NON-TYPEABLE *HAEMOPHILUS INFLUENZAE* AND RHINOVIRUS CO-INFECTION OF THE RESPIRATORY EPITHELIUM

Thesis submitted for the degree of Doctor of Philosophy
at University College London

Alina-Maria Petris

Infection, Immunity and Inflammation Research
and Teaching Department
UCL Great Ormond Street Institute of Child Health

AUGUST 21, 2019

I, Alina Maria Petris, confirm that the work presented in this thesis is my own. Where information has been derived from other sources, I confirm that this has been indicated in the thesis.

This research is supported by the NIHR GOSH BRC. The views expressed are those of the author and not necessarily those of the NHS, the NIHR or the Department of Health.

Abstract

Non-typeable *Haemophilus influenzae* (NTHi) and rhinovirus 16 (RV16) are strongly associated with symptomatic disease in healthy individuals and with disease exacerbations in patients with chronic lung conditions such as chronic obstructive pulmonary disease (COPD). Co-infection with RV16 and NTHi is thought to cause more severe exacerbations, although the mechanism behind this remains unknown. The hypothesis of this project was that RV16 and NTHi co-infection of the respiratory epithelium results in increased bacterial growth, greater epithelial damage and inflammation compared to single NTHi infection. To investigate this, healthy and COPD primary respiratory epithelial cells cultured at air-liquid interface for 6 days (pre-ciliation) or 28 days (ciliated) were infected with RV16 and 24 hours later challenged with NTHi.

In healthy and COPD ciliated epithelial cultures, NTHi bound to motile cilia within minutes, then formed filamentous morphotypes and biofilm-like aggregates which reduced ciliary beat amplitude by 24 hours post infection. NTHi epithelial invasion occurred preferentially in non-ciliated epithelial cells suggesting that ciliation may protect against NTHi invasion. This might be of importance in COPD cultures, where the number of ciliated cells was reduced, reflecting what is seen *in vivo*.

Co-infection of ciliated cultures with RV16 and NTHi resulted in a reduced ciliary beat frequency, epithelial barrier dysfunction and a more complex inflammatory response from healthy and COPD ciliated cultures, compared to NTHi single infection. RV16 co-infection also promoted mucin gene expression and enhanced NTHi growth by altering epithelial cell apical fluid secretion. In

contrast, pre-ciliation cultures showed markedly reduced responses to single RV16 or NTHi infection and their co-infection compared to ciliated cultures. However, pre-ciliation cultures were susceptible to NTHi invasion and promoted NTHi growth during co-infection with RV16, suggesting they may act like a niche for bacterial colonisation.

In conclusion, this study has shown that NTHi infection is able to affect ciliary function, form biofilm and invade the epithelium without epithelial barrier damage or induction of a complex inflammatory response, suggestive of a colonizer behaviour. In contrast, co-infection with RV16 and NTHi led to NTHi growth, a goblet cell-specific transcriptional profile, impaired ciliary function and epithelial barrier and increased inflammation which could result in increased bacterial dissemination and COPD exacerbation.

Impact statement

The primary impact of this research will be delivered through publications that will describe mechanisms which can be targeted therapeutically to limit airway colonisation by NTHi and NTHi growth during co-infection with RV. This would be of interest to academic researchers (microbiologists, immunologists, respiratory scientists, and pharmacologists), clinicians (respiratory medicine, infectious diseases), pharmaceutical companies such as GSK and patients.

This multi donor study describes the very early interaction of NTHi with the ciliated respiratory epithelium and has highlighted a number of mechanisms employed by NTHi to avoid clearance from the airways. For example the finding that NTHi undergoes conformational changes and forms a biofilm on the ciliated epithelium could be of interest to microbiologists, immunologists and respiratory scientists focused on studying mucociliary clearance, antibody mediate killing and immune cell phagocytosis of NTHi. Further identification of the factors responsible for enhanced growth of NTHi during co-infection with RV would allow their potential manipulation for therapeutic purposes and limitation of bacterial growth during viral co-infection. For example, inhaled therapies or manipulation of the immune system or of the bacteria to enhance bacterial clearance from the respiratory tract could reduce bacterial persistence and airway colonisation.

Pharmaceutical companies such as GSK with a focus on respiratory diseases will be interested in understanding the mechanisms that NTHi uses for invasion of the respiratory epithelium and how these could be manipulated for therapeutic purposes. This PhD project was funded by GSK and we have had

regular meetings to discuss the findings. They are interested in therapies that prevent epithelial invasion or long-term airway colonisation in patients with COPD.

Both academic researchers and pharmaceutical companies will benefit from the methods described here for primary cell culture, which highlight the markedly different results obtained in infection studies using undifferentiated versus differentiated epithelial cell cultures. Furthermore, it was shown here that findings from studies using epithelial cell lines could not be replicated in primary ciliated airway epithelial cell cultures. Thus, these findings emphasize the caution in interpretation of studies which use systems that are too far removed from primary human tissue.

Both healthy individuals and patients with COPD will benefit from the increasing attention given to research of this chronic lung disease. Publication of summaries of this research aimed at a non-scientific audience on social media outlets and web pages could help patients to understand the link of viral-bacterial co-infection in causing more severe exacerbations of their condition.

Acknowledgements

I would like to express my gratitude to my supervisor, Prof. Chris O'Callaghan for his guidance, patience and support throughout my PhD project. Thank you for allowing me to spend four unforgettable years in your laboratory during which I learnt so much and developed as a scientist and on a personal level. I would also like to thank Dr. Primrose Freestone, Dr. Claire Smith and Prof. Tim McHugh, who have helped me with numerous and valuable scientific discussions, laboratory guidance and essential encouragement and advice over the past 4 years. I thank Dr. Dale Moulding and Mark Turmaine, for their help with the confocal and electron microscope, respectively, as without their expertise, I would not have been able to perform my imaging studies.

During my PhD I was lucky enough to work with a great group of people from GlaxoSmithKline, who also funded my PhD project. Special thanks go to Dr. Rick Williamson and Dr. Soren Beinke for their scientific input into my project during our regular meetings as well as for their advice and guidance in my career. I would also like to thank Dr. Gareth Wayne for teaching me how to use the Image Stream and analyse the data, Dr. Ken Grace who helped me get more data in one week of running MSD, Luminex and PCR than in months previously and Dr. Augustin Amour, for his guidance on PI3K signalling and inhibition assays! I am thankful to Dr. Tanja Hoegg and Dr. Mark Lennon for their help with the statistical analysis, which has been invaluable for my project! I would also like to express my gratitude to Dr. Edith Hessel for her constant support of my career. My sincere thanks also go to Dr. Paul Redford and Dr. Nikolai Belyaev for always answering my PhD related questions, for their advice, encouragement and guidance over the past four years!

Thanks must also go to the girls of the O'Callaghan lab: Simona Velkova, Dani Lee and Dr. Daniela Cardinale! To Simona, we both know these past 4 years have not been easy, but we have worked so well together. I think we will both remember the endless hours of splitting co-cultures, of doing viable counts, of feeding ALI cultures as well as travelling to the US for the Gordon conference! I am grateful for our time and for how much we have learnt together! To Dani and Daniela, the princess has learnt how to prepare PBS and agar plates! Thank you both for all your patience and advice in the lab and I am especially thankful for our Friday night dinners at Daniela's –they make for great memories!

I would like to say a big thank you to my friends without whom I would not have been able to complete this PhD. Gabriela, I cannot thank you enough for being just a phone call away every time I needed to talk to someone and for always allowing me to share my thoughts unreservedly. Katie, thank you for our breakfasts at Bill's, for our photography trips around London and for being so understanding and always encouraging during difficult times. Andreea, thank you for our after work dinners, for helping me to re-discover my love for dancing and for being there for me when I needed to escape thesis writing. Linda and Cam, thank you for convincing me to go to Croatia, it has been the highlight of this summer, in the midst of a stressful period.

Last, but by no means least, I would like to wholeheartedly thank my parents for their continuous effort to support my studies in the UK, for their endless love, understanding, guidance and trust in me as without it I would not be where I am today.

Table of contents

Table of figures

Table of tables

List of abbreviations

ALI	Air liquid interface
BEBM	Bronchial epithelial basal medium
BEGM	Bronchial epithelial cell growth medium
CEACAM-1	Carcinoembryonic antigen related cell adhesion molecule 1
CFSE	Carboxyfluorescein succinimidyl ester
CFU	Colony forming units
COPD	Chronic obstructive pulmonary disease
DC	Dendritic cell
DMSO	Dimethyl sulfoxide
ENA-78	Epithelial-derived neutrophil-activating peptide 78
G-CSF	Granulocyte colony-stimulating factor
GM-CSF	Granulocyte-macrophage colony-stimulating factor
Gro-α	Growth related oncogene-α
ICAM-1	Intercellular adhesion molecule 1
IFN-λ	Interferon-λ

IL-8	Interleukin-8
IP-10	Interferon gamma-induced protein 10
MCP-1	Monocyte chemoattractant protein-1
MIP-3α	Macrophage inflammatory protein-3α
NAD	Nicotinamide adenine dinucleotide
NK cell	Natural killer cell
NTHi	Non-typeable Haemophilus influenzae
PAFR	Platelet activating factor receptor
PI3K	Phosphatidylinositol 3-kinase
qRT-PCR	Real-time quantitative reverse transcription polymerase chain reaction
RANTES	Regulated on activation, normal T cell expressed and secreted
RSV	Respiratory syncytial virus
RV	Rhinovirus
SEM	Scanning electron microscopy
Ser 473	Serine 473

SPDEF	SAM pointed domain-containing Ets transcription factor
TARC	Thymus and activation regulated chemokine
TEER	Trans-epithelial electrical resistance
Thr 308	Threonine 308
Th1 cell	T helper 1 cell
TNF-α	Tumor necrosis factor-α
TSLP-1	Thymic stromal lymphopoietin-1
ZO-1	Zonula occludens-1

Chapter 1: Introduction

1.1. The structure and function of the human respiratory epithelium

The epithelial layer lining the human airways is the first line of defence against inhaled environmental pathogens, particles and pollutants (Crystal et al., 2008). In addition to being a physical barrier for host protection, the epithelium also plays a central role in regulating airway immunity to infection as well as airway structure and function in health and disease (Proud and Leigh, 2011). The human airway epithelium is pseudostratified and consists of three major cells types: basal cells, secretory cells (including goblet and club cells) and ciliated cells (see Figure 1) (Rock and Hogan, 2011). Other rare cell types recently identified in the respiratory epithelium include brush or tuft cells, neuroendocrine cells and ionocytes (Montoro et al., 2018; Nevo et al., 2019; Plasschaert et al., 2018).

1.2. Basal cells

Basal cells are a population of undifferentiated cells with the capacity to self-renew or give rise to secretory, ciliated or rare cell types, thus often seen as the stem cells of the respiratory epithelium (Hackett et al., 2008; Rock and Hogan, 2011; Rock et al., 2009; Ruiz Garcia et al., 2018). Recent single cell RNA sequencing of the mouse and human respiratory epithelia have revealed that basal cells can be found in a range of physiological states, depending on their differentiation state, response to injury and airway location (Plasschaert et al., 2018; Ruiz Garcia et al., 2018; Vieira Braga et al., 2019)

In the adult mouse, basal cells are more abundant in the main bronchi and the trachea, where they represent 30% of the total cells in the epithelium, but their

frequency decreases distally to complete absence in the small airways (Rock et al., 2009). In human airways, a similar percentage of basal cells was identified in the epithelium lining large airways, with a 5 fold reduction in proportion along the smaller airways (below 0.5 mm in diameter) (Boers et al., 1998). Basal cells of the lung are characterised by high expression of the transcription factor transformation-related protein 63 (Trp63) as well as cytokeratins 5 and 14, nerve growth factor receptor (NGFR) and integrin alpha 6 (Rock et al., 2009).

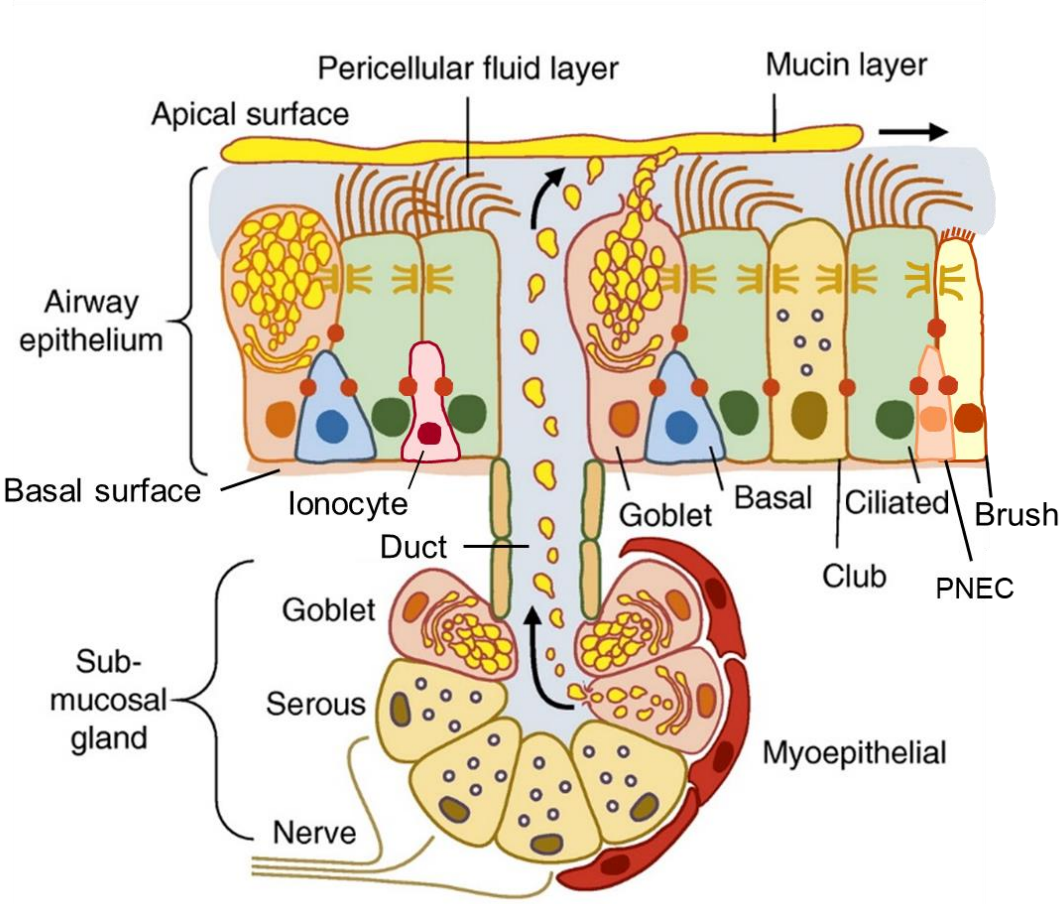

Figure 1. Structure of the respiratory epithelium and submucosal glands

The human airways are lined by a pseudostratified epithelium consisting of several cell types. Ciliated cells, through their continuous ciliary beating, move mucus secreted by goblet cells and submucosal glands along the respiratory tract in the process known as mucociliary transport. The pericellular fluid layer, formed of membrane tethered mucins and mucopolysaccharides, occupies the inter-ciliary space and sits underneath the mucus layer. Optimal hydration of the pericellular fluid is essential for normal ciliary beating and the cystic fibrosis transmembrane conductance regulator rich ionocytes play an important role in regulating its hydration (Button et al., 2012). Submucosal glands are lined by mucus producing goblet cells and serous cells that release electrolytes to regulate mucus hydration (Whitsett, 2018, Okuda et al., 2018). Innervated myoepithelial cells regulate mucus secretion from submucosal glands in response to neural inputs (Whitsett, 2018). Airway brush cells and pulmonary neuroendocrine cells (PNEC) are rarer cell types thought to act as oxygen and pathogen sensors (Nevo et al., 2019, Cutz et al., 2013). Club cells are direct descendants of

1.3. Club cells

Club cells are non-ciliated, cuboidal cells with an apical uterodome which contains electron-dense membrane bound granules (Boers et al., 1999; Reynolds and Malkinson, 2010; Rock and Hogan, 2011). These granules are filled with glycoproteins of the secretogoblin family, particularly SCGB1A1 (otherwise known as club cell secretory protein) which has anti-inflammatory effects (Reynolds and Malkinson, 2010; Rock and Hogan, 2011). Additionally, club cells produce a variety of mucins, antimicrobial peptides, proteases, surfactant apoproteins A, B, D, as well as cytokines and chemokines (Reynolds and Malkinson, 2010). The frequency of club cells along the airways can vary from approximately 22% in the terminal bronchioles to complete absence in the proximal airways (Boers et al., 1999; Okuda et al., 2019). Club cells are direct descendants of basal cells and act as progenitors which retain the capacity to self-renew and differentiate towards ciliated and goblet cell lineages, for example in response to injury (Montoro et al., 2018; Rawlins et al., 2009; Ruiz Garcia et al., 2018).

1.4. Goblet cells

Goblet cells of the respiratory epithelium are secretory cells which, together with submucosal glands, produce mucus (Fahy and Dickey, 2010) – Figure 1. Goblet cells can produce two types of mucins: membrane bound (MUC1, MUC3, MUC4, MUC12 and MUC13) and secreted mucins (MUC2, MUC5AC, MUC5B and MUC6) (Rose et al., 2001). While submucosal glands secrete predominantly MUC5B, goblet cells lining the airway epithelium produce both MUC5AC and MUC5B (Birchenough et al., 2015; Hovenberg et al., 1996;

Jackson, 2001; Okuda et al., 2019). In the healthy respiratory epithelium, mucins MUC5AC and MUC5B are secreted predominantly in the large airways, including the trachea and bronchi but their presence decreases in the smaller airways to complete absence in terminal bronchioles (Okuda et al., 2019). These polymeric mucin macromolecules such as MUC5AC and MUC5B sit on top of the periciliary layer – a liquid layer containing membrane attached mucins such as MUC1 and MUC4 and mucopolysaccharides and which fills up the space between the cilia- and, together with the ciliary movement, ensure mucociliary clearance of inhaled pathogens and particles (Button et al., 2012; Munkholm and Mortensen, 2014). A 'gel-on-brush' model has been proposed by Button and colleagues, whereby in a healthy individual, this tight mesh formed by mucins such as MUC4 and MUC1, which are attached to the cell membrane, cilia and microvilli, prevents particles larger than approximately 40nm – smaller than, for example, the Influenza A virus- to access the cell surface (Button et al., 2012). The level of hydration of the mucus layer is an influential factor in the efficiency of ciliary beating, with dehydrated mucus causing compression of the periciliary layer and collapse of cilia (Button et al., 2012). An important role in regulating airway hydration is played by the chloride channel cystic fibrosis transmembrane conductance regulator (CFTR) and the epithelial sodium channel (ENaC) which ensure secretion of Cl^- anions and absorption of Na^+, respectively (Boucher, 2019). An imbalance in the activities of these two channels leads to changes in airway surface fluid and affects mucus rheology and mucociliary clearance. This is the case in cystic fibrosis where mutations in CFTR lead to loss of Cl^- secretion

coupled with increased Na^+ absorption and subsequent airway dehydration and mucus stasis (Boucher, 2019; Moore and Tarran, 2018).

During epithelial differentiation and regeneration, goblet cells are successors of secretory club cells, being discriminated from these by higher production of mucins MUC5AC and MUC5B and expression of the transcription factor sterile alpha-motif pointed domain-containing E-twenty-six (SPDEF) (Chen et al., 2009; Rajavelu et al., 2015; Ruiz Garcia et al., 2018). Traditionally, goblet cells and ciliated cells have been considered as two very distinct differentiation lineages. However, with the advantage of single cell RNA sequencing technologies, two recent studies suggest that there is some plasticity between the two lineages as a small proportion of cells simultaneously expressing the goblet cell specific MUC5AC and ciliated cell specific transcription factor forkhead box J1 (FOXJ1) were detected (Rock and Hogan, 2011; Ruiz Garcia et al., 2018; Vieira Braga et al., 2019).

1.5. Ciliated cells

Ciliated cells propel mucus and mucociliary clearance plays a major role in clearing inhaled particles and pathogens (Norton et al., 2011). Ciliated cells are terminally differentiated cells, arising from secretory cells in absence of Notch signalling, a signalling pathway which regulates ciliated versus secretory cell fate choice (Rock and Hogan, 2011). Assembly of ciliary proteins then occurs under the control of a transcriptional network regulated by FOXJ1 (Whitsett, 2018). Ciliated cells have cilia on the apical side that beat in a coordinated fashion, at a frequency of approximately 10-16 Hertz, to ensure transport of the overlying mucus layer and any particles and organisms

attached to it (Chilvers and O'Callaghan, 2000). Each ciliated cell is estimated to have approximately 200-300 motile cilia on its surface with each cilia measuring approximately 6 µm in length (Rhodin, 1966; Thomas et al., 2012; Yaghi et al., 2012). The cilium is structured around a central pair of microtubules and nine peripheral microtubule doublets elongating from the basal body and aligned in parallel to form the axoneme, which is covered by the plasma membrane (Figure 2) (Ishikawa and Marshall, 2011). In order to move mucus along the respiratory tract, cilia beat in a cycle: the power stroke where the cilium elongates and moves forward in an almost perpendicular plane to the cell surface, with the tips of the cilia in close contact to the mucus layer, and the recovery stroke, where the cilium bends and moves backwards, in a plane closer to the cell surface and below the mucus layer (Sleigh et al., 1988; Tilley et al., 2015). For efficient mucus transport, cilia in the same area beat in a coordinated manner, creating a “metachronal wave” (Braiman and Priel, 2008). Ciliary beating is regulated by numerous factors, including cellular signalling pathways and external mechanosensitive factors (Boucher, 2019; Button et al., 2012; Salathe, 2007). The intracellular signalling pathways associated with regulating ciliary beating include: calcium signalling, the second messengers cyclic adenosine monophosphate (cAMP) and cyclic guanosine monophosphate (cGMP) and nitric oxide (Salathe, 2007). Activation of G-protein coupled receptors such as the P2 purinergic receptors by ATP or of muscarinic receptors by acetylcholine leads to activation of phospholipase C and elevation of the intracellular concentration of Ca^{2+}, which has been correlated with an increase in ciliary beat frequency (Braiman and Priel, 2008). It is believed that Ca^{2+} can exert its effects on modulating ciliary beat frequency

via the second messengers cAMP and cGMP. As such, elevated intracellular Ca^{2+} activates adenylate cyclase causing an increased production of cAMP and activation of the cAMP dependent protein kinase A. Protein kinase A localizes to the cilia and phosphorylates target axonemal proteins, leading to an increase in ciliary beat frequency (Braiman and Priel, 2008; Salathe, 2007). Ca^{2+} signalling can also activate the nitric oxide synthase, causing production of nitric oxide, subsequent activation of the cGMP- protein kinase G pathway and phosphorylation of target axonemal proteins (Braiman and Priel, 2008; Li et al., 2000). Extracellular factors that can affect ciliary function include: temperature, with higher temperature stimulating faster ciliary beating; pH, with acidic pH found to decrease ciliary beat frequency; changes in the periciliary layer, such as hydration of the periciliary fluid or its viscosity, determined by its content of mucin and other non-volatile solids, with dehydrated and viscous periciliary fluid causing a decrease in ciliary beating and even collapse of cilia (Boucher, 2019; Button et al., 2012; Clary-Meinesz et al., 1998; Clary-Meinesz et al., 1992). In addition, genetic mutations that affect proteins of the cilia structure can lead to abnormal ciliary beating and cause the respiratory disease primary ciliary dyskinesia (Horani et al., 2016). Abnormal ciliary beating can also affect cilia in brain ventricles and cause hydrocephalus, because of loss of cerebrospinal fluid flow, can lead to dysfunction of the reproductive system or to *situs inversus*, where internal organs are organised in a mirror image of their normal localisation (Fliegauf et al., 2007; Horani et al., 2016).

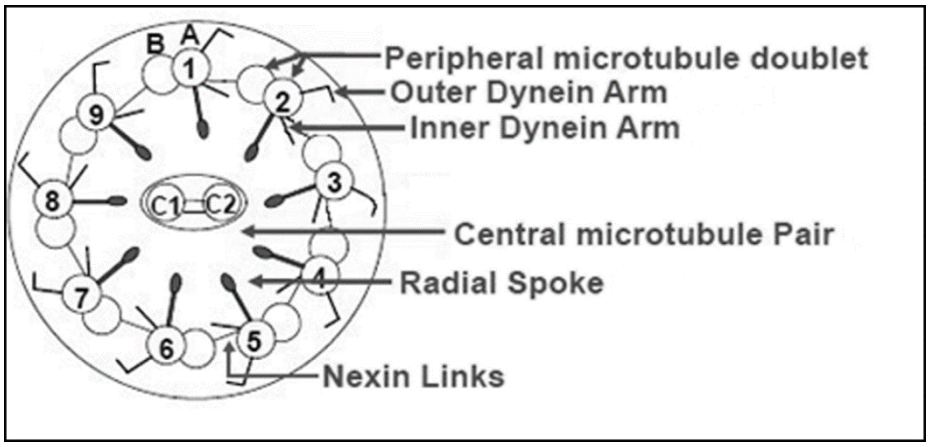

Figure 2. Structure of the motile cilium

Motile cilia have an evolutionary conserved axonemal structure organised around a pair of central microtubules surrounded by 9 pairs of peripheral microtubules, a structured known as 9+2. The microtubules are formed of α (A) and β (B) tubulin monomers. Nexin links form bridges connecting the peripheral microtubule pairs while radial spokes connect the central pair of microtubules with the peripheral pairs (Knowles et al., 2016; Tilley et al., 2015). The outer and inner dynein arms provide the energy for movement of the cilium by hydrolysis of ATP to ADP (Praveen et al., 2015). Picture adapted from (Knowles et al., 2016).

1.6. Other rare cell types

As mentioned earlier, much less abundant cell types have been identified in the airway epithelium, including neuroendocrine cells, brush cells and the recently discovered ionocytes (Montoro et al., 2018). Montoro and colleagues have shown, using single cells RNA sequencing, that these three cell types differentiate directly from basal cells, without the intermediate secretory cell stage that gives rise to ciliated and goblet cells (Montoro et al., 2018).

Neuroendocrine cells represent less than 1% of the total lung epithelial cells and possess characteristics of both hormone secreting endocrine cells and neurons, being the only innervated epithelial cell type (Branchfield et al., 2016; Kobayashi and Tata, 2018). Functionally, neuroendocrine cells are excitable

cells which act as oxygen and olfactory sensors and play a role in sensing inhaled allergens (Cutz et al., 2013; Gu et al., 2014; Sui et al., 2018). They can be found in clusters or as isolated cells and produce calcitonin-gene related peptide and gamma-aminobutyric acid which influences goblet cell differentiation and interaction with immune cells such as innate lymphoid cells (Sui et al., 2018).

Airway brush cells (also known as tuft cells) are multi-vesicular cells which present microvilli on the apical surface and account for approximately 1 to 7% of the epithelial cells (Reid et al., 2005). Their function in the respiratory epithelium is still incompletely understood but recent reports suggest they may have roles in innate immunity by being the main secretors of IL-25 in the epithelium (Bankova et al., 2018). It has also been suggested that they may act as chemosensors for bitter tasting bacterial products, producing acetylcholine as a result to stimulate vagal sensory nerve fibres and regulate breathing (Bankova et al., 2018; Krasteva et al., 2012; Nevo et al., 2019).

Pulmonary ionocytes are a recently identified epithelial cell type, representing 0.5-1.5% of the epithelial cells (Montoro et al., 2018; Plasschaert et al., 2018). Ionocytes express high levels of the chloride channel CFTR, thus playing essential roles in maintaining the airway surface fluid viscosity and mucociliary clearance (Montoro et al., 2018; Plasschaert et al., 2018).

1.7. Chronic obstructive pulmonary disease (COPD) causes and clinical characteristics

COPD is one of the leading causes of death and disability in the world. Epidemiological studies estimated that there were 384 million cases of COPD

in 2010 and 3 million deaths annually, but also highlighted that the prevalence of COPD is continuously increasing and expected to reach over 4.5 million deaths annually by 2030 (Agusti, 2018). The most common risk factor for developing COPD is cigarette smoking (Burney et al., 2014; Mannino and Buist, 2007). In non-smokers, it can arise as a result of α1-antitrypsin deficiency or exposure to occupational fumes, dust, vapours as well as outdoor and indoor air pollutants from burning biomass fuels (Burney et al., 2014; Mannino and Buist, 2007; Salvi and Barnes, 2009; Seemungal and Wedzicha, 2015).

COPD is defined by the Global Initiative for Chronic Obstructive Lung Disease (GOLD) as “a disease characterised by persistent respiratory symptoms and airflow limitation that is due to airway and/or alveolar abnormalities usually caused by significant exposure to noxious particles or gases” (Agusti, 2018). The disease is characterised by chronic inflammation which leads to development of emphysema, airway narrowing and remodelling, obstructive bronchiolitis, as well as chronic bronchitis (Agusti, 2018; Barnes, 2014; Barnes et al., 2003; Hogg and Timens, 2009). A diagnosis of COPD is made when there is a history of exposure to risk factors associated with presence of a chronic cough and dyspnoea and a post bronchodilator ratio of forced expiratory volume in 1 second (FEV1)/forced vital capacity (FVC) below 0.70 (Vestbo et al., 2013). COPD manifestations can extend beyond the lungs and induce a systemic inflammation associated with metabolic imbalances such as diabetes or obesity, bone disease or cardiovascular diseases. Individuals with COPD are also prone to develop depression, muscle weakness and lung cancer with squamous cell carcinoma being the most frequent type of cancer

seen (Auerbach et al., 1961; Barnes, 2010; de Torres et al., 2011; Kiri et al., 2010; Mouronte-Roibas et al., 2018; Wang et al., 2018a).

1.8. The respiratory epithelium in COPD

A consequence of the frequent exposure to tobacco smoke or pollution is seen in the increased baseline inflammation and changes in the structure and function of the respiratory epithelium (Schneider et al., 2010). These include basal cell hyperplasia, goblet cell hyperplasia and metaplasia, defective ciliary function, squamous metaplasia, epithelial to mesenchymal transition and loss of cell-cell junctions resulting in a leaky epithelium (Auerbach et al., 1961; Chung and Adcock, 2008; Crystal, 2014a; Milara et al., 2013; Shaykhiev et al., 2013b; Yaghi et al., 2012). The direct link between cigarette smoke exposure and development of COPD specific lung architecture has been investigated in studies using animal models of the disease which have shown that exposure of guinea pigs, mice, rats or ferrets repeatedly to cigarette smoke recapitulates human COPD phenotypes such as emphysema, mucus hypersecretion, goblet cell hyperplasia or small airway remodelling and inflammation (Ghorani et al., 2017; Jones et al., 2017; Raju et al., 2016; Vlahos and Bozinovski, 2014). Animal models of COPD can be valuable tools for mechanistic studies involving the whole organism, for drug target validation and safety and efficacy testing but their use for studying mechanisms of disease progression has remained somewhat limited. This is due in part to the nature of the disease which in humans develops over many years, presents much heterogeneity in phenotype and cannot be completely reproduced in animals which are routinely used in the laboratory and have a more limited life-span (Ghorani et al., 2017; Jones et al., 2017; Vlahos and Bozinovski, 2014). Therefore, most

of the current knowledge regarding the epithelial lesions that occur in the COPD lung come from *ex vivo* and *in vitro* studies using smokers' or COPD epithelia.

1.9. Basal cells in the pathogenesis of COPD

Early studies, which classified subjects only by their smoking status and did not account for a direct diagnosis of COPD, identified that basal cell hyperplasia was seen frequently in smokers who smoked more than one pack of cigarettes a day compared to non-smokers (Auerbach et al., 1979; Auerbach et al., 1961). More recently, exposure to cigarette smoke has been reported to affect the basal cell transcriptome (676 genes differentially expressed, compared to healthy non-smokers) as well as primary human bronchial epithelial cell differentiation at the air-liquid interface resulting in an increase of goblet and Club cells at the expense of ciliated cells (Cho et al., 2012; Ryan et al., 2014; Schamberger et al., 2015). Basal cells of COPD donors have been described as exhausted due to their reduced self-renewal capacity in clone forming assay and differentiation potential in cultures, where they resulted in differentiated epithelia with increased basal cells and mucus cells and over 80% fewer ciliated cells compared to differentiated epithelial cultures from subjects without COPD (Ghosh et al., 2018). One suggestion is that this may be a consequence of epigenetic modifications in basal cells of COPD patients, such as differential DNA methylation (Ghosh et al., 2018; Staudt et al., 2014). Smoking has also been linked to skewing basal cell differentiation towards an epithelial to mesenchymal transition and with reprogramming basal cells to a more human embryonic stem cell signature, which is similar to the early events which occur in the development of

aggressive forms of lung cancer (Shaykhiev et al., 2013a; Shaykhiev et al., 2013b). These studies indicate that through years of injury and exposure to noxious agents, basal cells of the COPD epithelium may be permanently imprinted towards an altered differentiation and therefore fail to regenerate a functional epithelium, limiting the protective capacity of the epithelial barrier and contributing to disease pathology.

1.10. Goblet cells, ciliated cells and mucociliary clearance in the pathogenesis of COPD

Goblet cell hyperplasia and an increase in goblet cell size, expansion of submucosal glands and increased mucus production are features of COPD that contribute to airway obstruction, formation of mucus plugs and inflammation (Fahy and Dickey, 2010; Innes et al., 2006; Kim et al., 2015; Rose et al., 2001; Saetta et al., 2000). Several mechanisms have been linked to induction of mucin secretion and goblet cell hyperplasia including inflammatory cytokines such as IL-13 and IL-17, up-regulation and stimulation of the epidermal growth factor (EGF) receptor by amphiregulin, cigarette smoke, bacterial products and neutrophil elastase or through activation of the Notch 3 signalling pathway by rhinovirus, the virus most commonly associated with COPD exacerbations (Atherton et al., 2003; Burgel and Nadel, 2004; Faris et al., 2016; Feldman et al., 2019; Jing et al., 2019; Rogers, 2003; Takeyama et al., 2001; Turner and Jones, 2009; Zuo et al., 2017).

Changes in the properties of mucus such as composition and viscosity, coupled with ciliary structure abnormalities and regions with loss of ciliated cells lead to an impaired mucociliary transport and accumulation of mucus

stores in the airways of smokers, which have been observed in many early studies (Auerbach et al., 1979; Auerbach et al., 1962; Lungarella et al., 1983; Stanley et al., 1986; Verra et al., 1995). The increased mucus stores seen in COPD airways are composed of a complex mixture of trapped immune cells, pathogens and cell debris that contribute to inflammation and fibrosis, causing further airway damage and disease progression (Fahy and Dickey, 2010; Hogg, 2004). Indeed, a more recent study identified that mucus obtained from bronchoscopic and sputum samples from subjects with chronic bronchitis had an increased content of mucins and non-volatile solids compared to the mucus of non-smokers and smokers without lung disease (Anderson et al., 2015). As expected, this is associated with decreased mucociliary clearance (Anderson et al., 2015). The predominant types of mucins were also found to change, with MUC5AC being the predominant form of mucin in the airways of smokers without COPD, while MUC5B was more abundant in airways of COPD patients (Caramori et al., 2004; Kirkham et al., 2008).

Smoking has long been associated with loss of airway ciliation in studies that investigated *ex vivo* epithelial strips by microscopy (Auerbach et al., 1961; 1962). More recent studies uncovered that cigarette smoke alters differentiation of primary human bronchial epithelial cells towards goblet and club cells at the expense of ciliated cells and leads to loss of ciliated cells in the airways of mice after 6-12 months of smoke exposure (Schamberger et al., 2015; Simet et al., 2010). Furthermore, airway repair and regeneration of ciliated cells was reduced when primary airway epithelial cells from COPD patients were grown in culture (Ghosh et al., 2018). In the study by Ghosh and colleagues, basal cells from COPD donors gave rise to 88% less ciliated cells

than basal cells from donors without COPD, highlighting an imprinted abnormal differentiation (Ghosh et al., 2018).

Several studies have analysed the effect of cigarette smoke on ciliary beat frequency and cilia length but results appear contradictory. All of the studies were carried out in nasal samples. One study reported no difference in the mean ciliary beat frequency of smokers versus non-smokers (Stanley et al., 1986) whilst Yaghi et al. (2012) described a significantly reduced ciliary beat frequency in moderate and severe COPD compared to control subjects. Contrary to this, a study by Zhou et al. (2009) reported an increase in the frequency of ciliary beating in smokers compared to non-smokers. Contradictory results have also been published with regards to a reduction in cilia length in COPD. Some studies described shorter cilia in bronchial samples from smokers and COPD patients compared to non-smokers (Brekman et al., 2014; Hessel et al., 2014; Leopold et al., 2009) while a study by Yaghi et al. (2012) reported no difference in the length of cilia between controls and COPD nasal samples.

In conclusion, further studies are required to understand the changes in ciliated cells and ciliary function caused by smoking, progression to COPD as well as by infectious agents. Future studies should also investigate other aspects of ciliary function, including ciliary beat pattern and ciliary beat amplitude, as ciliary beat frequency may be maintained despite an increase in ciliary dyskinesia, leading to overall ciliary function reduction (Smith et al., 2014).

1.11. The nasal versus bronchial epithelium in health and in COPD

Airway epithelial cells often used in respiratory research can be obtained from the nose through nasal brushing or from the lower respiratory tract by bronchial brushing, bronchial biopsy or isolated from resected lung tissue. The method of collection becomes particularly important when carrying out research on chronic respiratory diseases, as the ease of sample collection bears a big impact on study design and experimental reproducibility, particularly when comparisons between samples collected from healthy volunteers and patients with chronic respiratory diseases have to be made. Collection of nasal epithelial cells by nasal brushing is easier and more acceptable to both healthy and diseased donors, therefore increasing the likelihood of recruiting volunteers.

In samples collected from healthy volunteers, comparisons of nasal and bronchial epithelia suggest similarities in ciliary beat frequency (10.8 ±0.7 Hz in nasal cells and 11.8 ±2.3 Hz in bronchial cells), cell morphology, growth in culture and expression of receptors such as CD44, intercellular adhesion molecule-1 (ICAM-1), integrins αvβ3 and αvβ5 (Devalia et al., 1990; McDougall et al., 2008). Single cell RNA sequencing of nasal and bronchial brushings revealed the main cell types, including basal, ciliated and goblet cells are present in brushings from both locations but their proportions differ (Vieira Braga et al., 2019). As such, there were more goblet cells, less ciliated and a very small proportion of basal cells found in nasal brushings compared to bronchial brushings, where ciliated cells were the predominant type. In addition, nasal brushings lacked presence of club cells (Vieira Braga et al.,

2019). Cytokine release was found to be constitutively higher in nasal epithelial cells compared to bronchial (McDougall et al., 2008). However, in response to stimulation with interleukin-1β (IL-1β) and tumour necrosis factor-α (TNF-α), receptor expression changes were similar and the increase in cytokine release was correlated between nasal and bronchial samples (McDougall et al., 2008). Furthermore, differentiated primary bronchial epithelial cultures had lower baseline trans-epithelial electrical resistance and increased susceptibility to rhinovirus infection, including higher viral replication and inflammatory mediator production compared to differentiated nasal epithelial cultures (Lopez-Souza et al., 2009). However, effects seen after rhinovirus infection in nasal and bronchial epithelial cultures followed similar trends, suggesting a correlation between the two and the fact that healthy nasal epithelial cells could be used as surrogate for bronchial cells in infection studies (Lopez-Souza et al., 2009).

Several studies have addressed the comparison of upper and lower airway epithelia from smokers and patients with COPD. Firstly, upper airway involvement in COPD is supported by studies showing increased nasal inflammation and bacterial colonisation which was correlated with the degree of lower airway inflammation and bacterial load and by the presence of nasal symptoms which reflect pulmonary airflow impairment (Hurst et al., 2006a; Hurst et al., 2006b; Hurst et al., 2005). In addition, neutrophil and CD8+ T lymphocytes infiltrates were similar in nasal and bronchial mucosal samples, suggestive of similar inflammatory cell infiltrate between the two locations (Vachier et al., 2004). Two independent studies found similar gene expression profiles in nasal and bronchial epithelial samples collected from non-smokers

and similar smoking induced changes in the two locations, with one study reporting that only 27 genes were differentially induced in bronchial compared to nasal epithelia (Sridhar et al., 2008; Zhang et al., 2010). Furthermore, Boudewijn et al. (2017) performed genome wide gene expression analysis on nasal and bronchial epithelial brushings from two cohorts of COPD patients and found that the gene expression profile of COPD nasal epithelia overlaps the COPD bronchial gene expression profile. Separately, in a study by Talikka et al. (2017), nasal epithelial samples from current smokers and COPD patients were compared and their transcriptomics findings indicate that epithelial immune activation, oxidative stress and senescence responses were perturbed across three different anatomical locations: nasal, large airways and small airways. However, other responses such as signalling pathways activation, cell cycle or apoptosis responses varied depending on anatomical location. Furthermore, there were many similarities in the direction of network perturbations between nasal and large airway samples when comparisons between current smokers and patients with COPD were made. However, responses such as reactive oxygen species production under oxidative stress and senescence were found to change in opposite directions in nasal and large airway samples compared to lower airway samples when comparing current smokers with patients with COPD (Talikka et al., 2017). In subjects with COPD, analysis of bronchial and nasal biopsies revealed thicker epithelium and less squamous cell metaplasia in nasal samples compared to bronchial samples (Vachier et al., 2004). The basement membrane was similar in nasal and bronchial samples and overall thicker in COPD and smokers' samples compared to those of healthy volunteers (Vachier et al., 2004). In a study by

Comer et al. (2012) nasal and bronchial epithelial cells from COPD patients were cultured submerged, treated with cigarette smoke extract and then stimulated with *Pseudomonas aeruginosa* (*P. aeruginosa*) lipopolysaccharide. Following this treatment, toll like receptor 4 expression and IL-8 release were measured and found to be similar and in the case of IL-8, correlated, between nasal and bronchial cultures (Comer et al., 2012). In contrast, under the same conditions, IL-6 secretion was significantly higher in nasal epithelia compared to bronchial epithelium and IL-8 secretion in response to cigarette smoke extract was different in nasal versus bronchial epithelial cultures (Comer et al., 2012). Therefore, these studies indicate that there are many similarities between nasal and bronchial epithelia from healthy volunteers or COPD patients, including the involvement of the upper airway in disease symptoms and pathology. This supports the use of nasal epithelium in research studies due to its accessibility. However, as differences between nasal and bronchial epithelia have been flagged up, further studies are required to compare other aspects such as cellular composition of the epithelium, barrier function, response to infection and inflammation to validate their use as disease models. Ultimately, a better understanding of the differences between nasal and bronchial epithelium would clarify what compromises have to be made between disease relevance and ease of sample access when using nasal samples as a surrogate for the harder to access lower respiratory tract.

1.12. Inflammation and acute exacerbations of COPD

One of the clinical features of COPD is the chronic inflammation in the lungs, which is caused by both adaptive and innate immune mechanisms (Barnes, 2014; Hogg, 2004). B and T lymphocyte numbers are increased in the airways

of COPD patients, with T cells being predominantly CD8+ T cells, CD4+ T helper 1 (Th1) and CD4+ Th17 cell types (Barnes, 2016; Chung and Adcock, 2008; Hogg, 2004; Wang et al., 2018b). In terms of innate immune responses, epithelial cells, as well as neutrophils, macrophages and dendritic cells are the main cell types involved (Barnes, 2008b; Demedts et al., 2007). Activation of epithelial cells by smoke, inhaled pathogens and irritants stimulates production of several pro-inflammatory cytokines such as: TNF-α, IL-1β, IL-6 and chemotactic factors such as: growth related oncogene-α (Gro-α), monocyte chemotactic peptide-1 (MCP-1), IL-8, interferon inducible protein-10 (IP-10), eotaxin-1 or regulated on activation, normal T cell expressed and secreted (RANTES) (Barnes, 2016; Gao et al., 2015; Yi et al., 2018). IL-8, a neutrophil chemoattractant, is produced at higher levels by epithelial cells from COPD patients compared to healthy smokers and non-smokers, thus contributing to the mainly neutrophilic inflammation seen in COPD airways (Mio et al., 1997; Schulz et al., 2003). Neutrophils release oxidants and proteases such as neutrophils elastase, matrix metalloproteinase, myeloperoxidase or cathepsin G which can induce tissue damage and mucus secretion, thus promoting further airway damage (Barnes, 2014; Wang et al., 2018b). Similarly, monocytes migrate to the lung upon induction of MCP-1 production while dendritic cells respond to IP-10 (Barnes, 2008a; Gao et al., 2015). These chemokines can be secreted by macrophages and lymphocytes as well, therefore creating a continuously amplifying loop of immune cell migration to the lung and chemokine production resulting in chronic inflammation (Barnes, 2008a; Gadgil and Duncan, 2008).

Periods of increased inflammation and worse respiratory symptoms are called acute exacerbations of COPD (Vestbo et al., 2013). Symptoms of exacerbations include increased dyspnoea, cough and wheeze, sputum volume and purulence and arise as a consequence of the airway inflammation, increased mucus production and gas trapping (Agusti, 2018). COPD exacerbations, which tend to become more frequent as the disease becomes more severe, are associated with an accelerated decline in lung function, progression of the disease, a decline in the quality of life, higher mortality and account for most of the cost of COPD on healthcare systems (Agusti, 2018; Celli and Barnes, 2007; Mackay and Hurst, 2012). Over 70% of COPD exacerbations are triggered by bacterial and viral infections, although certain environmental factors can also contribute (Celli and Barnes, 2007; Mackay and Hurst, 2012; Papi et al., 2006). Viruses frequently associated with COPD exacerbations include rhinovirus (RV), respiratory syncytial virus, influenza virus and adenovirus while bacterial species include non-typeable *Haemophilus influenza* (NTHi)*, Streptococcus pneumoniae* (*S.pneumoniae*), *Moraxella catarrhalis* (*M.catarrhalis*) or *P. aeruginosa.* However, most COPD exacerbations are associated with RV and NTHi infections and bacterial and viral co-infection (Groenewegen and Wouters, 2003; Hutchinson et al., 2007; Papi et al., 2006; Patel et al., 2002; Seemungal et al., 2001; Wilkinson et al., 2017).

1.13. Rhinovirus: classification and characteristics

Rhinoviruses are the most common cause of upper respiratory tract infection, accounting for more than half of the cases of common cold annually (Blaas and Fuchs, 2016; Jacobs et al., 2013). RV belongs to the family of

Picornaviridae and it is a non-enveloped positive sense, single-stranded, RNA virus (Jacobs et al., 2013). An icosahedral capsid of approximately 30nm encases the 7200 base genome, which encodes for 4 structural viral proteins and 7 non-structural proteins with function in viral genome replication and assembly (Basnet et al., 2019; Fuchs and Blaas, 2010; Jacobs et al., 2013). More than 160 serotypes of RV have been discovered to date and have been classified as three species- A, B and C (Basnet et al., 2019; Palmenberg et al., 2009). RVs can also be classified based on the receptor they bind: the majority of both A and B types bind to the intercellular adhesion molecule-1 (ICAM-1) and are termed major group RVs whilst 12 serotypes of HRV-A bind to the low density lipoprotein receptor (LDLR) and are termed minor group. The receptor for RV-C has only recently been identified to be the cadherin-related family member-3 (CDHR3), which localizes preferentially to the basal bodies of ciliated cells (Blaas and Fuchs, 2016; Bochkov et al., 2015; Everman et al., 2019; Greve et al., 1989; Hofer et al., 1994).

Once bound to its receptor, the virus is internalised and enclosed into endosomes where it uncoats, the capsid is degraded inside lysosomes whereas viral RNA is released into the cytosol where it is replicated by the viral polymerase (Blaas and Fuchs, 2016). Single stranded viral RNA can be recognised by the endosomal toll like receptor (TLR)7 and TLR8 whereas replicated, double stranded RNA is recognised by TLR-3 (Jacobs et al., 2013). In the cytosol, pattern recognition receptors such as retinoic acid inducible gene I (RIG-I), melanoma differentiation-associated gene 5 (MDA5) or the cytosolic GAMP synthase (cGAS) molecule recognise presence of viral nucleic acids and trigger downstream production of cytokines and chemokines

(Goubau et al., 2013; McNab et al., 2015; Vareille et al., 2011). Upon infection by RV, respiratory epithelial cells respond by up-regulation of a wide range of mediators aimed at initiating and helping the host immune response through direct antiviral effects or recruitment of specialised leukocytes (Barnes, 2008a). These mediators include cytokines such as type I (IFN-α/β) and type III (IFN-λ1/2/3) interferons, interleukins 1, 6, 12, 15 and 18, growth factors such as vascular endothelial growth factor (VEGF), granulocyte-colony stimulating factor (G-CSF), granulocyte-macrophage colony stimulating factor (GM-CSF), chemokines such as IL-8, IP-10, RANTES, or defensins such as β-defensin 2 (Kennedy et al., 2012; Leigh et al., 2008; Papadopoulos et al., 2000; Piper et al., 2013; Proud et al., 2004; Rajan et al., 2013; Schroth et al., 1999; Spurrell et al., 2005; Wark et al., 2009). In particular, interferon secretion can have autocrine effects on epithelial cells, inducing production of the antiviral interferon stimulated genes proteins, which can directly affect viral replication by preventing viral entry into the cell, targeting virus proteins for degradation or degrade viral RNA (Haller and Kochs, 2011; Schneider et al., 2014; Silverman, 2007; Sun et al., 2012)

1.14. Rhinovirus infection of respiratory epithelial cells

It has been shown by several groups that epithelial cells are the main site of entry and replication for RVs (Arruda et al., 1995; Fuchs and Blaas, 2010; Gern et al., 1997; Lopez-Souza et al., 2004; Mosser et al., 2002; Papadopoulos et al., 2000; Wark et al., 2009). Recent studies have shown that RV16 and RV-C both preferentially infect ciliated cells of the airway epithelium, but not mucus producing goblet cells or basal cells, and cause ciliated cell shedding from the epithelial surface (Griggs et al., 2017; Jakiela et al., 2014; Tan et al., 2018).

In contrast, a previous study by Jakiela et al., suggested that basal cells of the differentiated airway epithelium could be more susceptible to infection by RV than suprabasal, differentiated epithelial cells (Jakiela et al., 2008). However the dual trypsin treatment used in this study to separate supra-basal and basal cells was not very cell-type specific and is unlikely to have isolated a pure basal cell population. The virus was also shown to be able to infect distally, in the lower airways as opposed to just the nasal mucosa (Gern et al., 1997; Lopez-Souza et al., 2009; Mosser et al., 2002; Papadopoulos et al., 2000). In addition, a study by Lopez-Sousa and colleagues indicates that *in vitro*, differentiated nasal epithelial cultures are more resistant to RV16 infection compared to differentiated bronchial cultures obtained from the same donor, in terms of both viral replication and inflammatory response (Lopez-Souza et al., 2009). While generally RV is not associated with significant cytotoxicity, it has been reported to affect the epithelial integrity and barrier function through downregulation of tight junction protein expression, allowing increased transmigration of bacterial pathogens such as NTHi (Looi et al., 2016; Sajjan et al., 2008).

1.15. Non-typeable *Haemophilus influenzae*

Haemophilus influenzae is a species of Gram negative coccobacilli that can be divided into typeable strains, which have a polysaccharide capsule, and non-typeable strains, which lack this capsule (King and Sharma, 2015). Whilst typeable strains can be further sub-divided into six subtypes named a to f, the NTHi is highly diverse, owing to variability in outer membrane proteins (St Geme et al., 1994). All types of *Haemophilus influenzae* have an obligatory requirement for hemin and nicotinamide adenine dinucleotide (NAD) for

growth, a characteristic which is also used clinically for identification from other bacterial species (Ahearn et al., 2017).

NTHi strains are the most common cause of *Haemophilus* respiratory infections, as these are commonly found in the nasopharynx of children and adults (Howard et al., 1988; King, 2012). In the upper airways of healthy individuals, NTHi is considered a commensal bacteria, with most children being transiently colonised in the first 2 years of life (Ahearn et al., 2017; King, 2012). However, when the bacteria spreads to the lower respiratory tract or when the respiratory tract is affected by disease or other infections, NTHi can become an opportunistic pathogen and cause symptomatic disease, including exacerbations of COPD or cystic fibrosis as well as pneumonia, otitis media or sinusitis (Clementi and Murphy, 2011).

1.16. NTHi interaction with the respiratory epithelium: adherence, biofilm formation and invasion

The first barrier encountered by the bacterium when it infects is the epithelial layer and NTHi possesses several mechanisms for adhering to it, as shown in Figure 3 (Clementi and Murphy, 2011). These include pili, autotransporter proteins, outer membrane proteins as well as lipopolysaccharides (St Geme, 2002). Pili are polymeric helical structures expressed on the surface of the bacteria which promote binding to epithelial cells and mucus (Kubiet et al., 2000; Loeb et al., 1988). Strains of NTHi that do not possess pili, use autotransporter proteins such as high molecular weight 1 (HMW1) and HMW2, *Haemophilus influenzae* adhesin (Hia) or the adhesion and penetration protein (Hap) to attach to the epithelial layer (Barenkamp and StGeme, 1996; Geluk

et al., 1998; Hendrixson and St Geme, 1998; St Geme, 2002). Outer membrane proteins such as P5 can promote binding to nasopharyngeal mucins as well as to the carcinoembryonic antigen-related cell adhesion molecule 1 (CEACAM1) and ICAM-1 (Avadhanula et al., 2006b; Euba et al., 2015; Hill et al., 2001; Reddy et al., 1996). Other outer membrane proteins such as Protein E (PE), P4 or PF can interact with the epithelium indirectly by binding to serum factors such as vitronectin, thus preventing complement mediated killing and allowing interaction with the epithelial vitronectin receptor, or by binding to extracelluar matrix proteins, including collagen IV, fibronectin, laminin or proteoglycan (Ahearn et al., 2017; Duell et al., 2016). In addition to proteins, attachment of NTHi to epithelial cells can also be mediated by lipooligosaccharides on the surface of the bacteria, with a particular phosphorylcholine (ChoP) moiety within lipooligosaccharides mediating adhesion to the platelet activating factor receptor (PAFR) on the host cell (Swords et al., 2000). Furthermore, despite early studies suggesting it does not bind to ciliated cells (Ketterer et al., 1999), a recent study contradicts this finding, showing early NTHi-cilia interaction during the course of infection of primary human air-liquid interface (ALI) cultured bronchial epithelial cells (Baddal et al., 2015).

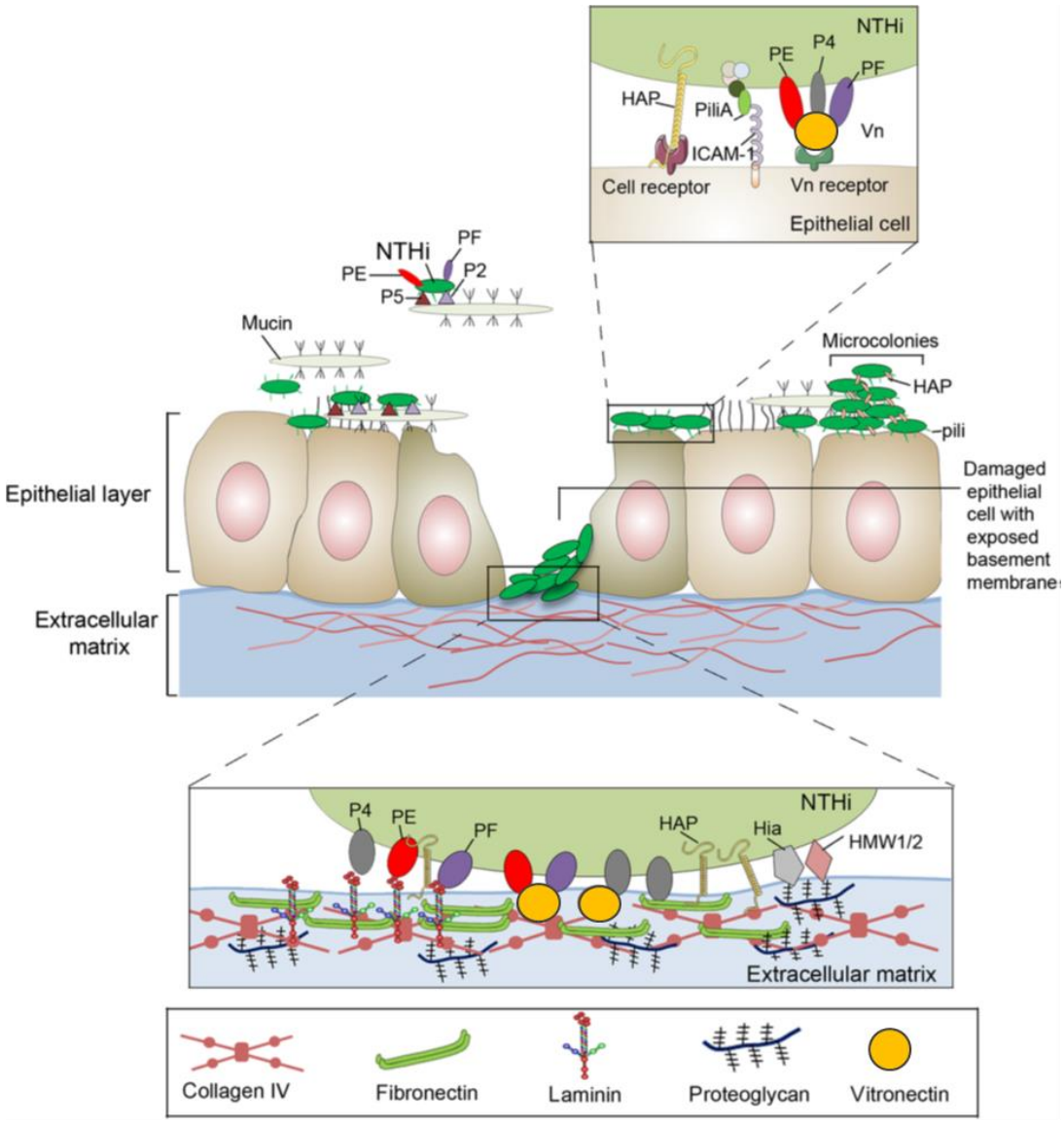

Figure 3. Mechanisms of NTHi adherence to the respiratory epithelium

NTHi possesses several mechanisms for adhesion to the epithelial layer and underlying extracellular matrix. These include pili, adhesins such as: high molecular weight (HMW 1/2), the autotransporter proteins *Haemophilus influenzae* adhesion (Hia) and Haemophilus adhesion protein (Hap), as well as outer membrane proteins such as Protein 2 (P2), P4, P5, PE, PF. Attachment to the epithelium and underlying extracellular matrix allows subsequent intracellular invasion and biofilm formation. Figure adapted from (Duell et al., 2016).

In addition to attachment to the epithelial layer of the respiratory tract, NTHi can avoid clearance from the airways by immune cells such as tissue resident macrophages and recruited neutrophils and antibiotic killing through biofilm formation and intracellular invasion (Ahearn et al., 2017; Langereis and Hermans, 2013; Slinger et al., 2006; Swords, 2012; van Schilfgaarde et al., 1999). Biofilm formation by NTHi has been documented in middle ear mucosal biopsies from children with otitis media, indicating the ability of NTHi to form biofilms during human disease (Hall-Stoodley et al., 2006). However, there is less evidence proving biofilm formation by NTHi in respiratory diseases such as cystic fibrosis or COPD. Only one study has so far provided evidence of NTHi biofilm formation in human lungs by imaging NTHi biofilms in broncho-alveolar lavage fluid from a patient with cystic fibrosis (Starner et al., 2006). *In vitro*, NTHi strains isolated from cystic fibrosis patients formed biofilm-like structures on air-liquid interface cultured Calu-3 cell line over 4 days of co-culture, resulting in large, matrix supported structures with a depth of over 20 µm (Starner et al., 2006). These structures also presented with an increased resistance to gentamicin killing, which was not due to bacterial loss of antibiotic susceptibility (Starner et al., 2006). Evidence of biofilm formation in COPD airways is limited to an *in vivo* mouse model of COPD, where mice were treated with a pulmonary bolus of elastase to replicate the emphysematous COPD airway, followed by NTHi infection 21 days later (Pang et al., 2008). In this study, elastase treated mice showed delayed bacterial clearance and displayed large aggregates of NTHi within the damaged tissue, in contrast to the individual bacteria distribution seen in control mice, which lacked symptoms of pathology following infection (Pang et al., 2008). However, further

studies are required to completely ascertain the role of biofilms in NTHi infection and persistence in the respiratory tract, including the role they play in resisting immune cell clearance, the mechanisms behind biofilm growth and enhanced antibiotic resistance (Swords, 2012).

Once attached to the surface of the epithelial cells, NTHi can enter human epithelial cells by various mechanisms, including macropinocytosis- mediated by cytoskeletal rearrangements involving lamellipodia formation and microvilli elongation- and receptor mediated endocytosis, involving the PAFR and the β-glucan receptor (Clementi and Murphy, 2011; Holmes and Bakaletz, 1997; Ketterer et al., 1999; Stgeme and Falkow, 1990; Swords et al., 2000). Following internalisation, the bacterium is trafficked through endolysosomes and normally would be killed in lysosomes (Clementi et al., 2014). However, NTHi uses the IgA protease to escape lysosome microbicidal activity by cleaving the lysosome-associated membrane protein 1 and disrupting lysosomal acidification, and survives intracellularly in a metabolically active but non-proliferative state (Clementi et al., 2014; Morey et al., 2011). Intracellular invasion of the epithelium provides a safe niche for NTHi persistence in the respiratory tract, due to its slow turnover which occurs approximately every 180 days, and as a shield against antibiotic killing (Clementi and Murphy, 2011; van Schilfgaarde et al., 1999).

1.17. Host signalling pathways involved in NTHi invasion of the respiratory epithelium

The interaction of NTHi with epithelial cells and subsequent bacterial internalisation is also dependent on host cell signalling pathways (Swords et

al., 2001). Binding of NTHi to the PAF receptor on the 16HBE14 bronchial epithelial cell line activates a pertussis toxin-sensitive G-protein complex, resulting in induction of phospholipase activity, in an increase in intracellular Ca^{2+} and activation of the phosphatidylinositol-3-kinase (PI3K) pathway, the latter two being required for NTHi internalisation (Swords et al., 2001). As the PI3K pathway plays important roles in regulating cytoskeletal re-arrangements in epithelial cells, a mechanism essential for bacterial internalisation, its role in NTHi invasion has been investigated more extensively. A study by Morey et al., confirmed that internalisation of NTHi by the A549 epithelial cell line results in phosphorylation of Akt, a measurement of PI3K pathway activation (as explained in more detail in 3.2.1.1), and that inhibition of this pathway by pan-PI3K inhibitors abrogated Akt phosphorylation and NTHi internalisation (Morey et al., 2011). Subsequently, the same group went on to investigate which pathways downstream of PI3K are important for NTHi internalisation into A549 epithelial cells (Lopez-Gomez et al., 2012). In their study, they re-confirmed that inhibition of Akt resulted in reduced bacterial invasion, whereas inhibition of phospholipase C- γ1 led to higher bacterial invasion (Lopez-Gomez et al., 2012). They identified that integrins β1 and α5 are important for bacterial invasion, as was their downstream signalling pathway involving protein tyrosine kinases and the Ras homologous (Rho) guanosine triphosphatase (GTPase) Rac-1, which regulates microtubule polymerisation and NTHi internalisation as a result (Lopez-Gomez et al., 2012). Additionally, the RhoA-Rho-associated, coiled-coil containing protein kinase (ROCK) pathway was shown to regulate NTHi internalisation by controlling microtubule stability and actin cytoskeleton, as loss of signalling through this pathway resulted in

increased bacterial invasion (Lopez-Gomez et al., 2012). Furthermore, the Forkhead box transcription factor family O (FOXO), a major downstream target of PI3K signalling, was also reported to be involved in regulating NTHi invasion (Brunet et al., 1999; Seiler et al., 2013). In a study using the Calu-3 cell line, silencing of FOXO 1/3 by siRNA resulted in increased bacterial internalisation (Seiler et al., 2013). As activation of the PI3K signalling pathway leads to phosphorylation of FOXO by Akt and its subsequent translocation from the nucleus to the cytosol where it is degraded by the proteasome, inhibition of the PI3K pathway would allow activation of FOXO which could then prevent bacterial invasion (Seiler et al., 2013).

In conclusion, these studies highlight the important role of the PI3K signalling pathway in regulating NTHi invasion. However, all of these studies have been carried out in different types of immortalised cell lines and their direct translation to differentiated primary respiratory epithelium has not been confirmed yet. Furthermore, none of these studies went on to identify which of the class I PI3K isoforms is essential for NTHi internalisation. This information would allow for a more targeted approach to inhibiting bacterial invasion therapeutically, which would be beneficial for diseases such as otitis media and respiratory conditions where NTHi is associated with disease exacerbations.

1.18. Rhinovirus and NTHi in exacerbations of COPD

The roles of rhinovirus and NTHi in exacerbations of COPD have been recognized both in epidemiological studies and in experimental infections of COPD patients with RV16, which were followed in a majority of patients by a

secondary bacterial infection (Bandi et al., 2003; George et al., 2014; Groenewegen and Wouters, 2003; Hurst et al., 2005; Hutchinson et al., 2007; Mallia et al., 2012; Mallia et al., 2011; McManus et al., 2008; Molyneaux et al., 2013; Patel et al., 2002; Rohde et al., 2003a; Rosell et al., 2005; Sethi et al., 2006; Wilkinson et al., 2017). Indeed, NTHi has been repeatedly reported to be the pathogen most frequently detected in the airways of COPD patients, both at stable state and during disease exacerbations, having been isolated in approximately 20-50% of samples, depending on whether PCR or culture detection methods were used (Bandi et al., 2001; Finney et al., 2014; Wilkinson et al., 2017). Similarly, RV accounts for the majority of virus induced exacerbations, being isolated in approximately 25-44% of COPD exacerbations (Bandi et al., 2001; Britto et al., 2017; Wilkinson et al., 2017). Furthermore, rhinovirus-NTHi co-infections have been associated with increased odds ratio of exacerbations, particularly when rhinovirus infection occurred in the presence of colonising NTHi (Wilkinson et al., 2017).

1.19. The role of rhinovirus in exacerbations of COPD

Rhinovirus induced exacerbations are often linked with a decrease in FEV1 and FVC, more severe symptoms and longer recovery times compared to non-infectious exacerbations (Patel et al., 2000; Seemungal et al., 2001). In an experimental human RV16 infection, Mallia et al. (2011) described higher blood and sputum neutrophilia, higher neutrophil elastase and greater viral loads in COPD patients compared to controls, which were also correlated with severity of respiratory symptoms. Furthermore, respiratory epithelial cells of COPD patients infected with RV39 had higher viral load and higher levels of IL-6, IL-8, IP-10 and type III interferon response compared to control donors,

thus confirming the repeatedly observed associations of higher inflammatory markers, particularly IL-6 and IP-10, with rhinovirus induced exacerbations (Mallia et al., 2011; Patel et al., 2000; Quint et al., 2010; Schneider et al., 2010; Seemungal et al., 2001). In addition to increasing epithelial secretion of pro-inflammatory mediators, RV infection also stimulates mucus production and goblet cell proliferation, thus contributing to the goblet cell hyperplasia and mucus obstruction seen in COPD airways (Jing et al., 2019; Tan et al., 2018). In a study by Faris et al., (2016), using a model of injured/regenerating primary tracheal epithelium, RV39 affected epithelial barrier function and altered differentiation with a skew towards more goblet cells and reduced ciliation (Faris et al., 2016). While this study did not compare between rhinovirus effects seen in healthy and COPD epithelia, it is an important indication as to the role of rhinovirus infection in disease progression, given how the COPD epithelium is continuously injured and regenerating.

1.20. The role of NTHi in exacerbations of COPD

NTHi is not normally identified in the lower airways of healthy individuals but it often colonises the lower airways of COPD patients, leading to more frequent exacerbations, more cough, increased severity of symptoms and sputum purulence at exacerbations, compared to non-colonised patients (Bandi et al., 2001; Hurst et al., 2005; Patel et al., 2002; Rosell et al., 2005; Sethi et al., 2006). The mechanisms by which NTHi induces acute exacerbations of COPD are not fully understood, but it has been reported that acquisition of a new strain, other than the one colonising the airway of a COPD patient, could be a trigger of exacerbation (Sethi et al., 2002). In addition, strains isolated from a COPD exacerbation induced more airway inflammation and neutrophil

recruitments in an *in vivo* mouse model than colonising strains (Chin et al., 2005). In an *in vitro* infection of primary airway epithelial cells, NTHi strains isolated at exacerbation had increased adherence to epithelial cells and induced higher expression of ICAM-1 and IL-8 by epithelial cells compared to colonizers (Chin et al., 2005). It has also been suggested that NTHi could use intracellular invasion of epithelial cells as a method of persistence and re-emergence in the airways (Hotomi et al., 2010; Murphy et al., 2004; van Schilfgaarde et al., 1999). Indeed, NTHi was detected inside epithelial cells in the lower respiratory tract of 33% of stable state patients and 87% of patients with exacerbations of chronic bronchitis, but not in healthy individuals (Bandi et al., 2001). In support of this hypothesis, a study by Murphy et al. (2004) indicated that the same strain of NTHi can persist in the airway of COPD patients for as long as 6 months, undetected by the usual sputum culture techniques, before re-emerging, emphasizing the persistent airway colonisation in COPD. Therefore, despite the fact that a causal relationship between NTHi infection and COPD exacerbations has been suggested in the studies mentioned, the cellular mechanisms by which NTHi interaction with the ciliated respiratory epithelium induces exacerbations of disease in certain conditions whilst being a silent coloniser in others have not been elucidated.

1.21. Rhinovirus and NTHi co-infection in exacerbations of COPD

While patients with COPD are in a stable state, both viral and bacterial pathogens are detected in only approximately 9%, increasing during exacerbations to 25-30%, depending on the method of detection employed (Wilkinson et al., 2017). This suggests that viral-bacterial co-infection is associated with exacerbation. In exacerbations where both viruses and

bacteria are detected, the severity of the exacerbation, bacterial loads and serum IL-6 levels are increased (Wilkinson et al., 2006). One hypothesis is that rhinovirus infection leads to secondary bacterial infections. Indeed, following experimental RV16 infection of patients with COPD, a secondary bacterial infection was detected in 60% of the patients compared to only 10% in individuals without COPD (Mallia et al., 2012). Of interest, in COPD patients, but not healthy controls, NTHi outgrowth from a pre-existing airway colonising community was reported approximately 15 days post rhinovirus infection (Molyneaux et al., 2013). Several mechanisms by which rhinovirus could promote secondary bacterial infections have been proposed, including alterations in antimicrobial peptides levels, delay of bacterial clearance through a reduction in IL-8 levels and subsequent neutrophil recruitment or by increasing bacterial (including NTHi) adherence to respiratory epithelial cells by up-regulating expression of receptors such as PAFR, ICAM-1, CEACAM or fibronectin (Avadhanula et al., 2006a; Bellinghausen et al., 2016; Hament et al., 2004; Ishizuka et al., 2003; Mallia et al., 2012; Unger et al., 2012; Wang et al., 2009). Another mechanism by which viral infections could pre-dispose to secondary bacterial infection or to growth of colonising bacteria could be alterations in nutritional immunity that virus infection can cause. Nutritional immunity refers to the sequestration of essential nutrients such as trace minerals or amino-acids by the host in order to limit pathogenicity during infection (Melvin and Bomberger, 2016). In support of this hypothesis, RSV or RV infection of cystic fibrosis bronchial epithelial cells induced increased *P. aeruginosa* biofilm formation during co-infection studies (Hendricks et al., 2016). This was a result of dysregulated iron homeostasis through up-

regulated apical release of the iron binding protein transferrin, thus allowing iron to be utilised as a nutrient source by the bacteria (Hendricks et al., 2016). Furthermore, RSV infection of cystic fibrosis epithelial cultures also stimulated *Staphylococcus aureus (S. aureus)* biofilm formation, but this was independent of iron availability and instead was promoted by increased availability of nutrients from the host and metabolic adaptations of the bacterium to promote growth and amino acid metabolism (Kiedrowski et al., 2018). As nutritional immunity has been described to affect NTHi biofilm architecture and invasive behaviour, it would be important to assess whether similar mechanisms are at play during rhinovirus-NTHi co-infection (Szelestey et al., 2013). Conversely, an interplay where an NTHi pre-infection alters the course of a subsequent viral infection has also been described. Proposed mechanisms include up-regulation of receptors such as ICAM-1 for RV, and changing the immune response of airway epithelial cells to RV, through alterations in cytokine and chemokine production and toll like receptor expression (Gulraiz et al., 2015; Sajjan et al., 2006). However, detailed knowledge of how NTHi interacts with the ciliated airway epithelium of the respiratory tract and the effect it has on it, as well as of the interplay between NTHi and respiratory viruses such as RV is limited. A better understanding of the mechanisms involved may contribute to the effort of improving the management and treatment of COPD exacerbations, particularly as the combination of these two pathogens accounts for induction a large proportion of disease exacerbations.

1.22. Hypothesis and aims of this project.

In this research project we were keen to investigate the effects of rhinovirus and NTHi infection of the ciliated respiratory epithelium given that infections with both pathogens can cause clinical symptoms in previously healthy individuals. However, as rhinovirus and NTHi infections and their co-infection are known to exacerbate disease in chronic lung conditions, we chose to investigate COPD to determine if the underlying cellular response was different in such a condition. We focused on primary nasal epithelial cells to allow comparison with results from cells derived from healthy individuals.

As most studies looking at viral and bacterial infection of respiratory cells have focused on cultures of cell lines or undifferentiated basal cells, we were interested to understand if differentiation to a ciliated phenotype, mimicking the host more closely, affected response to infection. To investigate this cells from individual donors were studied prior to ciliation and when the epithelium had differentiated into a ciliated phenotype.

Project hypothesis

Rhinovirus and NTHi co-infection of primary epithelial cultures from healthy and COPD donors results in increased bacterial growth and greater epithelial damage and inflammation compared to single NTHi infection

Project aims:

- To characterise primary epithelial cultures from healthy and COPD donors.
- To investigate the early interaction of NTHi with the ciliated respiratory epithelium.
- To investigate the effect of RV and NTHi co-infection on epithelial barrier function and inflammatory responses.
- To investigate the effect of RV co-infection on NTHi growth and interaction with the respiratory epithelium.
- To understand if epithelial differentiation affects the course of rhinovirus and NTHi infection and co-infection.

Chapter 2: Materials and Methods

2.1. Ethical statement

All of the primary human epithelial cell samples used in this study were collected with patient consent through the UCL Living Airway Biobank, which was approved by the NRES Committee North West-Liverpool East (project licence: 14/NW/0128) on the 7th of April 2014. This research project was approved following local ethical review by the UCL Research Ethics Committee.

2.2. Preparation of nasal or bronchial brushing for culture

Nasal brush biopsies were obtained by brushing the inferior nasal turbinate with a 2 mm cytology brush (Keymed, Southend-on-Sea, UK). Bronchial brush biopsies were obtained by brushing the trachea or a main bronchus using a 2mm cytology brush (Olympus, Tokyo, Japan). To release the cells, the brush was agitated into 2 ml of 20 mM HEPES buffered medium 199 containing 100 IU/ml penicillin, 100 µg/ml streptomycin, 20ug/ml gentamicin (all Gibco, Carlsbad, California, US) and 2.5 µg/ml fungizone (Invitrogen, Carlsbad, California, US). Cells were pelleted by spinning at 300 g for 5 minutes and re-suspended in 1 ml of culture medium (F-medium described in Section 2.4).

2.3. 3T3 J2F Mouse embryonic fibroblasts culture

3T3 J2F mouse embryonic fibroblasts, a gift from Prof. Samuel Janes (University College London), were cultured in Dulbecco's modified Eagle's medium (DMEM) (Gibco, Carlsbad, California, US) supplemented with 8% heat inactivated bovine serum (Invitrogen, Carlsbad, California, US), 100 IU/ml penicillin and 100 µg/ml streptomycin. Media was changed every 2-3 days until cells were 70-80% confluent, but were not allowed to reach 100% confluency.

When desired confluency was achieved, if the cells were to be passaged, the media was aspirated and cells rinsed once in PBS, followed by addition of 0.05% trypsin/EDTA (Sigma Aldrich, St. Louis, Missouri, US) and incubation for 3-5 minutes at 37^{o} C or until all cells detached, as confirmed by light microscopy. The trypsin was inactivated by addition of culture medium and the cell suspension collected. Cells were pelleted by centrifugation at 300 g for 5 minutes, the supernatant aspirated, the pellet re-suspended in culture medium and the suspension was split into 3-5 T75 or T175 flasks (Fisher Scientific, Loughborough, UK), depending on the growth rate desired. Fibroblasts were not passaged past passage 12.

When 70-80% confluent, fibroblasts used for preparing feeder layers were mitotically inactivated to prevent further proliferation by replacing the culture medium with fresh culture medium containing 4 µg/ml mitomycin (Sigma Aldrich, St. Louis, Missouri, US). The flask was returned to an incubator set at 37^{o} C, 5% CO_2 for 2-3 hours, after which cells were detached using trypsin/EDTA, harvested as above and seeded into the desired type of flask at the following densities: T25 flask = 0.45 x 10^6, T75 = 1.5-1.7 x 10^6. Fibroblasts were left to attach overnight and used within the next two days.

2.4. Primary human respiratory basal cell culture using conditional reprogramming

Basal cells were expanded by conditional reprogramming using the Rho-associated, coiled-coil containing protein kinase (ROCK) inhibitor. This involved co-culturing the human basal epithelial cells with a feeder layer of mitotically inactivated 3T3-J2F mouse embryonic fibroblasts, using a method

previously described by Butler et al. (2016). The culture medium -from here in called F-medium- used for co-cultures was prepared by mixing Ham's F-12 Nutrient Mix (Gibco, Carlsbad, California, US) in a ratio of 1:3 with DMEM containing 10% foetal bovine serum (Invitrogen, Carlsbad, California, US), 100 IU/ml penicillin and 100 µg/ml streptomycin. This mixture was subsequently supplemented with 25 ng/ml hydrocortisone, 5 µg/ml insulin, 0.1 nM cholera toxin (all Sigma Aldrich, St. Louis, Missouri, US), 0.125 ng/ml epidermal growth factor (Invitrogen, Carlsbad, California, US), 10 µg/ml gentamycin (Gibco, Carlsbad, California, US), 250 ng/ml amphotericin B (Fischer Scientific, Loughborough, UK) and 5 µM Y-2763 (Rock inhibitor) (Axxora, Farmingdale, New York, US). The cell suspension obtained from one brushing as described in section 2.2 was added to one flask or split into two T75 flasks (depending on the amount of tissue obtained from the brushing) containing mitotically inactive fibroblast feeder layer and 10 ml of F-medium. The F-medium bathing the cells was replaced every 2-3 days until 80-90% confluent (up to 7 days). Once basal cells reached 80-90% confluency, the F-medium was aspirated and the cells washed in 10 ml PBS. Then, fibroblasts were removed by adding 2-3 ml of 0.05% Trypsin/EDTA and incubating briefly while monitoring under light microscopy. Once all fibroblasts were detached, but not basal cell colonies, the trypsin containing fibroblasts feeder cells was removed and the cells washed again in 10 ml of PBS. To detach basal epithelial cells, 2-3 ml of TrypLE Select reagent (Life Technologies, Carlsbad, California, US) was added to the flask and incubated for 10-15 minutes at 37^{o}C or until all cells detached, as confirmed by light microscopy. In order to inactivate the TrypLE reagent, 10ml of F-medium was added to the flask and

the cells were pelleted by centrifugation at 300 g for 5 minutes. The supernatant was removed and the pellet re-suspended in F-medium. Cells were counted by trypan blue exclusion and seeded into new flasks containing mitotically inactive fibroblast feeder layer, at the following densities: T25 flask = 1.25 x 10^5, T75 = 5 x 10^5 in 5 or 10 ml of F-medium, respectively.

2.5. Collagen coating of plastic dishes

A 1% solution (v/v) of PureCol Collagen (CellSystems, Kirkland, Washington, US) was prepared by dilution of the stock solution (3mg/ml) into sterile phosphate buffered saline. The resulting collagen solution was added in sufficient volume to completely cover the surface of the dish. Following a minimum 1 hour incubation at room temperature the collagen solution was removed and the surface washed once with sterile tissue grade water. The dish was allowed to air dry in a sterile tissue culture hood and then stored in a sealed plastic bag at room temperature.

2.6. Air-liquid interface (ALI) culture of respiratory epithelial cells

Basal cells re-suspended in F-medium were seeded onto collagen-coated polyester membrane transwells (0.4 µm pore size, 6.5 mm diameter, Corning, New York, US) (see section 2.4) at 0.4-0.5 x 10^6 cells in 125 µl of culture medium per well. Then, 500 µl F-medium were added to the basolateral chamber. Cells were left to attach to the membrane for 24-48 hours after which the apical fluid was removed, leaving the cells exposed to air, while the basolateral medium was replaced with 500 µl of ALI medium. ALI medium was prepared by mixing basal epithelial growth medium (BEGM) - prepared from

bronchial epithelium basal medium (BEBM) supplemented with the BEGM SingleQuot Kit (Lonza, Slough, UK), except gentamicin - and Dulbecco's modified Eagle's medium (DMEM) (Gibco, Carlsbad, California, US) in a 50:50 proportion. Due to issues with BEGM availability from Lonza, some cultures were grown with the equivalent PromoCell Airway Epithelial Cell Growth Medium (PromoCell, Heidelberg, Germany), using the same recipe. The ALI medium mixture was subsequently supplemented with 100 nm retinoic acid (Sigma Aldrich, St. Louis, Missouri, US) and 100 IU/ml penicillin, 100 µg/ml streptomycin, 2.5 µg/ml fungizone and filtered through a 0.2 µm filter (Sartorius, Gottingen, Germany). The basolateral ALI medium was replaced every 2-3 days and cells were considered fully differentiated after 28 days of ALI culture. Differentiation was determined by regularly checking cultures using high-speed video microscopy, as described in section 2.8 and confirmed by immunofluorescence staining and confocal microscopy, as described in section 2.10.

2.7. Trans-epithelial electrical resistance measurement

Trans-epithelial electrical resistance (TEER) of cells cultured at ALI was used to assess the epithelial barrier integrity in a non-invasive manner (Srinivasan et al., 2015). TEER was measured with an EVOM^2 Epithelial Voltohmmeter voltmeter (World Precision Instruments, Sarasota, Florida, US) using two unequal length electrodes. Electrodes were sterilised by dipping into pure ethanol, left to air-dry and then dipped into sterile culture medium until calibrated. Final TEER values were calculated by multiplying the ohmic resistance value given by the voltmeter by the surface area of the membrane – 0.33 cm^2.

2.8. High speed video microscopy for ciliation scoring

Epithelial cultures were washed with 200 µl BEBM/ well and the holding plate was subsequently placed on an inverted Nikon Eclipse TiE microscope stage (Nikon, Kingston-upon-Thames, UK) with the temperature set to 37^{o} C and CO_2 to 5%. Each well was inspected using a x20 objective (numerical aperture=0.45) with collar adjusted for a long working distance and the Hamamatsu ORCA camera (Hamamatsu, Hamamatsu City, Japan) attached to the Nikon Eclipse TiE microscope. The level of epithelial culture ciliation was noted according to the scoring system shown in Table 6. For a video of a ciliated epithelial culture see Appendix 4 and Video 1 on the USB stick attached.

2.9. Flow cytometry

Epithelial cultures were washed once, apically and basolaterally in 200 µl and 700 µl of PBS respectively, followed by incubation with 200 µl StemPro Accutase Cell dissociation reagent (Life Technologies, Carlsbad, California, US) added apically and 500 µl of the reagent added basolaterally for 15 minutes at 37^{o} C. Cells were dissociated by gentle pipetting, collected in DMEM medium supplemented with 10% heat inactivated bovine serum spun at 300g for 5 min to collect the pellet. Epithelial cell counting and viability assessment was performed using trypan blue exclusion. Approximately 0.2-0.5x10^{6} cells/stain were then incubated with the Fc receptor blocking agent Human TruStain FcX (BioLegend, London, UK) at 1:50 dilution in buffer (PBS supplemented with 0.5% bovine serum albumin and 2.5mM EDTA (both Sigma Aldrich, St. Louis, Missouri, US) for 10 minutes at 4^{o} C. Cells were

subsequently washed by adding 200 µl of buffer and spinning at 300g for 5 minutes. The pellet was then incubated with antibodies in a 50 µl staining cocktail (Table 1) in buffer for 20 minutes at 4^{o} C in the dark. Cells were washed once in buffer and stained with 7AAD (eBioscience, San Diego, California, US) or Zombie UV Fixable viability kit (Biolegend, London, UK) for live/dead discrimination. Fluorescence minus one control stains were performed to confirm gating strategy. All data was recorded using a BD LSRII flow cytometer using the BD FACS Diva Software V8.0.1 (Becton Dickinson, Franklin Lakes, New Jersey, US) and analysed using FlowJo version 10 (Treestar Inc, Ashland, Oregon, US).

Table 1. Antibody cocktail for flow cytometry staining

Antibody	Clone	Fluorophore	Manufacturer	Volume/stain (µl)
CD271	C40-1457	Brilliant Violet 421	BD Biosciences, San Jose, California, US	2.5
CD49f	GoH3	PE	BD Biosciences, San Jose, California, US	5
CD133	AC133	APC	Miltenyi Biotec, Gladbach, Germany	10
CD66 a/c/e	ASL-32	FITC	BioLegend, London, UK	2
CD66 a/c/e/	ASL-32	Pe/Cy7	BioLegend, London, UK	5
CD54	HA58	Brilliant Violet 711	BD Biosciences, San Jose, California, US	5

2.10. Fixing and staining epithelial cells for confocal microscopy

Epithelial cultures were fixed by adding 200 µl of 4% paraformaldehyde (Sigma Aldrich, St. Louis, Missouri, US) to the apical chamber and at least 300 µl to the basolateral chamber for 1h at room temperature or overnight at 4^{o}C. Then, the cultures were washed with 200 µl of PBS apically and 500 µl of PBS basolaterally. To permeabilise epithelial cells and block non-specific binding of antibodies, cultures were incubated with 200 µl of a solution of 0.1% Triton-X and 3% bovine serum albumin in PBS (Sigma Aldrich, St. Louis, Missouri, US) added apically and 400 µl basolaterally at room temperature for 30-45 minutes. Then, a cocktail of primary antibodies (Table 2) diluted in a solution of 0.1% Triton-X and 1% bovine serum albumin was prepared and 50 µl of the mixture added apically to each well for 3 hours at room temperature. Each well was then washed 3 times in 200 µl of PBS added apically. The cocktail of secondary antibodies was diluted in a solution of 0.1% Triton-X and 1% bovine serum albumin and cultures were incubated with 100 µl of the mixture added apically for 1-2 hours at room temperature. Cultures were then washed twice in 200 µl of PBS. If cultures were stained with phalloidin-iFluor 555 (Abcam, Cambridge, UK), it was prepared by being diluted 1:1000 in a solution of 0.1% Triton-X and 1% bovine serum albumin and cultures were incubated with it for 1h at room temperature. Then, the phalloidin was removed and Hoescht nuclear stain (Sigma Aldrich, St. Louis, Missouri, US) was added apically and incubated at room temperature for 30 min. Cultures were then washed 3 times in 200 µl of PBS, membranes cut out from the transwell using a surgical blade and mounted onto glass slides (Fisher Scientific, Hampton, New Hampshire, US) with the ciliated side facing up. A single drop of n-propyl gallate (Sigma Aldrich,

St. Louis, Missouri, US) was added on top of the membrane which was then covered with a glass coverslip (Scientific Laboratory Supplies, Nottingham, UK) and sealed off using nail varnish.

Table 2. Antibodies used for immunostaining

Antibody	Host	Fluorophore	Dilution	Manufacturer
β-tubulin	rabbit	N/A	1:100	Abcam, Cambridge, UK
MUC5AC	mouse	N/A	1:100	Invitrogen, Carlsbad, California, United States
Rabbit IgG (H+L) Highly Cross-Adsorbed Secondary Antibody	Donkey	Alexa Fluor 594	1:250	Invitrogen, Carlsbad, California, United States
Anti-Mouse IgG	Goat	FITC	1:64	Sigma Aldrich, St. Louis, Missouri, US

2.11. Quantitative real-time reverse transcription PCR (qRT-PCR)

Epithelial cultures were lysed by adding 180 µl of Roche MagNA Pure LC RNA Isolation buffer (Roche, Basel, Switzerland) to each well and incubating at room temperature for 10 minutes to ensure complete lysis. Two wells per condition tested were pooled for each culture. Cell lysates were collected and stored at -80ºC until they were used. RNA was purified using the Roche

MagNA Pure 96 Cellular RNA Large Volume Kit (Roche, Basel, Switzerland) on a MagNA Pure 96 Instrument (Roche, Basel, Switzerland), according to manufacturer's instructions. Following RNA purification, the amount of RNA in each sample was quantified on a NanoDrop 8000 Spectrophotometer (Thermo Fisher Scientific, Waltham, Massachusetts, US) using 2 µl of sample. Complementary DNA (cDNA) was synthesised using the SuperScript IV VILO Master Mix (Invitrogen, Carlsbad, California, US) and mixing 20 µl of purified RNA with 20 µl cDNA reaction components, according to manufacturer's instruction. The Q Cycler 96 thermal cycler (Hain Lifescience, Nehren, Germany), was set to: 10 minutes at 25^{o}C, 30 minutes at 50^{o}C, 5 minutes at 85^{o}C and then on hold at 4^{o}C. For each sample, the cDNA thus obtained was mixed with the reaction mix prepared as follows: 412.5 µl of the LightCycler 480 Probes Master mix (Roche, Basel, Switzerland), which included the FastStart Taq DNA Polymerase, deoxynucleotide triphosphates and buffer, 146.5 µl of RNase/DNase free water and 41 µl of primer/probe, for commercial gene assays (Thermo Fisher Scientific, Waltham, Massachusetts, US) –see Table 3, or 154.5 µl of RNase/DNase free water and 33 µl of primer/probe for GSK in house assays (RV16 and gapd)- see Table 3. This reaction mix was enough for one 384 well plate. The mosquito HV robot (TTP Labtech, Melbourn, UK) was used to add 1.5 µl of cDNA to 4 µl of reaction mix in a white LightCycler 480 Multiwell Plate 384 plate (Roche, Basel, Switzerland), giving a final primer/probe concentration of 900 nM for commercial assays and 400nM for GSK in house assays. The real-time PCR amplification and detection was performed on a LightCycler 480 Instrument II running a LightCycler software v1.5.1.62 (both Roche, Basel, Switzerland). Data

obtained were analysed in Microsoft Excel (Microsoft, Redmont, Washington, US).

Table 3. qRT-PCR primer/probes reference

Gene	Primer/probe reference	Manufacturer
muc5ac	Hs00873651_mH	Thermo Fisher Scientific, Waltham, Massachusetts, US
muc5b	Hs00861588_m1	
muc4	Hs00366414_m1	
spdef	Hs00171942_m1	
claudin 8	Hs00273282_s1	
zo-1	Hs01551861_m1	
gapdh GSK in house	GAPD Forward CAAGGTCATCCATGACAACTTTG GAPD Reverse GGCCATCCACAGTCTTCTGG GAPD Probe ACCACAGTCCATGCCATCACTGCCA	
RV16 GSK in house	RV16 Forward GTTGTTCCCACCCAGATCAC RV16 Reverse CTCAGTTGTTTTTGCCCTTGTGG RV16 Probe TCAAGCACTTCTGTTTCCCCGGTCA	

2.12. High speed video microscopy for analysis of ciliary function

In order to assess ciliary beat frequency, ALI cultured ciliated epithelial cells were placed in a 37^{o} C and 5% CO2 humidified incubation chamber on an inverted Nikon Eclipse TiE microscope stage (Nikon, Kingston-upon-Thames, UK) and were allowed to adjust to the new environment for 30 minutes. All observations and videos were recorded using a Hamamatsu ORCA camera (Hamamatsu, Hamamatsu City, Japan) attached to the Nikon Eclipse TiE microscope, by focusing on the cilia using a x20 lens objective (numerical aperture= 0.45) with the collar set to a long viewing distance (See Appendix 4/ Video 1 on USB stick attached, as an example of a healthy ciliated culture imaged as described here). Prior to the start of the experiment, the x-y-z coordinates of 10 areas on the cell surface with at least 6 ciliated cells each were saved for each well using the NIS Elements AR software (Nikon, Kingston-upon-Thames, UK) and activating the Perfect Focusing System option (PFS). Videos were subsequently recorded at set time points for the duration of the experiment by returning to the same points in each well and using the settings described in Figure 4. The active shutter was set to close when measurements were not taken to prevent extensive light exposure of the samples.

2.13. Ciliary beat frequency analysis

Videos recorded using the Nikon Eclipse TiE microscope were subsequently converted to an .avi format using the NIS Elements AR software or a custom made FIJI (Schindelin et al., 2012) macro written by Dr. Dale Moulding (Confocal microscopy facility manager, UCL Great Ormond Street Institute of

Child Health). Then, the .avi video files were run through the CiliaFA software (Smith et al., 2012) installed as a plugin to ImageJ (National Institute of Health, USA) using the settings shown in Figure 4. The software uses a Fast Fourier transformation to determine ciliary beat frequency from recorded videos.

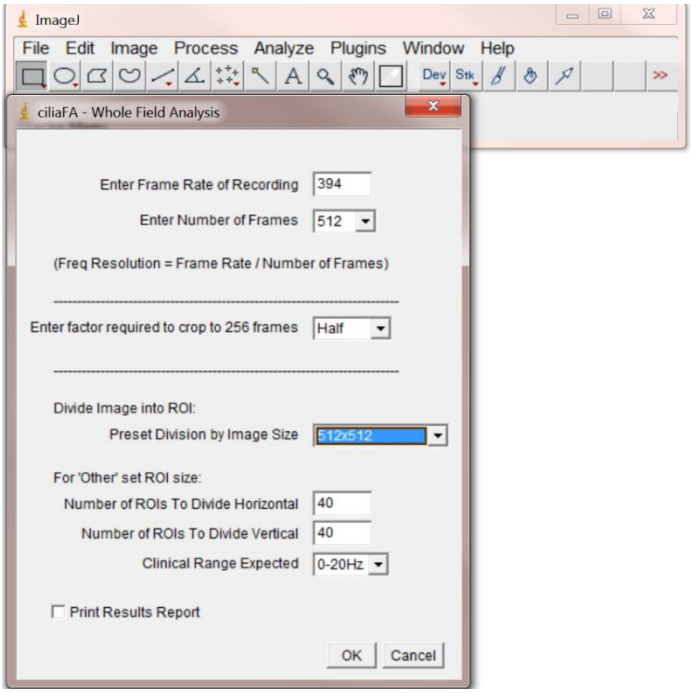

Figure 4. Settings used for high speed video microscopy recordings reflected in the ciliaFA software settings

Videos were recorded at set time points using a x20 objective (Numerical aperture =0.45) with the correction collar set to long viewing distance. In NIS Elements, the image size (region of interest) was set to 512x512 pixels. Under these settings, the pixel size measured 0.33 µm. High speed video imaging was performed by acquiring 512 frames at 394 frames per second with a 1 frame exposure. These acquisition settings were then input into the ciliaFA plug-in for Image J, for ciliary beat frequency analysis.

2.14. Ciliary amplitude measurements

As there is previously published evidence that ciliary beat pattern may be dyskinetic without a reduction in ciliary beat frequency, ciliary beat amplitude was also determine during NTHi infection of the ciliated epithelium. ALI

cultured ciliated epithelial cultures were infected with NTHi as described in 2.19 and incubated for 24 hours in an incubator set at 37º C and 5% CO_2. Prior to imaging, transwells were placed in glass dishes (WillCo Wells, Amsterdam, The Netherlands) with a custom made collar to adjust for the height of the transwell and keep it fixed in place. The dishes were then placed in a 37º C and 5% CO_2 humidified incubation chamber on an inverted Nikon Eclipse TiE microscope stage (Nikon, Kingston-upon-Thames, UK) and were allowed to adjust to the new environment for 30 minutes. All observations and videos were recorded using a Hamamatsu ORCA camera (Hamamatsu, Hamamatsu City, Japan) attached to the Nikon Eclipse TiE microscope by focusing on the cilia using a x60 lens objective (numerical aperture= 0.70) with the collar set to a long viewing distance. At least 10 videos per well were recorded. The cilia beat amplitude was measured using the NIS Elements AR software (Nikon, Kingston-upon-Thames, UK), using the distance measurement function. The start and end points of one cilium swipe were set and the software then calculated the distance between the two points.

2.15. Quantification of cytokines and chemokines in epithelial cell culture supernatants

Basolateral supernatants from epithelial cultures were collected and stored at -20ºC or -80ºC until they were analysed. Cytokines and chemokines were subsequently measured using MSD kits (MesoScaleDiscovery, Rockville, Maryland, US) and a Luminex kit (ThermoFischer Scientific, Vienna, Austria) platforms, as presented in Table 4, following manufacturer's instructions. MSD assays were read on an MSD SI6000 Sector Imager using Workbench software v4.0 (MesoScaleDiscovery, Rockville, Maryland, US). Luminex

assays were read on a Luminex Flexmap 3D, using the Luminex xPONENT v4.2 software (both Luminex Corporation, Austin, Texas, US) and analysed using the Bio-Rad Bioplex Manager v6.1 (Bio-Rad Laboratories, Hercules, California, US).

Table 4. Cytokine/ chemokine analysis kits

Analytes	Platform	Kit
IL-1β, IL-6, IL-8, TNF-α	MSD	V-Plex Human Proinflammatory Panel II (4plex)
TARC	MSD	V-Plex Human Tarc Kit (single plex)
IL-17C	MSD	V-Plex Human IL-17C Kit (single plex)
Interferon α2a, β, γ and λ	MSD	U-Plex Biomarker Group 1 (10 plex)
ENA-78, G-CSF, GRO-α, IL-1β, IL-15, IL-6, IL-8, IP-10, MCP-1, MIP-3α, RANTES, TNF-α	Luminex	Human Custom ProcartaPlex 12 plex

2.16. NTHi stock preparation

NTHi strain 49247 (ATCC, Manassas, Virginia, US) was originally isolated from the expectorated sputum of a 76-year old male who suffered from pneumonia. The strain was collected in January 1984 in Worcester, Massachusetts. NTHi was grown overnight on chocolate agar plates. Chocolate agar was prepared using sterile autoclaved Columbia agar base supplemented with 5% heat lysed de-fibrinated horse blood (both Oxoid, Basingstoke, UK). Bacterial colonies from chocolate agar plates were inoculated initially in 10 ml of brain-heart infusion (BHI) broth (Oxoid, Basingstoke, UK) supplemented with 10 µg/ml β-Nicotinamide adenine dinucleotide and Hemin (both Sigma Aldrich, St. Louis, Missouri, US), in a 50 ml tube with vented cap (Corning, Corning, New York, US). The tube was placed on a shaker set at 220-260 rpm in a humidified 5% CO_2 incubator set at 37^{o}C. After 16-18 hours, the optical density of the culture at 600 nm (OD_{600}) was measured using a BioPhotometer Plus spectrophotometer (Eppendorf, Hamburg, Germany) using supplemented BHI as blank. If an OD_{600} greater than 1 was observed (indicating stationary phase) the overnight culture was diluted 1:20 in fresh supplemented BHI and returned to the 37^{o}C with 5% CO_2 incubator and grown in the same manner as for the overnight culture until exponential. A growth curved was carried out with readings taken at 1 hour intervals to ensure collection of stock at mid-exponential phase. The culture intended for use as a stock was collected when an OD_{600} of approximately 0.7 was achieved. The bacterial suspension was mixed with 10% (v/v) glycerol (Sigma Aldrich, St. Louis, Missouri, US) (v/v), aliquoted in 500 µl aliquots and stored at -80^{o} C. To check the purity of the stock a sample of liquid was

streaked on a plate of chocolate agar. The plate was incubated overnight at 37^{o}C with 5% CO_2. The following day, the plate was visually inspected and if a single type of colonies were observed, the culture was considered pure.

2.17. Viable count of bacteria by the Miles Misra method

A vial of NTHi stock was retrieved from the -80^{o} C, thawed, washed 4 times in 1 ml BEBM medium by spinning at 6000 g for 4 minutes, then serially diluted in PBS and plated on chocolate agar in triplicate 10 µl spots per dilution. The following day, colonies were counted from the dilution where individual colonies could be clearly distinguished. The viable count was determined using the formula: colony forming units (CFU)/ml = average number of colonies x dilution factor x 100.

2.18. NTHi preparation for infection of epithelial cell cultures

On the day of the infection, a vial of NTHi was retrieved from the -80^{o} C freezer, thawed and washed 4 times in 1 ml BEBM by spinning at 6000 g for 4 minutes. The bacteria were re-suspended in BEBM, diluted to 2.5 x 10^7 CFU /ml and added to the epithelial culture in 200 µl/well. If NTHi was to be fluorescently labelled, the vial of NTHi was washed once in BEBM by spinning at 6000 g for 4 minutes, re-suspended in 1ml of BEBM and incubated with 3 µl of CFSE dye stain (Thermo Fisher Scientific, Waltham, Massachusetts, US) for 45 minutes at 37^{o} C, in the dark. The bacteria were then washed 3 times in BEBM and diluted at the required concentration in BEBM. In order to heat inactivate NTHi, the final concentration of bacteria required was incubated at 65^{o} C for 30 minutes and then streaked on a plate of chocolate agar to confirm inactivation, seen as a lack of bacterial growth.

2.19. NTHi infection of ALI cultured respiratory epithelial cells

The day before an NTHi infection, the basolateral medium of ALI epithelial cultures was replaced with 500 µl ALI media without antibiotics. To check the quality of the epithelial culture, 200 µl of ALI medium was added to the apical surface and trans-epithelial electrical resistance was measured as described in section 2.7, followed by ciliation level scoring as described in section 2.8. On the day of infection, the apical surface of the cells was washed again with 200 µl BEBM and the basolateral medium was replaced with fresh antibiotic free ALI medium. A vial of NTHi was retrieved and prepared as described in section 2.18. The final concentration of NTHi was added apically to each well in 200 µl of BEBM and the uninfected controls had 200 µl BEBM added apically as a mock. The plate was subsequently returned to 37º C and 5% CO_2, in a humidified environment. A viable count of the bacteria was performed to check the concentration of the inoculum.

2.20. Live confocal microscopy imaging

Epithelial cells were prepared for infection as previously described in section 2.19. On the day of the infection experiment, a fresh vial of NTHi was collected from -80º C and stained with green CFSE dye as described in section 2.18. During the staining time of NTHi, the ciliated epithelial cultures were washed once in BEBM and stained with 200 µl of 1.5X CellMask Deep Red Plasma membrane stain (Thermo Fisher Scientific, Waltham, Massachusetts, US) diluted in BEBM from the 1000X stock solution, and added apically, for 45 minutes, at 37º C, 5% CO_2. Epithelial cells were then washed apically 3 times in 200 µl of BEBM before addition of the bacteria. The transwells were placed

in glass dishes (WillCo Wells, Amsterdam, The Netherlands) with a custom made collar to adjust for the height of the transwell and in order to keep it fixed in place. Antibiotic free ALI medium was added to the bottom glass dish and the dish was sealed around with clear adhesive tape. The dishes were placed in a 37^{o} C incubation chamber on an inverted Zeiss LSM 710 confocal microscope stage and images were acquired using the Zen software (both Zeiss, Oberkochen, Germany). Live videos and Z-stacks were acquired using a x25 objective with a numerical aperture of 0.8 and water immersion. Excitation with 488 and 633nm lasers and detection of transmitted light (brightfield), green and far red fluorescence was performed as a single track experiment. Videos were recorded for either 100 or 1000 frames, and were subsequently converted to an .avi extension using the Imaris software, version 7.2 (Bitplane, Belfast, UK).

2.21. Scanning electron microscopy (SEM)

Following infection of ciliated cultures grown at the ALI with NTHi, the bacterial inoculum was removed and samples fixed in 2% (v/v) paraformaldehyde, 1.5% (v/v) glutaraldehyde (both Sigma Aldrich, St. Louis, Missouri, US) in PBS for 24 hours at 4^{o} C. Subsequently, the fixing agent was removed and samples transferred into PBS until further processing. Samples were then kindly processed by Mark Turmaine at the School of Pharmacy, UCL. Briefly, the samples were post fixed in 1% OsO_4/1.5% $K_4Fe(CN)_6$ in 0.1 M phosphate buffer, at 3°C for 45 minutes, washed in 0.1 M phosphate buffer followed by distilled water washing, and dehydrated in a graded ethanol-water series up to 100% ethanol. Dehydrated samples were then critical point dried using CO_2 and, using adhesive carbon tapes, mounted onto aluminium stubs where they

were coated with an approximately 7nm thick layer of Au using an Emitech coater (Emitech, Ashford, UK). Images were acquired using a FEI Quanta 200F FE SEM (FEI, Hillsboro, Oregon, US).

2.22. Image Cytometry

An aliquot of NTHi strain 1479 obtained from Dr. Simon Hall (GlaxoSmithKline, Stevenage) or of the in house NTHi strain 49247 was labelled with CFSE as described in section 2.18, then diluted to $2.5x10^7$ CFU/ml and added in 200µl of BEBM to the apical surface of in house nasal ciliated ALI cultures or bronchial epithelial cultures (Epithelix, Epithelix Sàrl, Genève, Switzerland) cultured at GlaxoSmithKline. At 24 hours post infection, the apical fluid and unattached bacteria were removed and the epithelial culture washed 3 times in BEBM. The epithelial cells were subsequently detached using StemPro Accutase Cell dissociation reagent and stained as described in section 2.9. The acquisition was performed using the ImageStream Mark II Imaging Flow Cytometer using the Inspire software and analysed using Ideas software (all Merck KGaA, Darmstadt, Germany). Dead cells were excluded based on size and complexity and by visually checking cells near the gate, rather than by using a dye.

2.23. Epithelial culture washing after NTHi infection

At the end of an NTHi infection of ALI cultured respiratory epithelial cell experiment, the apical fluid was removed by placing a pipette tip at the bottom of the transwell wall and collected for future analyses. Afterwards, the epithelial layer was gently washed 3 times with 200 µl of BEBM each by placing the tip of the pipette on the wall, at the top of the transwell, and pressing down the

pipette for 2-3 seconds. The fluid was immediately collected by moving the tip of the pipette on the opposite side of the transwell and placing it at the base of the wall, without tilting the transwell, and sucking out the liquid in approximately 2-3 seconds.

2.24. Intracellular invasion and adherence assay

The NTHi intracellular invasion and adherence assay was performed according to a method described previously (Clementi et al., 2014). Briefly, at the end of the experiment, the apical fluid was collected and the cells were washed as described before (section 2.23). The basolateral fluid was collected for future analysis and replaced with 500 µl BEBM or BEBM containing 50 µg/ml gentamicin (Gibco, Carlsbad, California, US). Then, 200 µl of BEBM or BEBM containing 50 µg/ml gentamicin were added to the apical surface and incubated for 2 hours at 37º C and 5% CO_2, in a humidified environment. The apical and basolateral fluids were then removed, cells washed 3 times with 200 µl of BEBM as before followed by addition of 180 µl of trypsin/EDTA to the apical chamber and 500 µl to the basolateral chamber. After a 10 minute incubation, the epithelial cells detached by trypsin/EDTA were collected and the enzyme was inactivated by mixing with of 10% (v/v) heat inactivated foetal calf serum (Sigma Aldrich, St. Louis, Missouri, US). Epithelial cells were pelleted by spinning at 6000 g for 3 minutes, the supernatant was removed and the pellet re-suspended in 200 µl of 0.8% (w/v) saponin (Sigma Aldrich, St. Louis, Missouri, US) diluted in PBS. The epithelial cells were incubated with saponin for 30 minutes at 37º C to break open the epithelial cell wall. Viable counts of bacteria in the stored apical fluid and the cell suspension were performed.

2.25. Inhibition of the PI3K signalling pathway

For studies investigating the role of the PI3 kinase pathway in epithelial invasion by NTHi, the basolateral medium of epithelial cultures was changed to 500 µl of antibiotic free medium 48 hours and again 24 hours prior to infection with NTHi. The commercial pan PI3K inhibitor LY-294002 hydrochloride (Sigma Aldrich, St. Louis, Missouri, US) was dissolved in DMSO to a stock concentration of 100mM, diluted 1:1000 in BEBM and 50 µl of this dilution was added to the basolateral medium, to a final concentration of 10 µM. The GSK987740A (GlaxoSmithKline, Stevenage, UK) Pan PI3K inhibitor was dissolved in DMSO to a stock concentration of 10mM, diluted 1:1000 in BEBM and 50 µl of this dilution was added to the basolateral medium, to a final concentration of 1 µM. Two control conditions were examined, an untreated control where 50 µl of fresh BEBM were added basolaterally and a vehicle control condition where 50 µl of a 1:1000 DMSO (compound solvent) in BEBM dilution was added basolaterally. One hour after the addition of inhibitors, cultures were challenged apically with 10 µl of BEBM or BEBM containing $5x10^6$ CFU /well of NTHi. The infection protocol was changed for Pi3K studies, as flooding of the epithelial cultures with 200 µl of BEBM resulted in strong activation of the PI3K pathway, as measured by the level of Akt phosphorylation (section 2.26) – See appendix 2. After 24 hours incubation, intracellular bacteria were quantified using the gentamicin killing assay, as described in section 2.24.

2.26. Quantification of Akt phosphorylation following NTHi infection of ciliated epithelial cultures

To quantify NTHi induced Akt phosphorylation (as a read-out of PI3K pathway activation, (Lopez-Gomez et al., 2012; Morey et al., 2011; Seiler et al., 2013) and confirm the inhibitory effect of the PI3K inhibitors, epithelial cultures were treated with LY294002 hydrochloride and GSK987740A as described in section 2.25 and 10 µl of BEBM or BEBM containing $5x10^6$ CFU / well of NTHi was added apically. To quantify phosphorylation of Akt at Serine 473 and Threonine 308, the Phospho (Ser473)/ Total Akt Whole Cell Lysate and Phospho-Akt (Thr308) Whole Cell Lysate kits (Meso Scale Discovery, Rockville, Maryland, US) were used. Briefly, at 2 hours or 24 hours post infection, the basolateral medium was removed and cultures were washed once apically with ice cold PBS. Fifty microliters of ice cold complete lysis buffer containing protease inhibitor and phosphatase inhibitors I and II were added apically to each well. The plates containing the epithelial cultures were then placed on ice for 45 minutes to ensure lysis had occurred. Cell lysates from 2 transwells per condition were pooled together and cellular debris were pelleted by spinning at 8000 g for 3 minutes. The supernatants were collected and frozen immediately on dry ice, followed by storage at -80 ^oC. The Akt assay was subsequently performed according to manufacturer's instructions, using 35µl of cell lysate/well and splitting the same cell lysate equally between the Serine 473 and Threonine 308 assays.

2.27. Rhinovirus culture and stock preparation

Rhinovirus serotype 16 (RV16) was a gift from Dr. Gary McLean (London Metropolitan University). RV16 is part of the RV A species, which is the predominant species associated with human disease, in both healthy individuals and patients with COPD (Choi et al., 2015; van der Linden et al., 2016). Furthermore, the genome of RV16 was sequenced and the serotype was identified as being more representative of human rhinoviruses than other experimentally used serotypes, such as RV2, RV39 or RV14 (Lee et al., 1995). While the epidemiology of RV in COPD is not well understood, human experimental infections using RV16 replicated the phenotype of virus induced disease exacerbations and promoted secondary bacterial infections, suggesting that it is an appropriate strain to use for studies in the mechanisms of COPD exacerbations (Mallia et al., 2012; Mallia et al., 2011).

RV16 was cultured and titrated for viral titre levels by Miss Simona Velkova. Briefly, Hela H1 cells, also gifted by Dr. Gary McLean, were grown to confluence in T175 flasks, in DMEM supplemented with 10% foetal calf serum (Sigma Aldrich, St. Louis, Missouri, US), 100 IU/ml penicillin and 100 µg/ml streptomycin. The Hela H1 cultures were washed twice in PBS and 5 ml of RV16 at a concentration of 1.35×10^7 tissue culture infectivity dose ($TCID_{50}$)/ml was added to the flask. The culture was supplemented with 7.5 ml of infection medium, prepared by mixing DMEM with 2% foetal calf serum, 100 IU/ml penicillin, 100 µg/ml streptomycin, 15mM HEPES and 15mM sodium bicarbonate (both Sigma Aldrich, St. Louis, Missouri, US). The flask was then incubated for 1h at room temperature with gentle shaking. Then, 12.5 ml of infection medium was added and the flask of cells was transferred to a

humidified 37^{O}C, 5% CO_2 incubator for up to 24 hours or until all cells had detached. The contents of the flask were subsequently frozen and thawed 3 times to ensure Hela cell lysis, after which the contents were spun down for 15 minutes at 3000 g and the supernatant filtered through a 0.2 µm filter (Sartorius, Gottingen, Germany). The resulting filtrate was concentrated using 100,000 MWCO Amicon Ultra-15 Centrifugal filter units (Merck Millipore, Burlington, Massachusetts, US) and followed by centrifugation at 4000 g for 30-60 minutes. The concentrated virus was precipitated by addition of 7% polyethylene glycol and 0.5M NaCl (both Sigma Aldrich, St. Louis, Missouri, US) and incubation on ice for 1 hour. The precipitated virus was pelleted by centrifugation at 4000 g for 1 hour at 4^{O}C, re-suspended in 15 ml of PBS, centrifuged again at 4000 g for 15 minutes and the supernatant filtered through a 0.2 µm filter. This filtrate was concentrated further using a 100,000 MWCO Amicon Ultra-15 Centrifugal filter unit to 0.5 ml of virus to which 2 ml of PBS were added to obtain 2.5 ml of purified RV16 stock, which was subsequently aliquoted and frozen at -80^{O}C.

2.28. Rhinovirus titration assay

Hela H1 cells were seeded into a flat bottom 96 well plate (Corning, New York, US) at 1.5 x 10^4 cells/well in 150 µl of infection medium. A 10 step 10-fold serial dilution of the RV16 stock was prepared in infection medium. Then, 50 µl of each dilution was added to 6 replicate wells of Hela H1 cells in the plate. Uninfected Hela H1 cells and medium alone were used as controls. The plate was incubated for 4 days at in a humidified incubator set 37^{o}C and 5% CO_2 after which wells presenting cytopathic effect at each dilution were scored. The

Spearman-Karber equation was used to calculate the virus titre (Puntener et al., 2011; Roulin et al., 2014).

2.29. Rhinovirus infection of primary epithelial cultures

Prior to infection with RV16, epithelial cultures were washed apically with 200 µl of BEBM and the basolateral ALI medium was exchanged with 500 µl of fresh ALI medium. Then, RV16 was added to the apical chamber at $1.5x10^6$ $TCID_{50}$/well in 100 µl of BEBM. An equivalent volume of BEBM only was used as mock. The culture was placed in a humidified incubator set at 37^OC with 5% CO_2. After 1 hour incubation the virus inoculum was removed and the cultures returned to the incubator.

2.30. Rhinovirus and NTHi co-infection of primary epithelial cultures

If the rhinovirus infection was followed by NTHi co-infection, then epithelial cultures were first fed basolaterally with antibiotic free ALI medium prior to RV16 infection. At 24h post RV16 infection, the apical surface was washed in 50 µl of BEBM. The basolateral medium was collected and replaced with 500 µl of fresh antibiotic free ALI medium. Subsequently, 200 µl of plain BEBM or BEBM containing $5x10^6$ CFU /well of NTHi was added apically and incubated for another 24 hours.

2.31. Incubation of NTHi with apical fluid from rhinovirus infected primary epithelial cultures

Following 48 hours of rhinovirus infection, 200 µl of apical fluid was collected from rhinovirus infected and control uninfected epithelial cultures. One hundred and fifty microliters of this apical fluid was then added to 50 µl of

BEBM containing $5x10^6$ CFU of NTHi, in a flat bottom 96 well plate (Corning, New York, US) and gently mixed by pipetting. Two control conditions were included: NTHi which was incubated with 150 µl of fresh BEBM only, or with BEBM containing $2.5x10^5$ TCID50/ml of RV16. The 96 well plate was placed in a humidified incubator set at 37^OC with 5% CO_2. After a 24 hour incubation and following vigorous resuspension, a viable count of NTHi was performed, as described in section 2.17.

2.32. Incubation of NTHi with iron and β-nicotinamide adenine dinucleotide in absence of epithelial cells

One hundred and eighty microliters of BEBM containing $5x10^6$ CFU / well of NTHi was added to wells of a flat bottom 96 well plate (Corning, New York, US). These were supplemented with 20 µl of BEBM, BEBM containing $Fe(NO_3)_3 9H_2O$ (Sigma Aldrich, St. Louis, Missouri, US) to a final concentration of 25 µM, BEBM containing β-NAD or hemin (both (Sigma Aldrich, St. Louis, Missouri, US) to a final concentration of 10 µg/ml, or BEBM containing $Fe(NO_3)_3 9H_2O$ and β-NAD or hemin and β-NAD. Bacteria were incubated with each of these supplements in a humidified incubator set at 37^OC with 5% CO_2. After a 24 hour incubation and following vigorous resuspension, a viable count of NTHi was performed, as described in section 2.17. This experiment was performed by the Masters student I supervised, Miss Anca Debora Balint.

2.33. Quantification of total iron in apical fluid from rhinovirus infected primary epithelial cultures

Following 48 hours of rhinovirus infection, 200 µl of apical fluid was collected from rhinovirus infected and control uninfected epithelial cultures and stored

frozen at -80^{o}C for subsequent analysis. To measure total iron release from epithelial cultures following rhinovirus infection, the QuantiChrom Iron Assay Kit (BioAssay Systems, Hayward, California, US) was used. The apical fluid was first centrifuged for 3 minutes at 2000 g to remove cellular debris. Fifty microliters of apical fluid were incubated with the working reagent and the assay performed following manufacturer's instructions. The colorimetric change was detected by measuring absorbance at 590nm using a Fluostar Optima plate reader (BMG LabTech, Ortenberg, Germany). When absorbance readings were analysed and converted to concentration values, the readings obtained from control BEBM/Promo Cell basal medium were used as blank, to account for the pink colour of the medium.

2.34. Quantification of nicotinamide adenine dinucleotide in apical fluid from rhinovirus infected primary epithelial cultures

Following 48 hours of rhinovirus infection, 200 µl of apical fluid was collected from rhinovirus infected and control uninfected epithelial cultures directly on dry ice and stored frozen at -80^{o}C for subsequent analysis. To measure the level of nicotinamide adenine dinucleotide (NAD) in this apical fluid, the NAD/NADH-Glo Assay (Promega, Madison, Wisconsin, US) was used. An NAD standard curve was generated as per manufacturer's instructions, using β-nicotinamide adenine dinucleotide (Sigma Aldrich, St. Louis, Missouri, US). Fifty microliters of apical fluid were used per assay and the assay performed according to manufacturer's instructions. The chemo-luminescence was detected using a Fluostar Optima plate reader (BMG LabTech, Ortenberg, Germany).

2.35. Statistical analysis

Statistical analysis support was provided by statisticians Dr. Mark Lennon and Dr. Tanja Hoegg (GSK) and an overall report of the statistical methods used for analysis of data presented in this thesis is included below. Detailed analysis of data presented in each figure is included in **Appendix 1**.

For experiments with more than two experimental conditions (e.g treatment levels, infection conditions, disease groups or time points), data were pooled across conditions and analysed jointly using linear modelling techniques. Separate analyses were run for different end-points or analytes. A modelling approach is preferable to a series of individual analyses (e.g. using t-tests) as it provides a more precise estimate of the variability in measurements, thereby increasing statistical power.

In most experiments, epithelial cells from each donor were exposed to all experimental conditions. Linear mixed effects models were applied in these contexts to account for dependence between measurements taken from cells of the same donor. For these models, experiment specific fixed effects were included for the different experimental conditions such as: disease groups (healthy/COPD), day (day 7/day 28), infection condition (Control, RV, NTHi, RV& NTHi), treatment (untreated/ PI3K inhibitors). In addition to fixed effects for the experimental conditions, these models included random effects for each donor to allow for donor-specific deviations from the means of the experimental conditions. In contrast to fixed effects, random effects were not estimated as part of the model fitting. Instead, it was assumed that random effects are generated from a mean-zero normal distribution. The standard deviation of this

distribution is a measure of between-donor variability and was estimated in place of the donor-specific deviations from the mean. Similarly, dependence between measurements may also be introduced by technical replication, therefore, for experiments where multiple wells were sampled for the same condition, an additional random effect for each well was included in the model. This approach is an alternative to averaging over technical replicates and can be appropriate when the number of technical replicates vary across samples. For most endpoints, measurements required a log10 transformation prior to model fitting to stabilize the variance and to ensure that the variability of measurements was of comparable size amongst all experimental conditions. Where this log10 transformation was performed, it is indicated in the figure legend.

The statistical significance of changes in the endpoints was assessed by hypothesis testing. For all tests, the null hypothesis is that there is no change in the endpoint; the alternative hypothesis is that there is a change. In experiments involving a large number of comparisons, p-values were adjusted for to account for multiple comparisons using the Benjamini-Hochberg (BH) method to reduce the chance of obtaining false positive findings (Benjamini and Hochberg, 1995). The method controls the false discovery rate per experiment, meaning that if p-values below 5% are considered statistically significant, 5% of findings are expected to be false.

All analyses were conducted using the statistical programming language R, Version 3.5.1.

Chapter 3: Results

3.1. Characterising ALI cultured primary epithelial cells from healthy and COPD donors

3.1.1. Introduction

Air-liquid interface (ALI) cultures of the human airway epithelium are arguably the gold standard in respiratory research, as they allow for investigation of most of the essential functions of the respiratory epithelium, including its cellular composition and morphology, barrier function, ion and fluid transport, innate immunity, infection and inflammation, cell signalling, ciliary function, regeneration and repair, in health or respiratory diseases (Butler et al., 2016; Comstock et al., 2011; Ghosh et al., 2018; Hirst et al., 2014; Jong et al., 1994; Pezzulo et al., 2011; Tan et al., 2018). ALI cultured primary human airway epithelial cells differentiate over 4 weeks to form a pseudostratified, polarised layer which recapitulates the structure of the human airway epithelium (Butler et al., 2016; Gray et al., 1996; Jong et al., 1994). This layer consists of basal, ciliated and secretory cells with apical presentation of microvilli (Butler et al., 2016; Gray et al., 1996; Jong et al., 1994).Transcriptional profiling of whole epithelium and a recent single cell RNA sequencing study which compared ALI cultured epithelia to *ex vivo* donor epithelia have further validated the resemblance of ALI cultured epithelium to the human respiratory epithelium in terms of cellular composition and signalling pathways (Pezzulo et al., 2011; Ruiz Garcia et al., 2018). Similar to the human airway epithelium, secretory cells found in ALI cultured epithelia produce mucins such as MUC5AC and MUC5B (Butler et al., 2016; Ross et al., 2007). Cultured ciliated cells present with motile cilia beating at an average of 10-16 Hz, which, together with the mucus and periciliary fluid, reproduce the process of mucociliary clearance

(Butler et al., 2016). The cystic fibrosis transmembrane conductance regulator (CFTR) and the epithelial sodium channel (ENaC) are both expressed and functional in ALI cultured airway epithelial cells, therefore allowing for regulation of airway surface fluid hydration and for studies investigating their function in health and disease (Brewington et al., 2018; Tipirneni et al., 2017). Furthermore, polarised airway epithelial cultures form an epithelial barrier with expression of junction proteins and are capable to respond to insult or infection by production of inflammatory cytokines and chemokines and expression of antimicrobial peptides (Baddal et al., 2015; Comstock et al., 2011; Jong et al., 1994; Ong et al., 2016; Tan et al., 2018).

ALI cultured airway epithelial cells have also been extensively used for the study of respiratory diseases, including COPD (Hirst et al., 2014; Jing et al., 2019; Staudt et al., 2014). They have contributed to our understanding of COPD mechanisms and changes that occur in the epithelium as a result of the prolonged exposure to cigarette smoke and other noxious particles which ultimately lead to airway pathology (Barnes et al., 2003). The changes that occur in the COPD epithelium have been described in Sections 1.8 to 1.10. Of interest here is that differentiation of epithelial cells from patients with COPD at the ALI has led to the generation of cultures with increased numbers of basal cells and goblet cells and over 80% fewer ciliated cells compared to differentiated epithelial cultures from healthy donors (Ghosh et al., 2018). These findings match observations from *ex vivo* studies analysing the epithelium of smokers which identified basal cell hyperplasia, accumulation of mucus and regions with loss of ciliation in samples from smokers (Auerbach et al., 1979; Auerbach et al., 1961; 1962; Kim et al., 2015; Lungarella et al.,

1983). In addition, COPD epithelia immuno-stained for two junctional proteins, namely occludin and tight junction protein 1, displayed abnormal organisation of cell-cell junctions when compared to samples from healthy volunteers (Heijink et al., 2014). This was identified in lung sections from COPD patients and in same donor epithelial cultures differentiated at ALI, thus suggesting a reduced epithelial barrier function in COPD (Heijink et al., 2014). More importantly, these findings suggest that basal cells obtained from COPD donors retain their disease phenotype when differentiated *in vitro* at the ALI.

Mucociliary clearance is believed to be impaired in the airways of COPD donors as a consequence of the increased mucus production and the reduced airway ciliation, as described previously in section 1.10. However, whether ciliary function is actually impaired in COPD airways is still unclear, with 3 studies that used nasal epithelial cells providing contradictory results, including no difference in the mean ciliary beat frequency of smokers versus non-smokers reported by Stanley et al. (1986). Yaghi et al. (2012) reported there was a significantly reduced ciliary beat frequency in moderate and severe COPD compared to control subjects, in contrast to a study by Zhou et al. (2009) who reported an increase in ciliary beat frequency in smokers compared to non-smokers. Previously, it has been shown that while ciliary beat frequency can be maintained, ciliary function can be affected by ciliary dyskinesia as a result of infection or epithelial disruption (Chilvers et al., 2001; Smith et al., 2014; Thomas et al., 2009). However, no study to date has investigated whether progression to COPD affects ciliary beat amplitude, which is another measure of ciliary function.

Another important feature of COPD is the presence of airway inflammation (Barnes, 2016). This pro-inflammatory environment is created by exposure to cigarette smoke, by increased presence of immune cells, particularly neutrophils and CD8+ T cells, as well as bacterial colonisation which collectively lead to a vicious circle of epithelial damage and continuously amplifying inflammation, as described in section 1.12. Previously, it has been reported that primary bronchial epithelial cells from COPD patients constitutively release more pro-inflammatory cytokines and chemokines such as IL-6, IL-8, GRo-α or MCP-1 compared to epithelial cultures from healthy volunteers, including when cultured at the ALI (de Boer et al., 2000; Ganesan et al., 2013; Schneider et al., 2010). Therefore, the airway epithelium in COPD is thought to be repeatedly damaged and continuously regenerating to repair the injuries inflicted by the numerous insults (Crystal, 2014b). However, there is very little understanding of how a regenerating epithelium responds to insults such as viral or bacterial infections which are often causes of disease exacerbations in COPD patients (Wilkinson et al., 2017).

Hypothesis:

Differentiation and baseline characteristics of COPD epithelial cultures grown at ALI are different from those of healthy cultures.

Aims:

- To establish a quality control protocol for epithelial cultures before use for experiments.
- To compare the differentiation of healthy and COPD epithelial cultures at the air liquid interface.
- To identify when ciliation begins in healthy and COPD cultures.
- To compare baseline ciliary function and inflammation in healthy and COPD epithelial cultures.

3.1.2. Clinical details of COPD patients and healthy volunteers who donated airway epithelial cells used in this project

Nasal epithelial cells were collected from 17 adult healthy donors and 12 patients with COPD by nasal brushing (section 2.2), following informed consent (section 2). The clinical characteristics of subjects are shown in Table 5. In a limited number of experiments, bronchial epithelial cells were used. These were collected from the same donors as nasal epithelial cells and therefore their characteristics are included in Table 5. Quantitative measurements reported in figures are exclusively from experiments using nasal epithelial cells whereas results obtained from studies using bronchial epithelial cells are only reported in text and not included in graphs.

Table 5. Clinical details of subjects who donated airway epithelial cells used for studies presented in this thesis

	Healthy	COPD
Number of donors	17	12
Male/Female	5/12	7/5
Age	54.5 (±10.7)	71.6 (±7)
FEV1	-	1.47 (±0.7)
FEV1 % predicted	-	45.8 (±15.7)
FVC	-	2.73 (±1)
FVC % predicted	-	78 (±20.5)
FEV1/FVC	-	0.53 (±0.12)
Current smokers	0	4
Number of donors with >2 exacerbations in previous year	0	11
Number of donors with other conditions (asthma/ hay fever/ allergies)	0/2/1	2/0/0

Abbreviations: FEV1, forced expiratory volume in 1 second; FVC, forced vital capacity; values presented as mean (± standard deviation).

3.1.3. Quality control assessment of nasal ciliated cultures from healthy and COPD subjects: ciliation level scoring and epithelial integrity measurement

Collection of primary epithelial cells by nasal or bronchial brushing from healthy volunteers and patients with COPD yielded a limited number of epithelial cells, approximately in the range of 1000- 50.0000 cells/ brushing. Therefore, epithelial cells thus obtained were cultured with mitotically

inactivated mouse embryonic fibroblasts to expand their numbers, following the method published by (Butler et al., 2016) and as described in section 2.4. This co-culture method produced an increased output of basal cells enabling use of cells from one donor for multiple experiments. Basal cells were subsequently cultured at an air—liquid interface to a ciliated phenotype (section 2.6). Due to observed inter- and intra-donor variability between differentiated epithelial cultures and to ensure that both healthy and COPD cultures were well differentiated prior to use for experiments, a quality control stage was implemented. This stage involved ciliation level scoring (section 2.8) and measurement of trans-epithelial electrical resistance (TEER) (section 2.7). Using high speed video microscopy for visual inspection, a ciliation score was developed to grade cultures from absence of any cilia to cilia covering the entire epithelial surface, as shown in Table 6. This improved the phenotyping of cultures during differentiation and prior to experiments. On the day before an experiment, the level of ciliation was documented and TEER measurement was performed and recorded. For certain experiments, the same culture batches were used for experiments at day 7 of epithelial differentiation and when cultures were fully differentiated at day 28. If at day 28 of differentiation the same culture batch did not differentiate properly and the quality control assessment revealed improper ciliation or reduced TEER, data obtained at day 7 for that donor was not used and the experiment at day 28 was not carried out.

Table 6. Scoring system for grading ciliation level and determining epithelial integrity in air-liquid interface epithelial cultures

Score	Description									
0	No moving cilia observed.									
1	A few individual ciliated cells scattered around the transwell (1-20 ciliated cells/well).									
2	Several ciliated cells in small groups but not forming extensive patches.									
3	Extensive patches of cilia (usually around edges). Cilia are usually absent in the centre of the transwell.									
4	A lawn of cilia all around the edges of the transwell. Cilia usually sparse in the middle of the transwell.									
5	Fully ciliated on edges and in the middle. A continuous lawn of cilia covering the entire surface of the transwell.									
Well number	I	II	III	IV	V	VI	VII	VIII	IX	X
Ciliation Score										
TEER reading										

Cultures with a ciliation level below 1 were not used for experiments, due to their suboptimal differentiation. The average score for healthy ciliated cultures was 3.3 (min 1.8-max 5) whereas for COPD cultures it was 2.9 (min 1- max 4.5) – Figure 5A. There was no statistically significant difference between the two groups in terms of ciliation (p=0.399), however a trend was observed of lower ciliation levels in COPD cultures, with an average scoring for COPD cultures being 0.4 units lower than that of healthy cultures. On average, the

intra-donor well to well variability in scoring, expressed as standard deviation of scores within donors, was estimated to be 0.232, confirming that wells used for experiments were similar in their ciliation level. Furthermore, an assessor bias test was carried out twice, blinded, with 2 other assessors and it confirmed agreement between scores awarded to different cultures. In the first instance, 9 wells from one donor were scored by myself and another assessor, with average scores awarded being 3.25(±0.41) for my own scoring and 3.685 (±0.47) for the other assessor. Upon comparing scores awarded, Cohen's Kappa for assessor agreement was 0.184, indicative of an agreement that while only slight, is better than by chance alone (ie. greater than 0). In the second test, 1 well each from 8 different donors was scored by myself and awarded an average score of 3.375 (±0.39) and a different assessor who awarded an average score of 3.625 (±0.31). In this case Cohen's Kappa was 0.304, suggestive of a fair agreement between assessors and again better than would have been expected from chance alone, thus suggesting no significant bias in individual scoring.

To confirm the integrity of the epithelial layer prior to use in experiments, the TEER of differentiated cultures was measured. Healthy epithelial cultures had an average TEER of 596 Ωxcm^2 (±284.2 Ωxcm^2), which was not significantly different (p=0.607) from that of COPD cultures - 654 Ωxcm^2 (±250.3 Ωxcm^2). - Figure 5B. The intra-donor well to well variability, across all donors measured, expressed as the standard deviation of TEER values within donors, was estimated as 152 Ωxcm^2, indicating that TEER was consistent between cultures of the same donor and the same culture batch. Cultures with a TEER

below 200 Ωxcm^2 were not used for experiments, as they were considered too low to reflect good barrier formation (Butler et al., 2016).

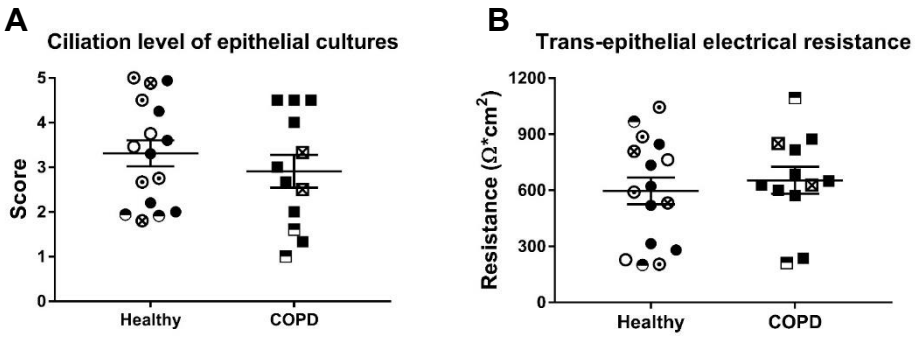

Figure 5. Ciliation scoring and TEER measurements of differentiated epithelial cultures

A. Differentiated nasal epithelial cultures were scored for their level of ciliation using high speed video microscopy prior to use for experiments (section 2.8). B. Epithelial integrity was assessed by measuring trans-epithelial electrical resistance (TEER) (section 2.7). Ciliation scoring and TEER measurements were carried out on 16 healthy cultures from 10 donors and 12 COPD cultures from 10 donors, by averaging measurements from a minimum of 4 wells/ donor. Where donor cells were cultured more than once, they were identified by the same symbol. Filled black symbol identifies a unique donor. Linear mixed effects models with a fixed effect for disease group (healthy/ COPD) and an experiment-specific random effect for each donor were used to compare ciliation levels and TEER values between healthy and COPD. Data are presented as mean ± standard error of the mean.

3.1.4. Characterisation of epithelial cultures from healthy donors and COPD patients during differentiation at ALI

To understand if COPD nasal epithelia differentiate in the same manner as healthy epithelia when grown in an ALI culture and to determine when ciliation begins, nasal epithelial cultures were analysed at 4 time points during the 28 days of differentiation. A flow cytometry characterisation method (section 2.9) was used to quantify the proportion of basal and ciliated cells in ALI epithelial cultures. In this analysis method, shown in Figure 6, live and then single cells were isolated and from these, basal cells were identified based on expression of CD271 (nerve growth factor receptor) and CD49f (integrin α6), (based on the method previously described by Rock et al., 2011, who identified CD271 and CD49f as cell surface markers of human basal cells). From the remaining, non-basal cells (CD271- CD49f- cells), ciliated cells were identified based on high expression of CD133 (or prominin 1) (GSK unpublished results) and lack of expression of CD66a/c/e. Two other distinct populations could be identified, namely CD133+CD66+ cells and CD133-CD66+ cells, which are likely to represent secretory progenitor cells and goblet cells, respectively (Ruiz Garcia et al., 2018). However, as the functional identity of each of these two populations remains unclear, as well as whether they represent homogenous populations containing a single cell type, they were excluded from further quantification and analysis.

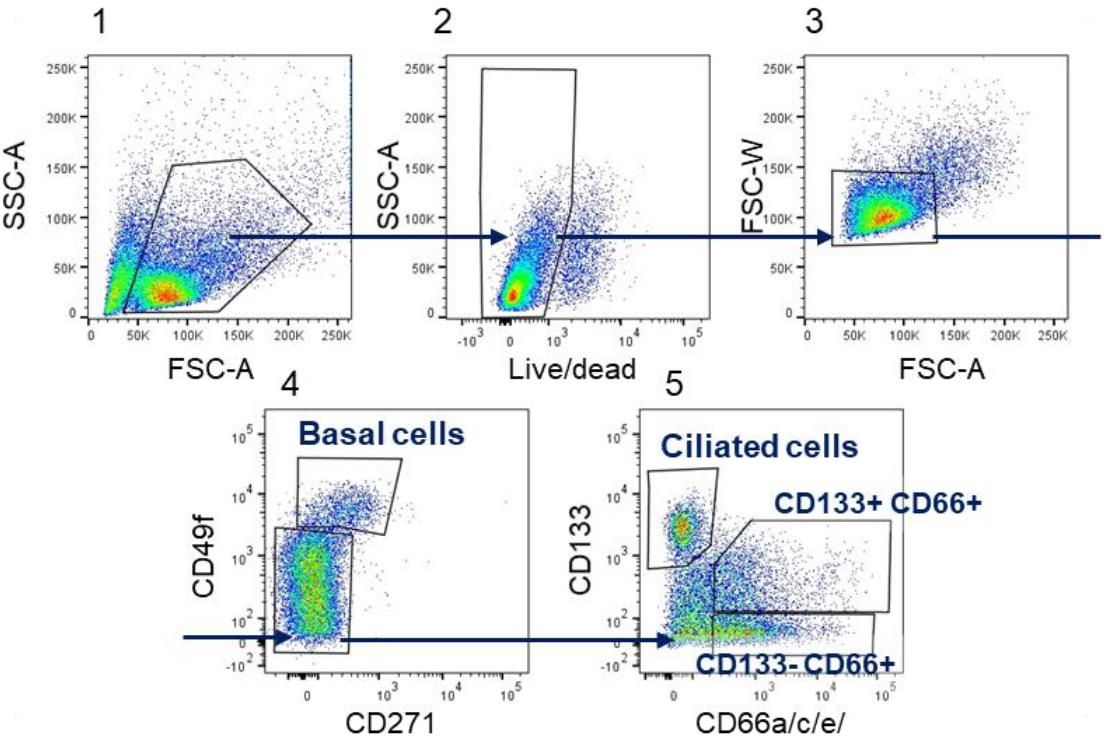

Figure 6. Representative gating strategy for characterisation of primary epithelial cultures by flow cytometry

Nasal epithelial cells cultured at ALI were analysed by multicolour flow cytometry (section 2.9) **1.** Cells were separated from debris. **2.** Live cells were separated from dead cells based on their lack of incorporation of the live/dead staining reagent. **3.** Single cells were separated from cell aggregates and clumps. **4.** Basal cells were separated from non-basal cells based on expression of CD271 and CD49f. **5.** From the CD271-CD49f- cells, ciliated cells were identified as CD133+CD66-. Two other distinct populations can be identified, namely CD133+CD66+ and CD133-CD66+.

Using this flow cytometry method, 6 healthy and 6 COPD cultures were analysed at day 0 (day when epithelial cultures are exposed to air apically), 7, 14 and 28 of differentiation. Epithelial cells were detached from 2 transwells per donor per time-point and the number of cells in suspension counted. The number and proportion of basal and ciliated cells were quantified at each stage out of the total number of live, single cells analysed, as shown in Figure 7A. The total number of cells counted per well was then used to extrapolate the number of each cell type per well from the number of events analysed.

This analysis revealed no significant change in the absolute number of basal cells during the differentiation period of healthy or COPD cultures (Figure 7B). However, in healthy epithelia there was strong evidence suggesting a decrease in the proportion of basal cells in culture at day 14 compared to day 0 ($p=0.058$) (Figure 7D). This decrease was significant at day 28 when compared to the percentage of basal cells at day 0 ($p=0.001$) and day 7 ($p=0.005$). This trend was not seen in COPD cultures, suggesting an altered differentiation pattern compared to healthy cultures. However, there was no significant difference in the number or proportion of basal cells between healthy and COPD epithelia at any time point.

The number and proportion of ciliated cells in healthy cultures (Figure 7 C & E) gradually increased as cells differentiated, with a small but significant increase in ciliation detected as early as day 7 compared to day 0 (comparison of numbers, $p=0.0002$, comparison of percentages $p=0.01$).

As expected, the number of ciliated cells was significantly higher at days 14 and 28 compared to the early stages of differentiation at day 0 and day 7

($p<0.0001$ for all comparisons). The proportion of ciliated cells followed a similar pattern as the number of ciliated cells, with the percentage increasing with differentiation. As such, the proportion of ciliated cells was significantly higher at days 14 and 28 compared to day 0 and day 7 ($p<0.0001$ for all comparisons). Interestingly, neither the number nor the proportion of ciliated cells increased significantly from day 14 to day 28 ($p>0.05$).

In COPD cultures, the number of ciliated cells was also significantly increased at days 14 and 28 compared to day 0 ($p<0.0001$) and day 7 ($p<0.001$ for all comparisons). Similarly, the proportion of ciliated cells was significantly increased at days 14 and 28 compared to day 0 and day 7 ($p<0.001$ for all comparisons). In contrast to healthy cultures, there was no significant increase in the number or proportion of ciliated cells in the early stages of differentiation- days 0 to 7. However, there was a significant increase in ciliated cell numbers from day 14 to day 28 ($p=0.012$), and strong evidence for an increase in ciliated cell proportion at the same time ($p=0.058$). Furthermore, there was strong evidence indicating a lower number of ciliated cells in COPD cultures compared to healthy cultures at day 14 of differentiation ($p=0.056$). At day 28, the average number of ciliated cells/ well was 2.3 times greater in healthy cultures than in COPD, but statistically this was not significantly different.

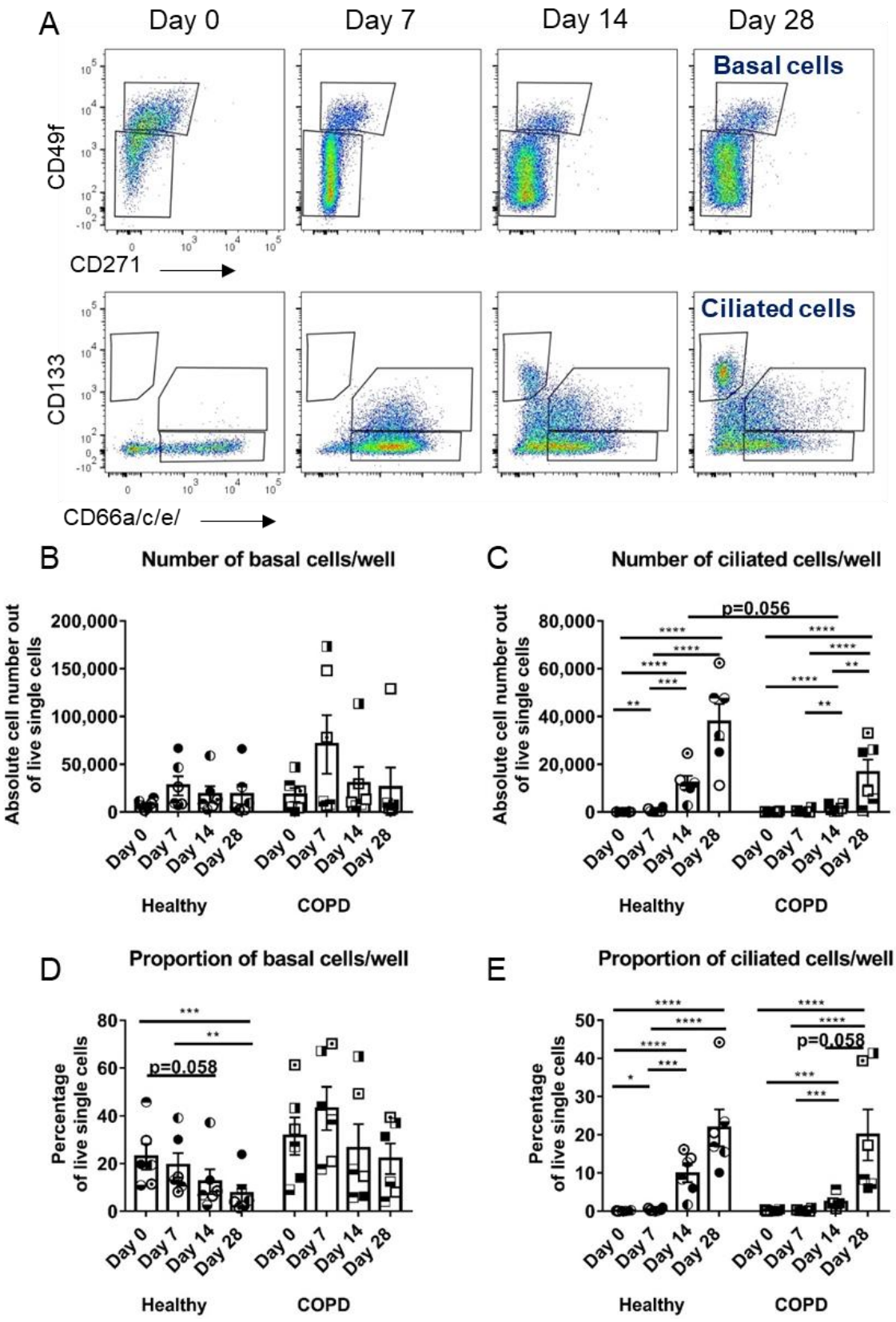
A
Day 0
Day 7
Day 14
Day 28
Basal cells
CD49f
CD271
Ciliated cells
CD133
CD66a/c/e/
B
Number of basal cells/well
Absolute cell number out of live single cells
200,000
150,000
100,000
50,000
0
Day 0
Day 7
Day 14
Day 28
Healthy
COPD
C
Number of ciliated cells/well
p=0.056
80,000
60,000
40,000
20,000
D
Proportion of basal cells/well
Percentage of live single cells
p=0.058
E
Proportion of ciliated cells/well
p=0.058

Figure 7. Quantification of basal and ciliated cells in epithelial cultures during differentiation at air-liquid interface

A. Representative plots of flow cytometric analysis of epithelial cultures at days 0, 7, 14 and 28 of differentiation of a healthy culture. Note the appearance of a ciliated cell population only after day 7. B&C Absolute number of basal and ciliated cells, respectively, calculated out of live single cells using flow cytometry analysis. D&E. Proportion of basal and ciliated cells, respectively, out of live, single cells. N= 6 healthy and 6 COPD donors. For statistical analysis, cell numbers and percentages were log10 transformed and analysed separately using linear mixed effects models with Benjamini-Hochberg adjustment for multiple comparisons. Data are presented as mean ± standard error of the mean. *=p<0.05, **=p<0.01, ***=p<0.001, ****=p<0.0001

In addition to flow cytometry, cultures were inspected by high-speed video microscopy and immuno-fluorescence staining to confirm appearance of cilia and mucus. To further investigate whether mucus and fully formed cilia are present at day 7 of epithelial differentiation and confirm differentiation at day 28, epithelial cultures were immuno-stained for mucin MUC5AC and β-tubulin for cilia and imaged by confocal microscopy (section 2.10). Indeed, as shown in Figure 8, fully extended cilia were not observed in cultures stained at day 7 although mucus secreting cells, identified by presence of the mucin MUC5AC were observed at this stage (Figure 8A). In one healthy donor, β-tubulin clusters could be observed, possibly indicating microtubule organisation prior to ciliogenesis. This aligned with observations made on the high speed video microscope, where mucus secretion started to be observed around day 7, but motile cilia could not be observed. As expected, at day 28 ciliated and mucus secreting cells were present in both healthy and COPD cultures, reflecting a differentiated epithelial layer (Figure 8B).

Goblet cell hyperplasia and mucus secretion are features of the COPD epithelium that have been reported in previous studies (Fahy and Dickey, 2010; Innes et al., 2006; Kim et al., 2015). In the absence of cell surface goblet cells markers that can selectively identify and quantify this population of cells from the other cell types in the epithelium, qRT-PCR was used to compare gene expression of the goblet cell specific mucins *MUC5AC* and *MUC5B* as well as expression of the transcription factor that regulates goblet cell differentiation, *SPDEF*, in healthy and COPD differentiated epithelial cultures (Park et al., 2007), as described in 2.11. As it can be seen in Figure 9., there was no significant difference in the expression levels of these 3 genes between healthy and COPD ($p>0.05$), suggesting there was no differential gene expression pattern of goblet cell associated genes in differentiated COPD nasal epithelia compared to healthy epithelia.

In conclusion the data described so far point towards an altered epithelial differentiation process in COPD cultures compared to healthy, with a sustained proportion of basal cell in the COPD epithelium which is not reduced like in healthy cultures and a delayed and reduced level of ciliation in COPD cultures compared to healthy. These results also identify day 7 of epithelial differentiation as a stage where mucus secreting cells are already present but which precedes the appearance of motile cilia. This could be considered representative for a regenerating epithelium and future studies in this project looked to compare responses to infection challenges of day 7 epithelial cultures to those of fully differentiated, day 28 ciliated cultures from healthy and COPD donors.

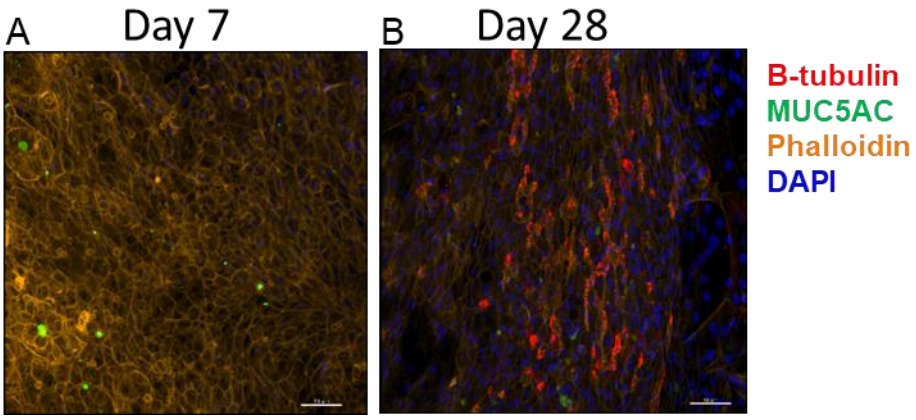

Figure 8. Immuno-fluorescence staining of mucus and cilia in respiratory epithelial cultures at day 7 and day 28 of differentiation

Confocal microscopy images of a healthy culture stained at day 7 (A) and day 28 (B) of differentiation. Cultures were stained for cilia β-tubulin (red), mucin MUC5AC (green), and f-actin using phalloidin (orange) and nuclei were stained with DAPI (blue). Images representative for 2 healthy donors and 2 COPD donors. Scale bar represents 50µm.

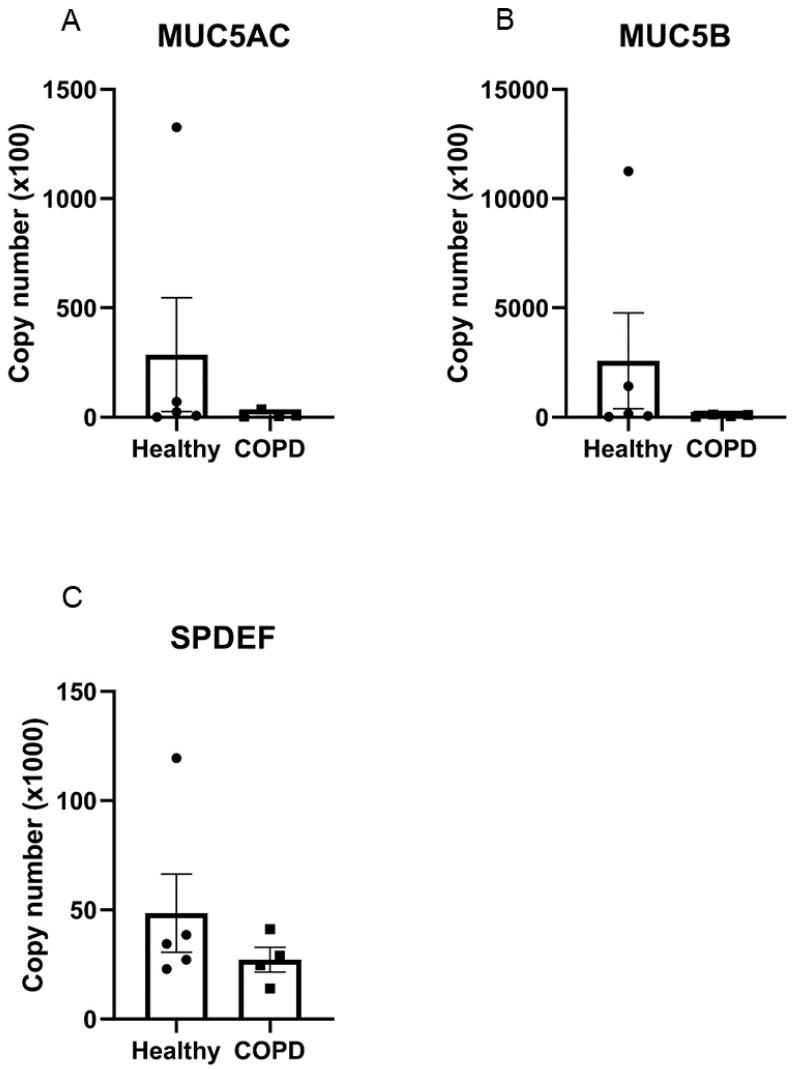

Figure 9. Expression of goblet cell specific genes by differentiated epithelial cultures

Expression of the genes encoding for the goblet cell specific mucins (A) MUC5AC and (B) MUC5B and of the transcription factor (C) SPDEF was quantified by qRT-PCR in fully differentiated (day 28) ALI cultured epithelial cells from healthy and COPD donors at baseline, as described in section 2.11. Two wells per donors were pooled together. N= 5 healthy, 4 COPD donors. Dots represent individual donors. For each analyte, separate linear mixed effects models were fitted, with a fixed effect for disease group (healthy/COPD). Data are shown as mean ± standard error or the mean.

3.1.5. Ciliary function assessment of healthy and COPD epithelial cultures

To assess ciliary function, including ciliary beat frequency and ciliary amplitude, healthy and COPD epithelial cultures were imaged using high-speed video microscopy (sections 2.13 and 2.14,). Ciliary beat frequency was determined from cultures kept at the ALI. Figure 10 shows that there was no significant difference in the average frequency of ciliary beating between healthy and COPD cultures ($p=0.33$). Ciliary amplitude was determined from control wells of infection experiments, where cultures had been submerged in BEBM for 24 hours. Again, ciliary amplitude of COPD cultures was similar to that of healthy cultures ($p=0.54$). These results suggest that these parameters of ciliary function are similar in the ALI cultured nasal ciliated cells of healthy volunteers and COPD patients.

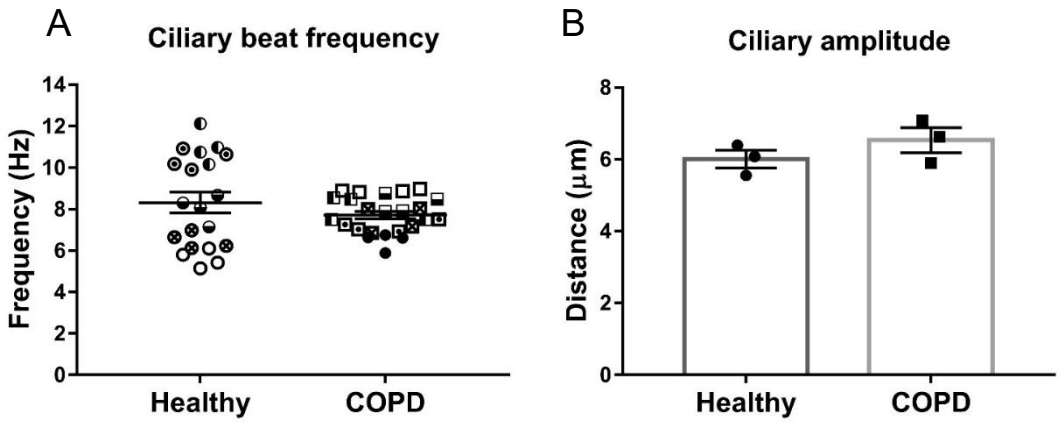

Figure 10. Ciliary function assessment in healthy and COPD epithelial cultures

Ciliary function measurements – ciliary beat frequency and amplitude- were determined from high speed video microscopy recordings of differentiated epithelial cultures. A. Cilia beat frequency was determined from 4 wells per donor prior to use for experiments. Wells from the same donor were labelled with the same symbol. N= 5 healthy donors and 6 COPD donors. B. Cilia amplitude was determined from at least ten amplitude measurements per donor, from control wells of infection experiments. Cultures were flooded with basal medium for 24 hours prior to video recordings. N=3 healthy and 3 COPD donors. For statistical analysis, ciliary beat frequency and amplitude values were log10 transformed and analysed separately using linear mixed effects models, with a fixed effect for disease group (healthy/COPD) and a random effect for each donor. Data are presented as mean ± standard error of the mean.

3.1.6. Inflammatory mediator production by primary epithelial cells from healthy donors and COPD patients at baseline

To further characterise nasal epithelial cultures from healthy donors and COPD patients, baseline levels of pro-inflammatory mediators were quantified as described in section 2.15. The selection of pro-inflammatory mediators analysed was based on a data set of gene expression changes from screening

infection experiments carried out at GSK. As shown in section 3.1.4, ciliation only appeared after day 7 of epithelial differentiation and cultures at this stage were considered representative for a regenerating epithelium, so level of cytokines and chemokines were measured in culture supernatants from cultures differentiated at the ALI for 7 days and for 28 days, when they were completely differentiated (Table 7). In healthy donors, culture supernatants showed no significant differences in levels of the cytokines and chemokines measured between day 7 and day 28. Similarly, in COPD cultures, the levels of cytokines and chemokines were not different between day 7 and day 28, with the exception of IL-8. There was significantly more IL-8 produced by COPD ciliated cultures (3.9 ±1.5 ng/ml) compared to day 7, pre-ciliation cultures (2.5 ± 1.8 ng/ml, p= 0.025), an increase not seen in supernatants from healthy cultures. However, there was no statistically significant difference between levels of cytokines or chemokines secreted by healthy and COPD cultures at either day 7 or day 28.

Table 7. Baseline cytokine and chemokine production by healthy and COPD epithelial cultures at a pre-ciliation (day 7) and fully differentiated (day 28) stage

Basolateral supernatants incubated with epithelial cultures for 24 hours were collected and cytokines and chemokines were quantified at day 7 and day 28, of epithelial differentiation. N= 7 healthy and 8 COPD donors. Cytokines and chemokines values were log10 transformed and analysed individually using linear mixed effects models with a fixed effect for disease group (healthy/COPD) and day (7/28) and a random effect for each donor. SD, standard deviation

	Day 7					**Day 28**					**Day 7 vs Day 28**	
Analyte	**Healthy**		**COPD**		**p value**	**Healthy**		**COPD**		**p value**	**Healthy**	**COPD**
	Mean (pg/ml)	SD	Mean (pg/ml)	SD		Mean (pg/ml)	SD	Mean (pg/ml)	SD		**p value**	**p value**
IL-1β	14.2	13.2	7.4	4.0	0.458	7.9	3.8	10.9	4.0	0.188	0.296	0.060
IL-6	44.2	104.6	16.8	20.9	0.843	30.3	42.2	27.3	32.5	0.892	0.188	0.206
TNF-α	11.6	9.4	7.5	4.5	0.333	8.1	3.4	4.4	2.2	0.095	0.548	0.106
IL-17	93.0	185.0	29.8	40.5	0.904	88.4	95.5	96.5	85.4	0.971	0.223	0.125
IFN-λ	0.4	0.6	1.7	1.2	0.974	1.1	0.9	1.4	0.3	0.895	0.974	0.997
IP-10	17.6	9.8	13.9	9.9	0.701	15.3	5.4	5.4	3.7	0.853	0.888	0.844
RANTES	6.4	3.0	6.0	2.2	0.983	5.9	1.3	7.0	2.5	0.865	0.983	0.828
TARC	1.9	0.9	1.7	0.4	0.970	2.0	1.6	2.5	1.6	0.921	0.965	0.876
IL-8	5197.7	4937.7	**2454.8**	**1755.5**	0.442	2870.6	1191.5	**3852.7**	**1531.5**	0.355	0.664	**0.025**
MCP-1	62.1	79.7	45.0	26.5	0.991	120.0	97.6	151.4	68.3	0.991	0.086	0.086
ENA-78	45.5	69.0	28.8	47.5	0.758	43.9	28.7	41.5	24.1	0.994	0.543	0.269

MIP-3α	193.9	114.5	146.5	83.3	0.936	175.7	42.4	157.5	51.0	0.936	0.936	0.958
G-CSF	111.8	54.3	99.5	48.1	0.855	111.7	38.6	106.6	44.1	0.923	0.998	0.893
Gro-α	1331.4	616.7	1066.3	823.7	0.968	1212.4	439.8	1153.9	494.1	0.989	0.989	0.989

3.1.7. Discussion

To study the effect of NTHi and RV on the airway epithelium, primary airway epithelial cells collected from healthy donors and COPD patients by nasal brushings were expanded by co-culture with mitotically inactivated mouse embryonic fibroblasts, as previously described by Butler et al. (2016). This method was preferred to the conventional BEGM culture as it has been shown to provide a higher output of basal cells and allow for extended passaging without loss of differentiation potential (Butler et al., 2016). In contrast, basal cells cultured by the conventional BEGM method lose their differentiation potential after passage 2, therefore limiting the number of experiments that can be carried out on cells from one donor (Butler et al., 2016; Gray et al., 1996). These characteristics have been validated by previous work in our laboratory, including in studies using primary ciliary dyskinesia epithelial cells, where expansion by the co-culture method followed by differentiation at ALI preserved the disease phenotype –in this case determined by the ciliary dysfunction- similarly to BEGM culture (results not shown).

Over a 28 day period, primary human basal cells differentiated into a multi-layered polarised epithelium containing ciliated, goblet, basal and progenitors cells which preserve the characteristics of the original donor, as has been reported by several studies using this method (Butler et al., 2016; de Borja Callejas et al., 2014; Gray et al., 1996; Hirst et al., 2010; Pezzulo et al., 2011). However, primary ciliated epithelial cell cultures can present with inter- and intra-donor variability. For this purpose, a quality control assessment sheet was developed for a rapid, non-invasive check of the quality of each well before the start of an experiment. The two main focuses of this assessment were the

level of ciliation of the culture - which can be visually determined by high speed video microscopy observations of the surface of each well and graded on a scale from 0 to 5 (Table 6) and the integrity of the epithelial layer as determined by the value of the TEER reading. This method allowed selection of cell cultures with similar characteristics for the same experiment, thus limiting intra-donor, well to well variability. It also ensured that cultures that failed at any point in the culture process were not used for experiments. As this scoring method can be subject to assessor bias, two separate validation tests were carried out, with two assessors who were blinded to the cultures they were scoring. In both cases, the agreement in scores was determined to be higher than by chance alone, indicating similarity in scores awarded. This scoring method indicated that intra-donor variability was low, with a standard deviation of 0.232. There were no statistically significant differences in ciliation levels observed in COPD cultures compared to healthy cultures (Figure 5). However, scores awarded to COPD cultures were on average 0.4 units lower than those awarded to healthy cultures, suggesting that maybe they did not ciliate as well as cultures from healthy epithelial cells and this was masked by high inter-donor variability. Epithelial barrier and integrity was also similar between healthy and COPD cultures, with no significant difference in TEER between the two groups (Figure 5). This is in agreement with previous reports which indicated no difference in TEER of healthy and COPD bronchial epithelial cultures and also recorded average TEER values of approximately 400 to 1000 $\Omega x cm^2$ (Amatngalim et al., 2017; Schneider et al., 2010). In contrast, findings from two other studies reported a decreased TEER in COPD bronchial epithelial cells cultured at ALI compared to healthy (Heijink et al., 2014; Staudt

et al., 2014). However, in both cases this was measured in early stages of epithelial differentiation (at day 10 or day 15), as opposed to when cultures were fully differentiated.

In light of previous studies suggesting that in COPD the airway epithelium is not regenerated in the same way as in healthy individuals, it was important to characterise the differentiation pattern of primary nasal epithelial cells from healthy and COPD donors, when cultured at ALI (Ghosh et al., 2018; Staudt et al., 2014). For this purpose, healthy and COPD cultures were analysed at 4 time points during the 28 days of differentiation, namely day 0, 7, 14 and 28.

Previous studies which investigated the cellular composition of the respiratory epithelium have often done so by means of microscopy imaging and manual or automated counting of the different cell types in the epithelial layer, either viewed from above or in cross section (Amatngalim et al., 2018; Butler et al., 2016; Ghosh et al., 2018; Schneider et al., 2010). To date there are no methods available that allow isolation and total quantification of the different cell types in the epithelial layer, primarily due to a lack of cell surface markers that can selectively identify ciliated, goblet and progenitor cells from basal cells. Basal cells of the respiratory epithelium can be identified based on expression of CD49f/ Integrin-α6 and CD271/NGFR, as identified by Rock et al. (2009). In order to quantify the number and percentage of basal and ciliated cells in epithelial cultures during differentiation, a novel, flow cytometry based analysis method was used (Figure 6). This relies on separation of basal cells based on expression of CD271 and CD49f, followed by isolation of ciliated cells based on expression of the cell surface marker CD133/Prominin 1 and lack of expression of CD66/CEACAM-1 (GSK intellectual property). CD133

was first identified as a potential ciliated cell marker based on its high up-regulation in a transcriptional profiling of gene expression changes during epithelial differentiation (Ross et al., 2007). It has subsequently been validated at GSK and the results reported in a manuscript currently under preparation. In addition to the CD133+CD66- ciliated cells, using this flow cytometry method, two other populations could be separated, CD133+CD66+ and CD133-CD66+. Based on their pattern of emergence, as shown in Figure 7, it is likely that the CD133+CD66+ and CD133-CD66+ populations represent secretory and intermediate progenitor populations, respectively, in accordance with recent single cell RNA sequencing data analysing the respiratory epithelium during differentiation at the ALI (Ruiz Garcia et al., 2018). In this study by Ruiz Garcia et al. (2018), cultures of upper airway epithelial cells at day 7 of epithelial differentiation were found to contain predominantly basal and secretory cells, in agreement with the presence of CD271+CD49f+ cells and CD133-CD66+ cells, respectively, in the flow cytometry analysis. Subsequently, in later stages of differentiation, suprabasal cells, with characteristics of intermediate progenitors for ciliated and goblet cells, were shown to emerge (Ruiz Garcia et al., 2018). It could be extrapolated that suprabasal cells are similar to the CD133+CD66+ cells. However, it remains to be determined whether these CD133-CD66+ and CD133+CD66+ cells represent homogenous populations as well as what their functional identity is.

While there was no difference in the number of basal cells in either healthy or COPD epithelia in the current study, their proportion decreased significantly as healthy cultures differentiated - Figure 7 B&D. This decrease in proportion of basal cells was not seen in COPD cultures, suggesting a different behaviour

of COPD basal cells compared to healthy during ALI differentiation. Furthermore, the proportion of basal cells present represents the relevant measurement of epithelial composition as it takes into account the possible differences in total cell number as well as the proportion of other cell types. As such, the significant decrease in proportion of basal cells in healthy cultures which was not seen in COPD cultures could indicate an altered homeostasis mechanism in COPD, with an increased proportion of basal cells at the expense of terminally differentiated cells such as ciliated cells. This agrees with previous reports indicating basal cell hyperplasia in COPD epithelia (Auerbach et al., 1979; Auerbach et al., 1961; Ghosh et al., 2018).

In quantifying and comparing the level of ciliation between healthy and COPD ALI cultured epithelial cells, it was the total number of ciliated cells that provided the essential information, given the cellular localisation of ciliated cells exclusively on the apical side of the epithelium. This is because the total number of ciliated cells becomes normalised to the same surface area (that of the transwell membrane). Interestingly, there was strong evidence to suggest a delayed increase in ciliated cell number in COPD epithelial cultures when compared to healthy epithelia at day 14 of differentiation (Figure 7C). Furthermore, in healthy epithelial cultures the number of ciliated cells was established by day 14 and did not increase significantly to day 28, but in COPD cultures, a significant increase was seen from day 14 to day 28. These observations appear to indicate a delay in establishing the population of ciliated cells in COPD cultures. Even at day 28, when cultures are considered completely differentiated, there were 2.3 times less ciliated cells in COPD cultures compared to healthy cultures, but this difference did not achieve

statistical significance, most likely due to high inter-donor variability. This is in agreement with visual scoring of COPD ciliated cultures which also reported a trend for lower average ciliation scores by 0.4 units compared to healthy culture scores. Ultimately, these data indicate an altered differentiation process of COPD epithelia compared to healthy epithelia where basal cells either proliferate more or do not differentiate towards ciliated cells. This finding is in agreement with results obtained by Ghosh et al. (2018) who reported that COPD bronchial epithelial cells differentiated at ALI showed increased numbers of basal cells and goblet cells and over 80% less ciliated cells compared to cultures from healthy donors. In their study, cell type quantification was performed by immunofluorescence staining of ALI cultures and imaging by confocal microscopy (Ghosh et al., 2018). It is therefore possible that the difference in the magnitude of the changes comes as a result of the different analysis methodologies used.

Currently, there is no cell surface marker available to allow isolation and quantification of secretory progenitors and goblet cells in the respiratory epithelium. In addition, staining cultures with an antibody against MUC5AC in order to visualise goblet cells led in many cases to identification of the secreted mucin on cilia and ciliated cells, making it inaccurate to attempt to quantify goblet cells by this method. Therefore, qRT-PCR was used to quantify the levels of gene expression of the transcription factor *SPDEF* and of the secretory cell specific mucins *MUC5AC* and *MUC5B* in healthy and COPD epithelial cultures. *SPDEF* is known to regulate goblet cell differentiation and its increased expression has been associated with goblet cell hyperplasia (Okuda et al., 2019; Park et al., 2007). Previous reports indicated higher

SPDEF expression in COPD ALI cultured epithelial cells compared to healthy cultures (Song et al., 2017). However, no statistically significant difference in the levels of *SPDEF* or mucins *MUC5AC* or *MUC5B* gene expression was detected in this study in differentiated COPD nasal epithelial cultures when compared to healthy (Figure 9), in agreement with results obtained by Amatngalim et al. (2017) who also found no significant difference in expression of *MUC5AC* in COPD differentiated bronchial epithelial cultures compared to healthy cultures. It would be of interest to understand if these findings correlate with levels of protein expression and goblet cells counts, if these were quantified in primary nasal epithelia.

The flow cytometry analysis of epithelial cultures during differentiation also pointed towards day 7 of epithelial differentiation as an interesting time point to study for further experiments, as it precedes ciliation and could provide useful information regarding a regenerating epithelium. Given the small number of ciliated cells detected by flow cytometry in healthy epithelia at day 7, it was necessary to confirm if they represented ciliated cells with fully formed cilia, particularly as CD133, the marker used for selection of ciliated cells by flow cytometry, is a marker of epithelial protrusions rather than cilia and has a cell surface localisation (Corbeil et al., 2000). Immunostaining of epithelial cultures for β-tubulin and MUC5AC at day 7 and day 28 confirmed a lack of extended cilia at day 7, although occasional flat tubulin networks could be observed, possibly indicating microtubule reorganisation preparing for ciliogenesis, as also observed by (Schamberger et al., 2015). These observations replicate previously published results showing ciliogenesis occurring after 7 days of epithelial differentiation, both by confocal microscopy

and by single cell RNA sequencing (Ruiz Garcia et al., 2018; Schamberger et al., 2015). In accordance with studies describing secretory cells as early differentiation progenitors and pre-cursors of goblet and ciliated cells, MUC5AC positive cells were identified at day 7 (Montoro et al., 2018; Ruiz Garcia et al., 2018). Therefore, day 7 of epithelial differentiation was identified as an important early differentiation stage which presents mucus secretory cells and precedes establishment of ciliation. Epithelial cultures differentiated for 7 days at ALI were previously used as a model of regenerating epithelium in a study investigating the effect of RV infection on primary epithelial differentiation at ALI (Faris et al., 2016). Therefore, epithelial cultures differentiated for 7 days were subsequently used for infection studies presented in chapters 3.2, 3.3 and 3.4 and results compared to those of cultures differentiated for 28 days, to understand how a regenerating epithelium responds to viral and bacterial infection and co-infection.

In terms of ciliary function, this study found there was no difference in the ciliary beat frequency between healthy and COPD epithelial cultures, in agreement with the work by Stanley et al. (1986), who reported no difference in the beat frequency of cilia from nasal samples of smokers versus non-smokers. In contrast, a later study reported a significantly reduced ciliary beat frequency in nasal samples collected from patients with moderate or severe COPD compared to those from control subjects (Yaghi et al., 2012). The difference in results of this study may be due to the use of freshly collected tissue for ciliary function measurement versus measurement in ALI cultured epithelial cells. Ciliary beat amplitude was also not different in cultures from COPD patients compared to healthy (Figure 10), but it is worth investigating in the future if this

finding holds true when measurements are carried out directly on patient samples.

As chronic inflammation is a hallmark of COPD, it was of interest to determine if inflammatory mediator secretion by ALI cultured nasal epithelial cells from COPD patients is different from that of healthy cells (Barnes, 2016). The concentration of cytokines IL-1b, IL-6, TNF-a, IL-17, G-CSF and IFN-l and of chemokines TARC, RANTES, MCP-1, ENA-78, GRO-α and MIP-3α did not differ in the supernatants from COPD cultures compared to those from healthy cultures (Table 7). Furthermore, there was also no significant difference in their baseline levels in day 7 cultures compared to day 28 cultures in either healthy or COPD. Interestingly, however, was that levels of the chemokine IL-8, a known neutrophil chemoattractant, were significantly higher in ciliated COPD cultures compared to day 7 cultures (Table 7) (Hammond et al., 1995). This increase in IL-8 concentration with epithelial differentiation was not detected in healthy cultures, suggesting that COPD epithelial cultures may be imprinted to produce more IL-8, leading to the predominantly neutrophilic inflammation seen in the COPD airways (Hoenderdos and Condliffe, 2013). In agreement with this, previous studies have also described higher baseline levels of IL-8 in supernatants from ALI cultured COPD bronchial epithelial cells than in cultures from healthy donors (Ganesan et al., 2013; Schneider et al., 2010; Schulz et al., 2003).

In conclusion, data presented in this chapter indicate that nasal epithelial cells from COPD patients, differentiated at the ALI to a ciliated phenotype, present with delayed and reduce ciliation compared to healthy cultures. Furthermore, unlike in healthy cultures where the proportion of basal cells decreases with

differentiation, in COPD cultures this is sustained, likely indicating an increased proportion of basal cells at the expense of ciliated cells. COPD epithelial cells also secreted more IL-8 when differentiated than at a pre-ciliation stage (day 7), indicating a different inflammatory behaviour than in healthy cultures. There was no difference in the expression levels of goblet cells specific genes, epithelial resistance, ciliary function or secretion of other cytokines and chemokines between healthy and COPD nasal epithelial cultures. Finally, day 7 of epithelial differentiation, which precedes appearance of cilia but presents with mucin producing secretory cells, was chosen as an epithelial differentiation stage representative for a regenerating epithelium and was investigated further during infection studies.

3.2. Investigating the early interaction of NTHi with the ciliated respiratory epithelium

3.2.1. Introduction

NTHi is a nasopharynx colonising commensal pathogen in the airways of healthy individuals (King, 2012). However, when the respiratory tract is affected by other infections or chronic diseases such as cystic fibrosis, primary ciliary dyskinesia or COPD, NTHi can become an opportunistic pathogen and cause respiratory disease exacerbations (Ahearn et al., 2017). In children, NTHi can also ascend to the middle ear and cause otitis media (Ahearn et al., 2017). In order to establish an infection within its human host, NTHi has to first interact with the respiratory epithelium. Several mechanisms by which NTHi can attach to the epithelium have been described in section 1.16. These include use of pili, autotransporter proteins, outer-membrane proteins and lipopolysaccharides which can interact with numerous epithelial receptors such as ICAM-1, CEACAM, PAFR, β-glucan receptor or extracellular matrix proteins such as laminin or collagen (Ahearn et al., 2017). However, there is little understanding of the very early interaction of NTHi with the ciliated respiratory epithelium as most of the previous studies have used cell lines or undifferentiated basal cells. It has been reported that NTHi can readily interact with mucus and that, through its pili and outer membrane proteins P2 and P5, it can bind to human nasal mucins (Kubiet et al., 2000; Read et al., 1991; Reddy et al., 1996). Contradictory results have been published regarding the interaction of NTHi with the motile cilia of the respiratory epithelium. Ketterer et al. (1999) have described in their study that NTHi attached specifically to non-ciliated cells and did not appear to adhere to cilia or ciliated cells of ALI

cultured epithelia. In contrast, Baddal et al. (2015) have presented confocal microscopy images showing NTHi attached to cilia within 1 hour of their addition to an ALI cultured epithelium but no measures of the effect on ciliary function were made. It is also unclear whether NTHi infection affects ciliary function in human ciliated epithelium. Clumps of ciliated epithelial cells collected from bovine bronchi were cultured for up to a week and then treated with bacteria free supernatants from NTHi cultures (Bailey et al., 2012). In this experiment, ciliary beat frequency was reduced by the NTHi culture supernatants but not by NTHi culture medium suggesting an effect of NTHi secreted factors on ciliary function (Bailey et al., 2012). Similarly, nasopharyngeal tissue specimens obtained from children and cultured embedded in agar were infected with NTHi and ciliary beat frequency was measured every 12 hours for 48 hours (Janson et al., 1999). In this study too, ciliary beat frequency was reduced by a protein D producing strain of NTHi, but not by a mutant lacking expression of this protein (Janson et al., 1999). However, both of these studies used tissue samples explanted from bovine or human airways and cultured for extended period of times, which could potentially make them more susceptible to the effects of bacterial infection than differentiated epithelial culture (Bailey et al., 2012; Janson et al., 1999). As such, the effect of NTHi infection on ciliary function in ALI cultured epithelia from healthy or from COPD donors remains unclear. Furthermore, in addition to ciliary beat frequency, ciliary beat amplitude is another aspect of ciliary function that can be affected during infection but remains unexplored. Indeed, respiratory syncytial virus and coronavirus have both been reported to cause ciliary dyskinesia without affecting ciliary beat frequency (Chilvers et al., 2001;

Smith et al., 2014). Therefore, further investigation is necessary to understand whether NTHi does in fact attach to cilia or ciliated cells early on in the infection process and whether it impacts ciliary function in healthy or COPD ciliated epithelia.

In the airways of patients with COPD, NTHi is the pathogen most frequently detected, both at stable state and during disease exacerbations (Wilkinson et al., 2017). In addition, in patients with COPD NTHi has been detected in the lower respiratory tract, where it is not normally encountered in healthy individuals (Bandi et al., 2001). As NTHi has been shown to invade epithelial cells and colonise the respiratory tract of patients with COPD, one hypothesis is that it uses intracellular invasion as a shield from immune cells, antibody mediated killing and antibiotics and as a means of persistence and re-emergence (Murphy et al., 2004; van Schilfgaarde et al., 1999). In support of this hypothesis, Pettigrew et al. (2018) reported that strains of NTHi were found to persist in airways of COPD patients for up to 1442 days. Similarly, Murphy et al. (2004) have reported that the same strain of NTHi was found to colonise the airways of COPD patients despite antibiotic therapy and over 6 months of negative sputum culture. These findings collectively imply an ability of NTHi to persist undetected in the airways and re-emerge at later times.

The process by which NTHi invades epithelial cells has been described in section 1.16 and involves cytoskeletal rearrangements by the epithelial cells to allow macropinocytosis or receptor mediated endocytosis (Clementi and Murphy, 2011; Holmes and Bakaletz, 1997; Ketterer et al., 1999; Stgeme and Falkow, 1990; Swords et al., 2000). The bacteria are then able to survive intracellularly by evading lysosome killing (Clementi et al., 2014).

One of the signalling pathways that has repeatedly been linked with regulation of NTHi internalisation into epithelial cells is the class I PI3K signalling pathway (Lopez-Gomez et al., 2012; Morey et al., 2011; Seiler et al., 2013). In mammals, eight isoforms of PI3K have been described and divided into 3 classes, based on structural characteristics and lipid substrate preference: class I PI3K contains the PI3K α, β, δ and γ isoform, class II PI3K contains three isoforms – PI3KC2α, PI3KC2β and PI3KC2γ, whereas there is only one class III PI3K isoform, also known as vacuolar sorting protein 34 (Vps34) (Okkenhaug, 2013). However, class I PI3 kinases have been studied the most in relation to bacterial invasion of the epithelium and for therapeutic purposes in COPD and will be the focus of this study.

3.2.1.1. Class I PI3K

The class I PI3Ks are heterodimeric proteins consisting of a catalytic subunit and an adapter subunit. Class IA PI3Ks use adapter proteins p50α, p55α, p85α, p85β, p55γ to bind to the catalytic subunits p110α, p110β, p110δ which ultimately denote the name of the PI3K isoform (Okkenhaug, 2013). The class IB PI3K γ isoform uses the p110 γ catalytic subunit and the p101 or p84 adaptor subunits (Okkenhaug, 2013). PI3Ks are recruited to the plasma membrane by activation of receptors which, either directly or indirectly, signal through protein tyrosine kinases, such as G-protein coupled receptors (GPCRs), B and T cell antigen receptors, integrins, Fc receptors, cytokine receptors, Toll-like receptors or receptor tyrosine kinases (Hawkins and Stephens, 2015). Activated protein tyrosine kinases in the intracellular domain of these receptors then bind to the adaptor subunits of PI3K via a Src homology 2 (SH2) domain to recruit the PI3Ks to the cell membrane and remove the

inhibitory effect of the regulatory subunit on the catalytic subunit (Vanhaesebroeck et al., 2010).

All activated class I PI3Ks use the substrate phosphatidylinositol 4,5-bisphosphate (PI(4,5)P2) and catalyse a reaction whereby the γ-phosphate group of ATP is transferred to PI(4,5)P2 to form phosphatidylinositol 3,4,5-trisphosphate (PI(3,4,5)P3), commonly known as PIP3 (Hawkins and Stephens, 2015). PIP3 then binds and recruits effector proteins with plekstrin-homology (PH) domains such as: the serine-threonine kinase protein Akt, the phosphoinositide-dependent kinase 1 (PDK1), regulators of small GTPases as well as signalling adaptors such as the growth factor receptor bound protein 2-associated protein 1 (GAB1/2) or the dual adaptor of phosphotyrosine and 3-phosphoinositides 1 (Hawkins and Stephens, 2015). The Akt Serine/Threonine kinase is predominantly activated downstream of PI3K and is often used as a surrogate readout for class I Pi3K activation (Fruman et al., 2017). For Akt to become activated following recruitment to the membrane, it requires phosphorylation by PDK1 or mechanistic target of rapamycin (mTOR) at Threonine 308 or Serine 473, respectively (Manning and Toker, 2017). Maximal Akt activation requires phosphorylation at both residues. Activated Akt then phosphorylates downstream substrate proteins such as the Forkhead box transcription factor family O (FOXO) or glycogen synthase kinase 3, among others (Manning and Toker, 2017). In order to terminate PI3K signalling, PIP3 is degraded by two different types of phosphatases –the SH2 containing phosphatases (SHIP) 1 and 2 which convert PIP3 into PI(3,4,)P2 and the phosphatase and tensin homologue (PTEN) which converts PIP3 back into PI(4,5)P2 (Hawkins and Stephens, 2015; Okkenhaug, 2013).

Cellular effects mediated by activation of class I PI3Ks and their downstream signalling pathways include regulation of transcription, translation, cell polarity, differentiation, metabolism, growth and survival, adhesion, movement and cytokine production (Hawkins and Stephens, 2015; Manning and Toker, 2017). These can be cell type dependent, with PI3Kα and β being ubiquitously expressed, whereas PI3Kδ expression is predominant on immune cells of the myeloid and lymphoid lineages (Fruman et al., 2017; Hawkins and Stephens, 2015). PI3Kγ expression is also cell and tissue type dependent, with highest expression levels detected in cells of myeloid lineage, although expression has been reported in endothelial cells, cardiac myocytes and T cells (Hawkins and Stephens, 2015).

3.2.1.2. PI3K signalling as a therapeutic target in COPD

In particular, in COPD, class I PI3Kδ and γ isoforms have been studied in detail, owing to their limited expression pattern, predominantly on immune cells, which made them an attractive strategy for controlling airway inflammation (Marwick et al., 2010; Sriskantharajah et al., 2013). In both asthma and COPD, dual inhibition of PI3Kγ and δ or either alone has been shown to reduce the inflammatory response by acting on macrophages, neutrophils, mast cells, T cells, eosinophils or B cells and regulating their function (Marwick et al., 2010). Recently, an inhaled selective PI3Kδ inhibitor GSK2269557 has shown a reduction in sputum IL-6 and IL-8 levels and an acceptable safety profile within a small COPD cohort, highlighting the predicted anti-inflammatory effect (Cahn et al., 2017). There is very limited information of the expression pattern and role of PI3Kδ expression in airway epithelial cells or its role during infection and disease (Jeong et al., 2018; Zhu et al., 2019). Therefore, further studies should investigate the

expression of isoform specific PI3K proteins in the primary airway epithelium and their specific roles during bacterial infection and epithelial invasion.

3.2.1.3. Role of PI3K signalling in NTHi invasion of the respiratory epithelium

As described in more detail in section 1.17, several studies have reported that NTHi invasion of epithelial cells is dependent on class I PI3K signalling (Morey et al., 2011; Seiler et al., 2013; Swords et al., 2001). Binding of NTHi to the PAF receptor on the 16HBE14 bronchial epithelial cell line activated the phosphatidylinositol-3-kinase (PI3K) pathway which was required for NTHi internalisation (Swords et al., 2001). Similarly, internalisation of NTHi by the A549 epithelial cell line resulted in phosphorylation of Akt and treatment with a pan PI3K inhibitor abrogated both Akt phosphorylation and NTHi internalisation (Morey et al., 2011). Subsequently, the same group went on to investigate which pathways downstream of PI3K are important for NTHi internalisation into A549 epithelial cells (Lopez-Gomez et al., 2012). In their study, they re-confirmed that inhibition of Akt resulted in reduced bacterial invasion (Lopez-Gomez et al., 2012). They also identified that NTHI can bind to integrins β1 and α5 and these are important for bacterial invasion, as was their downstream signalling effector Ras homologous (Rho) guanosine triphosphatase (GTPase) Rac-1 (Lopez-Gomez et al., 2012). Rac-1 was activated by NTHi infection and its inhibition reduced both NTHi internalisation and Akt phosphorylation (Lopez-Gomez et al., 2012). In a study using the Calu3 cell line, inhibition of PI3K signalling by the same pan-PI3K inhibitor again reduced NTHi invasion whereas silencing of FOXO 1/3 by siRNA resulted in increased bacterial internalisation (Seiler et al., 2013). As activation

of the PI3K signalling pathway leads to phosphorylation of FOXO by Akt and its subsequent translocation from the nucleus to the cytosol where it is degraded by the proteasome, inhibition of the PI3K pathway would allow activation of FOXO which could then prevent bacterial invasion (Seiler et al., 2013). The study by Seiler thus implicated FOXO transcription factors in regulation of NTHi invasion of epithelial cells.

In conclusion, these studies highlight the important role of the PI3K signalling pathway in regulating NTHi invasion. However, all of these studies have been carried out in different types of immortalised cell lines and their direct translation to differentiated primary respiratory epithelium, and in particular the COPD epithelium, has not been confirmed yet. Furthermore, none of these studies went on to identify which of the class I PI3K isoforms is essential for NTHi internalisation. Such knowledge would allow for a more targeted approach to inhibiting bacterial invasion therapeutically. This would be beneficial for diseases such as COPD where NTHi is associated with disease exacerbations and where specific PI3K inhibitors have already been investigated clinically for their role in immune cell mediated inflammation (Cahn et al., 2017; Marwick et al., 2010).

Hypothesis:

The early interaction of NTHi with the ciliated respiratory epithelium involves binding to cilia and epithelial invasion of the healthy and COPD primary epithelium in a PI3K dependent manner.

Aims:

- To study the very early interaction of NTHi with the ciliated respiratory epithelium.
- To determine if NTHi infection affects ciliary function.
- To determine if NTHi preferentially invades a specific epithelial cell type.
- To determine if epithelial differentiation affects NTHi adherence and invasion of the epithelium.
- To determine the role of PI3K signalling in NTHi invasion of the ciliated epithelium.

3.2.2. NTHi binds to motile cilia within minutes of addition to an epithelial culture and forms elongated chains within 24 hours.

To investigate the early interaction of NTHi with the ciliated respiratory epithelium, live confocal microscopy videos were recorded immediately after addition of either live or heat killed green fluorescent CFSE labelled NTHi to ciliated epithelial cultures stained with far red cell mask (sections 2.18 and 2.20). The first interaction of live NTHi with rapidly beating cilia was observed after approximately 5 minutes post addition to both healthy and COPD epithelial cultures, with individual bacteria observed attached to cilia (Figure 11A/ Video 11A) –See Appendix 4 and videos available on the USB stick attached. Heat inactivated NTHi also interacted with rapidly beating cilia and were bound within 5-10 minutes of addition to the culture. Interestingly, by 90 minutes, live NTHi formed chains of bacteria with a lattice like organisation, predominantly on ciliated areas (Figure 11B/ Video 11B), which were not apparent with heat inactivated bacteria (Figure 11E/Video 11E). In both healthy and COPD cultures, by 24 hours post infection, the lattice formed by live bacteria evolved into aggregates with a biofilm aspect that covered extensive areas of the ciliated culture (Figure 11C/Video 11C). Cilia beating could still be observed underneath the bacterial aggregates. Heat inactivated bacteria were still observed to form aggregates but these did not have the organised appearance of those formed by live NTHi (Figure 11F/Video 11F). These observations were confirmed in experiments using bronchial epithelial cultures from 1 healthy and 2 COPD donors.

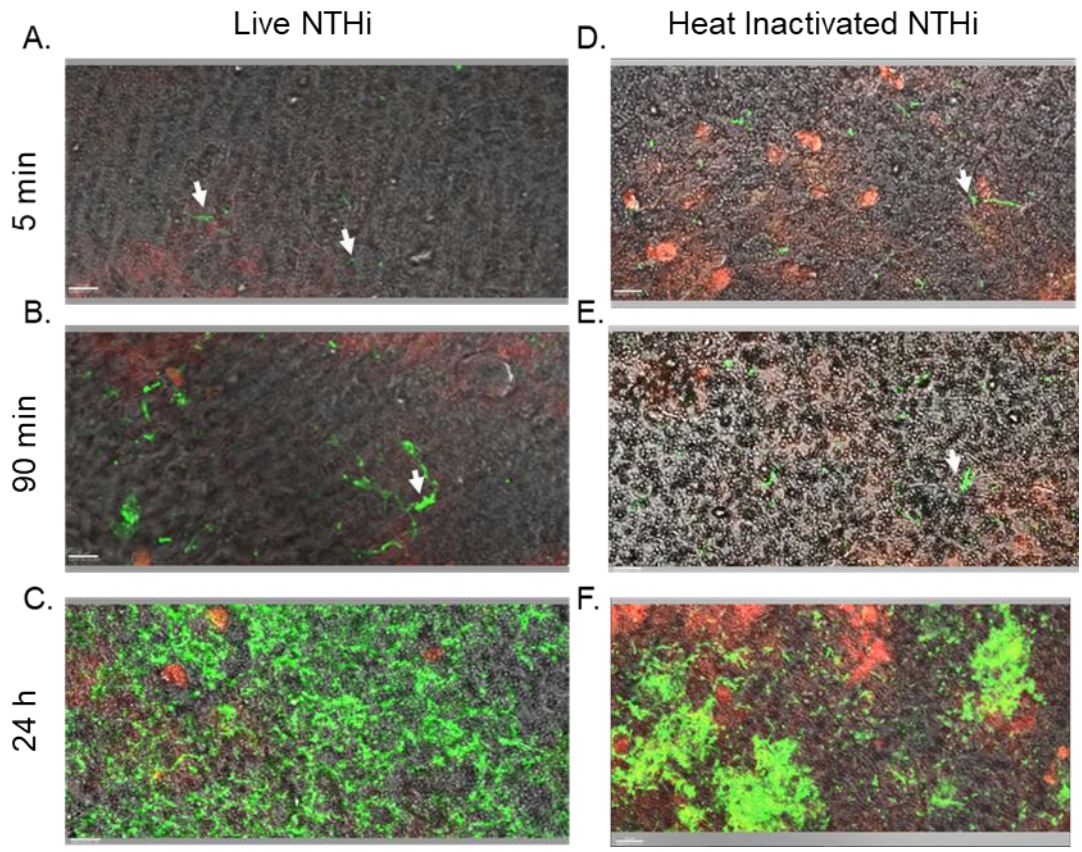

Figure 11. Screen captures of live confocal microscopy imaging of the interaction of live and heat inactivated NTHi with the ciliated respiratory epithelium

Live or heat inactivated NTHi strain 49247 (stained in green) was added to ciliated epithelial cultures (stained in red) at $5x10^6$ CFU/well and video imaged by live confocal microscopy. Videos available on USB stick attached. Live A. and heat killed D. NTHi interaction with motile cilia (arrows) at 5 minutes post addition to the culture. B. Live NTHi chain formation and lattice organisation on ciliated areas at 90 minutes (arrow) and C. Live NTHi biofilm at 24h post addition to ciliated cultures. E. Heat killed NTHI on ciliated cultures at 90 minutes post addition to the culture. F Heat killed NTHi aggregates at 24h. Scale bar represents 20 µm. Images are representative of experiments carried out in cultures from 3 healthy and 2 COPD donors.

To further investigate the conformational changes that NTHi was observed to undergo, healthy and COPD ciliated epithelial cultures were infected with live or heat inactivated NTHi and were imaged by scanning electron microscopy at 24 hours post infection. Despite the extensive washing and processing involved in the preparation of samples for scanning electron microscopy, both live and heat inactivated NTHi were observed attached to epithelial cultures (Figure 12). This suggested a firm attachment of NTHi to the epithelium and in particular to cilia, which was independent of NTHi being alive. Interestingly, heat inactivated NTHi was observed attached to the epithelial surface and to cilia in single bacteria or diploid conformation (Figure 12 E & F). In contrast, live NTHi underwent significant morphological changes (Figure 12 C & D), forming elongated chains with an average length of 4.03 ± 2.4 µm in healthy cultures and 4.225 ± 3.1 µm in COPD cultures (Figure 12G). These chains were significantly longer than the average length of heat inactivated bacteria on healthy cultures 1.7 ± 1.2 µm, $p<0.0001$, and 1.4 ± 0.8 µm, $p<0.0001$ on COPD cultures.

To understand if these morphological changes were a consequence of NTHi interaction with the epithelium, NTHi alone, either live or heat killed, was measured prior to addition to the culture, as well as after culturing live NTHi for 24h in basal epithelial medium in absence of epithelial cells. There was no significant difference between live NTHi and heat killed NTHi prior to addition to an epithelial culture ($p=0.581$) or when compared to heat killed NTHi attached to epithelial cultures at 24h post infection ($p>0.05$), confirming preservation of original morphology. Live NTHi cultured in basal epithelial medium formed chains that were longer compared to the size of the bacterium

at time 0, but on average these were not significantly longer than the length of NTHi at 0h ($p=0.315$). In contrast, when incubated on either healthy or COPD ciliated culture for 24 hours, NTHi chains were significantly longer compared to when bacteria was incubated in medium alone ($p<0.0001$), thus suggesting that interaction with the ciliated epithelium promotes NTHi morphological changes.

In conclusion, these results indicate that NTHi binds to motile cilia very early in the infection process, after which it undergoes morphological changes with formation of elongated chains and forms lattice like aggregates on healthy and COPD ciliated cultures.

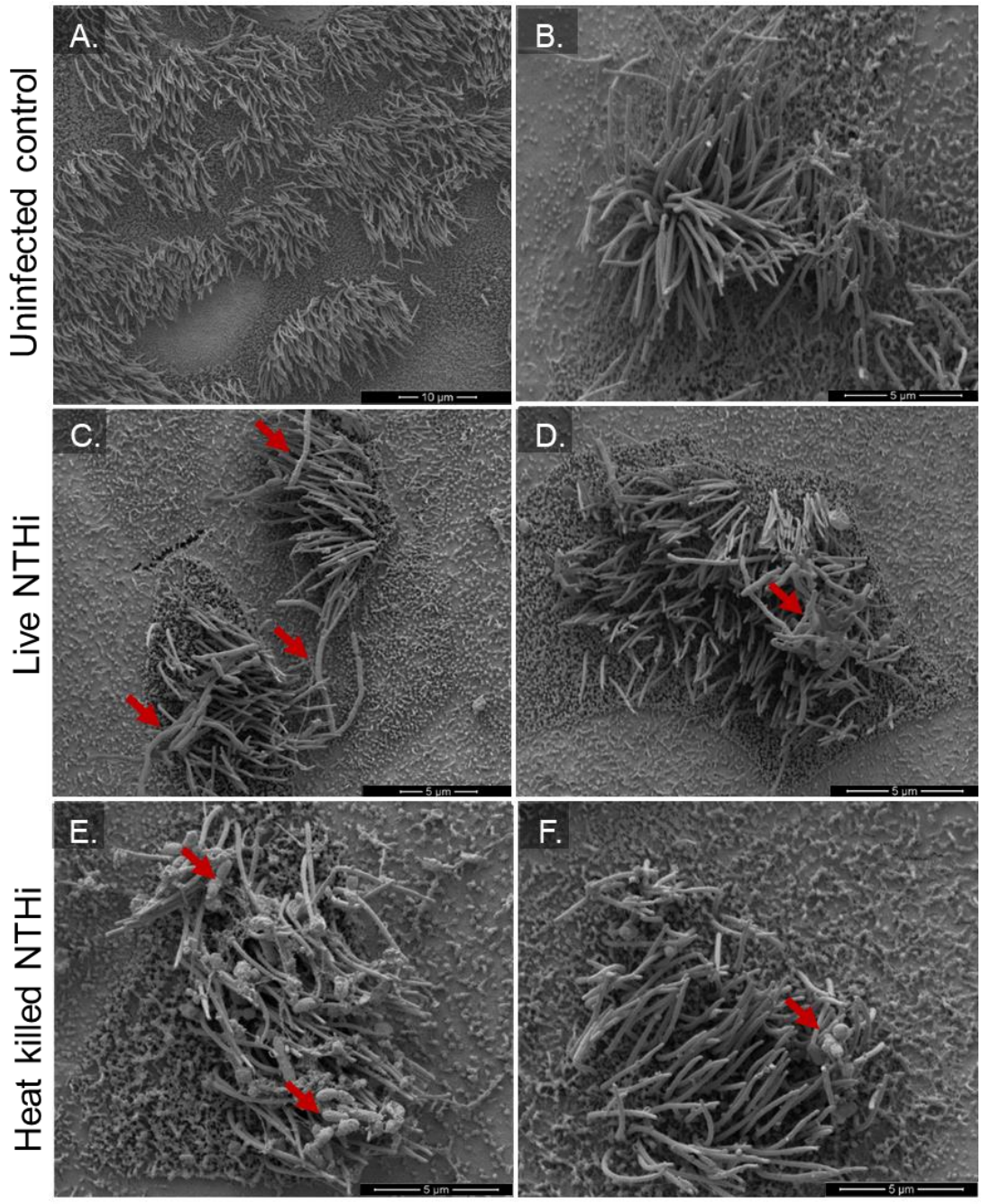
Uninfected control
Live NTHi
Heat killed NTHi
A.
B.
C.
D.
E.
F.
10 µm
5 µm

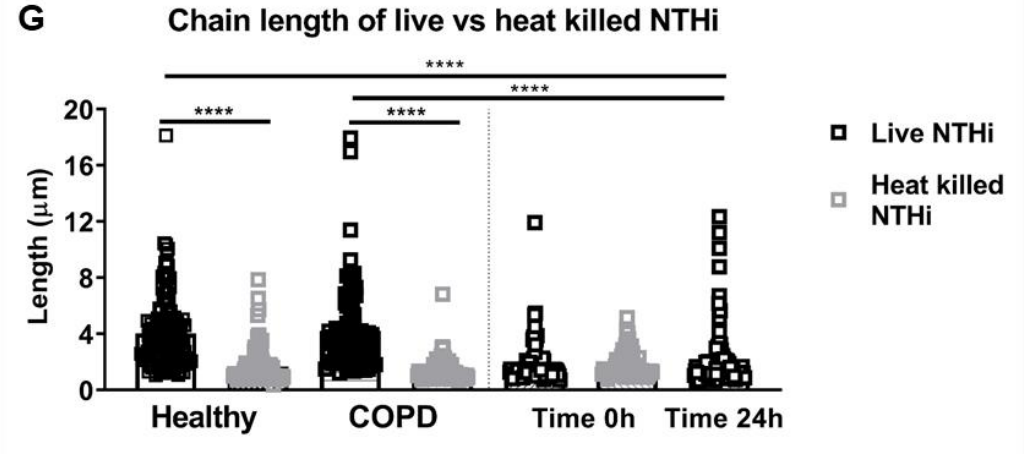
G
Chain length of live vs heat killed NTHi
Length (µm)
20
16
12
8
4
0
****
****
****
****
Healthy
COPD
Time 0h
Time 24h
Live NTHi
Heat killed NTHi

Figure 12. Scanning electron micrographs showing NTHi conformational change

Live or heat killed NTHi strain 49247 was added to ciliated epithelial cultures at $5x10^6$ CFU/well for 24 hours, fixed and imaged by scanning electron microscopy. A &B. Healthy uninfected ciliated epithelial culture. C & D. Healthy ciliated epithelial culture infected with live NTHi or E& F infected with heat inactivated NTHi. Arrows indicate NTHi attached to cilia. Scale bar represents 10 µm in A and 5 µm in B-F. G. Quantification of the length of live and heat killed NTHi chains, either attached to healthy or COPD epithelial cultures at 24 h post infection or in absence of epithelial cultures, at time 0h (prior to addition to the culture) or at 24h, following incubation in BEBM. Minimum 5 images per condition were analysed. N=2 healthy and 2 COPD cultures. For statistical analysis, chain length values were log10 transformed and a linear regression model was used to determine the mean length for each condition. P values were Benjamini-Hochberg adjusted for multiple comparisons. ****=p<0.0001.

3.2.3. NTHi aggregates affect ciliary function by reducing ciliary beat amplitude

It was then important to determine whether the direct binding of NTHi to cilia had an effect on ciliary function. For this purpose, ciliary beat frequency and ciliary beat amplitude were measured. Ciliary beat frequency was determined before infection of the epithelial cultures, immediately after addition of NTHi to the cultures and subsequently at 8 h and 24 h post infection, using high speed video microscopy recordings, as described in sections 2.12, 2.13 and 2.14. No statistically significant change in the frequency of cilia beating was determined in either healthy or COPD cultures following infection with NTHi at any of the time points (Figure 13A) ($p>0.05$). Interestingly, however, in healthy cultures, in both uninfected control wells and NTHi infected wells, a trend for an increase in ciliary beat frequency was observed with the average frequency increasing from 8.3±2.3 Hz and 8.7 ±1.9 Hz respectively, prior to infection to 11.7 ±2.3 Hz

in both groups at 24h post infection. In COPD cultures, this increase was smaller, of only approximately 1.3 Hz in uninfected cultures and 1Hz in NTHi infected cultures. It is possible that the increase in ciliary beat frequency was a consequence of fluid addition to the culture during bacterial infection. This increase was not statistically significant in either healthy or COPD.

When the experiment was replicated in ciliated bronchial epithelial cultures from 1 healthy and 2 COPD donors, ciliary beat frequency was, again, not affected by NTHi infection. However, a similar trend was observed whereby the frequency of ciliary beating in the healthy culture increased over time in both control and NTHi infected wells from an average of 11.5 ± 2.4 Hz and 11.9 ± 1.1 Hz, respectively, prior to infection, to 15.7 ± 1.5 Hz and 14.3 ± 1.3 Hz, respectively at 24h. In the COPD cultures, the average frequency before infection was 10 ± 0.7 Hz in the control cultures and 11.6 ± 1.3 Hz in the wells that were to receive NTHi, which then increased to 15.5 ± 1.1 Hz and 14.9 ± 1 Hz, respectively, at 24h post infection.

In contrast, at 24 h post NTHi infection, cilia beating amplitude was significantly reduced in areas covered by NTHi aggregates and biofilm (Figure 13B). Using high-speed video recordings, the distance travelled by individual cilia was measured, as described in section 2.14. In areas covered by bacterial aggregates this was reduced in both healthy and COPD cultures when compared to uninfected control wells (healthy: $p<0.0001$; COPD: $p<0.0001$). In NTHi infected wells, the amplitude of cilia covered by NTHi biofilm was significantly lower than that of cilia that lacked biofilm presence, in both healthy and COPD cultures (healthy: $p=0.0002$; COPD: $p<0.0001$). In healthy cultures, ciliary amplitude was also significantly reduced by NTHi infection even in

absence of biofilm, when compared to uninfected controls (p=0.0175). As ciliary amplitude measurements rely on visual interpretation, in order to confirm that measurements are reproducible, a test was carried out with two other assessors where each individual measured amplitude of ciliary beating from cilia from the same cells. Amplitude of cilia from two previously identified cells per video from 10 different videos were scored by each assessor. There was no significant difference in the average amplitude measured by each assessor (p=0.331) and the inter-assessor variability was estimated to be a standard deviation of 0.599 µm, therefore meaning that for approx. 95% of videos, amplitude measurements of the three assessors lie within 2*0.599 µm around their video-specific average.

In conclusion, these results indicate that presence of bacterial aggregates covering ciliated areas could affect ciliary function through a reduced beating amplitude rather than frequency.

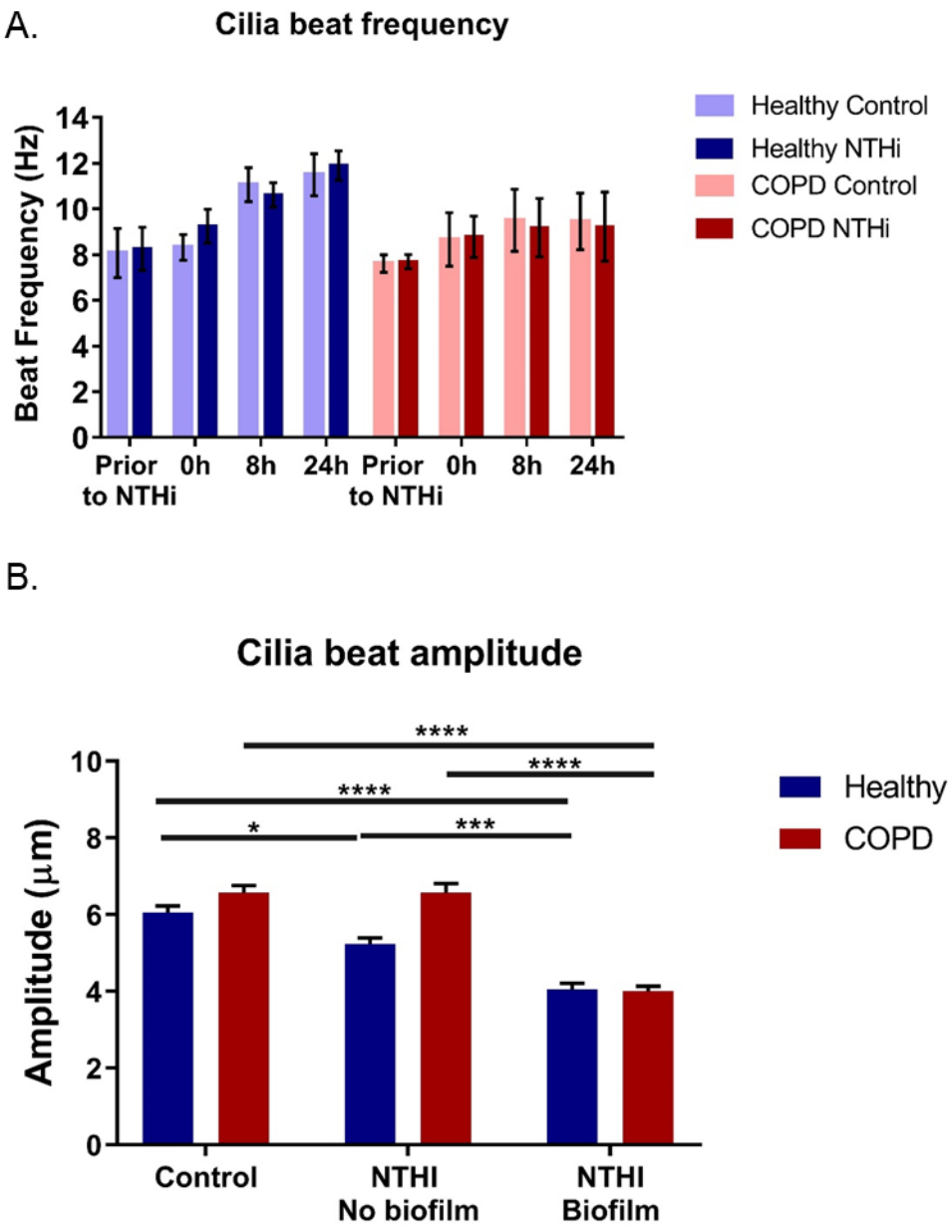

Figure 13. Ciliary function assessment following NTHi infection of epithelial cultures

A. Ciliary beat frequency was determined from high speed video microscopy recordings. Cultures were at air-liquid interface prior to NTHi strain 49247 addition ($5x10^6$ CFU/well) and subsequently submerged. At each time point, 10 videos per condition were recorded and used to determine average ciliary beat frequency for each donor. N= 5 healthy donors, 6 COPD donors. Data are presented as mean ± standard error of the mean. B. Cilia beat amplitude was determined using high speed video microscopy recordings at 24h post NTHi addition. For each condition, the distance travelled for at least 10 different cilia was measured. N= 3 healthy,

3 COPD donors. Data are presented as mean ± standard error of the mean. For statistical analysis, cilia beat frequency and beat amplitude values were log10 transformed and then analysed using separate mixed linear effects models with fixed effects for disease group (healthy/COPD), treatment (+/- NTHi) and time-point and a random effect for each donor. P values were adjusted for multiple comparisons using the Benjamini-Hochberg method. *=p<0.05, ***=p<0.001, ****=p<0.0001.

3.2.4. NTHi invades the ciliated respiratory epithelium, with a preference for non-ciliated epithelial cells

Following the initial interaction of NTHi with cilia of the respiratory epithelium, the bacterium has been previously reported to invade the epithelium (Clementi et al., 2014). In order to confirm this observation in ciliated nasal epithelial cultures, live confocal microscopy Z stack images were recorded at 24h post NTHi infection. For these experiments, NTHi was stained with green fluorescent CFSE dye and the epithelial layer with a red cell mask and infected cultures were imaged by live confocal microscopy (sections 2.18 and 2.20) (Figure 14 A&B). NTHi internalisation was observed in healthy and COPD nasal and bronchial epithelial cultures, with NTHi observed within the red epithelial layer (arrows, Figure 14A). Upon inspection of a single slice from the Z stack, NTHi could be seen within red stained epithelial cells, avoiding the dark area occupied by the nucleus (arrowheads, Figure 14B), thus confirming that NTHi is located inside the epithelial cells.

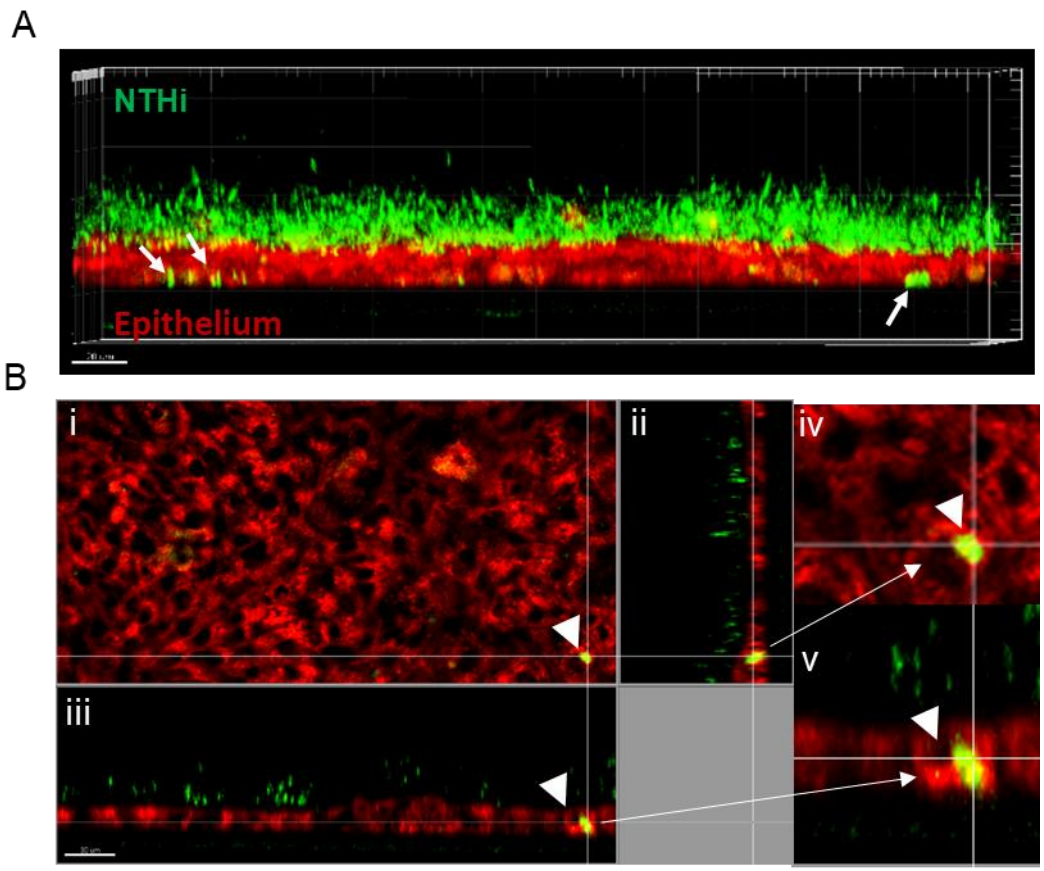

Figure 14. Live imaging of NTHi invasion of the ciliated epithelium

Ciliated epithelial cultures were inoculated with $5x10^6$ CFU/well of NTHi strain 49247 and imaged by live confocal microscopy at 24h post infection. A. Z-stack showing NTHi (green) biofilm on top of the epithelial layer (red) and NTHi which has invaded the epithelium, indicated by arrows. Scale bar represents 20 µm. B. One Z stack slice showing NTHi (green) within a red cell mask stained epithelial cell, indicated by arrowheads. Internalised NTHi bacteria are seen avoiding the dark area occupied by the nucleus. Panels show: i) top view the slice, ii) front and iii) side view and iv), v) zoom in on an NTHi invaded cell. Scale bar represents 30 µm.

To determine if NTHi invasion of the epithelium was targeted towards a specific cell type, two experiments were carried out using image cytometry, which combines confocal microscopy and flow cytometry. In the first experiment, commercially available healthy bronchial epithelial cells (cultured at GSK) were

infected with fluorescently labelled NTHi (strain 1479, GSK stock) for 24 hours, detached from the transwell membrane as described in section 2.22 and analysed on the Image Stream. Based on the intensity of NTHi fluorescence and the maximum pixel brightness, two separate population of NTHi positive events were separated. Upon visual inspection, the population with lower NTHi fluorescence but high maximum pixel brightness contained cells with extracellular NTHi. Conversely, the population with high NTHi fluorescence but lower maximum pixel brightness contained cells with intracellular NTHi. Cells in each population were then visually inspected and labelled as ciliated or non-ciliated. Results confirmed previous observations and showed that NTHi was attached to ciliated cells and in particular to cilia (Figure 15A). More specifically, of all the cells with NTHi bound extracellularly, 81% were ciliated and 19% were non-ciliated. Surprisingly, of the cells with intracellular NTHi, 93% were non-ciliated and 7% were ciliated. Figure 15B shows representative non-ciliated cells with intracellular NTHi.

In the second experiment, 1 nasal ciliated culture from a healthy donor and 2 COPD nasal ciliated cultures were infected with the in house strain of NTHi, either live or heat killed, for 24 hours. Subsequently, epithelial cells were stained for flow cytometry, as described in section 2.9 and analysed by Image Stream. The gating strategy shown in Figure 6, was applied. Basal cells (CD271+CD49f+) showed high-auto-fluorescence in uninfected samples and NTHi interaction with these cells could not be determined as cells were shown as fluorescent despite not being infected. NTHi presence in the populations of ciliated (CD133+CD66-) and non-ciliated epithelial cells (rest of cells, including CD133+CD66+ and CD133-CD66+ cells) was determined and separated by

fluorescence intensity. Cells with high NTHi fluorescence intensity were identified as those with extracellular NTHi and cells with lower fluorescence intensity were identified as having intracellular NTHi by visual inspection of individual events. Both ciliated and non-ciliated epithelial cells from all 3 donors presented attached, extracellular NTHi (Figure 15C&E). Interestingly, there was higher attachment of heat inactivated NTHi to both ciliated and non-ciliated cells in all three donors, compared to live NTHi (Figure 15 C&E). In contrast, live NTHi invasion of epithelial cells was identified in non-ciliated epithelial cells from all 3 donors (Figure 15F). Intracellular heat killed NTHi was also observed in the 3 donors, but at lower levels than seen with live NTHi. In one COPD donor, ciliated cells were identified that presented intracellular live NTHi and lower levels of heat killed NTHi (Figure 15D). In contrast the healthy donor and remaining COPD donor showed no NTHi invasion of ciliated cells.

In conclusion, these results suggest that NTHi preferentially invades non-ciliated cells while ciliated cells bind bacteria extracellularly, particularly to cilia.

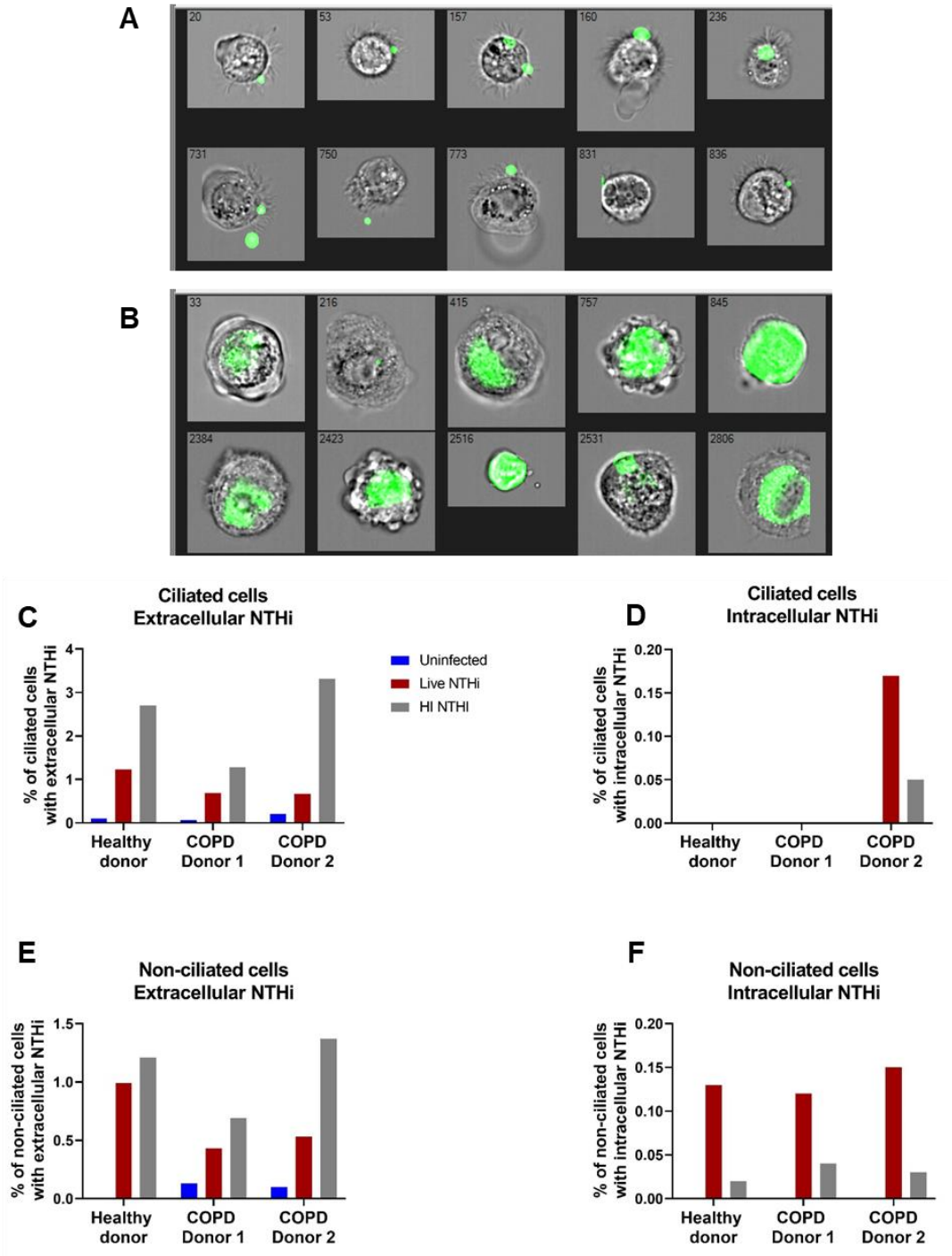

Figure 15. Quantification of NTHi invasion of ciliated versus non-ciliated epithelial cells by image cytometry

A&B. Commercially available ciliated bronchial epithelial cells from a healthy donor were infected with $5x10^6$ CFU/well of NTHi strain 1479 and analysed by image cytometry at 24 hours post infection. A. Ciliated cells with NTHi (green) attached, B. Non-ciliated cells with intracellular NTHi (green). C-F. Ciliated nasal epithelial cells from one healthy donor and 2 COPD patients were infected with $5x10^6$ CFU/well NTHi strain 49247, either live or heat killed.

At 24 hours post infection, epithelial cultures were analysed by image cytometry. The gating strategy described in Figure 6 was used to identify ciliated and non—ciliated cells. Due to high auto-fluorescence of uninfected basal cells, NTHi invasion of this population could not be determined. Percentages reported were determined as number of cells with NTHi associated out of the total population.

As imaging studies (Figure 15, Figure 12) suggested that NTHi preferentially bound to cilia but invaded non-ciliated epithelial cells, it was then of interest to determine how NTHi interacts with a pre-ciliation stage culture compared to a fully ciliated, differentiated epithelium. For this purpose, ALI cultures were differentiated for 7 days (a stage which precedes formation of cilia, as shown in section 3.1.4) of for 28 days when they were ciliated and then were infected with NTHi for 24 hours (section 2.19). At this time point, non-attached bacteria, adhered bacteria and intracellular bacteria were quantified (Figure 16), using a gentamicin killing assay (section 2.24). There was no difference in the average number of non-attached bacteria (Figure 16A) between pre-ciliation and ciliated cultures in either healthy ($p=0.99$) or COPD ($p=0.87$). Similarly, on average, bacterial adherence was not different between the two time points in either healthy ($p=0.8$) or COPD ($p= 0.9$) - Figure 16B. No difference in non-attached or attached bacteria was found between healthy or COPD cultures, irrespective of the time point analysed ($p>0.05$). In terms of bacterial invasion of the epithelium, shown in Figure 16C, a trend was present whereby in cultures from healthy donors, in 6 out of 7 donors, intracellular bacterial counts were lower in ciliated cultures than in pre-ciliation day 7 cultures. On average, NTHi invasion was 3.4 times as high in healthy pre-ciliation cultures compared to ciliated epithelia. However, this difference did not achieve statistical

significance (p= 0.297), possibly due to inter-donor variability. Unexpectedly, in cultures from COPD donors, an opposite trend was observed, where invasion was on average 3.4 times lower in pre-ciliation cultures compared to day 28, ciliated cultures, but this difference did not achieve statistical significance (p=0.234), again due to inter-donor variability. There was no significant difference between invasion of healthy and COPD epithelia at either day 7 (p= 0.061) or day 28 (p= 0.907).

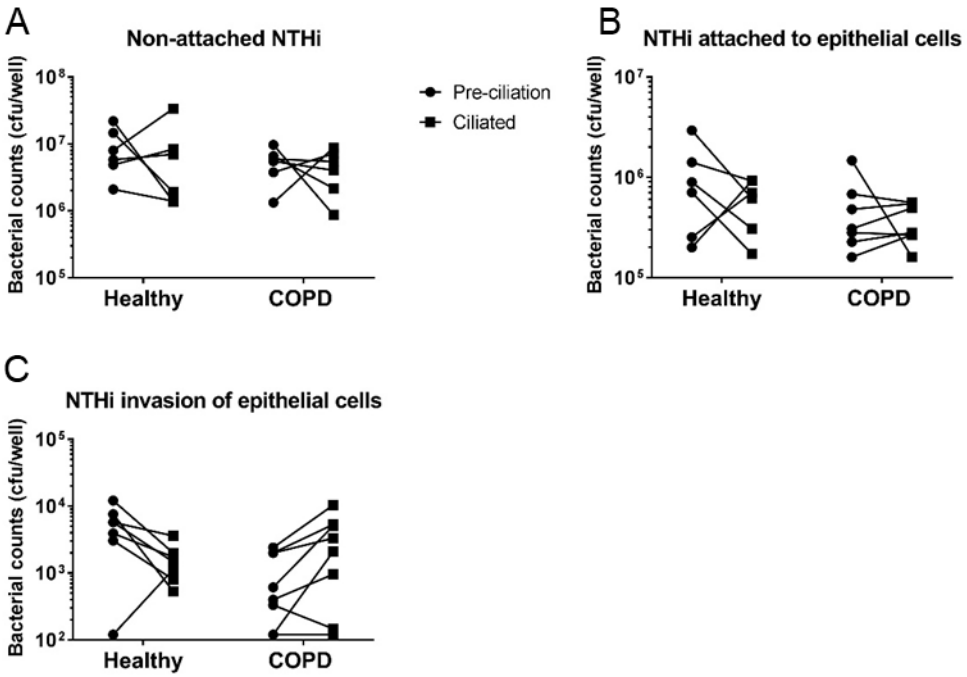

Figure 16. Quantification of non-attached, attached and intracellular NTHi in epithelial cultures at pre-ciliation day 7 and when ciliated at day 28

Pre-ciliation (day 7) and ciliated (day 28) epithelial cultures were infected with $5x10^6$ CFU/well of NTHi strain 49247 for 24 hours before quantification of non-attached NTHi (A), NTHi attached to the epithelium (B) and intracellular NTHi (C), using a gentamicin killing assay. N=7 healthy, 8 COPD donors. Lines connect same donor at pre-ciliation (day 7) and ciliated (day 28) stages. For statistical analysis, bacterial counts values were log10 transformed and subsequently analysed using separate linear mixed effects models for non-attached, attached and invasion counts. Fixed effects for disease groups (healthy/ COPD) and day (7/28) and

random donor effects were included and p values were adjusted for multiple comparisons using the Benjamini-Hochberg method.

3.2.5. Inhibition of the Pi3 kinase pathway does not reduce NTHi invasion of the ciliated epithelium.

Activation of the PI3K pathway by NTHi has been repeatedly reported in several studies, which also emphasize its role in regulating the process of invasion of respiratory epithelial cell lines by NTHi (Lopez-Gomez et al., 2012; Morey et al., 2011; Seiler et al., 2013). However, to date, no study has investigated the role of this pathway in NTHi invasion of primary ciliated epithelial cultures. Therefore, in order to understand whether the PI3K pathway regulates NTHi invasion in ALI epithelial cultures, ciliated epithelial cultures from healthy or COPD donors were treated with 2 different pan PI3K inhibitors: the commercially available LY-294002 hydrochloride and GSK987740A (section 2.25) and then infected with NTHi (section 2.19). At 24h post infection, NTHi invasion of the epithelium was quantified using a gentamicin killing assay (section 2.24) and the percentage of Akt phosphorylation at Ser473 and Thr308 out of total Akt expressed was quantified (section 2.26) as a measure of PI3K pathway activation. Initial experiments were carried out by adding NTHi to the apical surface of the epithelium in 200 µl of basal epithelial medium and incubating it for 24 hours, as described in section 2.19. However, preliminary data showed high levels of Akt phosphorylation at Ser473, ranging from 5% at 2h post infection to 20% at 24 h post infection, in both healthy and COPD cultures, uninfected control and NTHi infected wells (Figure shown in Appendix 2). These results suggested that flooding was stimulating PI3K activation and subsequent Akt phosphorylation and could have masked any

NTHi stimulated activation. The method was subsequently changed to deliver NTHi to epithelial cultures in a non-flooding volume of 10 µl of medium. All infection experiments in this section were carried out with this method, described in Section 2.25.

First, it was confirmed that the vehicle control (the solvent in which the Pi3K inhibitor compounds were dissolved, in this case DMSO) did not significantly change bacterial invasion in either healthy or COPD cultures when compared with the untreated control (healthy, p=0.758, COPD, p=0.696). Therefore, all subsequent comparisons were made against the vehicle control. Unexpectedly, treatment with LY-294002 did not significantly reduce NTHi invasion in healthy (p=0.696) or COPD cultures (p=0.696). Similarly, invasion was not reduced by the GSK987740A pan Pi3K inhibitor in either healthy or COPD (p=0.696 in both cases). Therefore, contrary to previously published studies, these data suggest that inhibition of the PI3K pathway does not affect NTHi invasion of ciliated epithelial cultures from healthy or COPD donors.

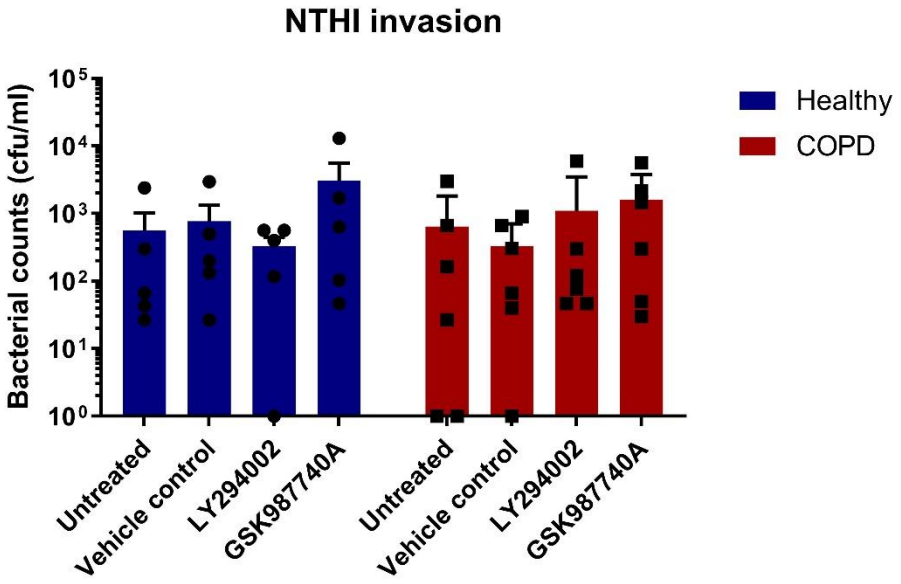

Figure 17. Effect of PI3K inhibition on NTHi invasion of ciliated epithelial cultures

Ciliated epithelial cultures were pre-treated basolaterally with either vehicle control or Pi3k inhibitor compound for 1h prior to NTHi 49247 addition ($5x10^6$ CFU/well) (section 2.25). NTHi invasion of the epithelium was quantified using a gentamicin killing assay at 24 hours post infection (section 2.24). N=5 healthy, 6 COPD donors. For statistical analysis, bacterial counts were log10 transformed and analysed using a linear mixed effects model with fixed effects for disease group and inhibitor type and a random donor effect. P values were Benjamini-Hochberg adjusted for multiple comparisons. Symbols represent individual donors. Data are presented as mean ± standard error of the mean.

3.2.6. NTHi does not stimulate Akt phosphorylation

Next it was important to determine whether the lack of effect of the two PI3K inhibitors on bacterial invasion was a consequence of the pathway not being activated by NTHi or of the inhibitors not having the predicted effect. Activation of the PI3K pathway leads to direct phosphorylation of the serine/threonine kinase Akt at two phosphorylation sites, namely Serine 473 and Threonine 308 (as described in the introduction of this chapter, section 3.2.1.1), and as such

it was used as a surrogate marker of PI3K activation (Fruman et al., 2017). Therefore, the percentage of Akt phosphorylated at these two sites out of the total Akt expressed was quantified following NTHi infection (Section 2.26).

The percentage of phosphorylated Akt out of total Akt was measured at 2 hours post NTHi infection, as an early infection time-point, and at 24 hours post NTHi infection, when bacterial invasion was also quantified (Figure 18). Contrary to published results, there was no increase in Akt phosphorylation following NTHi infection at either 2 hours or 24 hours post infection. When compared to the uninfected control, NTHi did not up-regulate Akt phosphorylation at either the Ser473 or Thr308, in either healthy or COPD cultures ($p>0.05$ in all cases).

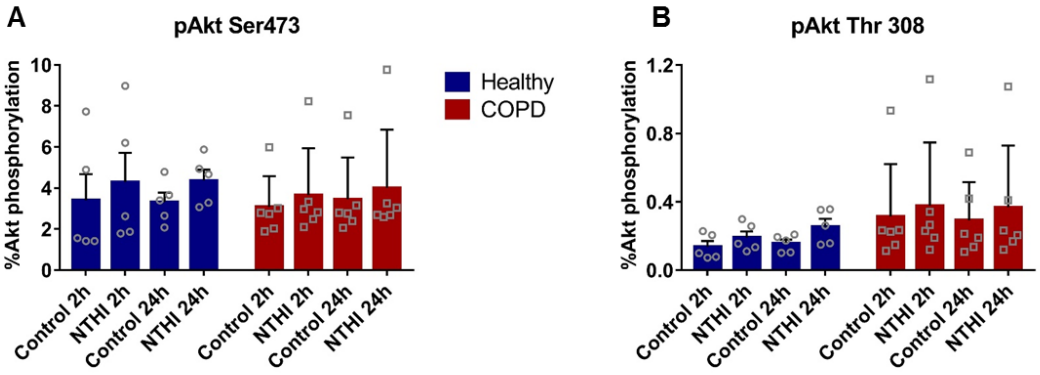

Figure 18. Quantification of Akt phosphorylation following NTHi infection of ciliated epithelial cultures

The percentage of phosphorylated Akt out of total Akt expressed, at Serine 473 and Threonine 308 sites, was quantified by MSD immunoassay as described in section 2.26., after 2 or 24 hours of NTHi 49247 infection (5x10^6 CFU/well) of ciliated epithelial cultures. Symbols indicate individual donors. N=5 healthy, 6 COPD donors. For statistical analysis, values for pAkt percentages were log10 transformed and linear mixed effects models were fitted separately for the Ser473 and Thr308 endpoints. Fixed effects were included for disease group, time and infection and a random effect for donors. P values were Benjamin- Hochberg corrected for multiple comparisons. Data are presented as mean ± standard error of the mean.

Next, it was important to confirm that the pan PI3K inhibitors were indeed functional and that they did inhibit activation of the PI3K signalling pathway. Thus, Akt phosphorylation at Ser473 and Thr308 was quantified after treatment of epithelial cultures with the LY294002 or the GSK987740A compounds, at either 2 hours or 24 hours post NTHi infection (Figure 19). It was first confirmed that vehicle control treatment of epithelial cultures did not affect the percentage of Akt phosphorylation compared to untreated cultures. The percentage of Akt phosphorylation was not significantly different in either healthy or COPD cultures, irrespective of time point, infection treatment or phosphorylation site analysed between untreated cultures or vehicle control

treated cultures ($p>0.05$). Therefore, all subsequent comparisons were carried out against the vehicle control treated cultures. As shown in Figure 19 A & B, the LY294002 and the GSK987740A compounds both significantly reduced phosphorylation of Akt at Ser473 when compared to the vehicle control condition, irrespective of the time point analyzed, disease group or infection treatment ($p<0.05$ in all cases). With the exception of the healthy uninfected group at 2h, the GSK987740A compound reduced Akt phosphorylation significantly more than the LY294002 compound in all treatment groups ($p<0.05$). Phosphorylation of Akt at Thr308 (Figure 19 C&D) was also significantly reduced by the GSK987740A compound at both time-points, irrespective of disease group or infection treatment ($p<0.001$ for all comparisons). With the exception of uninfected healthy cultures analyzed at 2h post infection where the LY294002 compound did not significantly reduce Akt phosphorylation ($p=0.084$), the compound significantly reduced levels of Akt in all other treatment groups ($P<0.05$). Comparisons of the levels of Akt phosphorylation between time-points or disease groups indicated no statistically significant difference ($p>0.05$), confirming that any pAkt detected is likely coming from background activation as opposed to external stimulation.

In conclusion, these data confirm that both the LY294002 and GSK987740A compounds were able to significantly reduce Akt phosphorylation. However, as NTHi did not up-regulate phosphorylation of Akt, thus not activating the PI3K pathway, it is likely that this is the reason why no effect on bacterial invasion was detected following treatment with the pan-PI3 kinase inhibitors.

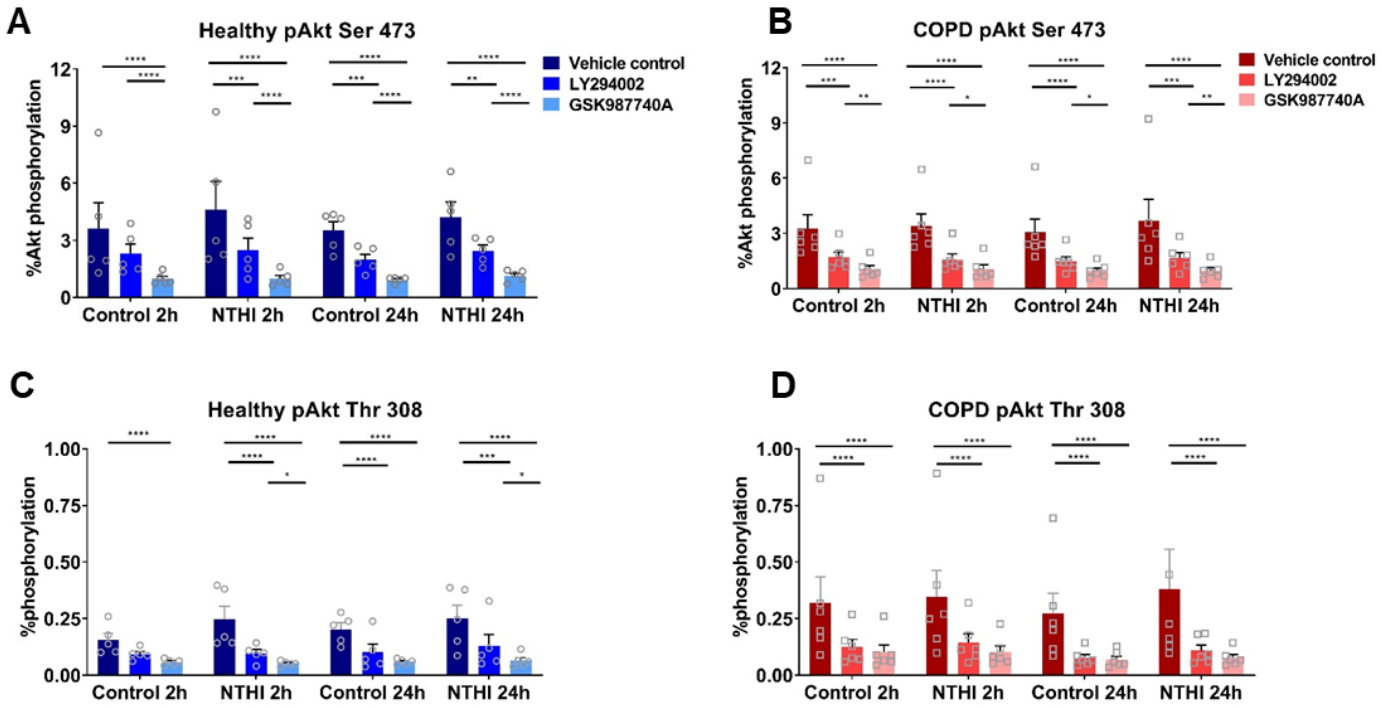

Figure 19. Effect of pan-PI3k inhibitors on Akt phosphorylation after NTHi infection of ciliated epithelial cultures

Epithelial cultures were pre-treated with vehicle control, LY294002 or GSK987740A compounds for 1h prior to infection with NTHi strain 49247 ($5x10^6$ CFU/well). The percentage of phosphorylated Akt out of total Akt was quantified at the Serine 473 and Threonine 308 sites at 2h and 24 h post NTHi infection by MSD immunoassay. Symbols represent individual donors. N= 5 healthy, 6 COPD donors. For statistical analysis, values for pAkt percentages were log10 transformed and linear mixed effects models were fitted separately for the Ser473 and Thr308 endpoints. Fixed effects were included for disease group, time, treatment and infection and a random effect for donors. P values were Benjamin- Hochberg corrected for multiple comparisons. Data are presented as mean ± standard error of the mean. *= p<0.05, **=p<0.01, ***=p<0.001, ****=p<0.0001.

3.2.7. Discussion

NTHi is known to commonly colonise the nasopharynx of healthy individuals as a commensal while numerous reports have described lower airway colonisation by NTHi in COPD (Ahearn et al., 2017; Bandi et al., 2001). However, despite NTHi being the most prevalent pathogen detected in the airways of patients with COPD at stable state and during disease exacerbations, there is very little understanding of the initial interaction of NTHi with the respiratory ciliated epithelium and the molecular events occurring within the host cell (Wilkinson et al., 2017). The current investigation provides evidence to show that within minutes of addition to a ciliated epithelial culture, NTHi was bound to rapidly beating cilia of both healthy and COPD cultures, as recorded live by confocal microscopy (Figure 11). This observation was subsequently reproduced by imaging NTHi attached to cilia by scanning electron microscopy as well as by image cytometry. By image cytometry both NTHi strains 1479 and 49247 attached to cilia of bronchial and nasal epithelial cultures, respectively, suggesting that the binding of NTHi to cilia is strong enough to resist the numerous processing steps involved in sample preparation for this method. This observation is in agreement with the report by Baddal et al. (2015), which showed NTHi attached to cilia at 1 hour post addition to a ciliated culture. In contrast, a different study has reported that NTHi does not bind to cilia or ciliated cells (Ketterer et al., 1999). It is possible that in their study the delivery method of NTHi to the apical surface of the epithelium in 10 µl of liquid medium favoured spread and interaction of NTHi with the surface epithelium whereas binding to motile cilia was limited. Interestingly, heat inactivated NTHi was also found to bind to cilia by all three

methods used (live confocal video microscopy, scanning electron microscopy, image cytometry), suggesting that binding to cilia does not require live bacteria and it might be a mechanism of host protection to prevent bacterial interaction with the epithelial surface. Following the initial interaction of NTHi with cilia, NTHi was found to invade the respiratory epithelial cultures from both healthy and COPD donors, in agreement with previous reports showing NTHi invasion of epithelial cell lines or of epithelial samples collected from the airways of COPD donors (Bandi et al., 2001; Clementi et al., 2014; Morey et al., 2011). Interestingly, however, was that live NTHi appeared to preferentially invade non-ciliated epithelial cells of both healthy and COPD cultures, as shown by image cytometry (Figure 15). Internalisation of heat killed NTHi was still predominantly in non-ciliated epithelial cells, but at much lower levels compared to live NTHi, suggesting that invasion occurs preferentially in non-ciliated cells and is dependent on the bacteria being alive. Furthermore, when invasion was quantified in healthy pre-ciliation day 7 epithelial cultures (Figure 16C) a trend was observed where invasion was higher than in ciliated epithelial cultures, suggesting that, prior to ciliation, healthy epithelial cultures are more susceptible to NTHi invasion. However, in COPD epithelial cultures the trend was reversed and it appeared that ciliated cultures were more susceptible to NTHi invasion compared to pre-ciliation cultures. Due to inter-donor variability, these observations did not achieve statistical significance. However, they do corroborate the fact that NTHi binds extracellularly to ciliated cells and to cilia and invades non-ciliated epithelial cells and it is therefore possible to speculate that the reduced ciliation of COPD cultures as shown in section 3.1.4 and reported previously could be one of the reasons why differentiated COPD

cultures are less protected against NTHi invasion (Auerbach et al., 1979; Ghosh et al., 2018). This is because it has been shown that cilia and the periciliary fluid containing a mesh of cell membrane tethered mucins form a protective barrier that prevents anything bigger than 40 nm from reaching the cell surface (Button et al., 2012). A similar mechanism might therefore also protect epithelial cells from NTHi internalisation provided ciliation is not disrupted and the epithelial surface exposed. In the future, characterisation of epithelial cell types and expression of receptors used by NTHi for adhesion and invasion could provide further understanding of the mechanisms that lead to a different invasive behaviour between healthy and COPD pre-ciliation and ciliated cultures and whether these can be targeted therapeutically.

In addition to binding to the ciliated and non-ciliated epithelial cells, NTHi was also observed to undergo morphological changes with formation of elongated chains within the first 24 hours of infection of healthy and COPD ciliated cultures (Figure 12.). Chains formed on epithelial cultures were significantly longer than chains formed by NTHi incubated in basal epithelial medium alone (Figure 12G), suggesting that long filaments form as a consequence of interaction with the ciliated epithelium. Chain formation by other bacterial species such as uropathogenic *Escherichia coli* (*E. coli*) has been described to provide a selective advantage against phagocytosis by immune cells such as neutrophils and macrophages (Horvath et al., 2011). This was shown by challenging mixed population of bacillary and filamentous *E. coli* with human or mouse macrophages and showed that bacillary forms of bacteria were preferentially killed over filamentous *E.coli* (Horvath et al., 2011). Therefore,

chain formation may also provide the same selective advantage for NTHi persistence on ciliated epithelium.

Availability of the essential nutrient iron has been linked to changes in NTHi morphology in a study where bacteria were grown in a defined medium in the presence or absence of heme-iron to generate heme-iron replete or restricted NTHi, respectively (Szelestey et al., 2013). In this study, heme-iron restricted NTHi formed filamentous morphotypes and a biofilm with a lace like architecture which was different to the mat-like biofilm formed by heme-iron replete NTHi, which predominantly contained rods (Szelestey et al., 2013). On ciliated cultures, NTHi formed aggregates with a lace-like architecture within the first 2 hours of addition to ciliated cultures which evolved to cover extensive areas of the epithelial surface by 24h post infection and which were observed to contain filamentous morphotypes. This indicates NTHi adapt to a hostile environment in which the host sequesters iron and essential nutrients. Biofilm formation by NTHi is also thought to be a mechanism of bacterial persistence in the respiratory tract, by hindering immune cell clearance and having increased resistance to antibiotic therapy compared to planktonic bacteria (Pang et al., 2008; Slinger et al., 2006; Starner et al., 2006; Swords, 2012). In the current investigation, NTHi was found to form aggregates resembling biofilms over ciliated epithelial cultures from both healthy and COPD donors within 24 hours. These aggregates were also found to reduce ciliary beat amplitude without affecting ciliary beat frequency (Figure 13), therefore likely impairing the process of muco-ciliary transport and bacterial clearance from the lungs. While there are no reports of ciliary amplitude assessment during NTHi infection, ciliary beat frequency was previously reported to be decreased

by NTHi in studies using *ex vivo* bovine and human epithelial tissue samples (Bailey et al., 2012; Janson et al., 1999). It is possible that several factors linked to the different methodologies and types of tissue used may account for the different results of these studies and the current investigation. These include the use of different bacterial strains, the fact that both of these studies were carried out on epithelial samples directly collected from airways and cultured for several days to weeks, which may alter their response to infection or this may already differ in comparison to that of ALI cultured and differentiated epithelial cells. Furthermore, the study by Bailey et al. (2012) did not use live bacteria for infection but rather NTHi culture supernatants. Ultimately, the infection method used in this present study involved flooding of the epithelial cultures which appeared to promote an increase in ciliary beat frequency, particularly noticeable in healthy cultures at 8h and 24h post infection, irrespective of infection treatment. As hydration of the airway surface fluid is known to increase ciliary beat frequency, it is possible that this effect may have masked the NTHi induced decrease in ciliary beat frequency (Boucher, 2019).

Epithelial invasion by NTHi was dependent on live NTHi, as shown in this study, but previous reports have indicated that epithelial cell signalling pathways are also important in mediating bacterial invasion. In particular, several studies have identified that Pi3K signalling is essential in regulating NTHi internalisation into the epithelial cell lines A549, Calu-3 or 16HBE14 (Lopez-Gomez et al., 2012; Morey et al., 2011; Seiler et al., 2013; Swords et al., 2001). These studies have shown that NTHi infection resulted into phosphorylation of Akt, a surrogate marker of Pi3K activation and subsequent

treatment with commercially available Pi3K inhibitors inhibited NTHi invasion (Lopez-Gomez et al., 2012; Morey et al., 2011; Seiler et al., 2013; Swords et al., 2001). In contrast, in the current study primary ciliated nasal epithelial cultures from healthy or COPD donors, NTHi did not induce activation of the Pi3K pathway, as determined by lack of increased phosphorylation of Akt at the Ser473 or Thr308 sites during infection (Figure 18). Furthermore, inhibition of the Pi3K signalling pathway with the same LY294002 Pi3K inhibitor compound used in previous studies (Lopez-Gomez et al., 2012; Morey et al., 2011; Seiler et al., 2013) or with the GSK987740A pan-Pi3K inhibitor did not reduce NTHi invasion (Figure 17), despite both inhibitors successfully reducing background levels of Akt phosphorylation (Figure 19), confirming their predicted inhibitory effect. It is possible that the different results obtained in the studies by Morey, Lopez-Gomez, Swords and Seiler using epithelial cell lines versus primary differentiated epithelial cells used in this study is a consequence of the methods used for immortalization of cell lines. In the process of transforming them to replicate indefinitely and behave like cancer cells, epithelial cell lines often suffer mutations in genes that encode for proteins with roles in cellular survival and proliferation (Tym et al., 2015). Among the hundreds of gene mutations identified in both A549 and Calu3 cell lines, both have mutations in the Rat Sarcoma (RAS) proto-oncogene which belongs to the small GTPase family (Tym et al., 2015). PI3k signaling is one of the many effector pathways downstream of RAS and therefore mutations in RAS may lead to enhanced activation of the Pi3K pathway (Castellano and Downward, 2011). An endogenous activation of the Pi3K pathway or other pathways interacting with PI3K-Akt signaling that play a role in bacterial

invasion may explain the results obtained in studies investigating NTHi invasion of epithelial cell lines and the different results seen when infection is carried out in primary ciliated epithelial cultures.

In conclusion, this investigation has provided evidence to show that NTHi interacted with rapidly beating cilia of both healthy and COPD cultures within minutes of addition to an epithelial culture, that NTHi was bound to ciliated cells extracellularly whereas invasion occurred preferentially within non-ciliated epithelial cells, thus suggesting that ciliation may offer a protective barrier against bacterial invasion. Furthermore, NTHi internalization into primary ciliated epithelial cultures from both healthy and COPD appeared to be independent of PI3K pathway activation. Over 24 hours, NTHi underwent conformational changes with formation of filamentous morphotypes, formed aggregates with a lattice like organization which evolved to cover large areas of the epithelial surface. Aggregate formation caused a reduction in ciliary beat amplitude, thus reducing ciliary function. Therefore, epithelial invasion by NTHi, formation of filamentous morphotypes, of biofilm-like aggregates and reduction in ciliary function are likely to prevent efficient clearance of NTHi from the airways by mucociliary transport or immune cells and allow persistence despite antibiotic therapy, which is particularly relevant in patients with COPD.

3.3. Studying the effect of RV and NTHi co-infection on epithelial barrier function and inflammatory mediator production

3.3.1. Introduction

Rhinovirus, the main cause of the common cold in healthy individuals, is also the main cause of virus induced exacerbations in patients with COPD (McManus et al., 2008; Rohde et al., 2003b; Seemungal et al., 2001). The causative role of RV in the induction of COPD exacerbations has been shown in human experimental infections (Mallia et al., 2011). In addition, following a naturally occurring or experimental RV infection, patients with COPD were predisposed to develop secondary bacterial infections (George et al., 2014; Mallia et al., 2012). The odds ratio of COPD exacerbation were found to be higher when RV16 and NTHi were detected together, compared to single infections, and in particular to NTHi infection alone (Wilkinson et al., 2017). NTHi, a silent commensal coloniser in healthy individuals, is the bacterial pathogen most frequently detected in the airways of patients with COPD, both at stable state and during disease exacerbations (Wilkinson et al., 2017; Wilkinson et al., 2006). Furthermore, COPD exacerbations where viral-bacterial co-infection was detected were found to be associated with more severe symptoms, increased inflammation and longer hospitalisation time, as discussed in section 1.21 (Wilkinson et al., 2006). However, it is still unclear whether an interplay between RV and NTHi may account for the increased risk of COPD exacerbations when both pathogens are detected and whether co-infection with RV could account for the switch in NTHi from being a silent coloniser to inducer of disease exacerbations.

In order to infect human hosts, respiratory pathogens such as RV and NTHi have to interact with the airway ciliated epithelium and disrupt its protective barrier function (Vareille et al., 2011). The airway epithelial layer possesses several mechanisms for host protection against infection and these include: mucociliary clearance, through ciliary beating and mucus production, a physical barrier through formation of tight junctions between epithelial cells, and production of antimicrobial peptides and inflammatory mediators to actively fight the infection and recruit specialised effector immune cells (Aghapour et al., 2018; Rezaee and Georas, 2014; Vareille et al., 2011).

However, knowledge about the direct effect of RV and NTHi infection on respiratory epithelial structure and barrier function remains incomplete and it is surprisingly limited in relation to RV and NTHi co-infection, which is particularly relevant for understanding their pathogenesis during COPD exacerbations. As presented in section 1.14, RV has been shown to infect and replicate in epithelial cells, particularly targeting ciliated cells, over goblet and basal cells, and causing ciliated cells to shed from the epithelium, consequently leading to a decrease in airway ciliation (Jakiela et al., 2014; Tan et al., 2018). However, the effect of RV on ciliary function and mucociliary clearance has not been studied in either healthy or COPD epithelium. In contrast, several studies have indicated a role for RV16 infection in stimulating mucus hypersecretion and goblet cell hyperplasia (Hewson et al., 2010; Jakiela et al., 2014; Jing et al., 2019; Liu et al., 2019; Tan et al., 2018). In particular, Hewson et al. (2010) detected increased epithelial release of MUC5AC in bronchoalveolar lavage and nasal lavage of healthy and asthmatic patients following human experimental RV infection and confirmed these

findings *in vitro*, by studying infections of airway epithelial cultures. More recently, Jing et al. (2019) identified that RV infection can induce goblet cells hyperplasia and up-regulation of mucin genes' expression which can be detected in cultures of primary tracheobronchial epithelial cells from COPD patients at 15 days post infection. In contrast, these changes were not seen in cultures from healthy individuals (Jing et al., 2019).

Knowledge of the effect of NTHi on ciliary function is also very limited and has been discussed in section 3.2.7 of this thesis. Briefly, two previous reports have suggested that ciliary function could be decreased by NTHi in models using human and bovine cultured tissue explants, whereas results of this investigation (Figure 13) indicated no effect of NTHi on ciliary beat frequency in either healthy or COPD cultures (Bailey et al., 2012; Janson et al., 1999). Instead, a decrease in ciliary beat amplitude was detected, as a result of NTHi aggregate formation over ciliated cells (Figure 13). Several studies have shown that *in vitro* NTHi is able to stimulate mucus production, in particular through up-regulation of *MUC5AC* (Chen et al., 2004; Komatsu et al., 2008; Konduru et al., 2017; Shen et al., 2008; Val et al., 2015). However, all these investigations were carried out using either respiratory or middle ear epithelial cell lines and some mimicked an NTHi infection by using NTHi cell lysates, as opposed to live bacteria for epithelial cell inoculation (Chen et al., 2004; Komatsu et al., 2008; Konduru et al., 2017; Shen et al., 2008; Val et al., 2015). More recently, RNA sequencing of primary ciliated epithelial cultures infected with NTHi revealed an up-regulation of mucin genes *MUC5B* and *MUC4*, but did not detect a change in *MUC5AC* (Baddal et al., 2015). No study to date has investigated the effect of a RV and NTHi co-infection on ciliary function

and mucus production by primary differentiated epithelial cells from either healthy or COPD donors.

Another mechanism by which the airway epithelium protects the host from inhaled pathogens and particulates is the formation of apical junctional complexes between neighbouring cells (Aghapour et al., 2018; Rezaee and Georas, 2014). Epithelial junctional complexes comprise the apically localised tight junctions, the more basolateral placed adherens junctions and the basal desmosomes (Aghapour et al., 2018; Rezaee and Georas, 2014). Tight junction complexes consist of trans-membrane proteins, occludin, claudin, junctional adhesion molecules and cytoplasmic molecules such as zonula occludens (ZO)-1,2,3 or cingulin (Aghapour et al., 2018). Through cytoplasmic molecules tight junction complexes can interact with the cell actin cytoskeleton to preserve their own stability (Aghapour et al., 2018). The adherens junction complexes consist of the type 1 transmembrane cadherin E-cadherin and the anchor proteins p120 catenin, β-catenin and α-catenin, which anchor the complex to the cytoskeleton (Aghapour et al., 2018; Niessen, 2007). An integral epithelial barrier ensures cell-cell adhesion, restricts transmigration of pathogens from the airway lumen, allows para-cellular transport of ions and certain molecules and plays important roles in signalling to establish apical-basal polarity during epithelial differentiation (Niessen, 2007; Rezaee and Georas, 2014). Disruption of the epithelial barrier has been linked with cigarette smoke exposure, oxidative stress and inflammatory cytokines, all of which are thought to increase epithelial permeability and contribute to airway inflammation, oedema and airway epithelium injury (Aghapour et al., 2018; Rezaee and Georas, 2014). However, an understanding of the role of

infectious pathogens on epithelial integrity is limited. Both RV and NTHi have individually been shown to affect epithelial barrier function during infection (Baddal et al., 2015; Comstock et al., 2011; Sajjan et al., 2008). RV infection of polarised airway epithelial cells was shown to decrease trans-epithelial electrical resistance and to allow NTHi trans-migration across the epithelium (Sajjan et al., 2008). Expression of several tight junction proteins was shown to be down-regulated by RV infection and these include: tight junction protein 1/ ZO-1, claudin 1, claudin 8, claudin 12 or occludin (Faris et al., 2016; Looi et al., 2018; Looi et al., 2016; Sajjan et al., 2008). Similarly, NTHi was shown to cause down-regulation of numerous genes encoding for proteins of the tight-junction complex, including *claudin 3*, *claudin 8* or *ZO-1* in a study using differentiated, ciliated epithelial cultures (Baddal et al., 2015). Infection of the A549 epithelial cell line by NTHi was shown to disrupt expression of the adherens junction protein E-cadherin (Kaufhold et al., 2017). However, a study involving long term co-culture of ciliated epithelial cultures with NTHi reported no decrease in trans-epithelial electrical resistance during 8 days of bacterial infection (Ren et al., 2012). Therefore, the consequence of NTHi infection on epithelial barrier integrity and junctional complex structure requires further investigation. Moreover, despite suggestions that both RV and NTHi can individually impact epithelial barrier function, there is no information on the effect that their co-infection would have on the epithelium junctional integrity and whether this is different in COPD epithelia compared to healthy. Ultimately, the airway epithelium also plays an innate immune function by secreting inflammatory mediators in response to viral and bacterial infection (Gomez and Prince, 2008; Vareille et al., 2011). Epithelial cells secrete

cytokines and chemokines which have roles in the recruitment and activation of innate immune cells such as neutrophils, macrophages, NK cells or eosinophils as well as of adaptive immune cells such as T and B lymphocytes and the antigen-presenting dendritic cells (Vareille et al., 2011). A list of pro-inflammatory mediators secreted by respiratory epithelial cells in response to viral or bacterial infection and some of their main functions is shown in Table 8. Of interest, RV infection of cultured COPD epithelial cells was shown to induce higher levels of inflammatory mediators (IL-6, IL-8, GRO-α, IFN-λ and IP-10) compared to levels found in supernatants from healthy cultures (Schneider et al., 2010). In contrast, no study has investigated the response of COPD epithelial cells to infection with NTHi, in comparison to that of healthy cells, which is surprising given the burden that NTHi represents in COPD pathology. In response to NTHi infection, healthy airway epithelial cells have been reported to produce IL-1β, IL-8, ENA-78, IP-10, MCP-1, RANTES or MIP-1α (Amatngalim et al., 2017; Baddal et al., 2015). In addition, only a very limited number of studies have investigated the effect of RV and NTHi co-infection on inflammatory mediators produced by respiratory epithelial cells. One study by Unger et al. (2012), reported that RV infection of a bronchial epithelial cell line reduced production of IL-8 during a subsequent NTHi infection and resulted in delayed neutrophil recruitment and bacterial clearance during *in vivo* infection of mice. In contrast, pre-treatment of primary bronchial epithelial cells with heat inactivated NTHi was found to up-regulate expression of the RV specific receptor ICAM-1 and induce an increased expression of pro-inflammatory mediators such as IL-6 and IL-8 during a subsequent RV16 infection (Gulraiz et al., 2015). Two other studies identified that simultaneous infection of

epithelial cells with RV and NTHi leads to synergistic induction of IL-8, CCL20 and IL-17C (Jamieson et al., 2019; Maciejewski et al., 2017). In particular, following RV1A and NTHi co-infection, COPD bronchial epithelial cells produced significantly more IL-17C compared to levels released by cells from non-smokers and healthy smokers (Jamieson et al., 2019). However, all of these studies were performed in epithelial cell lines or primary epithelial cultures grown as submerged monolayers, as opposed to differentiated, polarised cultures. Therefore, further investigations are required to understand the effect of RV and NTHi co-infection on the inflammatory response of well differentiated epithelia from healthy and COPD donors.

Table 8. Cytokines and chemokines produced by respiratory epithelial cells in response to viral or bacterial infection.

Analyte	Virus	Bacteria	Role in infection
IL-1β	x	x	Induction of the acute phase response Monocyte/macrophage recruitment DC maturation Th2 cell recruitment
IL-6	x	x	Induction of the acute phase response Activation of T lymphocytes
TNF-α	x	x	Induction of the acute phase response Monocyte/macrophage recruitment

IFN-α/β	x		NK cell recruitment and activation Activation of DCs and macrophages Direct antiviral effects
IFN-λ	x		Direct antiviral effect Activation of DCs and macrophages
IL-17C		x	Th17 cell activation Stimulates epithelial production of antimicrobial peptides
IL-8 /CXCL8	x	x	Neutrophil recruitment
Gro-α /CXCL1	x		Neutrophil recruitment
ENA-78 /CXCL5	x		Neutrophil recruitment
GM-CSF	x	x	Eosinophil recruitment
G-CSF		x	Neutrophil differentiation
Eotaxin-1 /CCL11	x		Eosinophil recruitment
Eotaxin-2 /CCL24	x		Eosinophil recruitment

RANTES/ CCL5	x		Eosinophil recruitment Th1 cell recruitment
IP-10 /CXCL-10	x	x	Th1 cell recruitment
MIP-1α /CCL3	x	x	NK cell recruitment and activation Monocyte/macrophage recruitment
MCP-1 /CCL2	x	x	Monocyte/macrophage recruitment
MIP-3α /CCL20	x		DC recruitment
IL-15	x		DC maturation
TSLP	x		DC maturation

References: (Baddal et al., 2015; Gomez and Prince, 2008; Ioannidis et al., 2013; Kusagaya et al., 2014; Message and Johnston, 2004; Murphy and Weaver, 2017; Pfeifer et al., 2013; Vareille et al., 2011; Wack et al., 2015; Yamaguchi et al., 2018)**.**

Hypothesis:

RV and NTHi co-infection of primary respiratory epithelial cultures from healthy and COPD donors causes more epithelial barrier disruption and inflammation than infection with NTHi alone.

Aims:

- To determine the effect of RV and NTHi co-infection of primary epithelial cultures on ciliary function.
- To determine the effect of RV and NTHi co-infection of primary epithelial cultures on mucin gene expression.
- To determine the effect of RV and NTHi co-infection on epithelial barrier integrity.
- To quantify the inflammatory response of primary epithelial cultures to RV and NTHi co-infection.
- To determine the effect of epithelial differentiation stage on the course of RV and NTHi co-infection and their effect on mucin gene expression, epithelial barrier integrity and inflammatory responses.

3.3.2. Rhinovirus and NTHi co-infection reduces ciliary beat frequency in healthy ciliated epithelial cultures

To determine the effect of RV and NTHi co-infection on epithelial barrier function, including ciliary function, mucus gene expression, epithelial integrity and inflammatory response, healthy and COPD nasal epithelial cultures were differentiated for either 6 days or 28 days before being infected with RV. Twenty four hours after RV infection, cultures were challenged with NTHi for another 24 hours (section 2.30).

Ciliary beat frequency was measured as described in sections 2.12 and 2.13 prior to RV infection and at 24 hours post RV infection, prior to addition of NTHi. Subsequently, ciliary beat frequency was measured, immediately following addition of NTHi, (in 200 µl of BEBM, as described in section 2.30), at 8 hours and 24 hours post NTHi challenge. As shown in Figure 20, in both healthy and COPD ciliated cultures, rhinovirus infection alone did not alter the frequency of ciliary beating in the first 24 hours of infection ($p>0.05$ for all comparisons). Immediately after addition of NTHi ciliary function was maintained in both healthy and COPD cultures ($p>0.05$ for all comparisons). However, in healthy cultures, at 8 hours post NTHi infection, ciliary beat frequency was significantly reduced by RV and NTHi co-infection compared to the uninfected control well ($p= 0.011$), but not by either RV or NTHi infection alone ($p>0.05$). At 24 hours post NTHi addition, ciliary beat frequency was still significantly reduced by the RV and NTHi co-infection when compared to the uninfected control ($p=0.015$) and to infection with NTHi alone ($p=0.015$), but not with RV infection alone. Neither pathogen alone caused a significant decrease in the frequency of ciliary beating at this time-point.

In COPD cultures, the decrease in ciliary beat frequency caused by RV and NTHi co-infection was not detected as beat frequency appeared to remain constant on average throughout the experimental time-frame ($p>0.05$ for all comparisons). However, the large inter-donor variability may have masked any infection induced effect on ciliary beat frequency.

Therefore, based on results obtained in healthy ciliated cultures, these data suggest that RV and NTHi co-infection may have a more detrimental effect on ciliary beat frequency than NTHi infection alone and may inhibit efficient pathogen clearance from the airway.

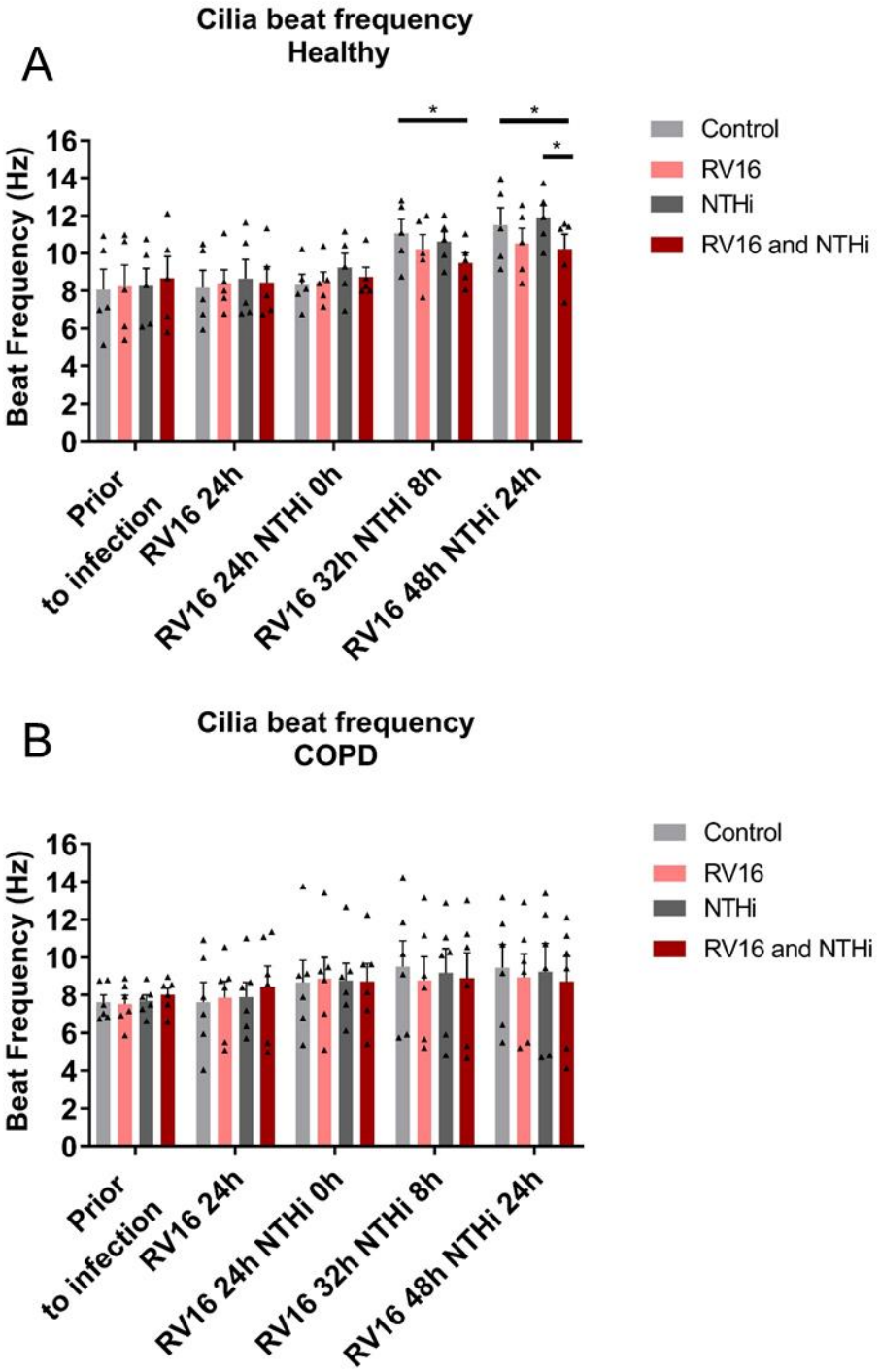

Figure 20. Effect of RV and NTHi co-infection on ciliary beat frequency

Ciliated cultures were infected with RV16 ($1.5x10^6$ $TCID_{50}$/well) for 24 hours, followed by challenge with NTHi 49247 ($5x10^6$ CFU/well). Cultures were at ALI prior to NTHi addition and subsequently submerged. At each time point, 10 high-speed videos per condition were recorded and used to determine average ciliary beat frequency for each donor. N= 5 healthy

donors, 6 COPD donors. For statistical analysis, cilia beat frequency values were log10 transformed and then analysed using a mixed linear effects model with fixed effects for disease group (healthy/COPD), infection (NTHi, RV) and time-point and a random effect for each donor. P values were adjusted for multiple comparisons using the Benjamini-Hochberg method. Data are presented as average ± standard error of the mean. *=p<0.05

3.3.3. Rhinovirus up-regulates expression of goblet cell specific transcription factor and mucin genes in ciliated cultures

To understand if RV and NTHi co-infection alters expression of the goblet cell specific transcription factor *SPDEF*, of secreted mucins *MUC5AC* and *MUC5B* as well as of the cell membrane tethered *MUC4*, pre-ciliation day 7 epithelial cultures and ciliated day 28 epithelial cultures from healthy and COPD donors were infected with RV alone, NTHi alone and both pathogens as described in section 2.30 (Button et al., 2012; Jing et al., 2019). Gene expression changes were analysed by qRT-PCR, as described in section 2.11.

In both healthy and COPD ciliated cultures, expression of the transcription factor *SPDEF* was upregulated by RV infection alone ($p<0.0001$ for both healthy and COPD) and by RV and NTHi co-infection ($p<0.0001$ for both healthy and COPD) when compared with uninfected control wells, as shown in Figure 21A. NTHi infection alone did not upregulate expression of *SPDEF* in either healthy or COPD ciliated cultures, when compared to uninfected control wells ($p>0.05$). As there was no significant difference in the expression of *SPDEF* in ciliated cultures infected with RV alone compared to those infected with RV and NTHi, it follows that the upregulation of *SPDEF* expression is driven by RV.

Similar to the up-regulation of *SPDEF* by RV, expression of *MUC5AC*, *MUC5B* and *MUC4* was also significantly increased by RV infection in both healthy and COPD ciliated cultures ($p<0.0001$ for all comparisons) (Figure 21 C,E,G). In contrast, NTHi infection alone only significantly increased expression of mucin *MUC5B* in COPD ciliated cultures compared to uninfected controls ($p=0.020$), but did not change expression of MUC5B in healthy ciliated cultures or of *MUC5AC* or *MUC4* in either healthy or COPD ciliated cultures ($p>0.05$ for all comparisons). RV and NTHi co-infection significantly up-regulated expression of *MUC5AC*, *MUC5B* and *MUC4* in both healthy and COPD ciliated cultures when compared to uninfected cultures ($p<0.0001$ for all comparisons). No significant difference was detected between mucin gene expression induced by RV alone or by RV and NTHi-co-infection, again indicating that the increased mucin gene expression was induced by the virus. No significant differences were detected between gene expression levels in healthy cultures compared to COPD, irrespective of infection treatment ($p>0.05$).

In contrast to ciliated epithelial cultures, the effect of RV on pre-ciliation day 7 epithelial cultures was very limited. As it can be seen in Figure 21 B, D, F, H, RV infection only caused significant increases in expression of *SPDEF* in healthy cultures, compared to uninfected control ($p=0.001$) and of *MUC5B* in COPD cultures, compared to uninfected control ($p=0.041$). In all cases, expression of *SPDEF*, *MUC5AC*, *MUC5B* or *MUC4* after RV infection, either alone or during co-infection with NTHi, was significantly lower than in ciliated cultures, for both healthy and COPD cultures ($p<0.01$). In addition, expression of *MUC5B* was significantly lower in day 7 epithelial cultures compared to ciliated cultures at baseline, in both healthy and COPD ($p<0.05$). No difference

in expression levels of any of the genes analysed was detected between healthy and COPD cultures at day 7 ($p>0.05$).

In conclusion, results of this study indicate that RV infection alone can induce up-regulation of the goblet cell specific transcription factor *SPDEF* and of mucin genes *MUC5AC*, *MUC5B* and *MUC4* in both healthy and COPD ciliated cultures whereas NTHi was only able to up-regulated expression of *MUC5B* in COPD cultures. These responses were significantly reduced or completely absent in day 7 pre-ciliation cultures.

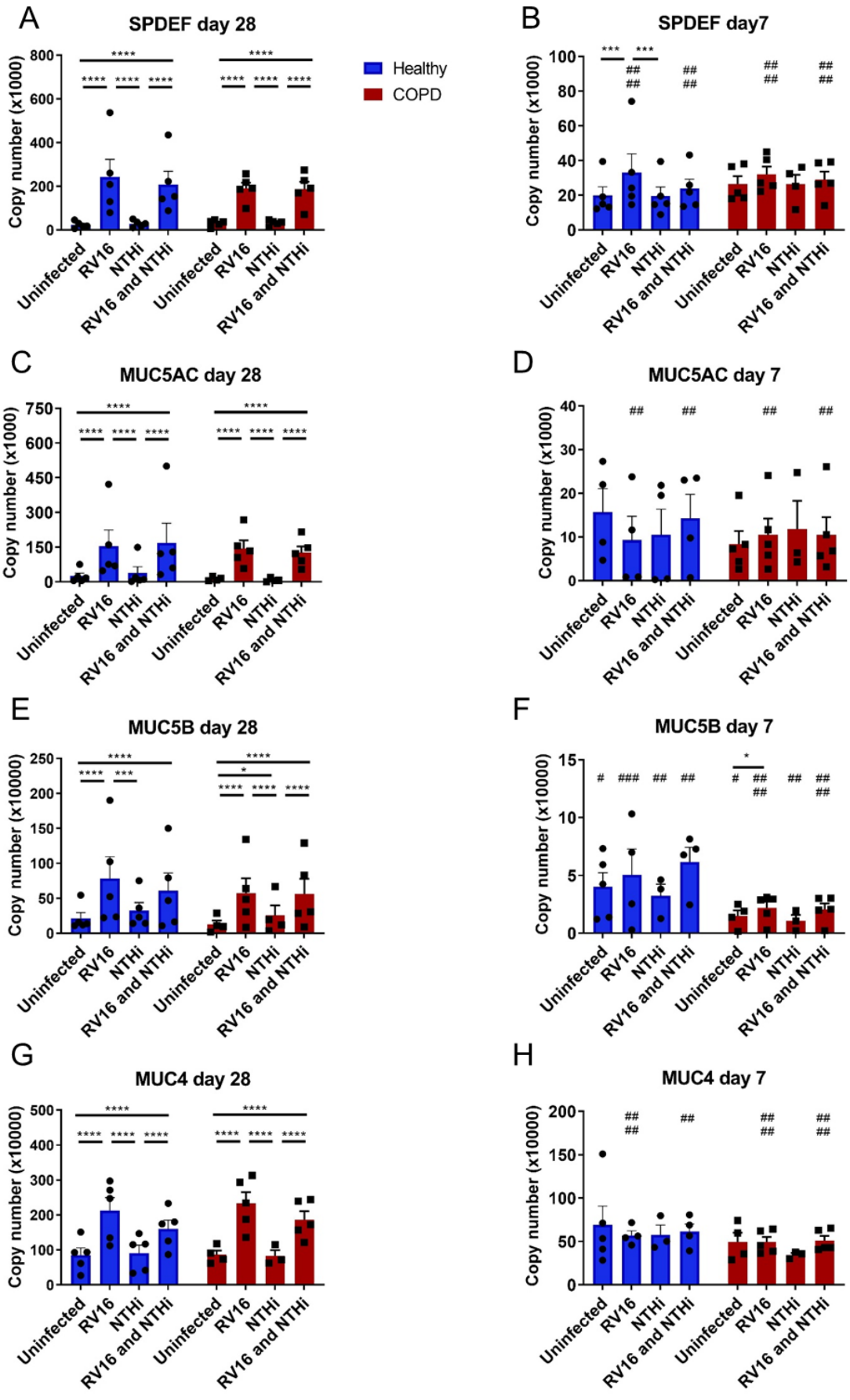
A
SPDEF day 28
Copy number (x1000)
Healthy
COPD
B
SPDEF day7
Copy number (x1000)
C
MUC5AC day 28
Copy number (x1000)
D
MUC5AC day 7
Copy number (x1000)
E
MUC5B day 28
Copy number (x10000)
F
MUC5B day 7
Copy number (x10000)
G
MUC4 day 28
Copy number (x10000)
H
MUC4 day 7
Copy number (x10000)
Uninfected
RV16
NTHi
RV16 and NTHi

Figure 21. *SPDEF* and mucin gene expression changes during RV and NTHi co-infection of primary epithelial cultures at day 7 and day 28 of differentiation

Gene expression levels of the transcription factor *SPDEF* (A,B) and mucins *MUC5AC* (C,D), *MUC5B* (E,F) and *MUC4* (G,H) were quantified by qRT-PCR in day 7 pre-ciliation cultures and fully differentiated ciliated epithelial cultures from healthy and COPD donors, following infection with RV16 alone ($1.5x10^6$ $TCID_{50}$/well), NTHi 49247 ($5x10^6$ CFU/well) alone or after RV-NTHi co-infection. Epithelial cells were pooled from 2 trans-wells/ condition for analysis. N=5 healthy and 5 COPD donors. Symbols represent individual donors. For statistical analysis, copy numbers were log 2 transformed and separate linear mixed effects models were fitted for each analyte, with fixed effects for disease group, day and infection and a day-specific random effect for each donor. P values were Benjamini-Hochberg adjusted for multiple comparisons. Data are shown as mean ± standard error of the mean. *=p<0.05, ***=p<0.001, ****=p<0.0001, #= denotes day 7 versus day 28 comparison within a treatment group, #=p<0.05, ##=p<0.01, ###=p<0.001, ####=p<0.0001.

3.3.4. Rhinovirus infection reduces epithelial barrier integrity in ciliated epithelial cultures

The maintenance of epithelial barrier function against infection is dependent on epithelial integrity. It has previously been reported that RV can lead to a decrease in epithelial resistance during infection (Comstock et al., 2011; Sajjan et al., 2008) and both RV and NTHi were individually reported to affect the structure of tight-junction complexes (Baddal et al., 2015; Looi et al., 2016; Sajjan et al., 2008). However, there is no understanding of the effect of RV and NTHi co-infection on epithelial integrity. As such, to answer this question, trans-epithelial electrical resistance (TEER) was measured in ciliated day 28 epithelial cultures and pre-ciliation day 7 epithelial cultures after infection with RV alone, NTHi alone or RV and NTHi co-infection, as described in section 2.7

In healthy ciliated cultures, RV infection caused a significant decrease in TEER, both during RV single infection ($p<0.0001$) and during co-infection with NTHi ($p<0.0001$), when compared to the uninfected control condition - Figure 22A. In COPD ciliated cultures, single RV infection caused a decrease in TEER compared to the uninfected control, but this was not statistically significant ($p=0.077$). During co-infection with NTHi, however, TEER was significantly reduced when compared to the uninfected control ($p<0.0001$) and to RV infection alone ($p=0.034$). Infection with NTHi alone did not affect TEER in healthy or COPD ciliated cultures (healthy: $p=0.552$, COPD: $p= 0.466$).

In contrast to ciliated cultures, the TEER of day 7 pre-ciliation cultures was not affected by RV infection alone, in either healthy or COPD cultures, when compared to the TEER of uninfected control wells ($p>0.05$), as shown in Figure 22B. In healthy cultures however, RV and NTHI co-infection significantly reduced TEER values when compared to the uninfected control ($p=0.018$). Despite this reduction in TEER during co-infection, TEER values of day 7 cultures after RV or RV and NTHi co-infection were still significantly higher than those of healthy ciliated cultures after RV infection ($p=0.004$) or after RV and NTHi co-infection ($p=0.026$), respectively, highlighting a different effect of RV on ciliated versus pre-ciliation epithelial cultures. In contrast, in pre-ciliation day 7 COPD cultures, RV and NTHi co-infection did not appear to affect TEER ($p>0.05$). A trend for lower TEER values in day 7 COPD cultures compared to day 7 healthy cultures was observed, however this did not achieve statistical significance ($p=0.055$ between untreated control healthy and COPD epithelial cultures).

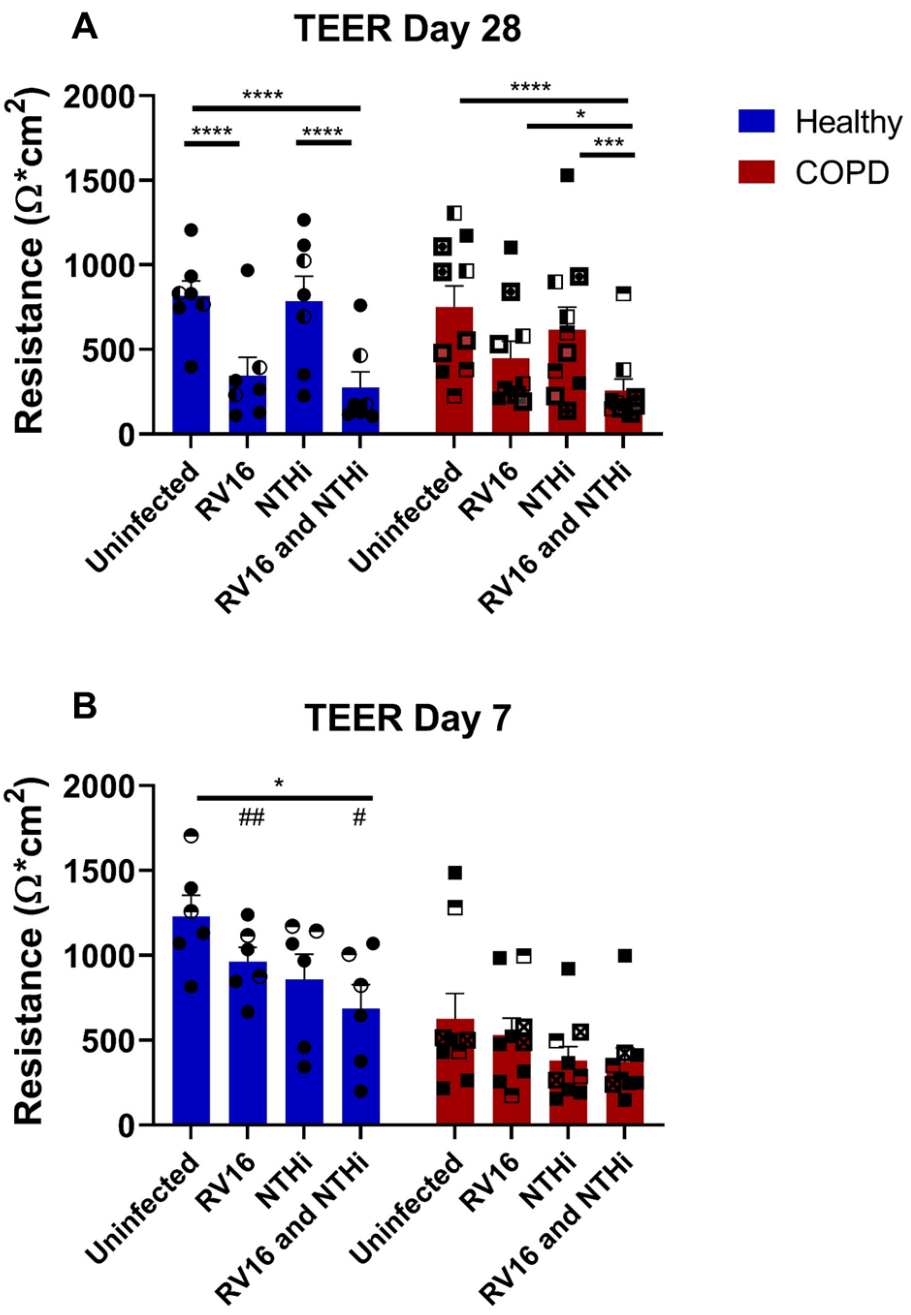

Figure 22. TEER during RV and NTHi single infection and co-infection of primary epithelial cultures at day 7 and day 28 of differentiation

Trans-epithelial electrical resistance (TEER) was quantified in nasal epithelial cultures when they were fully differentiated at day 28 (A) or pre-ciliation at day 7 (B) following infection with RV16 alone ($1.5x10^6$ $TCID_{50}$/well), NTHi 49247 ($5x10^6$ CFU/well) alone or RV and NTHi co-infection, as described in section 2.7. TEER was measured in one or two wells per condition. If technical replicates were performed, these were averaged to give one measurement per

condition. Where measurements were carried out more than once in the same donor during separate experiments, these are identified by the same symbol. Filled back symbols represent unique donors. For statistical analysis, TEER values were log10 transformed and a linear mixed effects model was fitted with fixed effects for disease group, day and infection and a day-specific random effect for each donor. P values were Benjamini-Hochberg adjusted for multiple comparisons. Data are presented as mean ± standard error of the mean. *=p<0.05, ***=p<0.001, ****=p<0.0001. # denotes comparison with same condition in day 28 culture, #=p<0.05, ##=p<0.01.

To further understand the effect of RV and NTHi single and co-infection on epithelial barrier integrity, the expression of genes encoding for tight junction proteins Claudin-8 and ZO-1 was assessed by qRT-PCR (as described in section 2.11) following infection with RV alone, NTHi alone or RV and NTHi co-infection.

Figure 23A shows that in both healthy and COPD day 28 ciliated cultures, RV infection caused a significant reduction in the expression of *Claudin 8,* both during single infection (healthy, p<0.0001, COPD, p=0.001) and during co-infection with NTHi (p<0.0001 in both cases) when compared to levels of expression in uninfected control wells. In contrast, NTHi infection did not alter expression of *Claudin 8* in ciliated cultures from either healthy or COPD (p>0.05 versus uninfected control). However, in healthy cultures, expression of *Claudin 8* was further reduced during RV and NTHi co-infection compared to RV infection alone (p=0.033), suggesting an additive effect during RV and NTHi co-infection in downregulating expression of *Claudin 8*. This effect was not detected in COPD cultures.

In contrast to ciliated cultures, in pre-ciliation day 7 cultures (Figure 23B) RV infection did not down-regulate expression of *Claudin 8*, in either healthy and COPD, when compared to expression levels in uninfected control cultures ($p=0.954$ in both cases). Moreover, expression levels of *Claudin 8* during RV infection were significantly higher compared to expression levels in the same groups in ciliated cultures, in both healthy and COPD cultures ($p<0.001$ for all comparisons).

In pre-ciliation, day 7 cultures, (Figure 23B) it was NTHi which caused a significant down-regulation of *Claudin 8* expression in both healthy and COPD cultures, when compared to expression levels in uninfected wells (healthy, $p=0.003$, COPD, $p=0.013$). The same effect was detected during co-infection with RV (healthy, $p=0.001$, COPD, $p=0.007$). There was no significant difference in expression levels between NTHi infection alone and RV and NTHi co-infection (healthy, $p=0.868$, COPD, $p=0.954$), indicating that the effect is caused by NTHi infection in both healthy and COPD. Despite the NTHi induced downregulation of *Claudin 8*, expression levels during RV and NTHi co-infection were significantly higher compared to expression levels in the same groups in ciliated cultures, in both healthy and COPD cultures ($p<0.01$ for all comparisons)

In terms of *ZO-1* expression in ciliated epithelial cultures, as shown in Figure 23C, this was found to be significantly up-regulated in both healthy and COPD ciliated cultures following RV infection alone and RV and NTHi co-infection, when compared to uninfected control expression levels ($p<0.0001$ in all cases). NTHi infection alone did not affect expression levels of *ZO-1* in either healthy or COPD cultures when compared to expression in uninfected cultures

(healthy, p=0.859, COPD, p=0.876). There was no significant difference in expression levels of *ZO-1* between RV infection alone and RV and NTHi co-infection in either healthy or COPD cultures, suggesting that the effect is mediated by RV alone (healthy, p= 0.184, COPD, p=0.397).

The up-regulation effect of RV on *ZO-1* gene expression (Figure 23D) was not detected in day 7 pre-ciliation cultures, where expression levels did not change during single RV infection, single NTHi infection or RV and NTHi co-infection ($p>0.05$ for all comparisons) in either healthy or COPD cultures. Moreover, in both healthy and COPD expression levels of *ZO-1* during single RV infection was significantly lower than in ciliated cultures, where it was up-regulated by virus infection (healthy, p= 0.011, COPD, p=0.005).

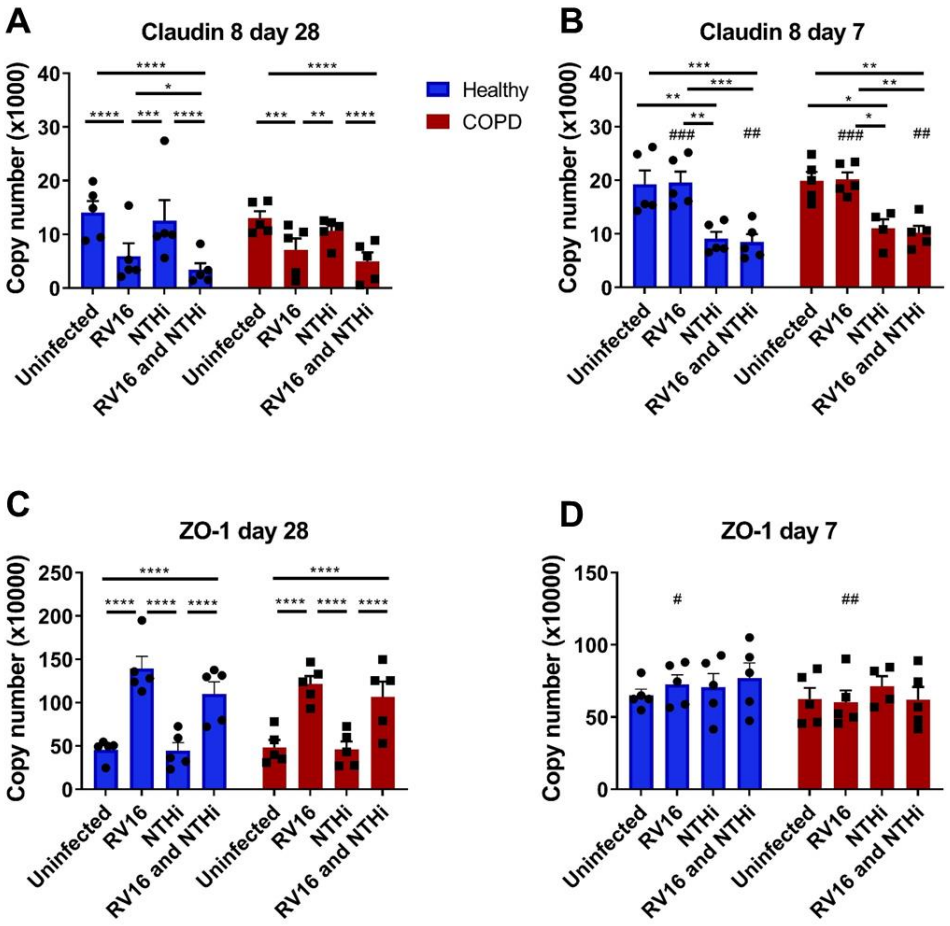

Figure 23. Expression of *Claudin 8* and *ZO-1* after infection with RV, NTHi or after RV and NTHi co-infection of primary epithelial cultures at day 7 and day 28 of differentiation.

Gene expression levels of *Claudin 8* (A,B) and *ZO-1* (C,D) were quantified by qRT-PCR in day 7 pre-ciliation cultures and fully differentiated ciliated epithelial cultures from healthy and COPD donors, as described in section 2.11., following infection with RV16 alone ($1.5x10^6$ $TCID_{50}$/well), NTHi 49247 ($5x10^6$ CFU/well) alone or after RV-NTHi co-infection. Following infection, epithelial cells were pooled for analysis from 2 trans-wells/ condition. N=5 healthy and 5 COPD donors. Symbols represent individual donors. For statistical analysis, copy number values were log2 transformed and separate linear mixed effects models were fitted for each analyte, with fixed effects for disease group, day and infection and a day-specific random effect for each donor. P values were Benjamini-Hochberg adjusted for multiple comparisons. Data are shown as mean ± standard error of the mean. *=p<0.05, ***=p<0.001, ****=p<0.0001, #= denotes day 7 versus day 28 comparison within a treatment group, #=p<0.05, ##=p<0.01, ###=p<0.001.

3.3.5. Cytokine responses of primary epithelial cultures to infection with RV alone, NTHi alone and RV and NTHi co-infection

To determine the effect of infection with RV alone, NTHi alone and RV and NTHi co-infection on epithelial inflammatory responses, cytokine production by nasal epithelial cultures from healthy and COPD donors was quantified. To do this, epithelial cultures were infected with RV for 24 hours then challenged with NTHi for another 24 hours, as described in section 2.30. Then, basolateral supernatants were collected and cytokines and chemokines measured as described in section 2.15.

As shown in Figure 24, it was found that single RV infection of both healthy and COPD day 28 ciliated cultures significantly up-regulated release of IL-1β, IL-6, TNF-α, IL-17 as well as of IFN-λ when compared to the respective uninfected control cultures ($p<0.05$ for all comparisons). G-CSF production was increased following RV infection of healthy cultures but not of COPD cultures ($p=0.033$). NTHi infection alone induced a significant up-regulation of IL-1β and TNF-α in both healthy and COPD ciliated cultures when compared to the uninfected controls ($p<0.05$ for all comparisons). However, NTHi did not stimulate release of IL-6, IL-17, IFN-λ or G-CSF in either healthy or COPD cultures compared to uninfected controls ($p>0.05$ for all comparisons). Rhinovirus and NTHi co-infection of ciliated cultures led to increased production of IL-1β, IL-6, TNF-α, IL-17 as well as IFN-λ in comparison to levels of the cytokines in uninfected control cultures from both healthy and COPD ($p<0.05$ for all comparisons), but did not affect G-CSF release in either healthy or COPD cultures. Given that NTHi did not up-regulate production of IL-6, IL-17 or IFN-λ and that there was no difference between the levels of these

cytokines in supernatants from RV single infection and those from RV and NTHi co-infection, it appears that the induction of cytokine production during co-infection is RV driven. There was no significant difference in the levels of IL-1β or TNF-α between infection treatments in either healthy or COPD cultures ($p>0.05$).

Of interest, cytokine responses of day 7 pre-ciliation cultures (Figure 24 B, D, F, H, J, L) were very different to those of ciliated cultures. With the exception of IFN-λ, RV did not increase synthesis of any of the other cytokines measured when compared to their respective uninfected control in healthy or COPD cultures ($p>0.05$). Expression of IFN-λ was significantly induced by RV during single infection and co-infection with NTHi, in both healthy and COPD cultures when compared to uninfected control cultures ($p<0.0001$ in both cases), but levels were still significantly lower than levels detected in supernatants of ciliated cultures from healthy and COPD donors ($p<0.05$ in all cases). Single NTHi infection did not significantly up-regulate expression of any of the cytokines measured in day 7 cultures. Interestingly, RV and NTHi co-infection led to a significant increase in IL-1β, IL-6, TNF-α and IL-17 production by COPD cultures, but not by healthy cultures, when compared to uninfected control conditions ($p<0.05$), suggesting a differential response to infection of COPD day 7 cultures compared to healthy cultures. In particular, IL-1β levels were significantly higher in COPD day 7 cultures during co-infection by RV and NTHi compared to RV infection alone ($p=0.049$). It is important to note, however, that levels of IL-1β, IL-6 and IL-17 were significantly lower in day 7 cultures during viral-bacterial coinfection compared to the same condition in ciliated cultures from both healthy and COPD ($p<0.05$).

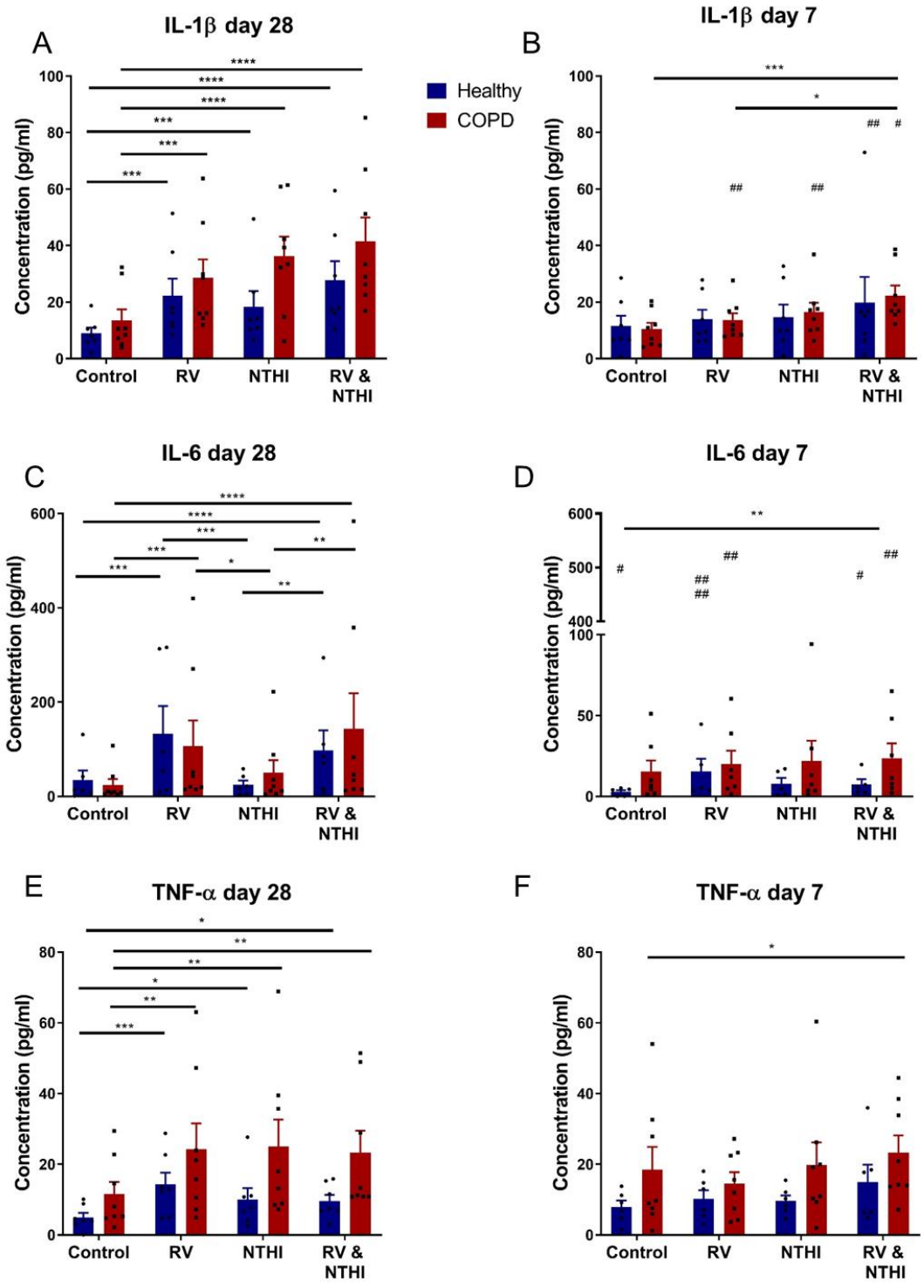
A
IL-1β day 28
Concentration (pg/ml)
Control
RV
NTHI
RV & NTHI
Healthy
COPD
B
IL-1β day 7
C
IL-6 day 28
D
IL-6 day 7
E
TNF-α day 28
F
TNF-α day 7

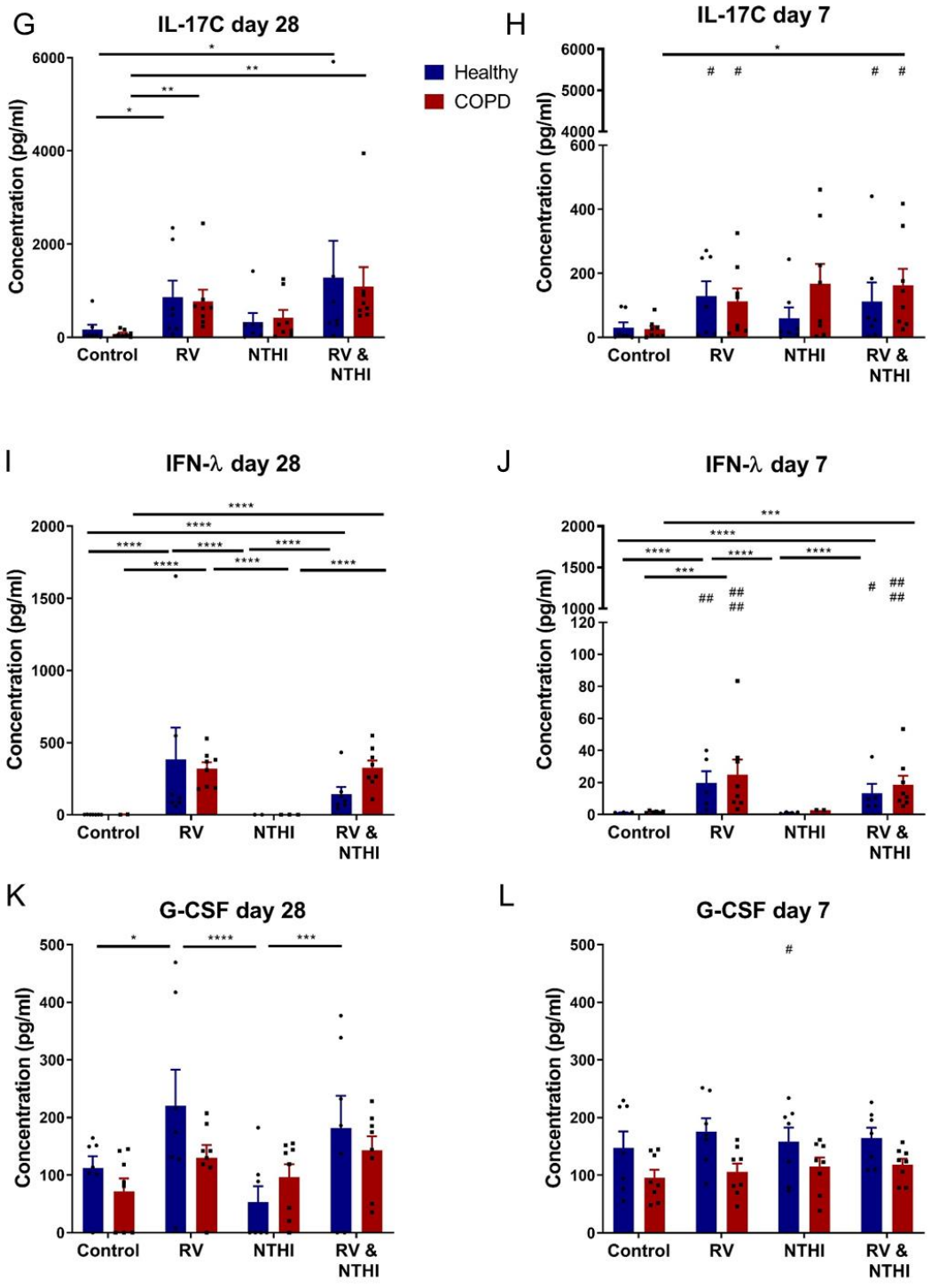

Figure 24. Cytokine responses of ciliated and day 7 pre-ciliation cultures to infection with RV alone, NTHi alone and RV and NTHi co-infection.

Cytokine release to basolateral medium of day 7 pre-ciliation cultures and fully differentiated day 28 ciliated epithelial cultures from healthy and COPD donors was quantified by MSD immunoassay following infection with RV16 alone ($1.5x10^6$ $TCID_{50}$/well), NTHi 49247 ($5x10^6$

CFU/well) alone or after RV-NTHi co-infection. N=7 healthy and 8 COPD donors. Symbols represent individual donors. For statistical analysis, concentrations were log10 transformed and cytokines were analysed individually using linear mixed effects models. Fixed effects for disease group, day, and treatment and random effect for each donor were included. P values were Benjamini-Hochberg adjusted for multiple comparisons. Data are shown as mean ± standard error of the mean. *=p<0.05, **p<0.01, ***=p<0.001, ****=p<0.0001, #= denotes day 7 versus day 28 comparison within a treatment group, #=p<0.05, ##=p<0.01, ####=p<0.0001.

3.3.6. Chemokine responses of primary epithelial cultures to infection with RV alone, NTHi alone and RV and NTHi co-infection

Production of chemokines by nasal epithelial cultures from healthy and COPD donors was investigated in pre-ciliation day 7 and ciliated epithelial cultures following RV and NTHi single infections and RV and NTHi co-infection. As shown in Figure 25 A, C, E, RV infection significantly increased levels of IL-8, IP-10 and RANTES in both healthy and COPD ciliated cultures when compared to uninfected control cultures ($p<0.01$ in all comparisons). In contrast, NTHi infection alone only stimulated release of IL-8 from both healthy and COPD ciliated cultures when compared to uninfected controls ($p<0.05$), but not of IP-10 or RANTES. RV and NTHi co-infection significantly increased levels of IL-8, IP-10 and RANTES when compared to uninfected controls of both healthy and COPD cultures ($p<0.05$ for all comparisons). As NTHi did not induce secretion of IP-10 or RANTES and there was no significant difference between levels of the chemokines during RV infection alone and RV and NTHi co-infection, it is likely that the up-regulation seen during viral-bacterial co-infection is RV driven in both healthy and COPD. There was no significant

difference in the levels of IL-8 between the different infection conditions in either healthy or COPD donors, although a trend for higher IL-8 levels in COPD cultures was observed following all three infections when compared to healthy cultures.

In day 7 pre-ciliation cultures, as shown in Figure 25 B, D, and F levels of IL-8 were only significantly increased in COPD cultures during RV and NTHI co-infection compared to uninfected controls ($p<0.05$), but not in healthy cultures. Despite the increased IL-8 production during viral-bacterial co-infection, levels were still significantly lower compared to the levels secreted by COPD ciliated cultures following co-infection ($p<0.01$). Secretion of IP-10 was significantly higher in both healthy and COPD cultures during RV single infection and during RV and NTHi co-infection, when compared to uninfected control cultures ($p<0.0001$ for all comparisons). However, levels of IP-10 were significantly lower in day 7 cultures than levels seen in supernatants from ciliated cultures in both healthy and COPD cultures, independent of single RV infection or co-infection ($p<0.05$ for all comparisons). NTHi infection alone did not stimulate production of either IL-8 or IP-10 in any day 7 cultures ($p>0.05$ for all comparisons). Furthermore, RANTES production was not induced by any of the infection conditions in either healthy or COPD culture.

In addition, levels of the chemokines TARC, MCP-1, ENA-78, MIP-3α and Gro-α were also quantified but no significant up-regulation was detected following single infection by RV or NTHi or their co-infection irrespective of disease state or differentiation stage. Results are shown in Appendix 3.

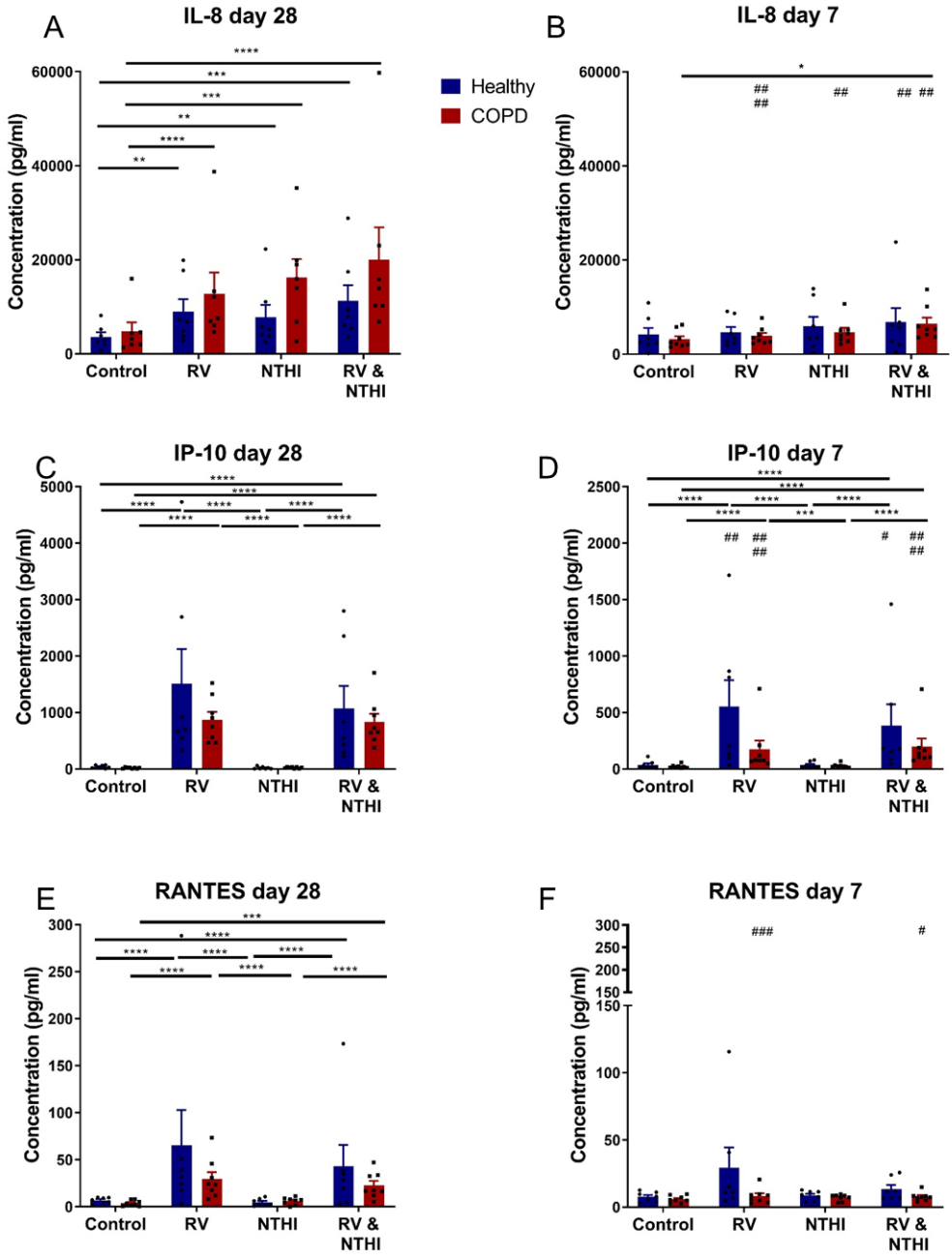

Figure 25. Chemokine responses of ciliated and day 7 pre-ciliation cultures to infection with RV alone, NTHi alone and RV and NTHi co-infection.

Chemokine release to basolateral medium of day 7 pre-ciliation cultures and fully differentiated day 28 ciliated epithelial cultures from healthy and COPD donors was quantified by MSD immunoassay, as described in section 2.15., following infection with RV16 alone ($1.5x10^6$ $TCID_{50}$/well), NTHi 49247 ($5x10^6$ CFU/well) alone or after RV-NTHi co-infection. N=7 healthy and 8 COPD donors. Symbols represent individual donors. For statistical analysis,

concentrations were log10 transformed and chemokines were analysed individually using linear mixed effects models. Fixed effects for disease group, day, and treatment and random effect for each donor were included. P values were Benjamini-Hochberg adjusted for multiple comparisons. Data are shown as mean ± standard error of the mean. *=p<0.05, **=p<0.01, ***=p<0.001, ****=p<0.0001, #= denotes day 7 versus day 28 comparison within a treatment group, #=p<0.05, ##=p<0.01, ###=p<0.001, ####=p<0.0001.

3.3.7. Rhinovirus replication is significantly higher in ciliated epithelial cultures compared to pre-ciliation day 7 cultures

Ultimately it was important to understand if the different effects induced by RV in ciliated versus pre-ciliation day 7 cultures were correlated with RV replication in these 2 culture conditions and whether RV replication is affected by NTHi co-infection. Therefore, RV expression was quantified by qRT-PCR in healthy and COPD day 7 pre-ciliation cultures and ciliated cultures after single RV infection or RV and NTHi co-infection, as described in section 2.11.

Interestingly, as shown in Figure 26, in both healthy and COPD, RV copy number was significantly lower in pre-ciliation day 7 cultures compared to ciliated epithelial cultures, irrespective of whether this was measured during single RV infection or co-infection with NTHi, ($p<0.0001$ in all cases). Co-infection with NTHi did not affect the course of RV infection, as there was no significant difference in RV copy number between RV single infection and co-infection with NTHi, irrespective of epithelial differentiation stage or disease group ($p>0.05$ for all comparisons). A trend was observed where RV copy number was lower in ciliated cultures from COPD donors compared to healthy donors, with the average RV copy number in ciliated COPD cultures being approximately half of that in healthy cultures, but this difference was not

statistically significant (p=0.348 during RV infection alone and during RV and NTHi co-infection).

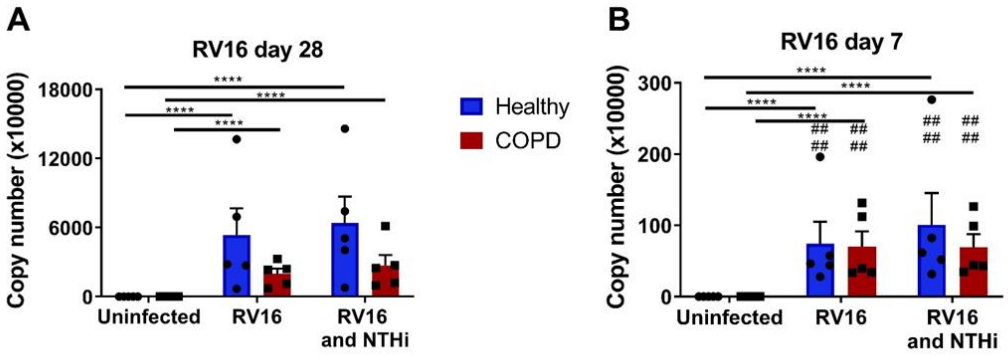

Figure 26. RV expression in ciliated and day 7 pre-ciliation epithelial cultures during RV single infection and RV and NTHi co-infection

The RV16 load in cells was quantified by qRT-PCR in fully differentiated, day 28 ciliated epithelial cultures (A) and day 7 pre-ciliation cultures (B) from healthy and COPD donors, as described in section 2.11., following infection with RV16 alone ($1.5x10^6$ $TCID_{50}$/well), or after RV16-NTHi (NTHi 49247, $5x10^6$ CFU/well) co-infection. Epithelial cells were pooled from 2 trans-wells/ condition for analysis. N=5 healthy and 5 COPD donors. For statistical analysis, copy numbers were log2 transformed and analysed using a linear mixed effects model with fixed effects for disease, day and infection and a donor specific random effect. P values were Benjamini-Hochberg adjusted for multiple comparisons. Symbols represent individual donors. Data are shown as mean ± standard error of the mean. ****=p<0.0001, #= denotes day 7 versus day 28 comparison within a treatment group, ####=p<0.0001.

3.3.8. Discussion

Current understanding of the effect of RV and NTHi infection and in particular their co-infection, on the barrier function of respiratory epithelium from COPD patients, where these pathogens are frequently associated with disease exacerbation, is surprisingly limited (Bandi et al., 2003; Molyneaux et al., 2013; Wilkinson et al., 2017; Wilkinson et al., 2006). In this study, the effect of single RV and NTHi infection and RV and NTHi co-infection on epithelial mucociliary function, barrier integrity and inflammatory responses was investigated using primary nasal epithelial cells from healthy and COPD donors. This was based on the hypothesis that RV and NTHi co-infection would lead to more epithelial barrier disruption and increased inflammatory responses compared to NTHi infection alone. For this study, cultures were differentiated for either 6 days, prior to ciliation, as a model of regenerating epithelium, (as discussed in section 3.1.7) or for 28 days when they were fully differentiated. At each time point, cultures were infected with RV and 24 hours later challenged with NTHi.

As the first interaction that either pathogen makes when infecting the human host is with the cilia of the ciliated epithelium, the effect of infection with RV alone, NTHi alone or their co-infection on ciliary beat frequency was investigated (Figure 20). Neither RV nor NTHi single infections were found to significantly reduce ciliary beat frequency in either healthy or COPD ciliated cultures over the course of the experiment (Figure 20). The effect of NTHi infection alone on ciliary beat frequency was shown in

Figure 13 and discussed in section 3.2.7. However, co-infection with RV and NTHi significantly reduced ciliary beat frequency in healthy cultures at 8h and

24h post NTHi infection when compared to uninfected cultures, and at the latter time point, also when compared to NTHi infection alone. In contrast, no such effect was observed in COPD cultures, as a result of inter-donor variability, therefore no conclusion could be drawn. However, based on the results obtained using healthy ciliated cultures, it appears that ciliary beat frequency is significantly impaired during RV and NTHi co-infection.

Furthermore, during NTHi infection alone it was possible to measure ciliary beat amplitude and as shown in Figure 13, this was reduced by NTHi aggregates formed over ciliated areas. During RV and NTHi co-infection, there was an increased growth of non-attached NTHi, as shown in Figure 27. Bacterial aggregates formed during co-infection were denser and also contained detached epithelial cells, (including ciliated cells which RV was shown to shed off the epithelial layer, Jakiela et al. (2014)), making it impossible to visually assess ciliary beat amplitude (See Appendix 4 and Videos 2-5 on USB stick attached for a comparison of aggregate formation during NTHi single infection versus during RV and NTHi co-infection). However, inferring from the results obtained during NTHi infection alone where it was bacterial aggregate formation that was associated with a decrease in ciliary amplitude, it is likely that the increased bacterial load and denser biofilms would have further decreased ciliary beat amplitude during RV and NTHi co-infection. Therefore, these observations collectively suggest that ciliary function, including beat frequency and beat amplitude, is further reduced during RV and NTHi infection compared to NTHi infection alone, which could ultimately reduce the efficiency of pathogen clearance from the airways.

In addition to ciliary function, mucus secretion is another factor that can affect mucociliary clearance. It has previously been described how increased mucin concentration in the mucus layer can cause compression of the periciliary layer, collapse of cilia and decreased mucociliary transport (Anderson et al., 2015; Boucher, 2019; Button et al., 2012). Infection with either RV or NTHi has been previously associated with an increase in mucus production by respiratory epithelial cells, but no study has assessed the effect of their co-infection on either healthy or COPD ciliated epithelia (Baddal et al., 2015; Chen et al., 2004; Hewson et al., 2010; Jakiela et al., 2014; Jing et al., 2019; Komatsu et al., 2008; Konduru et al., 2017; Liu et al., 2019; Tan et al., 2018) In the current investigation, Figure 21 showed that RV up-regulated expression of the goblet cell specific transcription factor *SPDEF*, of the secreted mucins *MUC5AC* and *MUC5B* as well as of the membrane tethered mucin *MUC4* in both healthy and COPD ciliated epithelial cultures. The up-regulation of *SPDEF* by RV in both healthy and COPD ciliated cultures, together with increased expression of secreted mucins, suggests that RV stimulates a goblet cell specific transcriptional profile, as *SPDEF* expression has previously been used as a marker of goblet cells (Jing et al., 2019). This is in agreement with the study by Jing et al. (2019) who reported that RV induced goblet cell hyperplasia in ciliated epithelial cultures from COPD donors and with results shown by Faris et al. (2016) who reported that RV infection of healthy epithelial cultures at day 7 of differentiation leads, 2-3 weeks later, to differentiated cultures with features of epithelial to mesenchymal transition and goblet cell hyperplasia. These findings suggest that at a transcriptional level, RV infection promotes up-regulation of genes associated with increased mucin secretion,

which is in agreement with previous reports which found that RV was able to up-regulate expression of *MUC5AC* and *MUC5B* following infection of ciliated epithelial cultures from either healthy or COPD donors (Jakiela et al., 2014; Jing et al., 2019; Liu et al., 2019; Tan et al., 2018). However, Jing et al. (2019) reported that up-regulation of *MUC5AC* and *MUC5B* was only observed in ciliated cultures from patients with COPD and not in healthy cultures, whereas Jakiela et al. (2014) and Liu et al. (2019) reported up-regulation of both *MUC5AC* and *MUC5B* in bronchial and nasal healthy cultures, respectively. It is very likely that the difference in results is a consequence of the time post infection at which the cultures were sampled and gene expression analysed. Jing et al. reported results at 15 days post RV infection, whereas Liu et al. reported results at 24 hours post infection and Jakiela et al. reported results at 48 hours post infection. Collectively, these findings indicate that mucin gene expression is up-regulated in both healthy and COPD epithelia in the early stages of RV infection, but only maintained in COPD cultures at later time points, as supported by Jing et al. (2019) as well as by *in vivo* studies carried out in mouse COPD models infected with RV (Ganesan et al., 2014; Sajjan et al., 2009). No previous studies have reported up-regulation of *MUC4* expression following RV infection of ciliated epithelial cultures from healthy or COPD, but given the role of this membrane tethered mucin in supporting the periciliary layer, if the increased transcription of the gene also translated into increased protein expression, the consistency of the periciliary layer would be affected, thus affecting ciliary function and mucociliary clearance (Button et al., 2012).

In contrast to RV, single NTHi infection of ciliated cultures did not increase expression of any of the mucin genes studied or of *SPDEF* in healthy ciliated cultures but induced a modest increased in *MUC5B* expression in COPD cultures (see Figure 21E). This is in contrast to previously published studies which reported an up-regulation of *MUC5AC* expression in epithelial cell lines or primary airway epithelial cells grown as submerged monolayers (Chen et al., 2004; Komatsu et al., 2008; Konduru et al., 2017; Shen et al., 2008; Val et al., 2015). This difference is likely a consequence of the use of undifferentiated epithelial cell lines or basal cells versus differentiated primary nasal epithelial cultures used in the current investigation. However, in a study where healthy ciliated epithelial cultures were infected with NTHi, transcription of *MUC4* and *MUC5B* was found to be up-regulated, but at later time points post NTHi infection (Baddal et al., 2015).

As NTHi did not alter expression of *SPDEF* or mucin genes and the increase detected in expression of all genes analysed during RV and NTHi co-infection was not different from levels detected during RV infection alone, it becomes clear that this is predominantly a RV driven effect without any synergy with NTHi.

It remains to be determined if the RV-induced increased transcription of *SPDEF* and mucin genes translates to goblet cell hyperplasia and increased mucus production, particularly in COPD cultures, as suggested by Jing et al. (2019). Furthermore, it would be of interest to quantify the amount of MUC5AC and MUC5B proteins produced by healthy and COPD ciliated cultures following RV or NTHi single infection and co-infection, as their proportion has been suggested to change during chronic respiratory disease, with MUC5B

becoming the predominant mucin in the sputum of COPD patients (Boucher, 2019; Kirkham et al., 2008).

In contrast to ciliated cultures, pre-ciliation day 7 cultures showed a significantly reduced response to single RV or NTHi infection as well as to their co-infection (Figure 21). A minimal up-regulation of *SPDEF* in healthy cultures and of *MUC5B* in COPD cultures was induced by RV. However, even in these cases the expression levels were significantly lower when compared to the same conditions in ciliated epithelial cultures. No other infection conditions up-regulated expression of *SPDEF*, *MUC5AC*, *MUC5B* or *MUC4* in pre-ciliation cultures from either healthy or COPD donors, most likely reflecting the incomplete differentiation of the epithelial cultures.

In addition to stimulating a goblet cell specific transcriptional profile, RV was also found to cause a significant reduction in TEER in healthy ciliated epithelial cultures, both during single infection and during co-infection with NTHi (Figure 22). In COPD ciliated cultures, a trend for a reduced TEER was also observed during RV single infection, although this did not achieve statistical significance. These results are in agreement with previous reports which have shown that RV infection of polarised epithelial cultures reduced TEER and increased epithelial permeability to dextran (Comstock et al., 2011; Looi et al., 2018; Sajjan et al., 2008). In contrast, an NTHi single infection did not alter epithelial resistance in either healthy or COPD ciliated cultures, which agrees with results reported from a long term co-culture of NTHi with ciliated epithelial cultures, where no effect of NTHi on epithelial resistance was detected over 8 days of incubation (Ren et al., 2012). Ultimately, this and the current study suggests that during RV and NTHi co-infection of healthy cultures, the

decrease in TEER is primarily RV driven. In COPD ciliated cultures, a small further reduction was detected during co-infection with NTHi compared to RV infection alone or to NTHi infection alone, suggesting a potential additive effect due to NTHi presence.

In order to determine whether the decrease in TEER following RV infection was also associated with destruction of junctional complexes, expression of *ZO-1* and *Claudin-8* were quantified by qRT-PCR. These proteins were chosen as their levels have been previously reported to be impacted by RV and NTHi single infection (Baddal et al., 2015; Sajjan et al., 2008). Replicating the pattern of TEER decrease following RV infection, *Claudin-8* expression was down-regulated in both healthy and COPD ciliated cultures by RV infection but not by NTHi (Figure 23). In contrast expression of *ZO-1* was significantly up-regulated by RV infection and unchanged by NTHi infection of healthy and COPD ciliated cultures. Previous studies have reported a downregulation by RV of genes encoding for tight junction proteins *Claudin 8* or *ZO-1* in primary airway epithelial cultures, but these were undifferentiated monolayers of epithelial cells (Looi et al., 2016). ZO-1 protein levels following RV infection of ciliated epithelial cultures were repeatedly found to be decreased and associated with epithelial tight junction destruction (Looi et al., 2016; Sajjan et al., 2008). No study has quantified protein levels of Claudin-8 following RV infection of epithelial cells. It is possible that the contrasting up-regulation of *ZO-1* gene expression detected in this study compared to the reported down-regulation of ZO-1 protein expression following RV infection reflects a differential transcriptional and translational regulation of ZO-1, which has been reported previously (Looi et al., 2018). Therefore, it could reflect a gene up-

regulation in a cellular attempt to replace the protein lost. Confirmation of this fact would require confocal microscopy validation of tight junction integrity by immuno-staining for both ZO-1 and Claudin-8 proteins following RV and NTHi single infection and RV and NTHi co-infection.

In contrast to results reported by Baddal et al. (2015) who showed a decrease in *Claudin-8* expression following NTHi infection of primary ciliated epithelial cultures, the current investigation found no effect of NTHi infection on *Claudin 8* expression (Figure 23). It is possible that the different results appeared as a consequence of the fact that Baddal et al. (2015) only used commercially available cultures from a single healthy donor for their experiments as opposed to the multi donor study presented in this chapter. Similar to the decrease in TEER during RV and NTHi co-infection, changes in gene expression levels of *ZO-1* and *Claudin 8* during RV and NTHi co-infection of ciliated cultures appeared to be driven by RV infection rather than NTHi, with no synergism detected in either healthy or COPD cultures.

In pre-ciliation day 7 cultures, changes in epithelial resistance were minimal, with a significant decrease in TEER only observed following RV and NTHi co-infection of healthy cultures, but not of COPD cultures (Figure 22B). Single NTHi infection did not alter TEER of either healthy or COPD day 7 cultures. The RV driven reduction in TEER observed during infection of ciliated cultures was not replicated in pre-ciliation cultures, suggesting a different behaviour of day 7 cultures to RV infection. Therefore, as NTHi did not appear to significantly affect TEER of day 7 pre-ciliation cultures, it was surprising to detect a significant decrease in expression of *Claudin 8* following NTHi single infection or RV and NTHi co-infection of both healthy and COPD pre-ciliation

cultures. As the decrease in *Claudin 8* expression was similar after RV and NTHi co-infection compared to NTHi single infection, while RV did not impact on *Claudin 8* expression, it follows that this is an NTHi driven effect in both healthy and COPD day 7 cultures. It would be of interest to validate this finding at a protein level, as it may highlight differential effects of NTHi infection on ciliated versus pre-ciliation cultures and it may be a mechanism of importance for NTHi internalisation into epithelial cultures, as shown in section 3.2. Neither RV nor NTHi infection altered expression of ZO-1 in either healthy or COPD day 7 cultures. There was no significant difference in TEER and expression of *ZO-1* or *Claudin 8* between healthy or COPD cultures, irrespective of infection condition, disease state or differentiation stage.

In this study the inflammatory response of healthy and COPD ciliated epithelia to infection with RV alone, NTHi alone or their co-infection was quantified. In both healthy and COPD ciliated cultures, RV was found to stimulate production of the acute phase reaction cytokines IL-1β, IL-6 and TNF-α. This suggests initiation of an acute inflammatory response, as was observed in previous *in vitro* studies and during experimental rhinovirus infection, where IL-6, TNF-α and C reactive protein were induced and their levels were correlated with virus load in the sputum of COPD patients (Gruys et al., 2005; Liu et al., 2019; Mallia et al., 2011; Piper et al., 2013; Schneider et al., 2010). As expected following a viral infection, RV also strongly up-regulated IFN-λ production in both healthy and COPD cultures, in agreement with previously published results (Schneider et al., 2010; Tan et al., 2018). RV was also a strong inducer of the chemokines IL-8, IP-10 and RANTES in both healthy and COPD ciliated cultures, thus contributing to the recruitment of immune cells such as neutrophils,

eosinophils, NK cells or Th1 lymphocytes to the respiratory epithelium, as previous studies have also described (Schneider et al., 2010; Schroth et al., 1999; Shelfoon et al., 2016; Spurrell et al., 2005). However, the study by Schneider et al. (2010) reported increased release of IL-6, IL-8, IP-10 and expression of *IFN-λ* from COPD ciliated cultures compared to healthy following RV39 infection. In contrast, no differences in the level of these cytokines and chemokines were detected between healthy and COPD ciliated cultures in the present study. A trend for higher levels of IL-1β, TNF-α and IL-8 produced following RV infection in COPD cultures was observed when compared to healthy, but this was not statistically significant, possibly due to inter-donor variability. Levels of G-CSF were stimulated by RV infection in healthy cultures, but not in COPD cultures, where a reduced induction of G-CSF may affect maturation of neutrophils recruited to the airways and lead to reduced immuno-regulation through decreased induction of tolerant dendritic cells and regulatory T cells (Franzke, 2006; Kato, 2016; Martins et al., 2010). Surprisingly, IL-17C was secreted by both healthy and COPD ciliated cultures following infection by RV, but not by NTHi, despite a previous report suggesting it is released following NTHi infection of epithelial cells (Pfeifer et al., 2013). In addition, no synergism in IL-17C release was detected during co-infection with RV and NTHi, with its production by both healthy and COPD cultures being attributed to RV alone. This finding is in contrast to the study by Jamieson et al. (2019) who found that simultaneous infection of bronchial epithelial cells grown as a submerged monolayer with RV and NTHi led to a significant and synergistic increase in IL-17C levels, but not when cells were infected with

either pathogen alone. It is possible that the different findings are related to the use of different epithelial cultures.

NTHi infection alone was found to induce up-regulation of IL-1β and TNF-α as well as levels of the chemokine IL-8, which is in agreement with results obtained by Baddal et al. (2015), who also detected increased IL-1β, TNF-α and IL-8 but not IL-6. A trend for higher levels of IL-1β, TNF-α and IL-8 in COPD ciliated cultures' supernatants compared to healthy was detected, but the difference did not achieve statistical significance. Moreover, in contrast to RV, NTHi did not stimulate release of IL-6, IFN-λ, IL-17, IP-10, RANTES or G-CSF, in either healthy or COPD ciliated cultures. These findings suggest a more limited contribution to inflammation and immune cell recruitment to the site of infection compared to RV infection, possibly reflecting the behaviour of a colonising pathogen (Murphy et al., 2004). In addition, during co-infection with RV, the inflammatory response of ciliated epithelial cultures from both healthy and COPD donors was driven by RV stimulated responses, with no additive effect from NTHi co-infection. This is in contrast to the suggestion that RV infection would down-regulate release of IL-8 in response to a subsequent NTHi infection, possibly because this study was carried out using a bronchial epithelial cell line, as opposed to primary differentiated epithelial cells used in the current investigation (Unger et al., 2012).

In contrast to ciliated epithelial cultures, pre-ciliation day 7 cultures presented with a significantly reduced release of all inflammatory mediators analysed. Of interest is that IL-1β, IL-6, TNF-α, IL-17 and IL-8 were significantly up-regulated by RV and NTHi co-infection of COPD epithelial cultures but not in healthy cultures when compared to their respective uninfected control

conditions, suggesting a more pro-inflammatory response of a regenerating COPD epithelium compared to healthy epithelium. Antiviral responses with production of IFN-λ and IP-10 were detected from both healthy and COPD day 7 cultures following RV infection but these were significantly lower than that of ciliated cultures. Interestingly, single NTHi infection of day 7 cultures from healthy or COPD did not stimulate a significant release of any of the mediators quantified, despite the fact that cultures were invaded by the bacterium at this stage, as shown in Figure 16.

It was important to determine if the different responses seen from day 7 pre-ciliation cultures compared to ciliated epithelial cultures in terms of mucin and tight junction proteins' gene expression changes as well as TEER and inflammatory mediator secretion were related to the viral and bacterial loads detected in the cultures at the two time points. Quantification of RV in epithelial cultures from healthy and COPD donors revealed that the virus readily replicated in ciliated cultures but viral copy numbers were significantly lower in day 7 epithelial cultures from both healthy and COPD donors (Figure 26). This was surprising given the lower levels of IFN-λ secreted by pre-ciliation cultures which could have provided less anti-viral responses compared to ciliated cultures (Figure 24). However, the lower viral load in pre-ciliation day 7 cultures may be explained by the fact that ciliated cells, which RV has been shown to preferentially infect and replicate within are absent in day 7 epithelial cultures (Jakiela et al., 2014; Tan et al., 2018). This difference is in agreement with results obtained by Jakiela et al. who also showed that RV replication in epithelial cultures differentiated for 8 days is lower than that seen in fully differentiated, ciliated epithelial cultures. Therefore, the reduced responses of

day 7 epithelial cultures to infection by RV, including changes in mucin and junctional proteins' gene expression, TEER change and inflammatory responses are likely to reflect not only their incomplete differentiation, but also the lower levels of viral replication allowed by these cells in comparison to ciliated cultures.

Furthermore, co-infection with NTHi did not affect RV viral load and this was not significantly different between healthy and COPD cultures at either day 7 or day 28. This is in contrast to results shown by Schneider et al. (2010), who reported higher viral load in COPD bronchial ciliated cultures compared to healthy bronchial cultures following infection with RV39. Similarly, in experimental RV infection of healthy volunteers or patients with COPD, higher viral loads were detected in nasal lavage and sputum samples from COPD patients compared to healthy volunteers. It is possible that the contrasting results are a consequence of the use of nasal epithelial cultures as opposed to bronchial cultures or of the fact that a similar type III interferon response was detected in healthy and COPD nasal cultures in the current investigation thus allowing similar levels of viral replication in cultures (Mallia et al., 2011; Schneider et al., 2010).

Quantification of NTHi at day 7 and 28 of epithelial differentiation, during single and co-infection, is shown in Figure 16, Figure 27 and Figure 28 and discussed in sections 3.2.7 and 3.4.7. Briefly, NTHi growth and attachment during single infection did not change with epithelial differentiation or disease state. However, as shown in Figure 16, NTHi invasion of the healthy epithelium appeared to decrease with ALI culture differentiation whereas in COPD cultures, NTHi invasion tended to increase with epithelial differentiation.

Furthermore, during RV and NTHi co-infection, there was a significant increase in NTHi growth compared to NTHi infection alone, coupled with a tendency for a decreased bacterial invasion, particularly in day 7 healthy cultures and ciliated COPD cultures (Figure 27). This suggests the following: firstly, that NTHi invasion of the airway epithelium occurred without a decrease in TEER values in both healthy or COPD cultures, (Figure 22); in future studies, it would be of interest to investigate the effect of NTHi on tight junction protein expression in pre-ciliation and ciliated cultures. Secondly, despite the increased bacterial growth during RV and NTHi co-infection in both healthy and COPD cultures, irrespective of differentiation stage, this was not matched by an increased up-regulation of mucin gene expression or inflammatory mediators' production in any culture condition, when compared to effects of single RV infection. Thirdly, pre-ciliation day 7 cultures of both healthy and COPD were susceptible to NTHi invasion and promoted NTHi growth during RV co-infection, but did not mount an appropriate immune response compared to differentiated ciliated cultures, potentially allowing for bacterial persistence and dissemination in the airways.

In conclusion, results presented in this chapter have shown that RV and NTHi co-infection of ciliated epithelium causes a decrease in ciliary function through reduced ciliary beat frequency and possibly ciliary amplitude. Furthermore, RV infection was shown to stimulate an increased goblet cell specific transcriptional profile during single infection and co-infection with NTHi. Therefore, it is possible to infer that the increased mucin secretion, decreased ciliary function and loss of ciliated cells that occur during RV and NTHi co-infection compared with single NTHi infection would impair mucociliary

transport, favouring airway muco-obstruction and preventing bacterial clearance from the airways *in vivo*. Moreover, effects seen during RV and NTHi co-infection, such as epithelial barrier dysfunction and inflammatory mediators' production were predominantly RV induced, as NTHi infection alone did not appear to alter barrier integrity and induced fewer inflammatory mediators. Therefore, this emphasizes increased epithelial barrier dysfunction and inflammation during RV and NTHi co-infection compared to infection by NTHi alone. Ultimately, the results shown in this chapter have highlighted the vastly different and usually reduced responses to infection of a regenerating, pre-ciliation epithelium compared to those of a fully differentiated epithelium, in both healthy and COPD cultures. These included reduced up-regulation of mucin gene expression in response to RV, preservation of TEER, reduced inflammatory responses and viral replication. However, regenerating epithelia allowed NTHi invasion and supported NTHi growth during co-infection with RV, making them a potential niche for NTHi persistence.

3.4. Investigating the effect of RV co-infection on NTHi growth and invasion of the respiratory epithelium

3.4.1. Introduction

Experimental rhinovirus infections carried out in patients with COPD have highlighted a causal relationship between viral infection and development of secondary bacterial infections in the airways of patients with COPD (Mallia et al., 2012). In this study, 60% of COPD subjects developed a secondary bacterial infection following rhinovirus challenge, in contrast to only approximately 10% of healthy smokers or non-smokers. Rhinovirus infection was shown to alter the airway bacterial microbiome by increasing the bacterial burden in subjects with COPD, but not in healthy subjects, with a significant outgrowth of NTHi from pre-existing colonising strains (Molyneaux et al., 2013). However, the mechanism by which RV induces the growth or virulence of NTHi during co-infection remains unclear.

Increased bacterial growth and biofilm formation following viral infection has been previously reported for several combinations of viral-bacterial co-infections and recent studies have investigated the role of nutritional immunity in this context (Hendricks et al., 2016; Kiedrowski et al., 2018; Siegel et al., 2014). Nutritional immunity refers to the sequestration of essential nutrients such as trace minerals or amino-acids by the host in order to limit pathogenicity during bacterial infection (Melvin and Bomberger, 2016). Enhanced *S. pneumoniae* growth and spread from the upper to lower respiratory tract of mice was observed during influenza virus co-infection when compared to mice infected with *S. pneumoniae* alone (Siegel et al., 2014). The enhanced

pneumococcus growth during influenza co-infection was found to be due to increased availability of carbon sources including sialic acid and sialylated mucins such as MUC5AC, stimulated by the viral infection (Siegel et al., 2014). Hendricks and colleagues observed an increased *P. aeruginosa* biofilm biomass both in *in vitro* RSV infected cultures of a cystic fibrosis epithelial cell line and in *in vivo* RSV infected mouse models compared to *P. aeruginosa* infection alone (Hendricks et al., 2016). RSV infection of a cystic fibrosis epithelial cell line was also shown to cause a dysregulation of iron homeostasis through up-regulation of apical release of the iron binding protein transferrin, thus promoting *P. aeruginosa* growth (Hendricks et al., 2016). Similarly, RSV promoted *S. aureus* biofilm growth during co-infection of cystic fibrosis epithelial cell line cultures, but in this case iron was not the factor stimulating bacterial biofilm growth (Kiedrowski et al., 2018). Bacterial growth was caused by a general increase in host-released nutrient and amino-acid availability that appeared as a result of RSV co-infection (Kiedrowski et al., 2018) This was evidenced by the up-regulation of bacterial genes associated with lipid, carbohydrate and amino acid metabolism, protein translation and ribosomal processes (Kiedrowski et al., 2018). Therefore, these studies collectively suggest that virus infection of the respiratory tract could affect the ability of the host to sequester nutrients from bacterial pathogens, thereby promoting bacterial growth, biofilm formation, aspiration and subsequent colonisation of airways (Hendricks et al., 2016; Kiedrowski et al., 2018; Siegel et al., 2014). None of these aspects have been investigated for RV and NTHi, the two main pathogens often isolated in the airways of COPD patients (Wilkinson et al., 2017). However, the ability of NTHi to respond to changes in nutrient

availability has been documented, with a focus on the role of heme-iron, due to its obligate requirement for extracellular sources of Fe (Szelestey et al., 2013). Heme iron availability has been shown to modulate NTHi morphology, biofilm architecture, invasive behaviour and disease severity in an otitis media chinchilla model of infection (Szelestey et al., 2013). Transiently heme-iron restricted NTHi switched to filamentous morphotypes and formed enhanced biofilms with a lace like architecture and increased height on abiotic surfaces and on chinchilla middle ear epithelial cells. The bacteria also displayed increased internalisation into chinchilla middle ear epithelial cells but overall caused a reduced pathology and disease severity during the *in vivo* studies compared to iron replete NTHi (Szelestey et al., 2013). The importance of heme-iron availability for NTHi virulence and survival is also highlighted by the numerous iron acquisition mechanisms expressed by the bacterium given its inability to synthesize the protoporphyrin ring required for Fe sequestration (Vogel et al., 2012). These include the heme-binding protein A, the haemoglobin/haemoglobin-haptoglobin binding proteins, the heme-utilization protein and Sap transporter (Morton et al., 2004a; Morton et al., 2009; Morton et al., 2004b; Vogel et al., 2012).

In addition to host Fe, NTHi has an obligate requirement for another host-acquired factor, namely NAD^+, due to a lack of biosynthetic enzymes for *de novo* NAD^+ synthesis or for salvaging NAD pre-cursors (Mesquita et al., 2016). Instead, NTHi possess two proteins essential for the uptake of NAD from the host, namely the outer membrane lipoprotein e(P4) and the NAD nucleotidase, a periplasmic enzyme (Kemmer et al., 2001; Mesquita et al., 2016; Reidl et al., 2000). In eukaryotic cells, NAD^+ is stored primarily intracellularly, in the cytosol

and mitochondria, either as NAD^+ or its reduced form NADH, its phosphorylated form NADP or a reduced, phosphorylated form NADPH, each stored in separate membrane bound cellular compartments and used by the cell for redox reactions (Belenky et al., 2007; Mesquita et al., 2016). Extracellularly, NAD^+ could be found at sites of injury through cell lysis, in addition to the extracellular transport of NAD^+ through gap junction channels (Belenky et al., 2007; Bou Saab et al., 2014). However, there is no current understanding of whether rhinovirus infection of respiratory epithelial cells affects availability of host-derived extracellular iron or NAD+ and whether these impact growth of NTHi during viral-bacterial co-infection.

Hypothesis:

Rhinovirus co-infection will stimulate NTHi growth and decrease bacterial invasion of primary respiratory epithelial cultures from healthy and COPD patients through up-regulation of NTHi-essential host-released nutrients.

Aims:

- To determine the effect of RV co-infection on NTHi growth on primary respiratory epithelial cultures.
- To determine the effect of RV co-infection on NTHi adherence and invasion of primary respiratory epithelial cultures.
- To determine whether epithelial differentiation stage affects the course of a RV and NTHi co-infection.
- To determine the effect of RV co-infection on epithelial apical release of iron and β-NAD, two of the nutrients essential for NTHi growth.

3.4.2. Rhinovirus co-infection stimulates planktonic NTHi growth

To determine the effect of RV co-infection on NTHi growth on the airway epithelium, primary epithelial cultures from healthy donors and patients with COPD were differentiated for either 6 days or 28 days before being infected with RV (as explained in section 2.29). Twenty four hours later, cultures were challenged with NTHi for another 24 hours (section 2.30). Non-attached NTHi was quantified as described in section 2.24.

In pre-ciliation day 7 cultures, for both healthy and COPD, there was a significantly higher number of non-attached NTHi (Figure 27) during RV and NTHi co-infection compared to NTHi infection alone (healthy, $p=0.034$, COPD, $p=0.023$). The same trend was seen in COPD ciliated (day 28) cultures, where the number of non-attached NTHi increased during RV co-infection when compared to NTHi infection alone ($p=0.002$). In healthy ciliated cultures there was evidence to indicate the same effect, but this was not statistically significant ($p=0.055$). These counts were matched by observations made by high-speed video microscopy where denser bacterial aggregates were observed during RV and NTHi co-infection, containing a mixture of bacterial structures and detached epithelial cells, compared to NTHi infection alone (See Appendix 4 and Videos 4 and 5 on USB stick attached, for a comparison of aggregate formation by NTHi alone and during RV and NTHi co-infection). There was no difference in NTHi growth during single infection or co-infection with RV between pre-ciliation day 7 cultures and ciliated day 28 cultures or between healthy and COPD cultures at either time point ($p>0.05$), indicating that this effect is independent of epithelial differentiation stage or disease state.

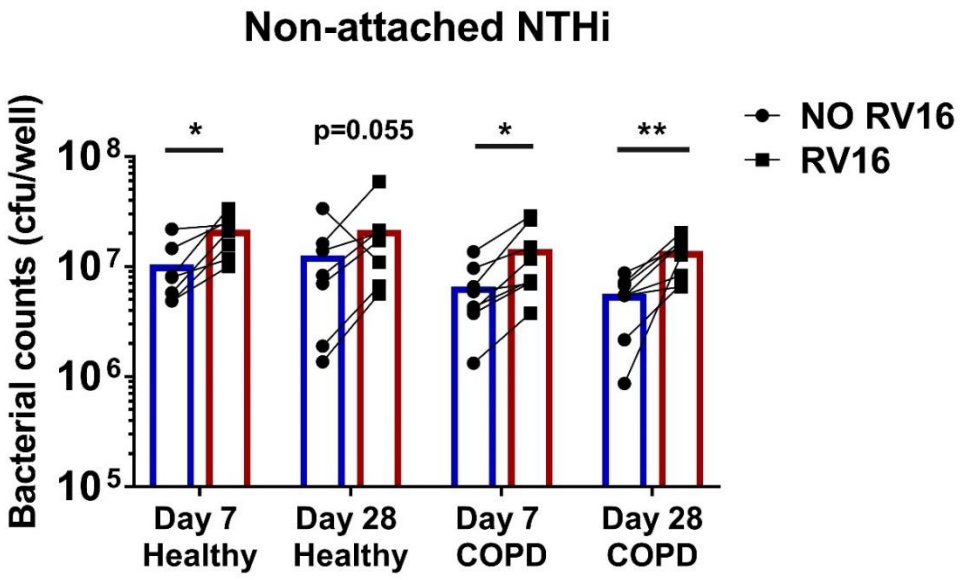

Figure 27. Quantification of non-attached NTHi during RV co-infection of primary epithelial cultures at day 7 and day 28 of differentiation

Pre-ciliation, day 7, and ciliated, day 28, nasal epithelial cultures from healthy and COPD donors were infected with RV16 ($1.5x10^6$ $TCID_{50}$/well) and after 24 hours challenged with NTHi 49247 ($5x10^6$ CFU/well) for another 24 hours. Non-attached bacteria were quantified by viable counts from apical fluid, as described in section 2.24. Symbols represent individual donors, with lines connecting the same donor during single and co-infection. Bars show mean bacterial counts. N=7 healthy, 8 COPD donors. For statistical analysis, bacterial counts values were log10 transformed and analysed using a linear mixed effects model with fixed effects for disease group, day and RV infection and a random day-specific donor effect. P values were adjusted using the Benjamini-Hochberg method for multiple comparisons. *=p<0.05, **=p<0.01.

3.4.3. Rhinovirus co-infection decreases NTHi invasion of ciliated COPD cultures, but does not affect NTHi attachment to the epithelium

At 48 hours post rhinovirus infection and 24 hours post NTHi infection, bacterial attachment and invasion of epithelial cultures was quantified as indicated in

section 2.24. Despite the higher number of viable NTHi in cultures during co-infection with RV, as shown in section 3.4.2, there was no change in bacterial attachment to the epithelium, in either ciliated or pre-ciliation cultures from healthy or COPD donors, when compared to NTHi attachment during single infection (Figure 28A) ($p>0.05$). However, NTHi internalisation was significantly decreased by RV co-infection in pre-ciliation day 7 healthy cultures when compared to invasion by NTHi alone (Figure 28B) ($p=0.032$). This effect was not seen in COPD cultures at day 7 ($p=0.82$). While in healthy ciliated cultures RV co-infection did not affect bacterial invasion significantly ($p=0.397$), in COPD ciliated cultures bacterial invasion was reduced during RV co-infection ($p=0.02$) compared to single NTHi infection.

Collectively, these data suggest that RV co-infection of nasal epithelial cultures supports growth of NTHi, independent of epithelial differentiation or disease state. Despite the increased availability of viable non-attached NTHi during RV co-infection compared to single NTHI infection, there was no change in bacterial adhesion to the epithelium coupled with a decreased invasion in non-ciliated healthy cultures and ciliated COPD epithelia. This led to the hypothesis that RV co-infection might change the behaviour of NTHi by promoting growth and reducing its invasiveness. One possibility is that RV infection might alter the composition of apical secretions released by epithelial cultures to increase nutrient availability, thus supporting NTHi growth and changing its invasive behaviour.

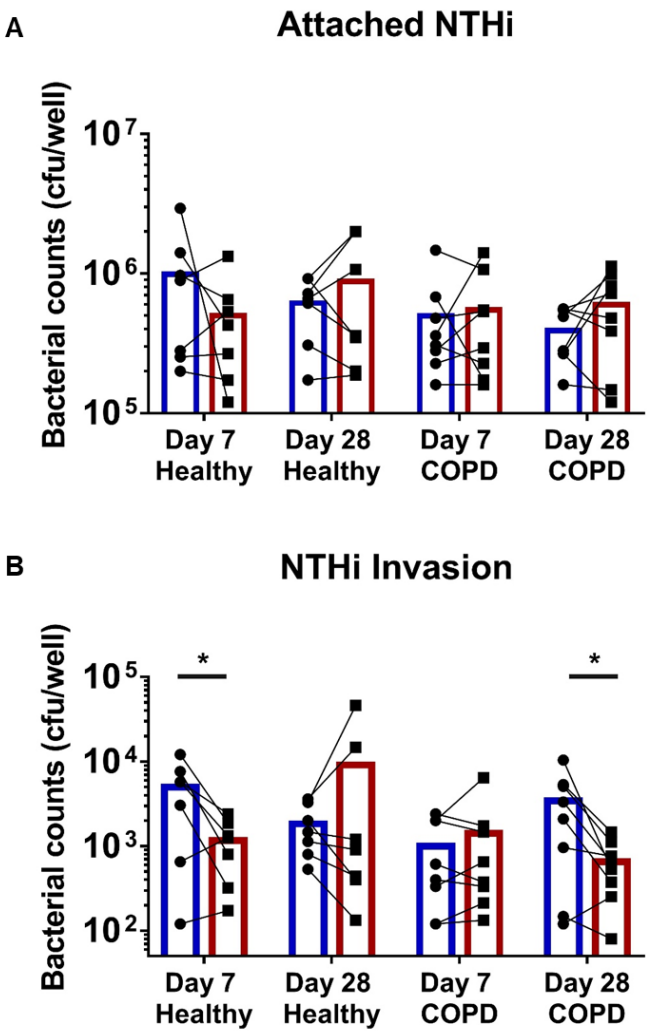

Figure 28. Quantification of NTHi attachment and invasion of primary respiratory epithelial cultures during co-infection with RV

Pre-ciliation day 7 cultures and ciliated day 28 nasal epithelial cultures from healthy and COPD donors were infected with RV16 ($1.5x10^6$ $TCID_{50}$/well) and after 24 hours challenged with NTHi 49247 ($5x10^6$ CFU/well) for another 24 hours. NTHi attachment (A) and invasion (B) were quantified using the gentamicin killing assay, as described in section 2.24. Symbols represent individual donors, with lines connecting the same donor during single and co-infection. Bars show mean bacterial counts. N=7 healthy, 8 COPD donors. For statistical analysis, bacterial counts values were log10 transformed and analysed using a linear mixed effects model with fixed effects for disease group, day and RV infection and a random donor effect. P values were adjusted using the Benjamini-Hochberg method for multiple comparisons.*=$p<0.05$.

3.4.4. Apical fluid from RV infected epithelial cultures supports growth of NTHi even in absence of epithelial cells

Next, it was important to determine if the increased NTHi growth on RV infected epithelial cultures was due to a change in epithelial secretions as a result of the viral infection. Therefore, apical fluid from pre-ciliation day 7, and ciliated day 28, healthy and COPD epithelial cultures, which were uninfected or infected with RV for 48 hours, was collected fresh and incubated with NTHi for 24 hours, as described in section 2.32. Viable counts of NTHi (Figure 29) indicated that irrespective of the disease state or differentiation stage of the epithelial cultures, apical fluid from cultures infected with RV supported growth of NTHi significantly more than apical fluid from control uninfected cultures ($p<0.0001$). This increase was not dependent on a direct effect of RV on NTHi, as in control experiments where NTHi was incubated with BEBM alone or BEBM containing $2.5x10^5$ TCID50/ml RV (the viral load determined from titration assays to quantify the amount of RV in apical fluid from nasal epithelial cultures, data not shown), the virus had no effect on overall NTHi viability after a 24 hour incubation ($p=0.99$). These results emphasize that a change in the content of the apical secretions during RV co-infection is responsible for the increased NTHi growth, rather than a direct virus effect. This led to the possibility that RV might increase availability of nutrients for NTHi growth, such as extracellular iron, as previously described during RSV and *P. aeruginosa* co-infection (Hendricks et al., 2016) or of NAD^+, the other essential factor required by NTHi for growth (Mesquita et al., 2016).

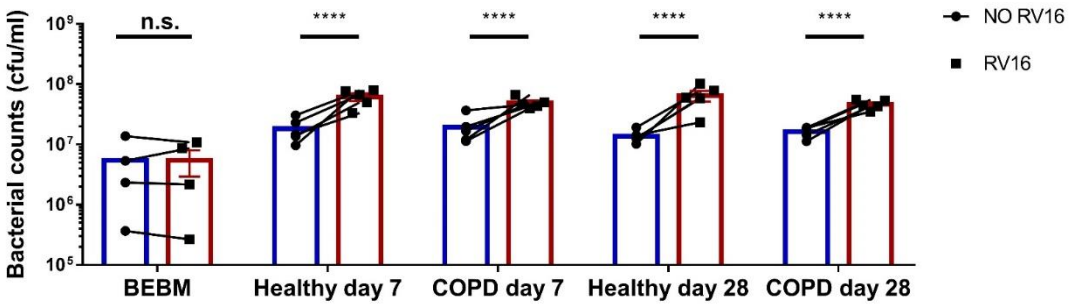

Figure 29. Effect of apical fluid from RV infected day 7 and day 28 epithelial cultures on NTHi growth

Pre-ciliation, day 7, cultures and ciliated, day 28, cultures from either healthy or COPD donors were infected with RV16 ($1.5x10^6$ $TCID_{50}$/well) for 48 hours, after which apical fluid was collected fresh and was incubated with NTHi 49247 ($5x10^6$ CFU/well) in absence of epithelial cells for 24 hours, as described in section 2.31. BEBM with or without RV16 was incubated with NTHi as a control. N=5 healthy, 5 COPD donors, 4 experimental repeats for control BEBM ± RV. Symbols represent individual culture donors with lines connecting same donor with or without RV. For control BEBM, symbols represent experimental repeats. Bacterial counts were log 10 transformed and analysed using a linear mixed effects model with fixed effects for disease group, RV infection and day and a random intercept for each donor. Bacterial counts from BEBM control experiments were analysed on the original scale using a paired t-test. Bars show mean bacterial counts ± standard error of the mean. ****=p<0.0001.

3.4.5. Do iron and β-NAD affect growth of NTHi in basal cell culture medium in absence of epithelial cells?

NTHi is a fastidious microorganism that requires exogenous sources of hemin, which provides iron- and NAD+ needed for growth and replication (Aich et al., 2015; Mesquita et al., 2016; Vogel et al., 2012). However, hemin, which is present in red blood cell haemoglobin, would not normally be available in

epithelial cultures for NTHi to use, but rather it is epithelial cell released iron that is more important (Aich et al., 2015; Hendricks et al., 2016). Therefore, in absence of epithelial cells, the effects of iron and β-NAD on NTHi growth in basal cell culture medium were tested - Figure 30; hemin addition was used as a positive control. When grown in BEBM alone, NTHi viability decreased significantly over 24 hours ($p=0.003$) compared to the initial inoculum count. However, when the BEBM was supplemented with both hemin and β-NAD, the two factors normally used to grow NTHi, bacterial survival was increased and cell numbers were significantly higher at 24 hours compared to medium alone ($p=0.003$). When each factor was added to the BEBM independently, β-NAD alone was able to sustain NTHi survival compared to medium alone ($p=0.005$) and to similar levels as when both hemin and β-NAD were present ($p=0.430$). Hemin alone, on the other hand, did not support NTHi survival when compared to medium alone ($p=1$). When hemin was replaced with ferric iron salt, similar results were obtained, in that addition of iron alone did not change NTHi survival when compared to medium alone ($p=1$), but addition of β-NAD and iron stimulated NTHi growth to the same levels as hemin and β-NAD ($p=1$). This experiment confirmed that exogenous β-NAD is essential for NTHi growth but also revealed that in its absence, iron or hemin availability is insufficient to support NTHi survival.

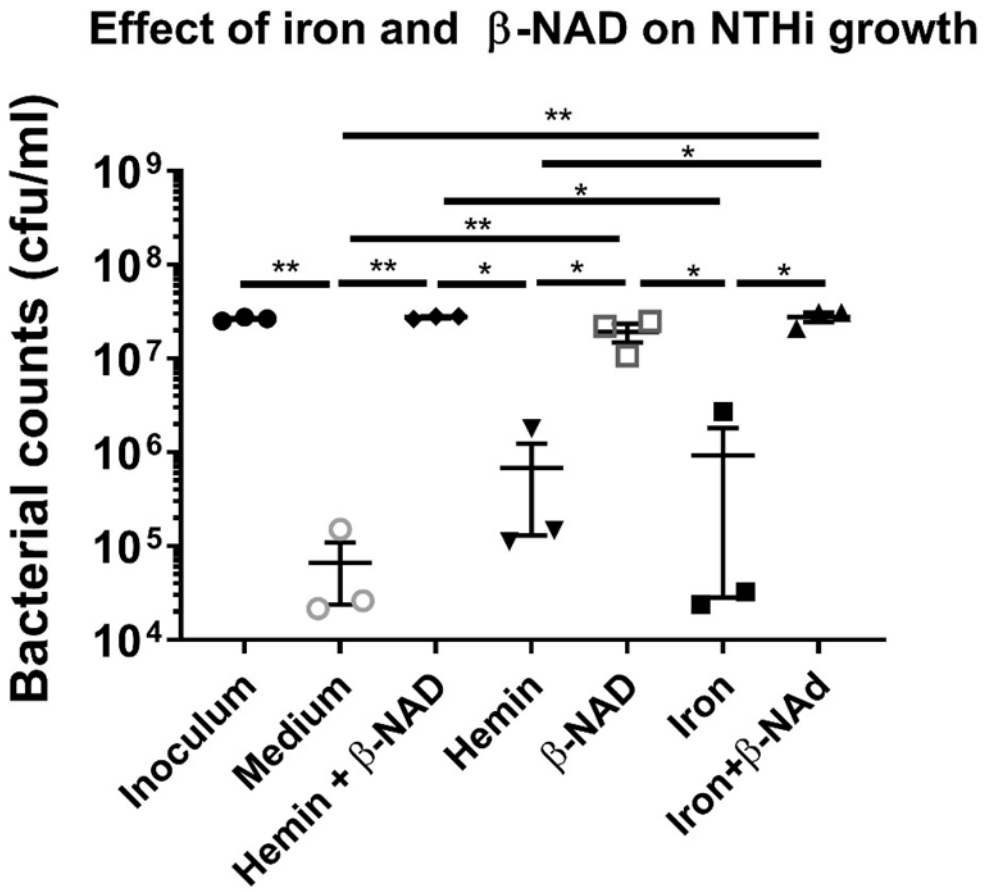

Figure 30. Effect of iron and NAD on NTHi growth in absence of epithelial cells

NTHi 49247 ($5x10^6$ CFU/well) was incubated with BEBM medium or BEBM containing 25 µM of $Fe(NO_3)39H_2O$, 10ug/ml Haemin and/or 10ug/ml β-NAD as described in Section 2.32 for 24 hours. N=3 experimental repeats. Symbols represent average from one experimental repeat with duplicate counts. For statistical analysis, average values were log10 transformed and analysed using a linear regression model with fixed effects for treatment and experiment. P values were adjusted for multiplicity using the Benjamini-Hochberg method. Data are shown as mean ±standard error of the mean. *=$p<0.05$, **=$p<0.01$.

3.4.6. Does RV infection of respiratory epithelial cultures stimulate apical release of iron or β-NAD?

To determine whether RV stimulated apical release of iron or NAD, the amount of total iron (Fe^{2+} and Fe^{3+}) and NAD in apical fluid from healthy or COPD epithelial cultures infected with RV for 48 hours was measured (Sections 2.33 and 2.34) (Figure 31). Interestingly, iron release was found to be significantly decreased in healthy day 7 cultures following RV infection compared to uninfected cultures ($p=0.036$) (Figure 31A). In the COPD day 7 cultures, as well as in ciliated healthy and COPD cultures, rhinovirus infection did not alter the iron content of the apical fluid when compared to their respective uninfected control cultures ($p>0.05$). It was also found that COPD uninfected ciliated cultures had a significantly lower iron content in apical fluid when compared to uninfected day 7 cultures ($p=0.036$). Similarly, following RV infection, apical fluid from COPD ciliated cultures contained significantly less iron than apical fluid from RV infected day 7 COPD cultures ($p=0.011$) but also compared to healthy, RV infected, ciliated cultures ($p=0.036$).

In conclusion, these data indicate that RV infection of healthy or COPD epithelial cultures does not increase apical free iron availability when measured at 48 hours post RV infection, but rather decreased it in day 7 healthy cultures. Therefore, in this study an increase in iron does not appear to be the factor that supports growth of NTHi during RV co-infection.

Next, the amount of NAD in apical fluid from RV infected healthy or COPD cultures was quantified as described in section 2.34, (Figure 31B). In this case too, rhinovirus infection did not stimulate apical release of NAD in either

healthy or COPD cultures, irrespective of their differentiation stage. This finding was also replicated in a COPD ciliated bronchial epithelial culture, where the concentration of NAD was similar to that of nasal ciliated cultures, namely 15.2nM prior to RV infection and 14.9nM following RV infection, suggesting no effect of RV on extracellular NAD availability.

What this analysis revealed, however, was a significantly higher availability of apical, extracellular, NAD in pre-ciliation cultures versus ciliated, day 28 cultures, in both healthy and COPD, irrespective of their infectious status ($p<0.0001$). In addition, apical fluid from healthy, day 7 cultures, contained more NAD than that of COPD day 7 cultures, in both control uninfected cultures and in RV infected cultures ($p=0.035$ in both cases).

In conclusion, these results point towards apical NAD availability not being increased following RV infection of epithelial cultures, therefore indicating that NAD is unlikely to be the factor that stimulates NTHi growth following RV infection of epithelial cultures. However, the striking difference in extracellular NAD availability between day 7 cultures and ciliated cultures is worth further investigation.

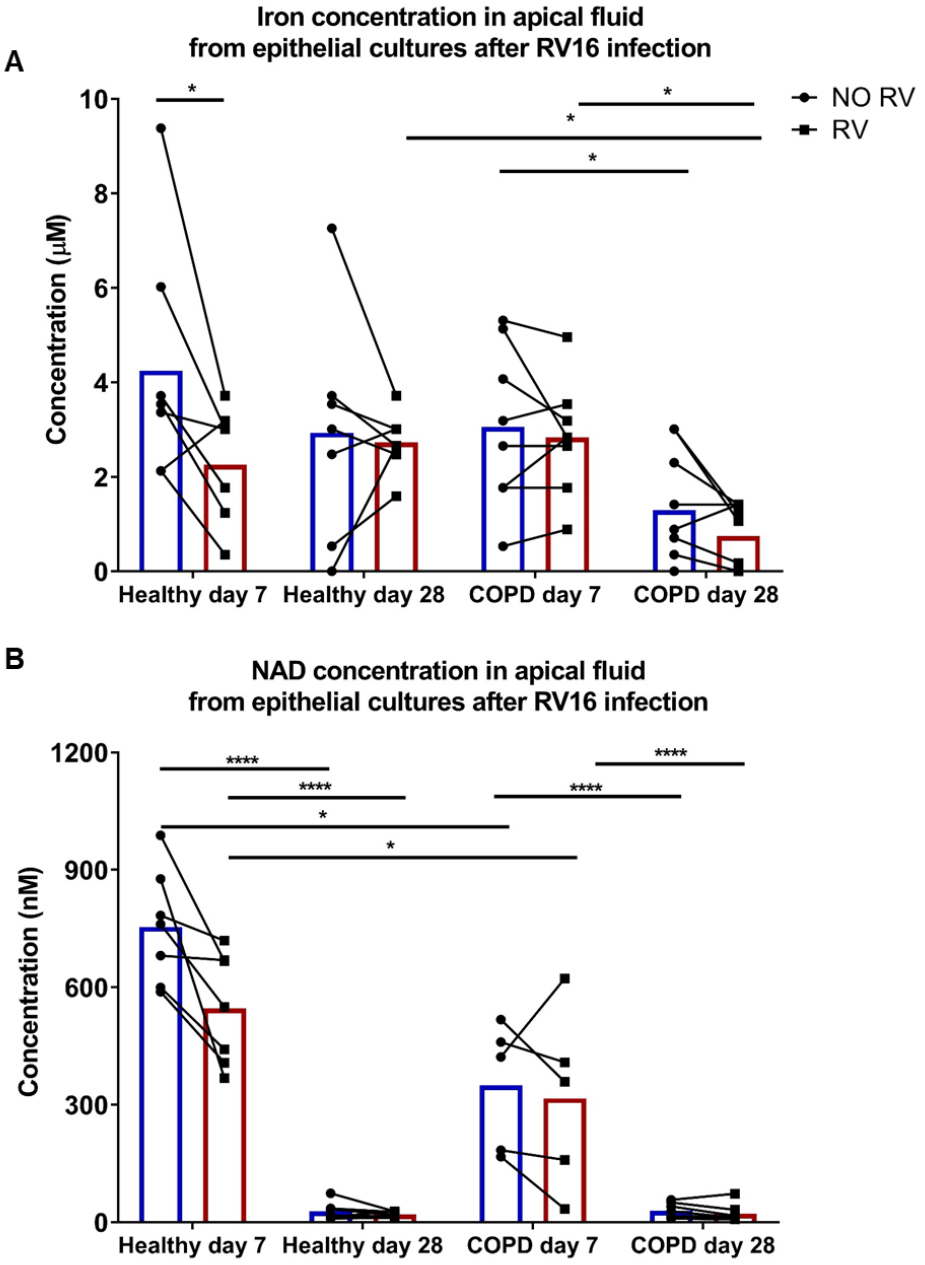

Figure 31. Quantification of total iron and NAD in apical fluid from RV infected day 7 and day 28 epithelial cultures

Total iron (A) or NAD (B) in apical fluid from uninfected or RV16 (1.5 $TCID_{50}$/well) infected cultures were quantified at 48 hours post infection using colorimetric and chemo-luminescence dedicated kits, respectively (sections 2.33 and 2.34 respectively). Symbols represent individual donors with lines connecting pre- and post RV concentrations within the same donor. Bars represent mean of the group. A. N=8 healthy day 7, 7 healthy day 28, 8 COPD day 7, 9 COPD day 28. B. N=7 healthy day 7 and day 28, 5 COPD day 7, 8 COPD day

28. For statistical analysis, NAD concentrations were log10 transformed, whereas iron concentration were analysed on the original scale. Iron and NAD concentrations were modelled separately suing linear mixed effects models with fixed effects for disease group, day and RV treatment and a random effect for each donor. P-values were Benjamini-Hochberg adjusted for multiple comparisons. *=p<0.05, ****=p<0.0001.

3.4.7. Discussion

An interplay between RV and NTHi in the pathogenesis of COPD exacerbations has been implied in clinical studies that highlight an increased association of exacerbations with presence of both pathogens and a significant growth of airway colonising NTHi following experimental rhinovirus infection (Molyneaux et al., 2013; Wilkinson et al., 2017). However, the mechanism by which RV could stimulate growth of NTHi in COPD airways has not been elucidated. In this study, healthy and COPD nasal epithelial cultures that were differentiated for 7 days or 28 days were infected with RV for 24h and then challenged with NTHi for another 24h, based on the hypothesis that RV would stimulate growth of NTHi and increase bacterial adhesion and invasion of the respiratory epithelium.

As predicted, an increase in non-attached NTHi was detected during co-infection with RV compared to NTHi infection alone (Figure 27), which appeared to be independent of disease state or differentiation stage of the epithelial cell cultures. Despite the difference in bacterial count between NTHi alone and NTHi and RV co-infection of healthy ciliated cultures not reaching statistical significance (p=0.055), bacterial growth during co-infection was observed in 6 out of 7 cultures, suggesting the effect of RV on NTHi growth is similar to that in the other 3 conditions tested. This result agrees with a

previous report showing that *in vitro*, RV14 infection of a cystic fibrosis epithelial cell line culture promoted growth of *P. aeruginosa* (Hendricks et al., 2016). Similarly, the same group have shown that RSV infection of cystic fibrosis epithelial cell line cultures could promote growth and biofilm formation of *P. aeruginosa* and *S. aureus*, albeit through different mechanisms of nutritional immunity changes (Hendricks et al., 2016; Kiedrowski et al., 2018). *P. aeruginosa* growth occurred due to an increased apical release of transferrin bound iron by cystic fibrosis epithelial cells as a result of RSV co-infection whereas *S. aureus* growth was independent of iron availability. In this case, *S. aureus* growth was due to higher amino acid availability and through up-regulation of genes associated with bacterial metabolism and protein synthesis during co-infection with RSV (Hendricks et al., 2016; Kiedrowski et al., 2018). Prior influenza infection was also shown to promote growth of *S. pneumoniae* in *in vivo* mouse studies, this time through up-regulation of host derived sialic acid, contained in glycoconjugates such as mucins (Siegel et al., 2014). More importantly, the enhanced growth of *S. pneumoniae* during influenza co-infection resulted in aspiration and bacterial spread to the lungs, resulting in lower airway colonisation (Siegel et al., 2014). In human studies, the dynamics of NTHi colonisation in children was changed during a viral infection, with higher bacterial counts detected when a virus was also present, independent of whether the child was symptomatic or asymptomatic (DeMuri et al., 2018).

These studies indicate that a similar process might occur in the airway of COPD patients, during rhinovirus and NTHi co-infection, particularly as NTHi is known to colonise the nasopharynx in healthy individuals, but it is often

identified in the lower respiratory tract of patients with COPD at exacerbation (Bandi et al., 2001). What is more, RV was shown to allow liberation of planktonic *P. aeruginosa* from biofilms formed on primary ciliated cystic fibrosis epithelial cultures, thus supporting the notion that a viral infection could lead to bacterial spread and colonisation of the lower respiratory tract (Chattoraj et al., 2011).

However, the mechanism by which RV could stimulate growth of NTHi in human airways remains elusive. Previous studies have only focused on the role of RV on NTHi adhesion to the epithelium. A study by Sajjan et al. (2008) reported that RV39 and RV1B could increase adherence of NTHi to primary ciliated respiratory epithelial cultures as well as bacterial transmigration across the epithelium, through a decrease in epithelial barrier function. Similarly, Wang et al. (2009) reported that RV infection of submerged, undifferentiated, primary nasal epithelial cultures leads to increased adherence of NTHi, possibly through viral induced up-regulation of receptors such as fibronectin, PAF-R and CEACAM. However, no previous studies quantified the effect of RV co-infection on NTHi adherence and invasion of primary epithelial cultures from healthy donors or patients with COPD. Interestingly, results of this study showed no effect of RV on NTHi adherence (Figure 28A) to the airway epithelium, irrespective of differentiation stage or disease group, which contrasts with previous reports. One possibility for the differing results compared to the study by Wang et al. (2009) is that air-liquid interface cultures were used in the current investigation, as opposed to submerged basal cell cultures, and results shown in chapter 3.3 indicate that the stage of epithelial cell differentiation bears a big impact on experimental read-outs and results.

Furthermore, they quantified NTHi adherence to the epithelium by fluorescence microscopy as opposed to viability counts used in this study (Wang et al., 2009). In their study, Sajjan et al. (2008) used ciliated primary epithelial cultures but three different isolates of NTHi, obtained from COPD patients, 2 different strains of RV (RV39 and RV1B) and a different experimental viral infection method whereby they left the viral inoculum on the culture for 24 hours, before addition of the bacteria, therefore results may not be directly comparable to those obtained in the current investigation

Surprisingly, in this study, NTHi invasion was decreased by RV co-infection of healthy, but not COPD, pre-ciliation day 7 epithelial cultures as well as of COPD ciliated cultures (Figure 28B). No clear effect of RV co-infection on NTHi invasion was observed in healthy ciliated cultures, possibly owing to inter-donor variability arising from use of multiple donors as opposed to epithelial cell lines or single donor studies. However, these findings of reduced or unchanged NTHi invasion are unexpected and somewhat counterintuitive considering the increased bacterial availability in the cultures, as demonstrated by the increased non-attached bacterial counts (Figure 27). Therefore, it was possible to hypothesize that a change in availability of nutrients as a consequence of the viral infection could alter the behaviour of NTHi, thus affecting its invasiveness and promoting growth. This type of behaviour alteration has been previously described for NTHi in response to heme-iron availability (Szelestey et al., 2013). It indicated that heme-iron restriction promoted internalisation of NTHi into chinchilla middle ear epithelial cells compared to heme-iron replete NTHi (Szelestey et al., 2013). By extrapolation, this study tested the hypothesis that RV infection of healthy and COPD primary

epithelial cultures could alter the availability of nutrients, thus promoting growth of NTHi and reducing its invasive behaviour. To confirm that the effect on bacterial growth was a consequence of a change in secretions from epithelial cultures, conditioned apical fluid collected following RV infection of epithelial cells was incubated with fresh NTHi in absence of epithelial cells. Irrespective of disease state or differentiation stage of the epithelium, apical fluid from RV infected cultures invariably promoted growth of NTHi compared to apical fluid from mock treated cultures (Figure 29). This effect was independent of the presence of RV in apical fluid, as incubation of NTHi with medium containing RV did not affect its viability when compared to incubation with BEBM alone, suggesting RV does not affect NTHi viability.

Given the previously documented requirement for iron and NAD+ for NTHi growth (Ahearn et al., 2017) it was intuitive to think of these two factors as nutrients that could easily boost NTHi growth following RV infection of epithelial cultures, particularly as virus effect on apical iron release has already been documented (Hendricks et al., 2016). Therefore, it was important to determine the effect of iron addition and β-NAD on NTHi growth in the basal culture medium used for epithelial culture infection. Interestingly, this experiment indicated that addition of iron alone to BEBM, either as an iron salt or as a complex in the form of hemin, cannot support NTHi growth in absence of β-NAD. Conversely, β-NAD alone was able to support growth of NTHi to levels similar to that of the positive control: β-NAD and hemin. This suggests that β-NAD alone might be an essential nutrient required for NTHi survival in BEBM.

Ultimately, the amount of iron and β-NAD in the conditioned apical fluid collected from epithelial cultures after RV infection was determined (Figure 31). Surprisingly, neither iron nor NAD were increased by RV infection. In contrast, iron availability was significantly decreased by RV infection in healthy pre-ciliation day 7 cultures whereas RV had no effect on extracellular NAD release. Therefore, it is possible that other factors are responsible for supporting the growth of NTHi during RV co-infection, such as sialic acid contained in mucins, particularly as RV was shown to up-regulate expression of mucin genes in section 3.3.3. In addition, clinically invasive NTHi strains were shown to have altered metabolic preferences for carbon sources such as sialic acid and reduced invasion of bronchial epithelial cells *in vitro,* possibly owing to metabolic adaptations during infection (Muda et al., 2019). A broader investigational approach, such as using quantitative mass spectrometry to look at proteomic and metabolomic profiles would allow a better understanding of the changes that occur in apical secretions from epithelial cultures following RV infection. Subsequently, it would be of interest to understand the transcriptional changes that occur in NTHi during co-infection with RV. Answering these questions would reveal if the changes in NTHi growth and invasive behaviour observed in this study are linked to a change in nutritional immunity or related to different mechanisms. One alternative possibility would be through alterations in antimicrobial levels in apical fluid from epithelial cultures. Previously Cole et al. (1999) have described the antimicrobial effect of nasal secretions on several different bacterial strains. Moreover, levels of the antimicrobial peptides secretory leukoprotease inhibitor and elafin were found to be reduced in sputum following experimental RV16 infection of

patients with COPD who developed secondary bacterial infections (Mallia et al., 2012). A reduction of antimicrobial peptides by RV co-infection would also explain the unrestricted growth of NTHi.

Another interesting finding of this study was that extracellular NAD was significantly lower in ciliated cultures, both healthy and COPD, compared to day 7 pre-ciliation cultures - Figure 31. The reason behind this striking difference in extracellular NAD levels between pre-ciliation day 7 cultures and ciliated day 28 cultures, remains unclear. The essential role of intra-cellular NAD in cellular processes such as energy metabolism, DNA repair or even apoptosis has been extensively studied, but the existence and function of extracellular NAD is only beginning to be uncovered and is still incompletely understood (Billington et al., 2006; Canto et al., 2015). So far, it is believed that NAD can translocate across cellular plasma membrane through hemichannels such as connexin 43, which is also expressed by respiratory epithelial cells, or it can be released locally at sites of injury and inflammation through cell lysis (Billington et al., 2006; Bou Saab et al., 2014). The mechanism of extracellular NAD secretion and the role it plays during human respiratory epithelium differentiation have not been studied yet. However, it is possible to speculate that changes in the levels of NAD are related to the differentiation stage of the cultures, as a few reports have suggested important roles for this molecule in regulation of cellular signalling pathways and stem cell differentiation (Gerth et al., 2004; Meng et al., 2018). As such, it is thought that airway epithelial cells express CD38, an ADP-ribosyl transferase which can translocate the ADP-ribose moiety from NAD to other acceptor proteins, but the downstream effects of this process are still unclear in epithelial cells (Uhlen, 2003; Uhlen et al.,

2015; Ziegler and Niere, 2004). A study of the effect of nicotinamide, a precursor of NAD+, on human pluripotent stem cells has uncovered that nicotinamide promoted cell survival and differentiation (Meng et al., 2018). Nicotinamide was found to act as a ROCK inhibitor and thus promote cell survival, but its effects extended beyond pathways regulated by ROCK signalling, inhibiting numerous other kinases. Of interest to this study was the fact that nicotinamide was found to initiate differentiation of the pluripotent stem cells by inhibition of casein kinase 1 and other kinases that regulate pluripotency. These effects were dose dependent, with only high concentrations of nicotinamide being able to induce the protein kinase inhibitory effects (Meng et al., 2018). Therefore, extrapolating from these findings, it is possible that high levels of NAD found in apical fluid of pre-ciliation epithelial cultures were required for the early differentiation stage and these ultimately decrease as epithelial differentiation is achieved. Previous reports described basal cell exhaustion in cultures from COPD patients and results shown in chapter 3.1 also indicated delayed and reduced ciliation in COPD epithelial cultures compared to healthy (Figure 7) (Ghosh et al., 2018). Therefore, it would be of interest to understand if the significantly lower levels of apical NAD in pre-ciliation, day 7 cultures from COPD patients compared to those from healthy donors are a cause of abnormal epithelial differentiation or a result of disease imprinting on basal and progenitor cells, resulting in reduced release of extracellular NAD.

In conclusion, this study has highlighted that RV co-infection of the respiratory epithelium stimulated growth of non-attached NTHi coupled with a decrease in NTHi invasion, particularly in healthy pre-ciliation cultures and COPD ciliated

cultures. Apical release of two nutrients essential for NTHi survival, iron and NAD was not increased by RV infection of epithelial cultures, indicating that they are unlikely to be the factors promoting NTHi growth. More comprehensive studies using proteomics and metabolomics approaches are required to understand the differences in apical secretions from epithelial cells in the presence and absence of RV infection.

Chapter 4. Discussion and future perspectives

4.1. Rationale of the study

The ciliated respiratory epithelium plays a crucial role in host protection against inhaled pathogens through its mucociliary transport, barrier protection and production of anti-microbial proteins and inflammatory mediators (Rezaee and Georas, 2014). It is also the main site of pathology in chronic respiratory conditions such as COPD, where exposure to cigarette smoke over numerous years leads to repeated insults and injury, thus damaging the epithelial barrier (Amatngalim and Hiemstra, 2018). Airway inflammation is another important feature of COPD, which is further increased during periods of disease exacerbation, causing loss of lung function, further epithelial damage and disease progression (Amatngalim and Hiemstra, 2018). Most disease exacerbations are triggered by respiratory viral and bacterial infections, with RV and NTHi being the pathogens most frequently detected (Papi et al., 2006; Wilkinson et al., 2017). While RV has been shown to be able to induce COPD exacerbations during a single infection, NTHi is mostly seen as an airway colonising pathogen which is thought to use intracellular invasion of the epithelium for persistence in the respiratory tract (Finney et al., 2014; Mallia et al., 2011; van Schilfgaarde et al., 1999). However, co-infection with RV and NTHi has been associated with higher odds ratio of COPD exacerbation as well as with increased inflammation and severity of symptoms (Papi et al., 2006; Wilkinson et al., 2017). Given the burden of these two pathogens in COPD progression, there is surprisingly little understanding of the mechanisms of their interaction with the ciliated respiratory epithelium and, in particular, the consequences of their co-infection on the airway epithelium.

In this project, it was hypothesised that RV and NTHi co-infection of the respiratory epithelium from healthy or COPD donors would result in more epithelial damage and inflammation as well as increased bacterial growth compared to NTHi infection alone. The specific aims of the project were to firstly characterise nasal epithelial cultures from healthy and COPD donors, to then investigate the early interaction of NTHi with the ciliated respiratory epithelium and ultimately to understand the effect of RV and NTHi co-infection on epithelial barrier function, bacterial growth and inflammatory responses. Another aim of the project was to understand if the differentiation stage of the epithelium affects the course of rhinovirus and NTHi single infection and their co-infection. The main findings presented in this thesis are summarised in Table 9, in the context of existing literature as well as future investigations, and discussed in more detail in the following sections of this chapter.

Table 9. Summary of findings presented in this thesis in the context of the existing literature and future studies

Chapter	Previous findings	Findings presented in this thesis	Main conclusion & *future studies*
3.1	▪ Increased levels of basal and goblet cells and decreased levels of ciliated cells in COPD epithelia compared to healthy. ▪ Primary respiratory epithelial cells from COPD donors give rise to differentiated cultures containing more goblet and less ciliated cells. ▪ Contradictory findings about changes in ciliary function in COPD. ▪ Increased baseline inflammatory mediator production in COPD compared to healthy, particularly IL-8.	▪ A decrease in basal cell number and proportion during differentiation of healthy epithelial cultures which was not seen in COPD cultures. ▪ No difference in goblet cell specific gene expression levels between healthy and COPD cultures. ▪ Decreased and delayed ciliation in COPD cultures compared to healthy. ▪ No difference in the baseline levels of ciliary beat frequency and amplitude between healthy or COPD. ▪ Increase in IL-8 production by ciliated COPD epithelial cultures compared to day 7 pre-ciliation cultures. No difference in healthy cultures.	▪ COPD epithelial cultures show altered differentiation, with reduced and delayed ciliation and a sustained basal cell population compared to healthy cultures. ▪ *Single cell transcriptomics could be used to assess cellular differences between healthy and COPD epithelia at a much higher resolution, help in identification of novel cell-type specific cell surface markers and understand COPD specific changes in epithelial composition.*

Chapter	Previous findings	Findings presented in this thesis	Main conclusion & *future studies*
3.2	▪ Contradictory findings regarding the interaction of NTHi with ciliated epithelial cells. ▪ Findings in human and bovine tissues explants suggested that NTHi may affect ciliary function. ▪ NTHi is an invasive bacterium, can invade and persist in epithelial cells despite antibiotic therapy. ▪ Studies in epithelial cell lines reported that NTHi invasion of the epithelium is dependent on PI3k pathway activation.	▪ NTHi binds to ciliated epithelial cells within minutes of addition to a ciliated culture, forms aggregates with a lattice like organisation which evolve into a biofilm like structure by 24 hours. ▪ NTHi forms elongated chains of bacteria at 24 hours post addition to healthy or COPD ciliated cultures. ▪ NTHi does not affect ciliary beat frequency but NTHi aggregates reduce ciliary beat amplitude. ▪ NTHi preferentially invades non-ciliated epithelial cells. ▪ NTHi invasion of the ciliated epithelium is not dependent on PI3K signalling.	▪ NTHi binds to cilia within minutes of addition to a ciliated epithelial culture and preferentially invades non-ciliated epithelial cells, suggesting ciliation may be protective against bacterial invasion. ▪ *Further dissect which specific cell type NTHi targets for invasion and the cell signalling pathways involved in invasion of primary epithelial cells.* ▪ *Development of novel antibiotic formulations to improve intracellular delivery of antibiotics could provide new therapeutic options for persistent NTHi infections.*

Chapter	Previous findings	Findings presented in this thesis	Main conclusion & *future studies*
3.3	▪ RV was shown to cause shedding of ciliated cells and to induce goblet cell hyperplasia. ▪ A limited number of suggestions indicating that NTHi could stimulate mucus hypersecretion. ▪ No knowledge of the effect of RV and NTHi co-infection on ciliary or goblet cell function. ▪ Both RV and NTHi have individually been shown to affect the epithelial barrier function and tight junction integrity. ▪ No study has investigated the effect of RV and NTHi co-infection on healthy or COPD primary epithelial barrier function and tight junctions.	▪ RV and NTHi co-infection led to a decrease in ciliary beat frequency, particularly in healthy donors. ▪ RV induced up-regulation of the goblet cell specific transcription factor *SPDEF* and of mucins *MUC5AC*, *MUC5B*, *MUC4* during single and co-infection with NTHi in healthy and COPD ciliated epithelial cultures. ▪ These effects were not seen in day 7 pre-ciliation cultures. ▪ TEER was reduced by RV infection and RV and NTHi co-infection in both healthy and COPD ciliated cultures. ▪ In day 7 pre-ciliation cultures, TEER was only reduced by RV and NTHI co-infection of healthy cultures.	▪ As shown in sections 3.3. and 3.4, RV and NTHi co-infection leads to NTHi growth, ciliary dysfunction, mucin gene up-regulation, epithelial barrier damage and increased inflammatory responses compared to NTHi infection alone. ▪ Pre-ciliation epithelial cultures were susceptible to NTHi invasion and growth of NTHi during co-infection with RV16, but were not able to mount appropriate host defence mechanisms, thus potentially serving as a niche for bacterial colonisation and dissemination.

Chapter	Previous findings	Findings presented in this thesis	Main conclusion & *future studies*
	▪ Both RV and NTHi have been shown to increase secretion of pro-inflammatory mediators by healthy epithelial cells. ▪ No study has investigated the inflammatory response of COPD epithelial cells to NTHi single infection. ▪ Synergistic induction of IL-8, CCL20 and IL-17C following simultaneous RV and NTHi co-infection of epithelial cell lines or submerged basal cells was reported.	▪ In both healthy and COPD ciliated cultures, RV16 infection reduced expression of *Claudin 8* and increased expression of *ZO-1* during single and co-infection with NTHi. ▪ In day 7 healthy and COPD cultures, *Claudin 8* expression was reduced by NTHi infection and RV-NTHi co-infection. *ZO-1* expression was not altered. ▪ Cytokines and chemokine secretion (IL-6, IL-17C, IFN-λ, G-CSF, IP-10, RANTES) was RV16 driven during single and co-infection with NTHi in both healthy and COPD ciliated cells; with the exception of IL-1β, TNF-β, and IL-8 which were also induced by NTHi, but no synergistic effect was detected.	▪ *Validation of changes observed at a gene expression level for mucins and tight junction proteins by quantification of protein levels would provide a better understanding of the effect of RV and NTHi co-infection on epithelial mucus secretion and barrier function in healthy and COPD.*

Chapter	Previous findings	Findings presented in this thesis	Main conclusion & *future studies*
	▪ RV was shown to preferentially replicate in ciliated cells; viral replication was reported lower in pre-ciliation epithelial cells compared to ciliated epithelial cells. ▪ Higher viral loads were reported in COPD epithelia cultures compared to healthy.	▪ Cytokines and chemokine secretion by day 7 cultures was significantly reduced in response to all infection treatments. ▪ Higher viral loads were detected in healthy and COPD ciliated cultures compared to day 7 pre-ciliation cultures. ▪ No difference between healthy and COPD viral loads at either time-point.	▪ *Mass spectrometry analysis of epithelial apical secretions and transcriptomic analysis of epithelial cell changes following RV16 infection would provide an insight into the changes that lead to the growth of NTHi during RV and NTHi co-infection.*
3.4	▪ Experimental human RV16 infection revealed that RV can lead to secondary bacterial infection and in particular growth of NTHi in COPD patients. ▪ Studies investigating different viral-bacterial co-infections (RSV+ *P. aeruginosa*, RSV+ *S. aureus*, influenza + *S. Pneumoniae*) have reported bacterial growth following virus infection of epithelial cells in vitro or in vivo in animal models.	▪ RV infection of healthy and COPD epithelial cultures stimulated NTHi growth in ciliated and pre-ciliation cultures, likely through changes in epithelial apical secretions and independent of RV16 presence. ▪ Epithelial invasion by NTHI was reduced during co-infection with RV in pre-ciliation healthy cultures and ciliated COPD cultures.	

Chapter	Previous findings	Findings presented in this thesis	Main conclusion & *future studies*
	▪ Bacterial growth was reported to be a consequence of increased availability of nutrients such as iron or sialic acid following virus infection. ▪ Iron and β-NAD are essential nutrients for NTHi growth.	▪ B-NAD alone was able to support NTHi growth in basal cell culture medium. ▪ RV16 infection of healthy or COPD epithelial cells did not increase iron and β-NAD apical secretion. ▪ B-NAD levels were significantly higher in day 7 healthy and COPD epithelial cultures compared to ciliated cultures, but lower in COPD day 7 cultures compared to healthy day 7 cultures.	▪ *It would be of interest to understand the role of extracellular NAD on epithelial cell differentiation and in relation to COPD.*

4.2. COPD epithelial cultures show delayed and reduced ciliation compared to healthy epithelial cultures

A comparative characterisation of healthy and COPD nasal epithelial cultures differentiated at the ALI revealed no significant differences between the two groups in their epithelial resistance, ciliary function or baseline production of inflammatory mediators. However, during differentiation at ALI, COPD epithelial cultures showed a delay in establishing ciliation and reduced overall ciliation compared to healthy cultures. In addition, healthy epithelial cultures presented with a decrease in the proportion of basal cells with increasing differentiation of the cultures, a trend not seen in COPD cultures. In this study, COPD cultures maintained a higher proportion of basal cells even at later stages of differentiation, indicating an abnormal differentiation and regeneration of the ciliated epithelium compared to healthy epithelium. These findings are in agreement with previous reports (Ghosh et al., 2018). Furthermore, as the epithelium of patients with COPD is repeatedly injured and continuously regenerating, it was important to investigate the role of viral and bacterial infection and co-infection on a regenerating epithelium. As ciliation was found to start after day 7 of differentiation in ALI cultures, this stage was chosen as representative for a regenerating epithelium and investigated further during infection studies presented in sections 3.2, 3.3 and 3.4.

4.2.1. Future perspectives

In this characterisation of healthy and COPD nasal epithelial cultures, it was only possible to accurately quantify basal and ciliated epithelial cells, based on a novel flow cytometry method which made use of cell type specific cell surface

markers. However, no such markers exist for the separation of goblet cells and intermediate progenitor cell types. Currently, the methods available for quantification of goblet cells include use of gene expression or mucin protein expression assays as a proxy for determining goblet cell presence, but neither measurements are true representations of actual goblet cell number in the ciliated epithelium (Feldman et al., 2019; Jing et al., 2019; Park et al., 2007). As goblet cells are one of the key cell types involved in COPD pathology and mucus obstruction, an understanding of the changes that occur in terms of goblet cell numbers, their activity and response to infection in COPD epithelia compared to healthy would be of great assistance in understanding disease mechanisms (Boucher, 2019). The recent rise in the use of single cell transcriptomics for identification of epithelial cell types in the lung, during differentiation and in chronic diseases, as shown in a number of very recent studies (Montoro et al., 2018; Plasschaert et al., 2018; Vieira Braga et al., 2019), could be employed for determining changes in the COPD epithelium in a less biased way and at a much higher resolution than previously possible. Information gained from such studies could help in the identification of novel cell surface markers for different epithelial cells types. In addition, single cell transcriptomic and phenotypic studies could provide an understanding of how much nasal epithelial cultures replicate the disease phenotype of lower respiratory conditions such as COPD. Such studies could also reveal how well respiratory epithelial cultures grown *in vitro* preserve the disease phenotype for heterogeneous disease such as COPD. Ultimately, a more detailed understanding of the *in vitro* system and its limitations could aide in the interpretation of studies and dictate appropriate methods for validation.

4.3. NTHi binds to cilia within minutes of addition to a ciliated epithelial culture and preferentially invades non-ciliated epithelial cells in a PI3K independent manner.

In this investigation it was shown that the early interaction of NTHi with the ciliated epithelium involves binding of the bacteria to cilia within minutes of addition to a culture, followed by formation of filamentous morphotypes and biofilm like-aggregates with a lattice like organisation over 24 hours. Bacterial aggregate formation affected ciliary function by reducing the amplitude of ciliary beating in both healthy and COPD epithelial cultures. In addition, filamentous morphotypes and biofilm formation have been previously described as methods employed by bacteria to resist clearance by immune cells and antibiotic killing (Horvath et al., 2011; Slinger et al., 2006). It was shown in the present study that while NTHi was bound to cilia and ciliated cells extracellularly, intracellular invasion occurred preferentially in non-ciliated epithelial cells from both healthy and COPD donors. It was also observed that in healthy cultures, epithelial invasion by NTHi appeared to decrease in ciliated cultures compared to pre-ciliation cultures, suggesting that differentiated ciliated cells are more resistant to invasion by NTHi. In contrast, in COPD, epithelial invasion appeared higher in ciliated cultures compared to pre-ciliation cultures. Collectively these results suggest a protective role of ciliation against NTHi invasion. Reduced ciliation in COPD airways, as shown in section 3.1.4, might be one of the factors accounting for the decreased protection against NTHi invasion. Reduced ciliation might leave areas of the epithelium exposed to bacterial invasion because of disrupted protection by the periciliary layer which has been shown to prevent anything bigger than 40

nm from reaching the epithelial cell surface (Button et al., 2012). As such, formation of filamentous morphotypes and biofilm-like aggregation and reduction in ciliary function are likely to prevent efficient clearance of NTHi from the airways by mucociliary transport. Epithelial cell invasion by NTHi may allow persistence despite the presence of immune cells and antibiotic therapy, as many antibiotics penetrate epithelial cell poorly. These factors are particularly relevant in patients with COPD.

Furthermore, based on previous reports describing an important role for PI3K signalling in NTHi invasion of epithelial cell lines, the role of this pathway in NTHi invasion of primary ciliated cultures was investigated (Lopez-Gomez et al., 2012; Morey et al., 2011; Seiler et al., 2013). Contrary to these published results, data obtained in this investigation showed that in primary differentiated epithelial cultures from healthy and COPD donors, NTHi did not activate the PI3K pathway and that PI3K signalling inhibition did not affect bacterial invasion. This highlights the contrasting results obtained in the studies mentioned (Lopez-Gomez et al., 2012; Morey et al., 2011; Seiler et al., 2013) which used epithelial cells lines and which could not be reproduced in this multi donor study using primary epithelial cell cultures. It also emphasizes a need for validation of results obtained using epithelial cell lines in human primary cultures before definitive conclusions can be drawn.

4.3.1. Future perspectives

As results shown in section 3.2 have emphasised a preference of NTHi to invade non-ciliated epithelial cultures, it would be of interest to further dissect which non-ciliated epithelial cell types are targeted. Technical difficulties with

high levels of auto-fluorescence from basal cells of ciliated epithelial cultures precluded quantification of their invasion by NTHi using image cytometry. Furthermore, due to a lack of cell surface markers for separation of progenitor and goblet cell types, they were treated as a collective population. The ability to separate these cell types into homogenous populations would allow for a better understanding of which cell type becomes preferentially invaded and whether the frequency of this cell type is changed in COPD compared to healthy epithelia.

Furthermore, as PI3K signalling was shown not to affect NTHi invasion of the epithelium, future studies should focus on understanding what cell signalling pathways are activated by NTHi infection. For example, EGFR signalling and the MAP kinase signalling pathway have been implicated in NTHi invasion of epithelial cell lines by Mikami et al. (2005) and Xu et al. (2011), and these findings should be validated in primary ciliated cultures. An understanding of the mechanisms involved in epithelial invasion by NTHi might provide new targets for inhibiting bacterial invasion and persistence in the respiratory tract. Additionally, from a clinical perspective, development of new antibiotic formulations that improve antibiotic delivery inside epithelial cells would provide another avenue for treatment of persistent NTHi infections. Many of the antibiotics used routinely to treat bacterial infections, such as azithromycin, ampicillin and gentamicin, have poor intracellular penetration (Ahren, 2002; Kratzer et al., 2007). The ability to reduce NTHi invasion and persistence in the airway would be of important help for patients with COPD who are colonised by NTHi.

4.4. RV and NTHi co-infection leads to NTHi growth, ciliary dysfunction, mucin gene up-regulation, epithelial barrier damage and increased inflammatory responses compared to NTHi infection alone

Clinical studies have repeatedly reported a role for RV and NTHi co-infection in exacerbations of COPD. Experimental human RV challenges carried out in patients with COPD have shown that RV infection leads to alterations in the airway microbiome and, in particular, to growth of NTHi (Mallia et al., 2011; Molyneaux et al., 2013). However, knowledge of their interaction with and effect on the respiratory epithelium during co-infection remains very limited. In sections 3.3 and 3.4 of this thesis, it was shown that ciliary function was reduced during RV and NTHi co-infection, with a reduction in ciliary beat frequency seen predominantly in cultures from healthy donors. During RV and NTHi co-infection of ciliated epithelial cultures, RV was found to also drive up-regulation of *SPDEF* and mucin gene expression as well as epithelial barrier damage, shown through the reduction in TEER and changes in expression of *Claudin 8* and *ZO-1*, in both healthy and COPD cultures. RV co-infection also stimulated NTHi growth in healthy and COPD ciliated cultures, when compared to NTHi infection alone. NTHi growth during RV co-infection was shown to occur through a change in apical secretions following RV infection of epithelial cultures, but was not dependent on iron or β-NAD availability. Ultimately, during RV and NTHi co-infection, increased inflammatory responses were also stimulated by RV with fewer cytokines and chemokines being induced by NTHi infection alone and no detection of synergism between the two pathogens.

Therefore, these findings suggest on the one hand, that, epithelial invasion by NTHi (shown in section 3.2.4) occurs without disruption of epithelial barrier integrity and with limited induction of inflammatory mediators for immune cell recruitment, suggestive of the behaviour of a colonising pathogen. On the other hand, during RV and NTHi co-infection, presence of the virus causes increased epithelial responses associated with more severe airway pathology compared to a single NTHi infection. Firstly, mucociliary clearance is affected by a reduction in ciliary beat frequency and a presumed decrease in ciliary beat amplitude through formation of denser aggregates containing more bacteria and RV-detached ciliated cells, (as shown by Jakiela et al. (2014). Secondly, a predicted increase in mucus production, based on results shown here and in previous reports (Jing et al., 2019), would lead to an increased mucus content and further decrease in the efficiency of mucociliary transport. Thirdly, increased epithelial barrier damage and inflammation were also observed during RV and NTHi infection compared to NTHi infection alone, owing to a RV driven effect. Lastly, as RV co-infection was shown to cause growth of NTHi, the decreased epithelial barrier function and reduced mucociliary clearance might provide a route for bacterial dissemination in the airways. It is possible that this phenomenon is more pronounced in COPD epithelia where ciliation is reduced, as shown here and also by Ghosh et al. (2018), and goblet cell hyperplasia and increased mucus production are thought to persist longer than in healthy epithelia (Jing et al., 2019). Collectively, these findings provide an insight into the mechanisms that could account for the increased risk of disease exacerbation observed clinically

during RV and NTHi co-infection compared to NTHi single infection (Wilkinson et al., 2017).

Furthermore, this study has also emphasized the striking differences in response to RV, NTHi and their co-infection of ciliated epithelial cultures compared to pre-ciliation cultures. Both healthy and COPD regenerating epithelia displayed significantly different and reduced responses during single infection and co-infection with RV and NTHi. While RV replication in pre-ciliation cultures was significantly lower than in ciliated cultures, pre-ciliation cultures of both healthy and COPD donors were susceptible to NTHi invasion and supported growth of NTHi during co-infection with RV. Therefore, these findings indicate that a regenerating epithelium would be more susceptible to NTHi infection or RV and NTHi co-infection and unable to mount the appropriate host defence mechanisms, thus potentially allowing bacterial dissemination to the airways and widespread colonisation.

4.4.1. Future perspectives

Investigation of the effect of single RV or NTHi infection and their co-infection revealed a RV induced up-regulation of goblet cell specific genes such as *SPDEF* and mucin genes. It would be important to validate these findings by quantifying the number of goblet and secretory cells in epithelial cultures following these three infection conditions as well as the protein level of mucins released by epithelial cells. This would allow for an understanding of whether the increased mucus production is a consequence of a change in epithelial differentiation leading to an increased presence of goblet cells or a transcriptional and translational response leading to increased protein

production. It would also further elucidate if this differs between healthy and COPD epithelia.

In addition, this study showed that TEER values changed during RV infection and RV and NTHi co-infection; changes in expression of genes encoding for tight junction proteins were also detected in both healthy and COPD cultures. It would be important to assess whether these gene expression changes translate to alteration in tight junction integrity following infections. Immuno-staining for the ZO-1 and Claudin 8 proteins and imaging by confocal microscopy would reveal if there is disruption of epithelial junctional integrity as well as whether this varies during single infection versus co-infection or between healthy and COPD cultures.

As iron and β-NAD concentrations in the apical fluid were not increased by RV infection, it appears unlikely that these were the factors responsible for simulating NTHi growth. It would therefore be of interest to investigate the contents of apical secretions from healthy and COPD epithelial cultures following RV infection using a broader analysis method such as mass spectrometry to assess metabolomic and proteomic changes. Alongside this, a transcriptomic analysis of the changes that occur in epithelial cells during RV and NTHi co-infection compared to NTHi single infection would provide further information as to what changes could be responsible for supporting NTHi growth. An alternative to the nutrient availability hypothesis would be a decrease in antimicrobial peptides as a consequence of the viral infection. This would lead to reduced restriction of NTHi growth, as it has been previously reported in clinical studies (Mallia et al., 2012). Ultimately, a surprising finding was the significantly higher levels of extracellular NAD found in pre-ciliation

cultures compared to ciliated cultures and the lower levels detected in COPD pre-ciliation cultures compared to healthy. As the role of extracellular NAD is only being recognised and has been linked with regulating stem cell differentiation (Gerth et al., 2004; Meng et al., 2018), it would be of interest to investigate its role during epithelial differentiation and in relation to COPD. It would be important to understand if the significantly lower levels of apical NAD in pre-ciliation cultures from COPD patients compared to those from healthy donors are a cause of abnormal epithelial differentiation or a result of disease imprinting on basal and progenitor cells, resulting in reduced release of extracellular NAD.

4.5. Overall summary and future project perspectives

In summary, this project has revealed a number of novel findings with regards to the interaction of NTHi and RV with the ciliated respiratory epithelium of healthy and COPD donors. Results of this study have highlighted mechanisms employed by NTHi to avoid clearance from the airways and promote silent colonisation of the respiratory tract. It has also been shown here that co-infection with RV and NTHi is associated with increased bacterial growth and greater epithelial damage and inflammation, which could lead to symptomatic disease in healthy individuals or disease exacerbations in patients with COPD. Ultimately, it was emphasized in these results that the choice of *in vitro* cell culture model bears a significant impact on study results and interpretation. As such, results obtained using immortalized cell lines or undifferentiated epithelial cell cultures were shown to be markedly different from responses of

ciliated epithelial cultures. Therefore, extreme caution must be exercised when interpreting studies carried out using epithelial cell lines or undifferentiated epithelial cells as they may not be representative of primary cell cultures or human tissues. In addition, conclusions of studies using epithelial cell lines or primary epithelial cells from a single donor may not be representative of a population or disease group. While multi donor studies using primary cell cultures are expensive, labour intensive and come with the difficulty of inherent inter-donor variability which can make drawing conclusions more difficult, they are more likely to be representative for the population group of interest. Therefore, findings obtained from such studies are more likely to be biologically relevant than single donor or cell line studies.

To further expand on the results shown in this thesis, future work could investigate if these can be reproduced using clinical strains of NTHi, which have been collected from COPD patients. Clinical strains of NTHi may have a different behaviour following interaction with the ciliated epithelium and during co-infection with RV, as a consequence of their pathogenic adaptation. In addition, a more biologically representative method of bacterial delivery to the epithelial culture through an aerosolization system could be used, instead of culture flooding with liquid medium as this may induce confounding effects such as artificial signalling pathway activation or stimulation of ciliary beat frequency. Prof. Chris O'Callaghan has developed a system that allows bacterial delivery to epithelial cultures through aerosolization. This system would provide a method of bacterial infection which resembles the natural infection route and could be used for long term infection studies and chronic colonisation models. While in this thesis an infection model where RV16

infection was followed by NTHi infection to mimic a viral infection followed by secondary bacterial infection, an aerosolisation model could allow for the set up of a chronic bacterial colonisation model subsequently followed by a viral challenge. This would be an insightful model for understanding the effect of a viral infection on an NTHi colonised respiratory epithelium. Furthermore, work done in our laboratory has developed a model system that allows investigation of the epithelial interaction with cells of the immune system such as neutrophils. Such research would be of particular importance to understand how epithelial infection with RV or NTHi can modulate recruitment of immune cells and their function in health and disease. This aspect is completely ignored in current cell culture systems and incompletely understood as a consequence, despite it being of great clinical relevance for respiratory diseases such as COPD, characterised by high levels of inflammation and immune cell infiltration.

Appendix 1.

Statistical analysis description with figure reference

Data in

Figure 5. Ciliation scoring and TEER measurements of differentiated epithelial cultures

TEER values and ciliation scores were modelled on their original scale using a linear mixed effects model. The model included a fixed effect for disease group (healthy/COPD) and an experiment-specific random effect for each donor. The estimated standard deviation of the model's residual error was used as an estimate of the intra-donor variability of TEER and ciliation score measurements. Agreement between assessors was quantified using Cohen's kappa. Cohen's kappa is a measure of agreement between categorical ratings of two assessors, taking values between -1 and 1. Cohen's kappa acknowledges that some agreement in ratings occurs as the result of chance alone. A value of 1 indicates perfect agreement between assessors, a value of zero represents agreement as good as chance.

Data in

Figure 7. Quantification of basal and ciliated cells in epithelial cultures during differentiation at air-liquid interface

Cell numbers and percentages of ciliated and basal cells were log10 transformed and analysed separately using linear mixed effects models. Each model included fixed effect for each combination of day (day 0/day 7/day 14/day 28) and disease group (healthy/COPD) as well as a random effect for

each donor. To enable log transformations of measurements of zero, small constants of 1 and 0.001 were added to counts and percentages, respectively. For each comparison, BH adjusted p-values for the test of no change in the endpoint are reported.

Data in

Figure 9. Expression of goblet cell specific genes by differentiated epithelial cultures

Ct measurements were converted to copy number using the formula

copy number=10^((40 -ct)/3.5)

and subsequently log2 transformed. Separate linear mixed effects models were fitted for all markers, which included a fixed effect for group (healthy/COPD). To account for variability in copy number due to differences in RNA loading, log2 transformed copy number of GAPDH was included in the initial models as a covariate. Hypothesis testing of the covariate's model parameter suggested no evidence of a relationship between the copy number of the housekeeper and the copy number of any marker. Therefore, housekeeper normalization was deemed unnecessary and GAPDH was removed from the final model.

Ciliary beat frequency in:

Figure 10. Ciliary function assessment in healthy and COPD epithelial cultures

Figure 13. Ciliary function assessment following NTHi infection of epithelial cultures

Figure 20. Effect of RV and NTHi co-infection on ciliary beat frequency

Ciliary beat frequencies (CBF) were log10 transformed and analysed using a linear mixed effects model. The model included fixed effects for each combination of disease group (healthy/COPD), treatment (CTRL/RV/NTHI/RVNTHI) and time point (T0/T24h RV/T24h RV T0 NTHI/T24h RV T8h NTHI/ T48h RV T24h NTHI). Because RV and NTHI were added sequentially over time, the model further assumes equal CBF means for all treatments at time 0, equal CBF means for control and NTHI conditions at 24 hours RV as well as equal CBF means for RV and RV NTHI co-infection at 24 hours RV. These assumptions introduce constraints on the fixed effects, thereby reducing the number of parameters to be estimated. Additionally, the model included a donor-specific random effect for each treatment level, each time point and each well. The latter accounts for pseudo-replication by repeated measurements of each well.

The statistical significance of CBF changes between disease groups was assessed using a likelihood ratio test. The likelihood ratio test is a single test to assess changes in CBF jointly for any treatment or time point, producing only one p-value rather than a p-value per treatment and time. If large, there is no evidence of a change in CBF between disease groups for any treatment or any point. If small, it suggests a difference for at least one treatment or time point. CBF changes between time points or treatments were assessed using individual tests, with p-values adjusted for multiple testing using the BH method.

Ciliary beat amplitude in:

Figure 10. Ciliary function assessment in healthy and COPD epithelial cultures

Figure 13. Ciliary function assessment following NTHi infection of epithelial cultures

Ciliary amplitude measurements were log10 transformed and analysed using a linear mixed effects model. The model included fixed effects for each combination of treatment (CTRL/NTHI no biofilm/biofilm) and disease group (healthy/COPD) and a random effect for each donor. To account for pseudo-replication from multiple technical replicates per donor and treatment, the model also included a random effect for each well. P-values for the tests of no change between treatments or disease groups are BH adjusted for multiplicity.

To assess whether there is a difference between average ciliary beat amplitude measurements of the assessors, a separate linear mixed effects models was fitted. The model included fixed effects for each assessor and random effects for each video. The null hypothesis that mean amplitude measurements are the same for all three assessors was first assessed by a global test. If the p-value of the global test is significant, pairwise tests are used to assess differences in mean measurements for each pair of assessors.

Inter-assessor variability in amplitude measurements was estimated by use of a linear mixed effects model. The models included a random effect for each video. The estimated standard deviation (σ) of the model's residuals is reported as a measure of the inter-assessor variability. Based on the residuals' normality assumption, ciliary beat amplitude measurements of the assessors are expected to lie within 2σ units around the video-specific average for 95% of videos.

Quantification of bacterial conformational changes in

Figure 12. Scanning electron micrographs showing NTHi conformational change

Bacteria length measurements were log10 transformed and a linear regression model was applied to estimate the mean length for condition. Because there were only two donors for the first four conditions (i.e. live healthy, HI healthy, live COPD, HI COPD), it was not possible to adjust for donor-to-donor variability in the model and measurements were pooled across donors for each condition. P-values for the tests of no change between groups were BH adjusted for multiplicity.

Bacterial counts in

Figure 16. Quantification of non-attached, attached and intracellular NTHi in epithelial cultures at pre-ciliation day 7 and when ciliated at day 28

Attached, non-attached and invasion counts were log10 transformed prior to modelling and analysed separately using linear mixed effects models. Each model included fixed effects for each combination of day (day 7/day 28) and disease group (healthy/COPD) and a random donor effect. Changes in bacterial counts between days or groups are reported as relative changes from baseline. P-values for the test of no change in counts are BH adjusted for multiplicity across the three endpoints.

Bacterial counts in

Figure 17. Effect of PI3K inhibition on NTHi invasion of ciliated epithelial cultures

Bacterial counts were log10 transformed and analysed using a linear mixed effects model. The model included fixed effects for each combination of disease group (healthy/COPD) and inhibitor type (CTRL/VC/Pan/LY) and a random donor effect. P-values for the test of no change in counts are BH adjusted.

Data in

Figure 18. Quantification of Akt phosphorylation following NTHi infection of ciliated epithelial cultures

Figure 19. Effect of pan-PI3k inhibitors on Akt phosphorylation after NTHi infection of ciliated epithelial cultures

Ser473 and Thr308 endpoints were analysed separately. Following a log10 transformation of all measurements, linear mixed effects models were fitted to the data. Both models included fixed effects for each combination of disease group (healthy/COPD), time (2h/24h), treatment (CTRL/VC/Pan/LY) and infection (uninfected/NTHI) as well as a random donor effect. Results from comparisons of concentrations between compounds, groups or time points are reported as relative changes from baseline. P-values for the test of no change in concentrations are Benjamini-Hochberg adjusted.

PCR data in

Figure 21. SPDEF and mucin gene expression changes during RV and NTHi co-infection of primary epithelial cultures at day 7 and day 28 of differentiation

Figure 23. Expression of Claudin 8 and ZO-1 after infection with RV, NTHi or after RV and NTHi co-infection of primary epithelial cultures at day 7 and day 28 of differentiation.

Figure 26. RV expression in ciliated and day 7 pre-ciliation epithelial cultures during RV single infection and RV and NTHi co-infection

Ct measurements were converted to copy number using the formula

copy number=10^((40 -ct)/3.5)

and subsequently log2 transformed. Separate linear mixed effects models were fitted for all markers, which included fixed effects for each combination of treatment (Ctrl/RV/NTHi/RV+NTHi), day (day 7/day 28) and group (healthy/COPD) and a day-specific random effect for each donor. To account for variability in copy number due to differences in RNA loading, log2 transformed copy number of GAPDH was included in the initial models as a covariate. GAPDH was included as a covariate in the final model, but with a parameter constrained to 1 and not estimated from the data. Thus, it is assumed that one unit change in log2 copy number of GAPDH leads to one unit change in log2 copy number of the marker. The decision to constrain the parameter to 1 was motivated by findings in initial analyses of these data that suggested inadequate adjustment for RV-related differences in RNA loading under the unconstrained model. This analysis is closely related to housekeeper normalization using the ΔΔ Ct method, which analogously assumes that a unit change in housekeeper cycle time leads to a unit change in the cycle time of the marker. P-value for the test of no change in expression are BH adjusted for multiple testing across all markers.

Data in:

Figure 22. TEER during RV and NTHi single infection and co-infection of primary epithelial cultures at day 7 and day 28 of differentiation

TEER values were log10 transformed and averaged over technical replicates where available. A linear mixed effects model was fitted to these data including fixed effects for each combination of treatment (CTRL/RV/NTHI/RV+NTHI), day (day7/day28) and group (COPD/healthy) and a day-specific random effect for each donor. P-values for the test of no change between conditions are BH adjusted for multiplicity.

Data in:

Figure 24. Cytokine responses of ciliated and day 7 pre-ciliation cultures to infection with RV alone, NTHi alone and RV and NTHi co-infection.

Figure 25. Chemokine responses of ciliated and day 7 pre-ciliation cultures to infection with RV alone, NTHi alone and RV and NTHi co-infection.

Table 7. Baseline cytokine and chemokine production by healthy and COPD epithelial cultures at a pre-ciliation (day 7) and fully differentiated (day 28) stage

Cytokines/chemokines were analysed individually using linear mixed effects models. Each model included fixed effects for each combination of disease group (healthy/COPD), treatment (CTRL/NTHI/RV/NTHI+RV), time (24 hr/48 hr) and day (day 7/day 28) and a random effect for each donor. Concentrations were log10 transformed prior to modelling, with the exception of MIP3a, G-CSF, Gro-a, which were analysed on the original scale. To avoid problems with

log transformations of concentrations of zero, a small constant of 1 was added to all measurements. P-values for the tests of no change in concentration were BH adjusted for multiplicity.

Bacterial counts in:

Figure 27. Quantification of non-attached NTHi during RV co-infection of primary epithelial cultures at day 7 and day 28 of differentiation

Figure 28. Quantification of NTHi attachment and invasion of primary respiratory epithelial cultures during co-infection with RV

Data on attached, non-attached and invasion bacterial counts were log10 transformed and analysed separately using linear mixed effects models. All models included fixed effects for each combination of disease group (healthy/COPD), day (day 7/day 28) and RV infection (no RV/RV). The model for attached bacterial counts included a random donor effect, while the models for non-attached and invasion counts included random day- and treatment-specific donor effects. For all three endpoints, the statistical significance of changes in bacterial counts between disease groups at any day or for any treatment was assessed jointly using a likelihood ratio test. If significant at the 5% level, changes were then assessed individually for all time points and for all treatment levels. Changes in bacterial counts between days or treatments were assessed using individual hypothesis tests, with p-values BH adjusted for multiplicity.

Bacterial counts in Figure 29. Effect of apical fluid from RV infected day 7 and day 28 epithelial cultures on NTHi growth

Bacterial counts were analysed on the log10 scale using a linear mixed effect model. The model included fixed effects for each combination of group (healthy/COPD), treatment (no RV/RV) and day (day 7/day 28) and a random intercept for each donor. In a separate analysis, bacterial counts from culture media experiments were analysed on the original scale using a paired t-test.

Bacterial counts in Figure 30. Effect of iron and NAD on NTHi growth in absence of epithelial cells

Two replicates per treatment and experiment were averaged and log10 transformed prior to modelling. The resulting data were analysed using a linear regression model with fixed effects for each treatment and each experiment. The latter aims to account for systematic changes in bacterial counts due to experimental factors. Because counts for Hemin, Medium and Iron showed more variability than the counts for treatments involving β-NAD, the model also allowed for different variances between these two groups of treatments. P-values are adjusted for multiplicity using the BH method.

Data in: Figure 31. Quantification of total iron and NAD in apical fluid from RV infected day 7 and day 28 epithelial cultures

Iron and NAD concentrations were modelled separately using linear mixed effects models. Both models included fixed effects for each combination of day (day 7/day 28), group (healthy/COPD) and treatment (no RV/RV) and a random effect for each donor. NAD concentrations were analysed on the log10 scale while Iron concentrations were analysed on the original scale. P-values for the tests of no change in mean concentration are BH adjusted.

Appendix 2.

Percentage of Akt phosphorylated at Ser473 following NTHi infection using the flooding method.

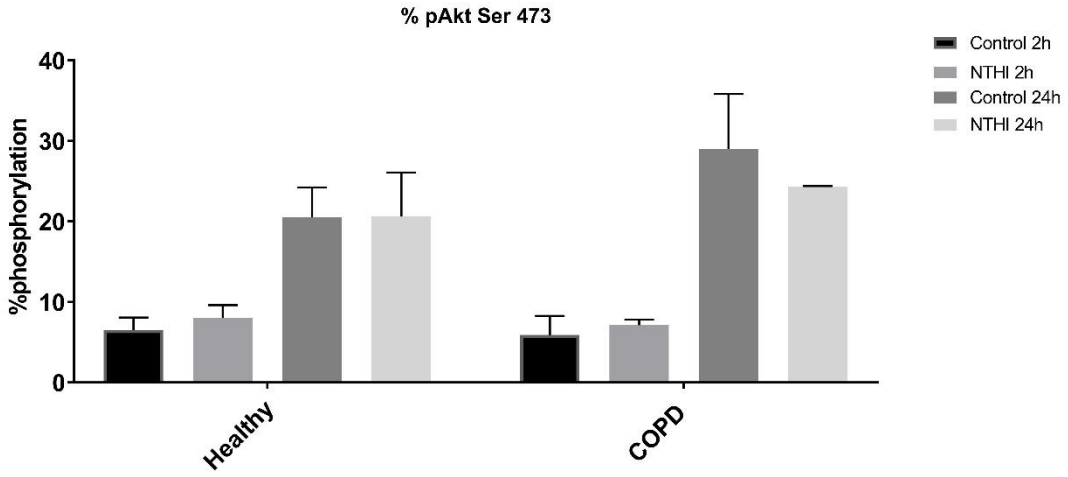

Quantification of pAkt following NTHi infection of ciliated cultures using the flooding method.

The percentage of Akt phosphorylated at Serine 473 out of total Akt expressed was quantified by MSD immunoassay as described in section 2.26., after 2 or 24 hours of NTHi 49247 infection ($5x10^6$ CFU/well) of ciliated epithelial cultures, carried out as described in section 2.19. N=3 healthy, 2 COPD donors. Data are presented as mean ± standard error of the mean.

Appendix 3.

Chemokines measured in cell culture supernatants that were not up-regulated by NTHi and RV or their co-infection.

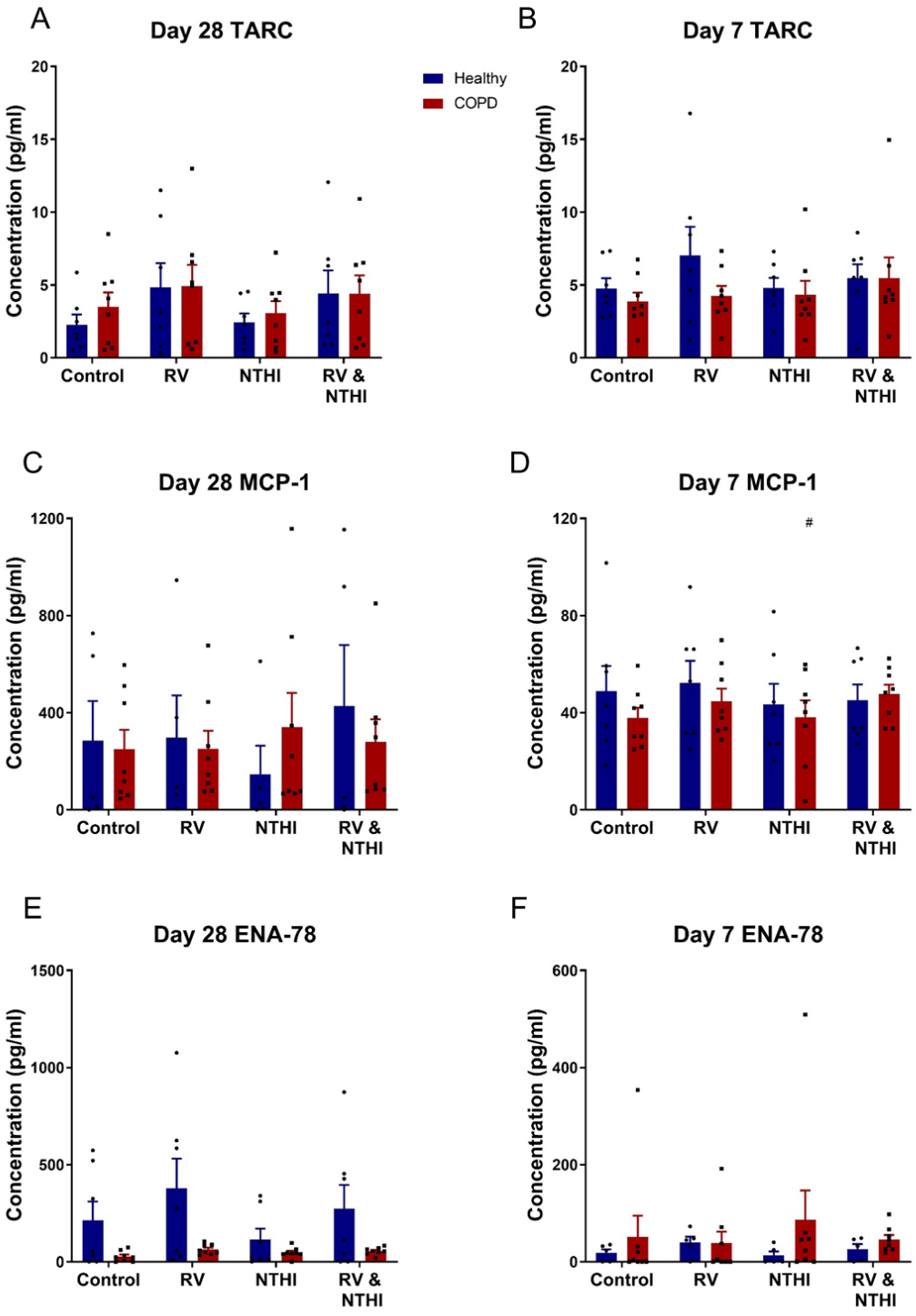

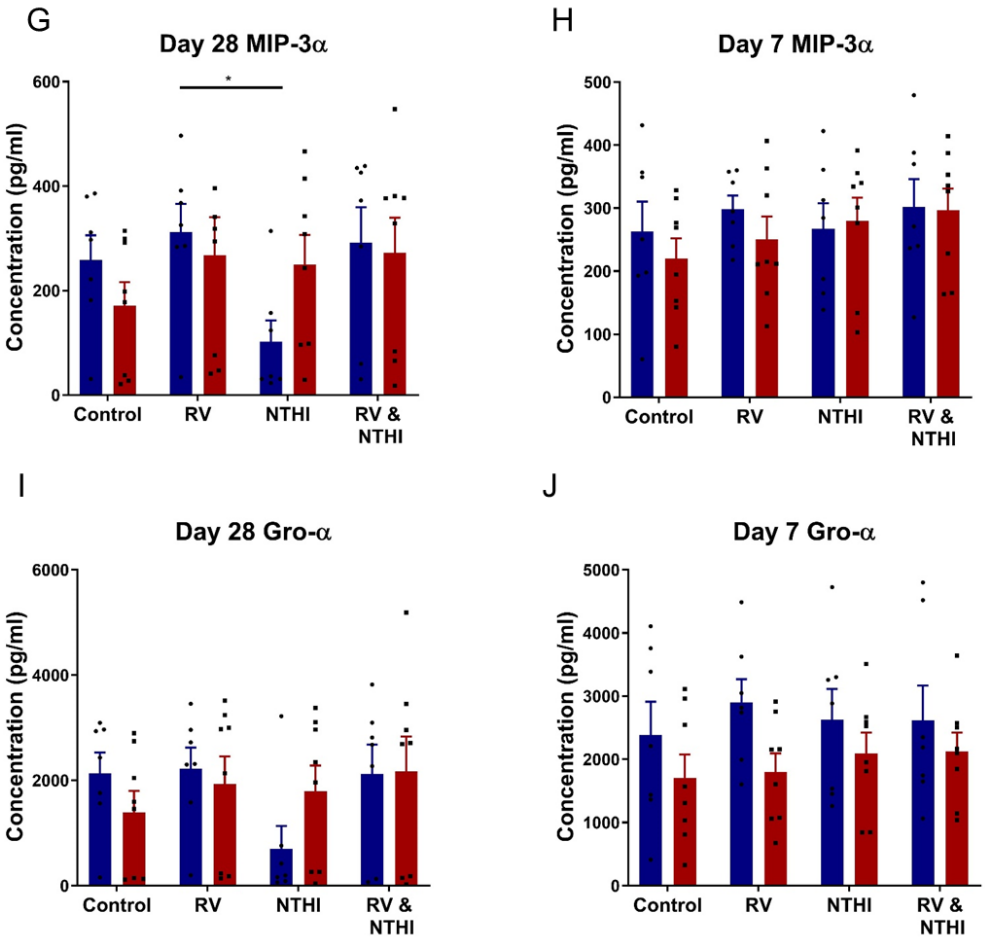

Chemokines measured in supernatants of ciliated and day 7 pre-ciliation cultures after infection with RV alone, NTHi alone and RV and NTHi co-infection.

Chemokine release to basolateral medium of day 7 pre-ciliation cultures and fully differentiated day 28 ciliated epithelial cultures from healthy and COPD donors was quantified by MSD or Luminex immunoassays as described in section 2.15., following infection with RV16 alone (1.5 x10^6 $TCDID_{50}$/well), NTHi 49247 alone (5x10^6 CFU/well) or after RV-NTHi co-infection. N=7 healthy and 8 COPD donors. Symbols represent individual donors. For statistical analysis, concentrations were log10 transformed and cytokines were analysed individually using linear mixed effects models. Fixed effects for disease group, day, and treatment and random effect for each donor were included. P values were Benjamini-Hochberg adjusted for multiple comparisons. Data are shown as mean ± standard error of the mean. *=p<0.05, #= denotes day 7 versus day 28 comparison within a treatment group, #=p<0.05.

Appendix 4.

Legend of videos included on USB stick attached.

Video 1 – Healthy ciliated epithelial culture imaged as described in section 2.12.

Video 2 – Healthy ciliated epithelial culture, control for infection experiment, flooded with BEBM for 24 hours.

Video 3 - Healthy ciliated epithelial culture, 48 hours post RV16 infection, flooded with BEBM for 24 hours

Please observe detached epithelial cells on the apical surface.

Video 4 - Healthy ciliated epithelial culture, flooded and infected with NTHi for 24 hours.

Please observe bacterial aggregates over ciliated areas.

Video 5 – Healthy ciliated epithelial culture, 48 hours post RV16 infection, 24 hours post NTHI infection.

Please observe dense biofilm like structure which also contains detached epithelial cells.

Videos 11A-11F are labelled according to the labelling presented in Figure 11.

Chapter 5. List of references

Aghapour M, Raee P, Moghaddam SJ, Hiemstra PS and Heijink IH (2018) Airway epithelial barrier dysfunction in chronic obstructive pulmonary disease: role of cigarette smoke exposure. *American Journal of Respiratory Cell and Molecular Biology* **58**:157-169.

Agusti AG (2018) Global strategy for the diagnosis, management and prevention of chronic obstructive pulmonary disease (2018 Report), p 142, Global Initiative for Chronic Obstructive Lung Disease, https://goldcopd.org/.

Ahearn CP, Gallo MC and Murphy TF (2017) Insights on persistent airway infection by non-typeable *Haemophilus influenzae* in chronic obstructive pulmonary disease. *Pathogens and Disease* **75**.

Ahren IL (2002) Comparison of the antibacterial activities of ampicillin, ciprofloxacin, clarithromycin, telithromycin and quinupristin/dalfopristin against intracellular non-typeable *Haemophilus influenzae*. *Journal of Antimicrobial Chemotherapy* **50**:903-906.

Aich A, Freundlich M and Vekilov PG (2015) The free heme concentration in healthy human erythrocytes. *Blood, Cells, Molecules and Diseases* **55**:402-409.

Amatngalim GD and Hiemstra PS (2018) Airway epithelial cell function and respiratory host defense in chronic obstructive pulmonary disease. *Chinese Medical Journal* **131**:1099-1107.

Amatngalim GD, Schrumpf JA, Dishchekenian F, Mertens TCJ, Ninaber DK, van der Linden AC, Pilette C, Taube C, Hiemstra PS and van der Does AM (2018) Aberrant epithelial differentiation by cigarette smoke dysregulates respiratory host defence. *European Respiratory Journal* **51**.

Amatngalim GD, Schrumpf JA, Henic A, Dronkers E, Verhoosel RM, Ordonez SR, Haagsman HP, Fuentes ME, Sridhar S, Aarbiou J, Janssen RAJ, Lekkerkerker AN and Hiemstra PS (2017) Antibacterial defense of human airway epithelial cells from chronic obstructive pulmonary disease patients induced by acute exposure to non-typeable *Haemophilus influenzae*: modulation by cigarette smoke. *Journal of Innate Immunity* **9**:359-374.

Anderson WH, Coakley RD, Button B, Henderson AG, Zeman KL, Alexis NE, Peden DB, Lazarowski ER, Davis CW, Bailey S, Fuller F, Almond M, Qaqish B, Bordonali E, Rubinstein M, Bennett WD, Kesimer M and Boucher RC (2015) The relationship of mucus concentration (hydration) to mucus osmotic pressure and transport in chronic bronchitis. *American Journal of Respiratory and Critical Care Medicine* **192**:182-190.

Arruda E, Boyle TR, Winther B, Pevear DC, Gwaltney JM, Jr. and Hayden FG (1995) Localization of human rhinovirus replication in the upper respiratory tract by in situ hybridization. *The Journal of Infectious Diseases* **171**:1329-1333.

Atherton HC, Jones G and Danahay H (2003) IL-13-induced changes in the goblet cell density of human bronchial epithelial cell cultures: MAP kinase and phosphatidylinositol 3-kinase regulation. *American Journal of Physiology-Lung Cellular and Molecular Physiology* **285**:L730-L739.

Auerbach O, Hammond EC and Garfinkel L (1979) Changes in bronchial epithelium in relation to cigarette smoking, 1955-1960 vs 1970-1977. *New England Journal of Medicine* **300**:381-386.

Auerbach O, Stout AP, Hammond EC and Garfinkel L (1961) Changes in bronchial epithelium in relation to cigarette smoking and in relation to lung cancer. *New England Journal of Medicine* **265**:253-&.

Auerbach O, Stout AP, Hammond EC and Garfinkel L (1962) Changes in bronchial epithelium in relation to sex, age, residence, smoking and pneumonia *New England Journal of Medicine* **267**:111-&.

Avadhanula V, Rodriguez CA, Devincenzo JP, Wang Y, Webby RJ, Ulett GC and Adderson EE (2006a) Respiratory viruses augment the adhesion of bacterial pathogens to respiratory epithelium in a viral species- and cell type-dependent manner. *Journal of Virology* **80**:1629-1636.

Avadhanula V, Rodriguez CA, Ulett GC, Bakaletz LO and Adderson EE (2006b) Non-typeable *Haemophilus influenzae* adheres to intercellular adhesion molecule 1 (ICAM-1) on respiratory epithelial cells and upregulates ICAM-1 expression. *Infection and Immunity* **74**:830-838.

Baddal B, Muzzi A, Censini S, Calogero RA, Torricelli G, Guidotti S, Taddei AR, Covacci A, Pizza M, Rappuoli R, Soriani M and Pezzicoli A (2015) Dual RNA-seq of non-typeable *Haemophilus influenzae* and host cell transcriptomes reveals novel insights into host-pathogen cross talk. *MBio* **6**:e01765-01715.

Bailey KL, LeVan TD, Yanov DA, Pavlik JA, DeVasure JM, Sisson JH and Wyatt TA (2012) Non-typeable *Haemophilus influenzae* decreases cilia beating via protein kinase C epsilon. *Respiratory Research* **13**.

Bandi V, Apicella MA, Mason E, Murphy TF, Siddiqi A, Atmar RL and Greenberg SB (2001) Non-typeable *Haemophilus influenzae* in the lower respiratory tract of patients with chronic bronchitis. *American Journal of Respiratory and Critical Care Medicine* **164**:2114-2119.

Bandi V, Jakubowycz M, Kinyon C, Mason EO, Atmar RL, Greenberg SB and Murphy TF (2003) Infectious exacerbations of chronic obstructive pulmonary disease associated with respiratory viruses and non-typeable *Haemophilus influenzae*. *FEMS Immunology & Medical Microbiology* **37**:69-75.

Bankova LG, Dwyer DF, Yoshimoto E, Ualiyeva S, McGinty JW, Raff H, von Moltke J, Kanaoka Y, Austen KF and Barrett NA (2018) The cysteinyl leukotriene 3 receptor regulates expansion of IL-25-producing airway brush cells leading to type 2 inflammation. *Science Immunology* **3**.

Barenkamp SJ and StGeme JW (1996) Identification of a second family of high-molecular-weight adhesion proteins expressed by non-typable *Haemophilus influenzae*. *Molecular Microbiology* **19**:1215-1223.

Barnes PJ (2008a) The cytokine network in asthma and chronic obstructive pulmonary disease. *Journal of Clinical Investigation* **118**:3546-3556.

Barnes PJ (2008b) Immunology of asthma and chronic obstructive pulmonary disease. *Nature Reviews Immunology* **8**:183-192.

Barnes PJ (2010) Chronic obstructive pulmonary disease: effects beyond the lungs. *Plos Medicine* **7**.

Barnes PJ (2014) Cellular and molecular mechanisms of chronic obstructive pulmonary disease. *Clinics in Chest Medicine* **35**:71-86.

Barnes PJ (2016) Inflammatory mechanisms in patients with chronic obstructive pulmonary disease. *The Journal of Allergy and Clinical Immunology* **138**:16-27.

Barnes PJ, Shapiro SD and Pauwels RA (2003) Chronic obstructive pulmonary disease: molecular and cellular mechanisms. *European Respiratory Journal* **22**:672-688.

Basnet S, Palmenberg AC and Gern JE (2019) Rhinoviruses and their receptors. *Chest* **155**:1018-1025.

Belenky P, Bogan KL and Brenner C (2007) NAD+ metabolism in health and disease. *Trends in Biochemical Sciences* **32**:12-19.

Bellinghausen C, Rohde GGU, Savelkoul PHM, Wouters EFM and Stassen FRM (2016) Viral-bacterial interactions in the respiratory tract. *Journal of General Virology* **97**:3089-3102.

Benjamini Y and Hochberg Y (1995) Controlling the false discovery rate: a practical and powerful approach to multiple testing. *Journal of the Royal Statistical Society* **57**:289-300.

Billington RA, Bruzzone S, De Flora A, Genazzani AA, Koch-Nolte F, Ziegler M and Zocchi E (2006) Emerging functions of extracellular pyridine nucleotides. *Molecular Medicine* **12**:324-327.

Birchenough GMH, Johansson MEV, Gustafsson JK, Bergstrom JH and Hansson GC (2015) New developments in goblet cell mucus secretion and function. *Mucosal Immunology* **8**:712-719.

Blaas D and Fuchs R (2016) Mechanism of human rhinovirus infections. *Molecular and Cellular Pediatrics* **3**:21.

Bochkov YA, Watters K, Ashraf S, Griggs TF, Devries MK, Jackson DJ, Palmenberg AC and Gern JE (2015) Cadherin-related family member 3, a childhood asthma susceptibility gene product, mediates rhinovirus C binding and replication. *Proceedings of the National Academy of Sciences of the United States of America* **112**:5485-5490.

Boers JE, Ambergen AW and Thunnissen F (1998) Number and proliferation of basal and parabasal cells in normal human airway epithelium. *American Journal of Respiratory and Critical Care Medicine* **157**:2000-2006.

Boers JE, Ambergen AW and Thunnissen F (1999) Number and proliferation of Clara cells in normal human airway epithelium. *American Journal of Respiratory and Critical Care Medicine* **159**:1585-1591.

Bou Saab J, Losa D, Chanson M and Ruez R (2014) Connexins in respiratory and gastrointestinal mucosal immunity. *FEBS letters* **588**:1288-1296.

Boucher RC (2019) Muco-obstructive lung diseases. *New England Journal of Medicine* **380**:1941-1953.

Boudewijn IM, Faiz A, Steiling K, van der Wiel E, Telenga ED, Hoonhorst SJM, Ten Hacken NHT, Brandsma CA, Kerstjens HAM, Timens W, Heijink IH, Jonker MR, de Bruin HG, Sebastiaan Vroegop J, Pasma HR, Boersma WG, Wielders P, van den Elshout F, Mansour K, Spira A, Lenburg ME, Guryev V, Postma DS and van den Berge M (2017) Nasal gene expression differentiates COPD from controls and overlaps bronchial gene expression. *Respiratory Medicine* **18**:213.

Braiman A and Priel Z (2008) Efficient mucociliary transport relies on efficient regulation of ciliary beating. *Respiratory Physiology & Neurobiology* **163**:202-207.

Branchfield K, Nantie L, Verheyden JM, Sui P, Wienhold MD and Sun X (2016) Pulmonary neuroendocrine cells function as airway sensors to control lung immune response. *Science (New York, NY)* **351**:707-710.

Brekman A, Walters MS, Tilley AE and Crystal RG (2014) FOXJ1 prevents cilia growth inhibition by cigarette smoke in human airway epithelium in vitro. *American Journal of Respiratory Cell and Molecular Biology* **51**:688-700.

Brewington JJ, Filbrandt ET, LaRosa FJ, 3rd, Moncivaiz JD, Ostmann AJ, Strecker LM and Clancy JP (2018) Brushed nasal epithelial cells are a surrogate for bronchial epithelial CFTR studies. *Journal of Clinical Investigation* **3**.

Britto CJ, Brady V, Lee S and Dela Cruz CS (2017) Respiratory viral infections in chronic lung diseases. *Clinics in Chest Medicine* **38**:87-96.

Brunet A, Bonni A, Zigmond MJ, Lin MZ, Juo P, Hu LS, Anderson MJ, Arden KC, Blenis J and Greenberg ME (1999) Akt promotes cell survival by phosphorylating and inhibiting a Forkhead transcription factor. *Cell* **96**:857-868.

Burgel PR and Nadel JA (2004) Roles of epidermal growth factor receptor activation in epithelial cell repair and mucin production in airway epithelium. *Thorax* **59**:992-996.

Burney P, Jithoo A, Kato B, Janson C, Mannino D, Nizankowska-Mogilnicka E, Studnicka M, Tan W, Bateman E, Kocabas A, Vollmer WM, Gislason T, Marks G, Koul PA, Harrabi I, Gnatiuc L, Buist S and Burden of Obstructive Lung Disease S (2014) Chronic obstructive pulmonary disease mortality and prevalence: the associations with smoking and poverty--a BOLD analysis. *Thorax* **69**:465-473.

Butler CR, Hynds RE, Gowers KHC, Lee DDH, Brown JM, Crowley C, Teixeira VH, Smith CM, Urbani L, Hamilton NJ, Thakrar RM, Booth HL, Birchall MA, De Coppi P, Giangreco A, O'Callaghan C and Janes SM (2016) Rapid expansion of human epithelial stem cells suitable for airway tissue engineering. *American Journal of Respiratory and Critical Care Medicine* **194**:156-168.

Button B, Cai LH, Ehre C, Kesimer M, Hill DB, Sheehan JK, Boucher RC and Rubinstein M (2012) A periciliary brush promotes the lung health by separating the mucus layer from airway epithelia. *Science (New York, NY)* **337**:937-941.

Cahn A, Hamblin JN, Begg M, Wilson R, Dunsire L, Sriskantharajah S, Montembault M, Leemereise CN, Galinanes-Garcia L, Watz H, Kirsten AM, Fuhr R and Hessel EM (2017) Safety, pharmacokinetics and dose-response characteristics of GSK2269557, an inhaled PI3Kdelta inhibitor under development for the treatment of COPD. *Pulmonary Pharmacology & Therapeutics* **46**:69-77.

Canto C, Menzies KJ and Auwerx J (2015) NAD(+) metabolism and the control of energy homeostasis: a balancing act between mitochondria and the nucleus. *Cell Metabolism* **22**:31-53.

Caramori G, Di Gregorio C, Carlstedt I, Casolari P, Guzzinati I, Adcock IM, Barnes PJ, Ciaccia A, Cavallesco G, Chung KF and Papi A (2004) Mucin expression in peripheral airways of patients with chronic obstructive pulmonary disease. *Histopathology* **45**:477-484.

Castellano E and Downward J (2011) RAS interaction with PI3K: more than just another effector pathway. *Genes Cancer* **2**:261-274.

Celli BR and Barnes PJ (2007) Exacerbations of chronic obstructive pulmonary disease. *European Respiratory Journal* **29**:1224-1238.

Chattoraj SS, Ganesan S, Jones AM, Helm JM, Comstock AT, Bright-Thomas R, LiPuma JJ, Hershenson MB and Sajjan US (2011) Rhinovirus infection liberates planktonic bacteria from biofilm and increases chemokine responses in cystic fibrosis airway epithelial cells. *Thorax* **66**:333-339.

Chen G, Korfhagen TR, Xu Y, Kitzmiller J, Wert SE, Maeda Y, Gregorieff A, Clevers H and Whitsett JA (2009) SPDEF is required for mouse pulmonary goblet cell differentiation and regulates a network of genes associated with mucus production. *Journal of Clinical Investigation* **119**:2914-2924.

Chen R, Lim JH, Jono H, Gu XX, Kim YS, Basbaum CB, Murphy TF and Li JD (2004) Non-typeable *Haemophilus influenzae* lipoprotein P6 induces MUC5AC mucin transcription via TLR2-TAK1-dependent p38 MAPK-AP1 and IKKbeta-IkappaBalpha-NF-kappaB signaling pathways. *Biochemical and Biophysical Research Communications* **324**:1087-1094.

Chilvers MA, McKean M, Rutman A, Myint BS, Silverman M and O'Callaghan C (2001) The effects of coronavirus on human nasal ciliated respiratory epithelium. *European Respiratory Journal* **18**.

Chilvers MA and O'Callaghan C (2000) Local mucociliary defence mechanisms. *Paediatric Respiratory Reviews* **1**:27-34.

Chin CL, Manzel LJ, Lehman EE, Humlicek AL, Shi L, Starner TD, Denning GM, Murphy TF, Sethi S and Look DC (2005) *Haemophilus influenzae* from patients with chronic obstructive pulmonary disease exacerbation induce more inflammation than colonizers. *American Journal of Respiratory and Critical Care Medicine* **172**:85-91.

Cho MH, Castaldi PJ, Wan ES, Siedlinski M, Hersh CP, Demeo DL, Himes BE, Sylvia JS, Klanderman BJ, Ziniti JP, Lange C, Litonjua AA, Sparrow D, Regan EA, Make BJ, Hokanson JE, Murray T, Hetmanski JB, Pillai SG, Kong X, Anderson WH, Tal-Singer R, Lomas DA, Coxson HO, Edwards LD, MacNee W, Vestbo J, Yates JC, Agusti A, Calverley PM, Celli B, Crim C, Rennard S, Wouters E, Bakke P, Gulsvik A, Crapo JD, Beaty TH and Silverman EK (2012) A genome-wide association study of COPD identifies a susceptibility locus on chromosome 19q13. *Human Molecular Genetics* **21**:947-957.

Choi SH, Hong SB, Kim T, Kim SH, Huh JW, Do KH, Lee SO, Kim MN, Lim CM, Kim YS, Koh Y, Woo JH, Choi SH and Sung H (2015) Clinical and molecular characterization of rhinoviruses A, B, and C in adult patients with pneumonia. *Journal of Clinical Virology* **63**:70-75.

Chung KF and Adcock IM (2008) Multifaceted mechanisms in COPD: inflammation, immunity, and tissue repair and destruction. *European Respiratory Journal* **31**:1334-1356.

Clary-Meinesz C, Mouroux J, Cosson J, Huitorel P and Blaive B (1998) Influence of external pH on ciliary beat frequency in human bronchi and bronchioles. *European Respiratory Journal* **11**:330-333.

Clary-Meinesz CF, Cosson J, Huitorel P and Blaive B (1992) Temperature effect on the ciliary beat frequency of human nasal and tracheal ciliated cells. *Biology of the Cell* **76**:335-338.

Clementi CF, Hakansson AP and Murphy TF (2014) Internalization and trafficking of non-typeable *Haemophilus influenzae* in human respiratory epithelial cells and roles of IgA1 proteases for optimal invasion and persistence. *Infection and Immunity* **82**:433-444.

Clementi CF and Murphy TF (2011) Non-typeable *Haemophilus influenzae* invasion and persistence in the human respiratory tract. *Frontiers in Cellular and Infection Microbiology* **1**.

Cole AM, Dewan P and Ganz T (1999) Innate antimicrobial activity of nasal secretions. *Infection and Immunity* **67**:3267-3275.

Comer DM, Elborn JS and Ennis M (2012) Comparison of nasal and bronchial epithelial cells obtained from patients with COPD. *PloS One* **7**:e32924.

Comstock AT, Ganesan S, Chattoraj A, Faris AN, Margolis BL, Hershenson MB and Sajjan US (2011) Rhinovirus-induced barrier dysfunction in polarized airway epithelial cells is mediated by NADPH oxidase 1. *Journal of Virology* **85**:6795-6808.

Corbeil D, Roper K, Hellwig A, Tavian M, Miraglia S, Watt SM, Simmons PJ, Peault B, Buck DW and Huttner WB (2000) The human AC133 hematopoietic stem cell antigen is also expressed in epithelial cells and targeted to plasma membrane protrusions. *Journal of Biological Chemistry* **275**:5512-5520.

Crystal RG (2014a) Airway basal cells the "smoking gun" of chronic obstructive pulmonary disease. *American Journal of Respiratory and Critical Care Medicine* **190**:1355-1362.

Crystal RG (2014b) Airway basal cells. The "smoking gun" of chronic obstructive pulmonary disease. *American Journal of Respiratory and Critical Care Medicine* **190**:1355-1362.

Crystal RG, Randell SH, Engelhardt JF, Voynow J and Sunday ME (2008) Airway epithelial cells current concepts and challenges. *Proceedings of the American Thoracic Society* **5**:772-777.

Cutz E, Pan J, Yeger H, Domnik NJ and Fisher JT (2013) Recent advances and contraversies on the role of pulmonary neuroepithelial bodies as airway sensors. *Seminars in Cell and Developmental Biology* **24**:40-50.

de Boer WI, Sont JK, van Schadewijk A, Stolk J, van Krieken JH and Hiemstra PS (2000) Monocyte chemoattractant protein 1, interleukin 8, and chronic airways inflammation in COPD. *The Journal of Pathology* **190**:619-626.

de Borja Callejas F, Martinez-Anton A, Alobid I, Fuentes M, Cortijo J, Picado C, Roca-Ferrer J and Mullol J (2014) Reconstituted human upper airway epithelium as 3-d in vitro model for nasal polyposis. *PloS One* **9**:e100537.

de Torres JP, Marin JM, Casanova C, Cote C, Carrizo S, Cordoba-Lanus E, Baz-Davila R, Zulueta JJ, Aguirre-Jaime A, Saetta M, Cosio MG and Celli BR (2011) Lung cancer in patients with chronic obstructive pulmonary disease incidence and predicting factors. *American Journal of Respiratory and Critical Care Medicine* **184**:913-919.

Demedts IK, Bracke KR, Van Pottelberge G, Testelmans D, Verleden GM, Vermassen FE, Joos GF and Brusselle GG (2007) Accumulation of dendritic cells and increased CCL20 levels in the airways of patients with chronic obstructive pulmonary disease. *American Journal of Respiratory and Critical Care Medicine* **175**:998-1005.

DeMuri GP, Gern JE, Eickhoff JC, Lynch SV and Wald ER (2018) Dynamics of bacterial colonization with *Streptococcus pneumoniae*, *Haemophilus influenzae*, and *Moraxella catarrhalis* during symptomatic and asymptomatic viral upper respiratory tract infection. *Clinical Infectious Diseases* **66**:1045-1053.

Devalia JL, Sapsford RJ, Wells CW, Richman P and Davies RJ (1990) Culture and comparison of human bronchial and nasal epithelial cells in vitro. *Respiratory Medicine* **84**:303-312.

Duell BL, Su YC and Riesbeck K (2016) Host-pathogen interactions of non-typeable *Haemophilus influenzae*: from commensal to pathogen. *FEBS letters* **590**:3840-3853.

Euba B, Moleres J, Viadas C, de Los Mozos IR, Valle J, Antonio Bengoechea J and Garmendia J (2015) Relative contribution of P5 and hap surface proteins to non-typable *Haemophilus influenzae* interplay with the host upper and lower airways. *PloS One* **10**.

Everman JL, Sajuthi S, Saef B, Rios C, Stoner AM, Numata M, Hu D, Eng C, Oh S, Rodriguez-Santana J, Vladar EK, Voelker DR, Burchard EG and Seibold MA (2019) Functional genomics of CDHR3 confirms its role in HRV-C infection and childhood asthma exacerbations. *The Journal of Allergy and Clinical Immunology*.

Fahy JV and Dickey BF (2010) Airway mucus function and dysfunction. *New England Journal of Medicine* **363**:2233-2247.

Faris AN, Ganesan S, Chattoraj A, Chattoraj SS, Comstock AT, Unger BL, Hershenson MB and Sajjan US (2016) Rhinovirus delays cell repolarization in a model of injured/regenerating human airway epithelium. *American Journal of Respiratory Cell and Molecular Biology* **55**:487-499.

Feldman MB, Wood M, Lapey A and Mou H (2019) SMAD signaling restricts mucous cell differentiation in human airway epithelium. *American Journal of Respiratory Cell and Molecular Biology*.

Finney LJ, Ritchie A, Pollard E, Johnston SL and Mallia P (2014) Lower airway colonization and inflammatory response in COPD: a focus on *Haemophilus*

influenzae. *International Journal of Chronic Obstructive Pulmonary Disease* **9**:1119-1132.

Fliegauf M, Benzing T and Omran H (2007) When cilia go bad: cilia defects and ciliopathies. *Nature Reviews Molecular Cell Biology* **8**:880.

Franzke A (2006) The role of G-CSF in adaptive immunity. *Cytokine & Growth Factor Reviews* **17**:235-244.

Fruman DA, Chiu H, Hopkins BD, Bagrodia S, Cantley LC and Abraham RT (2017) The PI3K pathway in human disease. *Cell* **170**:605-635.

Fuchs R and Blaas D (2010) Uncoating of human rhinoviruses. *Reviews in Medical Virology* **20**:281-297.

Gadgil A and Duncan SR (2008) Role of T-lymphocytes and pro-inflammatory mediators in the pathogenesis of chronic obstructive pulmonary disease. *International Journal of Chronic Obstructive Pulmonary Disease* **3**:531-541.

Ganesan S, Comstock AT, Kinker B, Mancuso P, Beck JM and Sajjan US (2014) Combined exposure to cigarette smoke and non-typeable *Haemophilus influenzae* drives development of a COPD phenotype in mice. *Respiratory Research* **15**:11-11.

Ganesan S, Unger BL, Comstock AT, Angel KA, Mancuso P, Martinez FJ and Sajjan US (2013) Aberrantly activated EGFR contributes to enhanced IL-8 expression in COPD airways epithelial cells via regulation of nuclear FoxO3A. *Thorax* **68**:131-141.

Gao W, Li L, Wang Y, Zhang S, Adcock IM, Barnes PJ, Huang M and Yao X (2015) Bronchial epithelial cells: the key effector cells in the pathogenesis of chronic obstructive pulmonary disease? *Respirology* **20**:722-729.

Geluk F, Eijk PP, van Ham SM, Jansen HM and van Alphen L (1998) The fimbria gene cluster of nonencapsulated *Haemophilus influenzae*. *Infection and Immunity* **66**:406-417.

George SN, Garcha DS, Mackay AJ, Patel AR, Singh R, Sapsford RJ, Donaldson GC and Wedzicha JA (2014) Human rhinovirus infection during naturally occurring COPD exacerbations. *European Respiratory Journal* **44**:87-96.

Gern JE, Galagan DM, Jarjour NN, Dick EC and Busse WW (1997) Detection of rhinovirus RNA in lower airway cells during experimentally induced infection. *American Journal of Respiratory and Critical Care Medicine* **155**:1159-1161.

Gerth A, Nieber K, Oppenheimer NJ and Hauschildt S (2004) Extracellular NAD+ regulates intracellular free calcium concentration in human monocytes. *Biochemical Journal* **382**:849-856.

Ghorani V, Boskabady MH, Khazdair MR and Kianmeher M (2017) Experimental animal models for COPD: a methodological review. *Tobacco Induced Diseases* **15**:25.

Ghosh M, Miller YE, Nakachi I, Kwon JB, Baron AE, Brantley AE, Merrick DT, Franklin WA, Keith RL and Vandivier RW (2018) Exhaustion of airway basal progenitor cells in early and established chronic obstructive pulmonary disease. *American Journal of Respiratory and Critical Care Medicine* **197**:885-896.

Gomez MI and Prince A (2008) Airway epithelial cell signaling in response to bacterial pathogens. *Pediatric Pulmonology* **43**:11-19.

Goubau D, Deddouche S and Reis e Sousa C (2013) Cytosolic sensing of viruses. *Immunity* **38**:855-869.

Gray TE, Guzman K, Davis CW, Abdullah LH and Nettesheim P (1996) Mucociliary differentiation of serially passaged normal human tracheobronchial epithelial cells. *American Journal of Respiratory Cell and Molecular Biology* **14**:104-112.

Greve JM, Davis G, Meyer AM, Forte CP, Yost SC, Marlor CW, Kamarck ME and McClelland A (1989) The major human rhinovirus receptor is ICAM-1. *Cell* **56**:839-847.

Griggs TF, Bochkov YA, Basnet S, Pasic TR, Brockman-Schneider RA, Palmenberg AC and Gern JE (2017) Rhinovirus C targets ciliated airway epithelial cells. *Respiratory Medicine* **18**:84.

Groenewegen KH and Wouters EFM (2003) Bacterial infections in patients requiring admission for an acute exacerbation of COPD; a 1-year prospective study. *Respiratory Medicine* **97**:770-777.

Gruys E, Toussaint MJ, Niewold TA and Koopmans SJ (2005) Acute phase reaction and acute phase proteins. *Journal of Zhejiang University Science* **6**:1045-1056.

Gu X, Karp PH, Brody SL, Pierce RA, Welsh MJ, Holtzman MJ and Ben-Shahar Y (2014) Chemosensory functions for pulmonary neuroendocrine cells. *American Journal of Respiratory Cell and Molecular Biology* **50**:637-646.

Gulraiz F, Bellinghausen C, Bruggeman CA and Stassen FR (2015) *Haemophilus influenzae* increases the susceptibility and inflammatory response of airway epithelial cells to viral infections. *The FASEB Journal* **29**:849-858.

Hackett T-L, Shaheen F, Johnson A, Wadsworth S, Pechkovsky DV, Jacoby DB, Kicic A, Stick SM and Knight DA (2008) Characterization of side population cells from human airway epithelium. *Stem Cells* **26**:2576-2585.

Hall-Stoodley L, Hu FZ, Gieseke A, Nistico L, Nguyen D, Hayes J, Forbes M, Greenberg DP, Dice B, Burrows A, Wackym PA, Stoodley P, Post JC, Ehrlich GD and Kerschner JE (2006) Direct detection of bacterial biofilms on the middle-ear mucosa of children with chronic otitis media. *Jama* **296**:202-211.

Haller O and Kochs G (2011) Human MxA protein: an interferon-induced dynamin-like GTPase with broad antiviral activity. *Journal of Interferon & Cytokine Research* **31**:79-87.

Hament JM, Aerts PC, Fleer A, Van Dijk H, Harmsen T, Kimpen JL and Wolfs TF (2004) Enhanced adherence of *Streptococcus pneumoniae* to human epithelial cells infected with respiratory syncytial virus. *Pediatric Research* **55**:972-978.

Hammond ME, Lapointe GR, Feucht PH, Hilt S, Gallegos CA, Gordon CA, Giedlin MA, Mullenbach G and Tekamp-Olson P (1995) IL-8 induces neutrophil chemotaxis predominantly via type I IL-8 receptors. *The Journal of Immunology* **155**:1428-1433.

Hawkins PT and Stephens LR (2015) PI3K signalling in inflammation. *Biochimica et Biophysica Acta* **1851**:882-897.

Heijink IH, Noordhoek JA, Timens W, van Oosterhout AJ and Postma DS (2014) Abnormalities in airway epithelial junction formation in chronic obstructive pulmonary disease. *American Journal of Respiratory and Critical Care Medicine* **189**:1439-1442.

Hendricks MR, Lashua LP, Fischer DK, Flitter BA, Eichinger KM, Durbin JE, Sarkar SN, Coyne CB, Empey KM and Bomberger JM (2016) Respiratory syncytial virus infection enhances *Pseudomonas aeruginosa* biofilm growth through dysregulation of nutritional immunity. *Proceedings of the National Academy of Sciences of the United States of America* **113**:1642-1647.

Hendrixson DR and St Geme JW (1998) The *Haemophilus influenzae* Hap serine protease promotes adherence and microcolony formation, potentiated by a soluble host protein. *Molecular Cell* **2**:841-850.

Hessel J, Heldrich J, Fuller J, Staudt MR, Radisch S, Hollmann C, Harvey BG, Kaner RJ, Salit J, Yee-Levin J, Sridhar S, Pillai S, Hilton H, Wolff G, Bitter H, Visvanathan S, Fine J, Stevenson CS, Crystal RG and Tilley AE (2014) Intraflagellar transport gene expression associated with short cilia in smoking and COPD. *PloS One* **9**:e85453.

Hewson CA, Haas JJ, Bartlett NW, Message SD, Laza-Stanca V, Kebadze T, Caramori G, Zhu J, Edbrooke MR, Stanciu LA, Kon OM, Papi A, Jeffery PK, Edwards MR and Johnston SL (2010) Rhinovirus induces MUC5AC in a human infection model and in vitro via NF-kappaB and EGFR pathways. *European Respiratory Journal* **36**:1425-1435.

Hill DJ, Toleman MA, Evans DJ, Villullas S, van Alphen L and Virji M (2001) The variable P5 proteins of typeable and non-typeable *Haemophilus influenzae* target human CEACAM1. *Molecular Microbiology* **39**:850-862.

Hirst RA, Jackson CL, Coles JL, Williams G, Rutman A, Goggin PM, Adam EC, Page A, Evans HJ, Lackie PM, O'Callaghan C and Lucas JS (2014) Culture of primary

ciliary dyskinesia epithelial cells at air-liquid interface can alter ciliary phenotype but remains a robust and informative diagnostic aid. *PloS One* **9**:e89675.

Hirst RA, Rutman A, Williams G and O'Callaghan C (2010) Ciliated air-liquid cultures as an aid to diagnostic testing of primary ciliary dyskinesia. *Chest* **138**.

Hoenderdos K and Condliffe A (2013) The neutrophil in chronic obstructive pulmonary disease. *American Journal of Respiratory Cell and Molecular Biology* **48**:531-539.

Hofer F, Gruenberger M, Kowalski H, Machat H, Huettinger M, Kuechler E and Blaas D (1994) Members of the low density lipoprotein receptor family mediate cell entry of a minor-group common cold virus. *Proceedings of the National Academy of Sciences of the United States of America* **91**:1839-1842.

Hogg JC (2004) Pathophysiology of airflow limitation in chronic obstructive pulmonary disease. *The Lancet* **364**:709-721.

Hogg JC and Timens W (2009) The pathology of chronic obstructive pulmonary disease. *Annual Review of Pathology* **4**:435-459.

Holmes KA and Bakaletz LO (1997) Adherence of non-typeable *Haemophilus influenzae* promotes reorganization of the actin cytoskeleton in human or chinchilla epithelial cells in vitro. *Microbial Pathogenesis* **23**:157-166.

Horani A, Ferkol TW, Dutcher SK and Brody SL (2016) Genetics and biology of primary ciliary dyskinesia. *Paediatric Respiratory Reviews* **18**:18-24.

Horvath DJ, Jr., Li B, Casper T, Partida-Sanchez S, Hunstad DA, Hultgren SJ and Justice SS (2011) Morphological plasticity promotes resistance to phagocyte killing of uropathogenic Escherichia coli. *Microbes and Infection* **13**:426-437.

Hotomi M, Arai J, Billal DS, Takei S, Ikeda Y, Ogami M, Kono M, Beder LB, Toya K, Kimura M and Yamanaka N (2010) Non-typeable *Haemophilus influenzae* isolated from intractable acute otitis media internalized into cultured human epithelial cells. *Auris, Nasus, Larynx* **37**:137-144.

Hovenberg HW, Davies JR and Carlstedt I (1996) Different mucins are produced by the surface epithelium and the submucosa in human trachea: Identification of MUC5AC as a major mucin from the goblet cells. *Biochemical Journal* **318**:319-324.

Howard AJ, Dunkin KT and Millar GW (1988) Nasopharyngeal carriage and antibiotic resistance of *Haemophilus influenzae* in healthy children. *Epidemiology and Infection* **100**:193-203.

Hurst JR, Kuchai R, Michael P, Perera WR, Wilkinson TM and Wedzicha JA (2006a) Nasal symptoms, airway obstruction and disease severity in chronic obstructive pulmonary disease. *Clinical Physiology and Functional Imaging* **26**:251-256.

Hurst JR, Perera WR, Wilkinson TM, Donaldson GC and Wedzicha JA (2006b) Systemic and upper and lower airway inflammation at exacerbation of chronic obstructive pulmonary disease. *American Journal of Respiratory and Critical Care Medicine* **173**:71-78.

Hurst JR, Wilkinson TM, Perera WR, Donaldson GC and Wedzicha JA (2005) Relationships among bacteria, upper airway, lower airway, and systemic inflammation in COPD. *Chest* **127**:1219-1226.

Hutchinson AF, Ghimire AK, Thompson MA, Black JF, Brand CA, Lowe AJ, Smallwood DM, Vlahos R, Bozinovski S, Brown GV, Anderson GP and Irving LB (2007) A community-based, time-matched, case-control study of respiratory viruses and exacerbations of COPD. *Respiratory Medicine* **101**:2472-2481.

Innes AL, Woodruff PG, Ferrando RE, Donnelly S, Dolganov GM, Lazarus SC and Fahy JV (2006) Epithelial mucin stores are increased in the large airways of smokers with airflow obstruction. *Chest* **130**:1102-1108.

Ioannidis I, Ye F, McNally B, Willette M and Flano E (2013) Toll-like receptor expression and induction of type I and type III interferons in primary airway epithelial cells. *Journal of Virology* **87**:3261-3270.

Ishikawa H and Marshall WF (2011) Ciliogenesis: building the cell's antenna. *Nature Reviews Molecular Cell Biology* **12**:222-234.

Ishizuka S, Yamaya M, Suzuki T, Takahashi H, Ida S, Sasaki T, Inoue D, Sekizawa K, Nishimura H and Sasaki H (2003) Effects of rhinovirus infection on the adherence of *Streptococcus pneumoniae* to cultured human airway epithelial cells. *The Journal of Infectious Diseases* **188**:1928-1939.

Jackson AD (2001) Airway goblet-cell mucus secretion. *Trends in Pharmacological Sciences* **22**:39-45.

Jacobs SE, Lamson DM, St George K and Walsh TJ (2013) Human rhinoviruses. *Clinical Microbiology Reviews* **26**:135-162.

Jakiela B, Brockman-Schneider R, Amineva S, Lee WM and Gern JE (2008) Basal cells of differentiated bronchial epithelium are more susceptible to rhinovirus infection. *American Journal of Respiratory Cell and Molecular Biology* **38**:517-523.

Jakiela B, Gielicz A, Plutecka H, Hubalewska-Mazgaj M, Mastalerz L, Bochenek G, Soja J, Januszek R, Aab A, Musial J, Akdis M, Akdis CA and Sanak M (2014) Th2-type cytokine-induced mucus metaplasia decreases susceptibility of human bronchial epithelium to rhinovirus infection. *American Journal of Respiratory Cell and Molecular Biology* **51**:229-241.

Jamieson KC, Traves SL, Kooi C, Wiehler S, Dumonceaux CJ, Maciejewski BA, Arnason JW, Michi AN, Leigh R and Proud D (2019) Rhinovirus and bacteria

synergistically induce IL-17C release from human airway epithelial cells to promote neutrophil recruitment. *The Journal of Immunology* **202**:160-170.

Janson H, Carlen B, Cervin A, Forsgren A, Magnusdottir AB, Lindberg S and Runer T (1999) Effects on the ciliated epithelium of protein D-producing and -nonproducing non-typeable *Haemophilus influenzae* in nasopharyngeal tissue cultures. *The Journal of Infectious Diseases* **180**:737-746.

Jeong JS, Lee KB, Kim SR, Kim DI, Park HJ, Lee HK, Kim HJ, Cho SH, Kolliputi N, Kim SH and Lee YC (2018) Airway epithelial phosphoinositide 3-kinase-delta contributes to the modulation of fungi-induced innate immune response. *Thorax* **73**:758-768.

Jing YX, Gimenes JA, Mishra R, Pham D, Comstock AT, Yu DH and Sajjan U (2019) NOTCH3 contributes to rhinovirus-induced goblet cell hyperplasia in COPD airway epithelial cells. *Thorax* **74**:18-32.

Jones B, Donovan C, Liu G, Gomez HM, Chimankar V, Harrison CL, Wiegman CH, Adcock IM, Knight DA, Hirota JA and Hansbro PM (2017) Animal models of COPD: What do they tell us? *Respirology* **22**:21-32.

Jong PMd, Sterkenburg MAv, Hesseling SC, Kempenaar JA, Mulder AA, Mommaas AM, Dijkman JH and Ponec M (1994) Ciliogenesis in human bronchial epithelial cells cultured at the air-liquid interface. *American Journal of Respiratory Cell and Molecular Biology* **10**:271-277.

Kato T (2016) Subchapter 35C - Granulocyte Colony-Stimulating Factor, in *Handbook of Hormones* (Takei Y, Ando H and Tsutsui K eds) pp 323-335, Academic Press, San Diego.

Kaufhold I, Osbahr S, Shima K, Marwitz S, Rohmann K, Dromann D, Goldmann T, Dalhoff K and Rupp J (2017) Non-typeable *Haemophilus influenzae* (NTHi) directly interfere with the regulation of E-cadherin in lung epithelial cells. *Microbes and Infection* **19**:560-566.

Kemmer G, Reilly TJ, Schmidt-Brauns J, Zlotnik GW, Green BA, Fiske MJ, Herbert M, Kraiss A, Schlor S, Smith A and Reidl J (2001) NadN and e (P4) are essential for utilization of NAD and nicotinamide mononucleotide but not nicotinamide riboside in *Haemophilus influenzae*. *Journal of Bacteriology* **183**:3974-3981.

Kennedy JL, Turner RB, Braciale T, Heymann PW and Borish L (2012) Pathogenesis of rhinovirus infection. *Current Opinion in Virology* **2**:287-293.

Ketterer MR, Shao JQ, Hornick DB, Buscher B, Bandi VK and Apicella MA (1999) Infection of primary human bronchial epithelial cells by *Haemophilus influenzae*: Macropinocytosis as a mechanism of airway epithelial cell entry. *Infection and Immunity* **67**:4161-4170.

Kiedrowski MR, Gaston JR, Kocak BR, Coburn SL, Lee S, Pilewski JM, Myerburg MM and Bomberger JM (2018) *Staphylococcus aureus* biofilm growth on cystic

fibrosis airway epithelial cells is enhanced during respiratory syncytial virus coinfection. *mSphere* **3**:e00341-00318.

Kim V, Oros M, Durra H, Kelsen S, Aksoy M, Cornwell WD, Rogers TJ and Criner GJ (2015) Chronic bronchitis and current smoking are associated with more goblet cells in moderate to severe COPD and smokers without airflow obstruction. *PloS One* **10**:e0116108.

King P (2012) *Haemophilus influenzae* and the lung (*Haemophilus* and the lung). *Clinical and Translational Medicine* **1**:10-10.

King PT and Sharma R (2015) The lung immune response to non-typeable *Haemophilus influenzae* (Lung immunity to NTHi). *The Journal of Immunology*.

Kiri VA, Soriano JB, Visick G and Fabbri LM (2010) Recent trends in lung cancer and its association with COPD: an analysis using the UK GP Research Database. *Primary Care Respiratory Journal* **19**:57-61.

Kirkham S, Kolsum U, Rousseau K, Singh D, Vestbo J and Thornton D (2008) MUC5B is the major mucin in the gel phase of sputum in chronic obstructive pulmonary disease. *American Journal of Respiratory and Critical Care Medicine* **178**:1033-1039.

Knowles MR, Zariwala M and Leigh M (2016) Primary ciliary dyskinesia. *Clinics in Chest Medicine* **37**:449-461.

Kobayashi Y and Tata PR (2018) Pulmonary neuroendocrine cells: sensors and sentinels of the lung. *Developmental Cell* **45**:425-426.

Komatsu K, Jono H, Lim JH, Imasato A, Xu H, Kai H, Yan C and Li JD (2008) Glucocorticoids inhibit non-typeable *Haemophilus influenzae*-induced MUC5AC mucin expression via MAPK phosphatase-1-dependent inhibition of p38 MAPK. *Biochemical and Biophysical Research Communications* **377**:763-768.

Konduru AS, Matsuyama S, Lee BC, Komatsu K and Li JD (2017) Curcumin inhibits NTHi-induced MUC5AC mucin overproduction in otitis media via upregulation of MAPK phosphatase MKP-1. *International Journal of Inflammation* **2017**:4525309.

Krasteva G, Canning BJ, Papadakis T and Kummer W (2012) Cholinergic brush cells in the trachea mediate respiratory responses to quorum sensing molecules. *Life Sciences* **91**:992-996.

Kratzer C, Graninger W, Macfelda K, Buxbaum A and Georgopoulos A (2007) Comparative activities of antibiotics against intracellular non-typeable *Haemophilus influenzae*. *Wiener klinische Wochenschrift* **119**:297-302.

Kubiet M, Ramphal R, Weber A and Smith A (2000) Pilus-mediated adherence of *Haemophilus influenzae* to human respiratory mucins. *Infection and Immunity* **68**:3362-3367.

Kusagaya H, Fujisawa T, Yamanaka K, Mori K, Hashimoto D, Enomoto N, Inui N, Nakamura Y, Wu R, Maekawa M, Suda T and Chida K (2014) Toll-like receptor-mediated airway IL-17C enhances epithelial host defense in an autocrine/paracrine manner. *American Journal of Respiratory Cell and Molecular Biology* **50**:30-39.

Langereis JD and Hermans PW (2013) Novel concepts in non-typeable *Haemophilus influenzae* biofilm formation. *FEMS Microbiology Letters* **346**:81-89.

Lee WM, Wang W and Rueckert RR (1995) Complete sequence of the RNA genome of human rhinovirus 16, a clinically useful common cold virus belonging to the ICAM-1 receptor group. *Virus Genes* **9**:177-181.

Leigh R, Oyelusi W, Wiehler S, Koetzler R, Zaheer RS, Newton R and Proud D (2008) Human rhinovirus infection enhances airway epithelial cell production of growth factors involved in airway remodeling. *The Journal of Allergy and Clinical Immunology* **121**:1238-1245 e1234.

Leopold PL, O'Mahony MJ, Lian XJ, Tilley AE, Harvey BG and Crystal RG (2009) Smoking is associated with shortened airway cilia. *PloS One* **4**:e8157.

Li D, Shirakami G, Zhan X and Johns RA (2000) Regulation of ciliary beat frequency by the nitric oxide-cyclic guanosine monophosphate signaling pathway in rat airway epithelial cells. *American Journal of Respiratory Cell and Molecular Biology* **23**:175-181.

Liu T, Zhou YT, Wang LQ, Li LY, Bao Q, Tian S, Chen MX, Chen HX, Cui J and Li CW (2019) NOD-like receptor family, pyrin domain containing 3 (NLRP3) contributes to inflammation, pyroptosis, and mucin production in human airway epithelium on rhinovirus infection. *The Journal of Allergy and Clinical immunology*.

Loeb MR, Connor E and Penney D (1988) A comparison of the adherence of fimbriated and nonfimbriated *Haemophilus influenzae* type b to human adenoids in organ culture. *Infection and Immunity* **56**:484-489.

Looi K, Buckley AG, Rigby PJ, Garratt LW, Iosifidis T, Zosky GR, Larcombe AN, Lannigan FJ, Ling KM, Martinovich KM, Kicic-Starcevich E, Shaw NC, Sutanto EN, Knight DA, Kicic A and Stick SM (2018) Effects of human rhinovirus on epithelial barrier integrity and function in children with asthma. *Clinical & Experimental Allergy* **48**:513-524.

Looi K, Troy NM, Garratt LW, Iosifidis T, Bosco A, Buckley AG, Ling KM, Martinovich KM, Kicic-Starcevich E, Shaw NC, Sutanto EN, Zosky GR, Rigby PJ, Larcombe AN, Knight DA, Kicic A and Stick SM (2016) Effect of human rhinovirus infection on airway epithelium tight junction protein disassembly and transepithelial permeability. *Experimental Lung Research*:1-16.

Lopez-Gomez A, Cano V, Moranta D, Morey P, Garcia del Portillo F, Bengoechea JA and Garmendia J (2012) Host cell kinases, alpha5 and beta1 integrins, and

Rac1 signalling on the microtubule cytoskeleton are important for non-typable *Haemophilus influenzae* invasion of respiratory epithelial cells. *Microbiology* **158**:2384-2398.

Lopez-Souza N, Dolganov G, Dubin R, Sachs LA, Sassina L, Sporer H, Yagi S, Schnurr D, Boushey HA and Widdicombe JH (2004) Resistance of differentiated human airway epithelium to infection by rhinovirus. *American Journal of Physiology-Lung Cellular and Molecular Physiology* **286**:L373-381.

Lopez-Souza N, Favoreto S, Wong H, Ward T, Yagi S, Schnurr D, Finkbeiner WE, Dolganov GM, Widdicombe JH, Boushey HA and Avila PC (2009) In vitro susceptibility to rhinovirus infection is greater for bronchial than for nasal airway epithelial cells in human subjects. *The Journal of Allergy and Clinical Immunology* **123**:1384-1390 e1382.

Lungarella G, Fonzi L and Ermini G (1983) Abnormalities of bronchial cilia in patients with chronic bronchitis. An ultrastructural and quantitative analysis. *Lung* **161**:147-156.

Maciejewski BA, Jamieson KC, Arnason JW, Kooi C, Wiehler S, Traves SL, Leigh R and Proud D (2017) Rhinovirus-bacteria coexposure synergistically induces CCL20 production from human bronchial epithelial cells. *American Journal of Physiology-Lung Cellular and Molecular Physiology* **312**:L731-L740.

Mackay AJ and Hurst JR (2012) COPD exacerbations causes, prevention, and treatment. *Medical Clinics of North America* **96**:789-+.

Mallia P, Footitt J, Sotero R, Jepson A, Contoli M, Trujillo-Torralbo M-B, Kebadze T, Aniscenko J, Oleszkiewicz G, Gray K, Message SD, Ito K, Barnes PJ, Adcock IM, Papi A, Stanciu LA, Elkin SL, Kon OM, Johnson M and Johnston SL (2012) Rhinovirus infection induces degradation of antimicrobial peptides and secondary bacterial infection in chronic obstructive pulmonary disease. *American Journal of Respiratory and Critical Care Medicine* **186**:1117-1124.

Mallia P, Message SD, Gielen V, Contoli M, Gray K, Kebadze T, Aniscenko J, Laza-Stanca V, Edwards MR, Slater L, Papi A, Stanciu LA, Kon OM, Johnson M and Johnston SL (2011) Experimental rhinovirus infection as a human model of chronic obstructive pulmonary disease exacerbation. *American Journal of Respiratory and Critical Care Medicine* **183**:734-742.

Manning BD and Toker A (2017) AKT/PKB signaling: navigating the network. *Cell* **169**:381-405.

Mannino DM and Buist AS (2007) Global burden of COPD: risk factors, prevalence, and future trends. *The Lancet* **370**:765-773.

Martins A, Han J and Kim SO (2010) The multifaceted effects of granulocyte colony-stimulating factor in immunomodulation and potential roles in intestinal immune homeostasis. *IUBMB Life* **62**:611-617.

Marwick JA, Chung KF and Adcock IM (2010) Phosphatidylinositol 3-kinase isoforms as targets in respiratory disease. *Therapeutic Advances in Respiratory Disease* **4**:19-34.

McDougall CM, Blaylock MG, Douglas JG, Brooker RJ, Helms PJ and Walsh GM (2008) Nasal epithelial cells as surrogates for bronchial epithelial cells in airway inflammation studies. *American Journal of Respiratory Cell and Molecular Biology* **39**:560-568.

McManus TE, Marley AM, Baxter N, Christie SN, O'Neill HJ, Elborn JS, Coyle PV and Kidney JC (2008) Respiratory viral infection in exacerbations of COPD. *Respiratory Medicine* **102**:1575-1580.

McNab F, Mayer-Barber K, Sher A, Wack A and O'Garra A (2015) Type I interferons in infectious disease. *Nature Reviews Immunology* **15**:87-103.

Melvin JA and Bomberger JM (2016) Compromised defenses: exploitation of epithelial responses during viral-bacterial co-infection of the respiratory tract. *PLoS Pathogens* **12**:e1005797.

Meng Y, Ren Z, Xu F, Zhou X, Song C, Wang VY, Liu W, Lu L, Thomson JA and Chen G (2018) Nicotinamide promotes cell survival and differentiation as kinase inhibitor in human pluripotent stem cells. *Stem Cell Reports* **11**:1347-1356.

Mesquita I, Varela P, Belinha A, Gaifem J, Laforge M, Vergnes B, Estaquier J and Silvestre R (2016) Exploring NAD+ metabolism in host-pathogen interactions. *Cellular and Molecular Life Sciences* **73**:1225-1236.

Message SD and Johnston SL (2004) Host defense function of the airway epithelium in health and disease: clinical background. *Journal of Leukocyte Biology* **75**:5-17.

Mikami F, Gu H, Jono H, Andalibi A, Kai H and Li JD (2005) Epidermal growth factor receptor acts as a negative regulator for bacterium non-typeable *Haemophilus influenzae*-induced Toll-like receptor 2 expression via an Src-dependent p38 mitogen-activated protein kinase signaling pathway. *Journal of Biological Chemistry* **280**:36185-36194.

Milara J, Peiro T, Serrano A and Cortijo J (2013) Epithelial to mesenchymal transition is increased in patients with COPD and induced by cigarette smoke. *Thorax* **68**:410-420.

Mio T, Romberger DJ, Thompson AB, Robbins RA, Heires A and Rennard SI (1997) Cigarette smoke induces interleukin-8 release from human bronchial epithelial cells. *American Journal of Respiratory and Critical Care Medicine* **155**:1770-1776.

Molyneaux PL, Mallia P, Cox MJ, Footitt J, Willis-Owen SA, Homola D, Trujillo-Torralbo MB, Elkin S, Kon OM, Cookson WO, Moffatt MF and Johnston SL (2013) Outgrowth of the bacterial airway microbiome after rhinovirus

exacerbation of chronic obstructive pulmonary disease. *American Journal of Respiratory and Critical Care Medicine* **188**:1224-1231.

Montoro DT, Haber AL, Biton M, Vinarsky V, Lin B, Birket SE, Yuan F, Chen SJ, Leung HM, Villoria J, Rogel N, Burgin G, Tsankov AM, Waghray A, Slyper M, Waldman J, Nguyen L, Dionne D, Rozenblatt-Rosen O, Tata PR, Mou HM, Shivaraju M, Bihler H, Mense M, Tearney GJ, Rowe SM, Engelhardt JF, Regev A and Rajagopal J (2018) A revised airway epithelial hierarchy includes CFTR-expressing ionocytes. *Nature* **560**:319.

Moore PJ and Tarran R (2018) The epithelial sodium channel (ENaC) as a therapeutic target for cystic fibrosis lung disease. *Expert Opinion on Therapeutic Targets* **22**:687-701.

Morey P, Cano V, Marti-Lliteras P, Lopez-Gomez A, Regueiro V, Saus C, Bengoechea JA and Garmendia J (2011) Evidence for a non-replicative intracellular stage of non-typable *Haemophilus influenzae* in epithelial cells. *Microbiology* **157**:234-250.

Morton DJ, Bakaletz LO, Jurcisek JA, VanWagoner TM, Seale TW, Whitby PW and Stull TL (2004a) Reduced severity of middle ear infection caused by non-typeable *Haemophilus influenzae* lacking the hemoglobin/hemoglobin–haptoglobin binding proteins (Hgp) in a chinchilla model of otitis media. *Microbial Pathogenesis* **36**:25-33.

Morton DJ, Seale TW, Bakaletz LO, Jurcisek JA, Smith A, VanWagoner TM, Whitby PW and Stull TL (2009) The heme-binding protein (HbpA) of *Haemophilus influenzae* as a virulence determinant. *International Journal of Medical Microbiology* **299**:479-488.

Morton DJ, Smith A, Ren Z, Madore LL, VanWagoner TM, Seale TW, Whitby PW and Stull TL (2004b) Identification of a haem-utilization protein (Hup) in *Haemophilus influenzae*. *Microbiology* **150**:3923-3933.

Mosser AG, Brockman-Schneider R, Amineva S, Burchell L, Sedgwick JB, Busse WW and Gern JE (2002) Similar frequency of rhinovirus-infectible cells in upper and lower airway epithelium. *The Journal of Infectious Diseases* **185**:734-743.

Mouronte-Roibas C, Leiro-Fernandez V, Ruano-Ravina A, Ramos-Hernandez C, Abal-Arca J, Parente-Lamelas I, Botana-Rial M, Priegue-Carrera A and Fernandez-Villar A (2018) Chronic obstructive pulmonary disease in lung cancer patients: prevalence, underdiagnosis, and clinical characterization. *Respiration* **95**:414-421.

Muda NM, Nasreen M, Dhouib R, Hosmer J, Hill J, Mahawar M, Schirra HJ, McEwan AG and Kappler U (2019) Metabolic analyses reveal common adaptations in two invasive *Haemophilus influenzae* strains. *Pathogens and Disease* **77**.

Munkholm M and Mortensen J (2014) Mucociliary clearance: pathophysiological aspects. *Clinical Physiology and Functional Imaging* **34**:171-177.

Murphy K and Weaver C (2017) *Janeway's Immunobiology*, Garland Science, United States of America.

Murphy TF, Brauer AL, Schiffmacher AT and Sethi S (2004) Persistent colonization by *Haemophilus influenzae* in chronic obstructive pulmonary disease. *American Journal of Respiratory and Critical Care Medicine* **170**:266-272.

Nevo S, Kadouri N and Abramson J (2019) Tuft cells: from the mucosa to the thymus. *Immunology Letters* **210**:1-9.

Niessen CM (2007) Tight junctions/adherens junctions: basic structure and function. *Journal of Investigative Dermatology* **127**:2525-2532.

Norton MM, Robinson RJ and Weinstein SJ (2011) Model of ciliary clearance and the role of mucus rheology. *Physical Review E* **83**.

Okkenhaug K (2013) Signaling by the phosphoinositide 3-kinase family in immune cells. *Annual Review of Immunology* **31**:675-704.

Okuda K, Chen G, Subramani DB, Wolf M, Gilmore RC, Kato T, Radicioni G, Kesimer M, Chua M, Dang H, Livraghi-Butrico A, Ehre C, Doerschuk CM, Randell SH, Matsui H, Nagase T, O'Neal WK and Boucher RC (2019) Localization of secretory mucins MUC5AC and MUC5B in normal/healthy human airways. *American Journal of Respiratory and Critical Care Medicine* **199**:715-727.

Ong HX, Jackson CL, Cole JL, Lackie PM, Traini D, Young PM, Lucas J and Conway J (2016) Primary air-liquid interface culture of nasal epithelium for nasal drug delivery. *Molecular Pharmaceutics* **13**:2242-2252.

Palmenberg AC, Spiro D, Kuzmickas R, Wang S, Djikeng A, Rathe JA, Fraser-Liggett CM and Liggett SB (2009) Sequencing and analyses of all known human rhinovirus genomes reveal structure and evolution. *Science (New York, NY)* **324**:55-59.

Pang B, Hong W, West-Barnette SL, Kock ND and Swords WE (2008) Diminished ICAM-1 expression and impaired pulmonary clearance of non-typeable *Haemophilus influenzae* in a mouse model of chronic obstructive pulmonary disease/emphysema. *Infection and Immunity* **76**:4959-4967.

Papadopoulos NG, Bates PJ, Bardin PG, Papi A, Leir SH, Fraenkel DJ, Meyer J, Lackie PM, Sanderson G, Holgate ST and Johnston SL (2000) Rhinoviruses infect the lower airways. *The Journal of Infectious Diseases* **181**:1875-1884.

Papi A, Bellettato CM, Braccioni F, Romagnoli M, Casolari P, Caramori G, Fabbri LM and Johnston SL (2006) Infections and airway inflammation in chronic obstructive pulmonary disease severe exacerbations. *American Journal of Respiratory and Critical Care Medicine* **173**:1114-1121.

Park K-S, Korfhagen TR, Bruno MD, Kitzmiller JA, Wan H, Wert SE, Hershey GKK, Chen G and Whitsett JA (2007) SPDEF regulates goblet cell hyperplasia in the airway epithelium. *Journal of Clinical Investigation* **117**:978-988.

Patel I, Seemungal T, Wilks M, Lloyd-Owen S, Donaldson G and Wedzicha J (2002) Relationship between bacterial colonisation and the frequency, character, and severity of COPD exacerbations. *Thorax* **57**:759-764.

Patel IS, Wilks M, Whiley AC, Lloyd-Owen S, Seemungal TAR and Wedzicha JA (2000) Relationship between exacerbation frequency and bacterial colonisation in COPD. *Thorax* **55**:A16-A16.

Pettigrew MM, Ahearn CP, Gent JF, Kong Y, Gallo MC, Munro JB, D'Mello A, Sethi S, Tettelin H and Murphy TF (2018) *Haemophilus influenzae* genome evolution during persistence in the human airways in chronic obstructive pulmonary disease. *Proceedings of the National Academy of Sciences of the United States of America* **115**:E3256-E3265.

Pezzulo AA, Starner TD, Scheetz TE, Traver GL, Tilley AE, Harvey B-G, Crystal RG, McCray PB and Zabner J (2011) The air-liquid interface and use of primary cell cultures are important to recapitulate the transcriptional profile of in vivo airway epithelia. *American Journal of Physiology - Lung Cellular and Molecular Physiology* **300**:L25-L31.

Pfeifer P, Voss M, Wonnenberg B, Hellberg J, Seiler F, Lepper PM, Bischoff M, Langer F, Schafers HJ, Menger MD, Bals R and Beisswenger C (2013) IL-17C is a mediator of respiratory epithelial innate immune response. *American Journal of Respiratory Cell and Molecular Biology* **48**:415-421.

Piper SC, Ferguson J, Kay L, Parker LC, Sabroe I, Sleeman MA, Briend E and Finch DK (2013) The role of interleukin-1 and interleukin-18 in pro-inflammatory and anti-viral responses to rhinovirus in primary bronchial epithelial cells. *PloS One* **8**:e63365.

Plasschaert LW, Zilionis R, Choo-Wing R, Savova V, Knehr J, Roma G, Klein AM and Jaffe AB (2018) A single-cell atlas of the airway epithelium reveals the CFTR-rich pulmonary ionocyte. *Nature* **560**:377.

Praveen K, Davis EE and Katsanis N (2015) Unique among ciliopathies: primary ciliary dyskinesia, a motile cilia disorder. *F1000 Prime Reports* **7**:36-36.

Proud D and Leigh R (2011) Epithelial cells and airway diseases. *Immunological Reviews* **242**:186-204.

Proud D, Sanders SP and Wiehler S (2004) Human rhinovirus infection induces airway epithelial cell production of human beta-defensin 2 both in vitro and in vivo. *The Journal of Immunology* **172**:4637-4645.

Puntener D, Engelke MF, Ruzsics Z, Strunze S, Wilhelm C and Greber UF (2011) Stepwise loss of fluorescent core protein V from human adenovirus during entry into cells. *Journal of Virology* **85**:481-496.

Quint JK, Donaldson GC, Goldring JJ, Baghai-Ravary R, Hurst JR and Wedzicha JA (2010) Serum IP-10 as a biomarker of human rhinovirus infection at exacerbation of COPD. *Chest* **137**:812-822.

Rajan D, Gaston KA, McCracken CE, Erdman DD and Anderson LJ (2013) Response to rhinovirus infection by human airway epithelial cells and peripheral blood mononuclear cells in an in vitro two-chamber tissue culture system. *PloS One* **8**:e66600.

Rajavelu P, Chen G, Xu Y, Kitzmiller JA, Korfhagen TR and Whitsett JA (2015) Airway epithelial SPDEF integrates goblet cell differentiation and pulmonary Th2 inflammation. *Journal of Clinical Investigation* **125**:2021-2031.

Raju SV, Kim H, Byzek SA, Tang LP, Trombley JE, Jackson P, Rasmussen L, Wells JM, Libby EF, Dohm E, Winter L, Samuel SL, Zinn KR, Blalock JE, Schoeb TR, Dransfield MT and Rowe SM (2016) A ferret model of COPD-related chronic bronchitis. *Journal of Clinical Investigation* **1**:e87536.

Rawlins EL, Okubo T, Xue Y, Brass DM, Auten RL, Hasegawa H, Wang F and Hogan BLM (2009) The role of Scgb1a1(+) Clara cells in the long-term maintenance and repair of lung airway, but not alveolar, epithelium. *Cell Stem Cell* **4**:525-534.

Read RC, Wilson R, Rutman A, Lund V, Todd HC, Brain APR, Jeffery PK and Cole PJ (1991) Interaction of non-typable *Haemophilus influenzae* with human respiratory mucosa in vitro. *The Journal of Infectious Diseases* **163**:549-558.

Reddy MS, Bernstein JM, Murphy TF and Faden HS (1996) Binding between outer membrane proteins of non-typeable *Haemophilus influenzae* and human nasopharyngeal mucin. *Infection and Immunity* **64**:1477-1479.

Reid L, Meyrick B, Antony VB, Chang LY, Crapo JD and Reynolds HY (2005) The mysterious pulmonary brush cell: a cell in search of a function. *American Journal of Respiratory and Critical Care Medicine* **172**:136-139.

Reidl J, Schlor S, Kraiss A, Schmidt-Brauns J, Kemmer G and Soleva E (2000) NADP and NAD utilization in *Haemophilus influenzae*. *Molecular Microbiology* **35**:1573-1581.

Ren D, Nelson KL, Uchakin PN, Smith AL, Gu XX and Daines DA (2012) Characterization of extended co-culture of non-typeable *Haemophilus influenzae* with primary human respiratory tissues. *Diagnostic Microbiology and Infectious Disease* **237**:540-547.

Reynolds SD and Malkinson AM (2010) Clara cell: Progenitor for the bronchiolar epithelium. *International Journal of Biochemistry & Cell Biology* **42**:1-4.

Rezaee F and Georas SN (2014) Breaking barriers. New insights into airway epithelial barrier function in health and disease. *American Journal of Respiratory Cell and Molecular Biology* **50**:857-869.

Rhodin JAG (1966) Ultrastructure and function of the human tracheal mucosa. *American Review of Respiratory Disease* **93**:1-15.

Rock JR and Hogan BLM (2011) Epithelial progenitor cells in lung development, maintenance, repair and disease. *Annual Review of Cell and Developmental Biology* **27**:493-512.

Rock JR, Onaitis MW, Rawlins EL, Lu Y, Clark CP, Xue Y, Randell SH and Hogan BLM (2009) Basal cells as stem cells of the mouse trachea and human airway epithelium. *Proceedings of the National Academy of Sciences of the United States of America* **106**:12771-12775.

Rogers DF (2003) The airway goblet cell. *The International Journal of Biochemistry & Cell Biology* **35**:1-6.

Rohde G, Wiethege A, Borg I, Kauth M, Bauer TT, Gillissen A, Bufe A and Schultze-Werninghaus G (2003a) Respiratory viruses in exacerbations of chronic obstructive pulmonary disease requiring hospitalisation: a case-control study. *Thorax* **58**:37-42.

Rohde G, Wiethege A, Borg I, Kauth M, Bauer TT, Gillissen A, Bufe A and Schultze-Werninghaus G (2003b) Respiratory viruses in exacerbations of chronic obstructive pulmonary disease requiring hospitalisation: a case-control study. **58**:37-42.

Rose MC, Nickola TJ and Voynow JA (2001) Airway mucus obstruction: mucin glycoproteins, MUC gene regulation and goblet cell hyperplasia. *American Journal of Respiratory Cell and Molecular Biology* **25**:533-537.

Rosell A, Monsó E, Soler N and et al. (2005) Microbiologic determinants of exacerbation in chronic obstructive pulmonary disease. *Archives of Internal Medicine* **165**:891-897.

Ross AJ, Dailey LA, Brighton LE and Devlin RB (2007) Transcriptional profiling of mucociliary differentiation in human airway epithelial cells. *American Journal of Respiratory Cell and Molecular Biology* **37**:169-185.

Roulin PS, Lotzerich M, Torta F, Tanner LB, van Kuppeveld FJ, Wenk MR and Greber UF (2014) Rhinovirus uses a phosphatidylinositol 4-phosphate/cholesterol counter-current for the formation of replication compartments at the ER-Golgi interface. *Cell Host Microbe* **16**:677-690.

Ruiz Garcia S, Deprez M, Lebrigand K, Paquet A, Cavard A, Arguel M-J, Magnone V, Caballero I, Leroy S, Marquette CH, Marcet B, Barbry P and Zaragosi L-E (2018) Single-cell RNA sequencing reveals novel cell differentiation dynamics during human airway epithelium regeneration. *BioRxiv*.

Ryan DM, Vincent TL, Salit J, Walters MS, Agosto-Perez F, Shaykhiev R, Strulovici-Barel Y, Downey RJ, Buro-Auriemma LJ, Staudt MR, Hackett NR, Mezey JG and Crystal RG (2014) Smoking dysregulates the human airway basal cell transcriptome at COPD risk locus 19q13.2. *PloS One* **9**:e88051.

Saetta M, Turato G, Baraldo S, Zanin A, Braccioni F, Mapp CE, Maestrelli P, Cavallesco G, Papi A and Fabbri LM (2000) Goblet cell hyperplasia and epithelial inflammation in peripheral airways of smokers with both symptoms of chronic bronchitis and chronic airflow limitation. *American Journal of Respiratory and Critical Care Medicine* **161**:1016-1021.

Sajjan U, Ganesan S, Comstock AT, Shim J, Wang Q, Nagarkar DR, Zhao Y, Goldsmith AM, Sonstein J, Linn MJ, Curtis JL and Hershenson MB (2009) Elastase- and LPS-exposed mice display altered responses to rhinovirus infection. *American Journal of Physiology-Lung Cellular and Molecular Physiology* **297**:L931-944.

Sajjan U, Wang Q, Zhao Y, Gruenert DC and Hershenson MB (2008) Rhinovirus disrupts the barrier function of polarized airway epithelial cells. *American Journal of Respiratory and Critical Care Medicine* **178**:1271-1281.

Sajjan US, Jia Y, Newcomb DC, Bentley JK, Lukacs NW, LiPuma JJ and Hershenson MB (2006) H. influenzae potentiates airway epithelial cell responses to rhinovirus by increasing ICAM-1 and TLR3 expression. *The FASEB Journal* **20**:2121-2123.

Salathe M (2007) Regulation of mammalian ciliary beating. *Annual Review of Pathology* **69**:401-422.

Salvi SS and Barnes PJ (2009) Chronic obstructive pulmonary disease in non-smokers. *The Lancet* **374**:733-743.

Schamberger AC, Staab-Weijnitz CA, Mise-Racek N and Eickelberg O (2015) Cigarette smoke alters primary human bronchial epithelial cell differentiation at the air-liquid interface. *Scientific Reports* **5**:8163.

Schneider D, Ganesan S, Comstock AT, Meldrum CA, Mahidhara R, Goldsmith AM, Curtis JL, Martinez FJ, Hershenson MB and Sajjan U (2010) Increased cytokine response of rhinovirus-infected airway epithelial cells in chronic obstructive pulmonary disease. *American Journal of Respiratory and Critical Care Medicine* **182**:332-340.

Schneider WM, Chevillotte MD and Rice CM (2014) Interferon-stimulated genes: a complex web of host defenses. *Annual Review of Immunology* **32**:513-545.

Schroth MK, Grimm E, Frindt P, Galagan DM, Konno SI, Love R and Gern JE (1999) Rhinovirus replication causes RANTES production in primary bronchial epithelial cells. *American Journal of Respiratory Cell and Molecular Biology* **20**:1220-1228.

Schulz C, Wolf K, Harth M, Kratzel K, Kunz-Schughart L and Pfeifer M (2003) Expression and release of interleukin-8 by human bronchial epithelial cells from patients with chronic obstructive pulmonary disease, smokers, and never-smokers. *Respiration* **70**:254-261.

Seemungal T, Harper-Owen R, Bhowmik A, Moric I, Sanderson G, Message S, MacCallum P, Meade TW, Jeffries DJ, Johnston SL and Wedzicha JA (2001) Respiratory viruses, symptoms, and inflammatory markers in acute exacerbations and stable chronic obstructive pulmonary disease. *American Journal of Respiratory and Critical Care Medicine* **164**:1618-1623.

Seemungal TAR and Wedzicha JA (2015) Update in chronic obstructive pulmonary disease 2014. *American Journal of Respiratory and Critical Care Medicine* **192**:1036-1044.

Seiler F, Hellberg J, Lepper PM, Kamyschnikow A, Herr C, Bischoff M, Langer F, Schafers HJ, Lammert F, Menger MD, Bals R and Beisswenger C (2013) FOXO transcription factors regulate innate immune mechanisms in respiratory epithelial cells. *The Journal of Immunology* **190**:1603-1613.

Sethi S, Evans N, Grant BJ and Murphy TF (2002) New strains of bacteria and exacerbations of chronic obstructive pulmonary disease. *New England Journal of Medicine* **347**:465-471.

Sethi S, Maloney J, Grove L, Wrona C and Berenson CS (2006) Airway inflammation and bronchial bacterial colonization in chronic obstructive pulmonary disease. *American Journal of Respiratory and Critical Care Medicine* **173**:991-998.

Shaykhiev R, Wang R, Zwick RK, Hackett NR, Leung R, Moore MAS, Sima CS, Chao IW, Downey RJ, Strulovici-Barel Y, Salit J and Crystal RG (2013a) Airway basal cells of healthy smokers express an embryonic stem cell signature relevant to lung cancer. *Stem Cells* **31**:1992-2002.

Shaykhiev R, Zuo W-L, Chao I, Fukui T, Witover B, Brekman A and Crystal RG (2013b) EGF shifts human airway basal cell fate toward a smoking-associated airway epithelial phenotype. *Proceedings of the National Academy of Sciences of the United States of America* **110**:12102-12107.

Shelfoon C, Shariff S, Traves SL, Kooi C, Leigh R and Proud D (2016) Chemokine release from human rhinovirus-infected airway epithelial cells promotes fibroblast migration. *The Journal of Allergy and Clinical Immunology* **138**:114-122 e114.

Shen H, Yoshida H, Yan F, Li W, Xu F, Huang H, Jono H and Li JD (2008) Synergistic induction of MUC5AC mucin by non-typeable *Haemophilus influenzae* and *Streptococcus pneumoniae*. *Biochemical and Biophysical Research Communications* **365**:795-800.

Siegel SJ, Roche AM and Weiser JN (2014) Influenza promotes pneumococcal growth during coinfection by providing host sialylated substrates as a nutrient source. *Cell Host Microbe* **16**:55-67.

Silverman RH (2007) Viral encounters with 2',5'-oligoadenylate synthetase and RNase L during the interferon antiviral response. *Journal of Virology* **81**:12720-12729.

Simet SM, Sisson JH, Pavlik JA, Devasure JM, Boyer C, Liu X, Kawasaki S, Sharp JG, Rennard SI and Wyatt TA (2010) Long-term cigarette smoke exposure in a mouse model of ciliated epithelial cell function. *American Journal of Respiratory Cell and Molecular Biology* **43**:635-640.

Sleigh MA, Blake JR and Liron N (1988) The propulsion of mucus by cilia. *American Review of Respiratory Disease* **137**:726-741.

Slinger R, Chan F, Ferris W, Yeung SW, St Denis M, Gaboury I and Aaron SD (2006) Multiple combination antibiotic susceptibility testing of non-typeable *Haemophilus influenzae* biofilms. *Diagnostic Microbiology and Infectious Disease* **56**:247-253.

Smith CM, Djakow J, Free RC, Djakow P, Lonnen R, Williams G, Pohunek P, Hirst RA, Easton AJ, Andrew PW and O'Callaghan C (2012) ciliaFA: a research tool for automated, high-throughput measurement of ciliary beat frequency using freely available software. *Cilia* **1**:14.

Smith CM, Kulkarni H, Radhakrishnan P, Rutman A, Bankart MJ, Williams G, Hirst RA, Easton AJ, Andrew PW and O'Callaghan C (2014) Ciliary dyskinesia is an early feature of respiratory syncytial virus infection. *European Respiratory Journal* **43**:485-496.

Song J, Heijink IH, Kistemaker LEM, Reinders-Luinge M, Kooistra W, Noordhoek JA, Gosens R, Brandsma CA, Timens W, Hiemstra PS, Rots MG and Hylkema MN (2017) Aberrant DNA methylation and expression of SPDEF and FOXA2 in airway epithelium of patients with COPD. *Clinical Epigenetics* **9**:42.

Spurrell JC, Wiehler S, Zaheer RS, Sanders SP and Proud D (2005) Human airway epithelial cells produce IP-10 (CXCL10) in vitro and in vivo upon rhinovirus infection. *American Journal of Physiology-Lung Cellular and Molecular Physiology* **289**:L85-95.

Sridhar S, Schembri F, Zeskind J, Shah V, Gustafson AM, Steiling K, Liu G, Dumas YM, Zhang X, Brody JS, Lenburg ME and Spira A (2008) Smoking-induced gene expression changes in the bronchial airway are reflected in nasal and buccal epithelium. *BMC Genomics* **9**:259.

Srinivasan B, Kolli AR, Esch MB, Abaci HE, Shuler ML and Hickman JJ (2015) TEER measurement techniques for in vitro barrier model systems. *Journal of Laboratory Automation* **20**:107-126.

Sriskantharajah S, Hamblin N, Worsley S, Calver AR, Hessel EM and Amour A (2013) Targeting phosphoinositide 3-kinase delta for the treatment of respiratory diseases. *Annals of the New York Academy of Sciences* **1280**:35-39.

St Geme JW (2002) Molecular and cellular determinants of non-typeable *Haemophilus influenzae* adherence and invasion. *Cellular Microbiology* **4**:191-200.

St Geme JW, Takala A, Esko E and Falkow S (1994) Evidence for capsule gene-sequences among pharyngeal isolates of non-typeable *Haemophilus influenzae* *The Journal of Infectious Diseases* **169**:337-342.

Stanley PJ, Wilson R, Greenstone MA, MacWilliam L and Cole PJ (1986) Effect of cigarette smoking on nasal mucociliary clearance and ciliary beat frequency. *Thorax* **41**:519-523.

Starner TD, Zhang N, Kim G, Apicella MA and McCray PB, Jr. (2006) *Haemophilus influenzae* forms biofilms on airway epithelia: implications in cystic fibrosis. *American Journal of Respiratory and Critical Care Medicine* **174**:213-220.

Staudt MR, Buro-Auriemma LJ, Walters MS, Salit J, Vincent T, Shaykhiev R, Mezey JG, Tilley AE, Kaner RJ, Ho MW and Crystal RG (2014) Airway basal stem/progenitor cells have diminished capacity to regenerate airway epithelium in chronic obstructive pulmonary disease. *American Journal of Respiratory and Critical Care Medicine* **190**:955-958.

Stgeme JW and Falkow S (1990) *Haemophilus influenzae* adheres to and enters cultured human epithelial cells. *Infection and Immunity* **58**:4036-4044.

Sui P, Wiesner DL, Xu J, Zhang Y, Lee J, Van Dyken S, Lashua A, Yu C, Klein BS, Locksley RM, Deutsch G and Sun X (2018) Pulmonary neuroendocrine cells amplify allergic asthma responses. *Science (New York, NY)* **360**.

Sun Y, Han M, Kim C, Calvert JG and Yoo D (2012) Interplay between interferon-mediated innate immunity and porcine reproductive and respiratory syndrome virus. *Viruses* **4**:424-446.

Swords WE (2012) Non-typeable *Haemophilus influenzae* biofilms: role in chronic airway infections. *Frontiers in Cellular and Infection Microbiology* **2**:97.

Swords WE, Buscher BA, Li KVS, Preston A, Nichols WA, Weiser JN, Gibson BW and Apicella MA (2000) Non-typeable *Haemophilus influenzae* adhere to and invade human bronchial epithelial cells via an interaction of lipooligosaccharide with the PAF receptor. *Molecular Microbiology* **37**:13-27.

Swords WE, Ketterer MR, Shao J, Campbell CA, Weiser JN and Apicella MA (2001) Binding of the non-typeable *Haemophilus influenzae* lipooligosaccharide to the PAF receptor initiates host cell signalling. *Cellular Microbiology* **3**:525-536.

Szelestey BR, Heimlich DR, Raffel FK, Justice SS and Mason KM (2013) *Haemophilus* responses to nutritional immunity: epigenetic and morphological contribution to biofilm architecture, invasion, persistence and disease severity. *PLoS Pathogens* **9**:e1003709.

Takeyama K, Jung B, Shim JJ, Burgel PR, Pick TD, Ueki IF, Protin U, Kroschel P and Nadel JA (2001) Activation of epidermal growth factor receptors is responsible for mucin synthesis induced by cigarette smoke. *American Journal of Physiology-Lung Cellular and Molecular Physiology* **280**:L165-L172.

Talikka M, Martin F, Sewer A, Vuillaume G, Leroy P, Luettich K, Chaudhary N, Peck MJ, Peitsch MC and Hoeng J (2017) Mechanistic evaluation of the impact of smoking and chronic obstructive pulmonary disease on the nasal epithelium. *Clinical Medicine Insights: Circulatory, Respiratory and Pulmonary Medicine* **11**:11795484-17710928.

Tan KS, Ong HH, Yan Y, Liu J, Li C, Ong YK, Thong KT, Choi HW, Wang DY and Chow VT (2018) In vitro model of fully differentiated human nasal epithelial cells infected with rhinovirus reveals epithelium-initiated immune responses. *The Journal of Infectious Diseases* **217**:906-915.

Thomas B, Aurora P, Spencer H, Elliott M, Rutman A, Hirst RA and O'Callaghan C (2012) Persistent disruption of ciliated epithelium following paediatric lung transplantation. *European Respiratory Journal* **40**:1245-1252.

Thomas B, Rutman A and O'Callaghan C (2009) Disrupted ciliated epithelium shows slower ciliary beat frequency and increased dyskinesia. *European Respiratory Journal* **34**:401-404.

Tilley AE, Walters MS, Shaykhiev R and Crystal RG (2015) Cilia dysfunction in lung disease. *Annual Review of Physiology* **77**:379-406.

Tipirneni KE, Grayson JW, Zhang S, Cho DY, Skinner DF, Lim DJ, Mackey C, Tearney GJ, Rowe SM and Woodworth BA (2017) Assessment of acquired mucociliary clearance defects using micro-optical coherence tomography. *International Forum of Allergy & Rhinology* **7**:920-925.

Turner J and Jones CE (2009) Regulation of mucin expression in respiratory diseases. *Biochemical Society Transactions* **37**:877-881.

Tym JE, Mitsopoulos C, Coker EA, Razaz P, Schierz AC, Antolin AA and Al-Lazikani B (2015) canSAR: an updated cancer research and drug discovery knowledgebase. *Nucleic Acids Research* **44**:D938-D943.

Uhlen M (2003) The Human Protein Atlas version 18.1, CD38- Cell Type Expression, in *https://wwwproteinatlasorg/ENSG00000004468-CD38/tissue/primary+data*, [Accessed: 16.08.2019].

Uhlen M, Fagerberg L, Hallstrom BM, Lindskog C, Oksvold P, Mardinoglu A, Sivertsson A, Kampf C, Sjostedt E, Asplund A, Olsson I, Edlund K, Lundberg E,

Navani S, Szigyarto CA, Odeberg J, Djureinovic D, Takanen JO, Hober S, Alm T, Edqvist PH, Berling H, Tegel H, Mulder J, Rockberg J, Nilsson P, Schwenk JM, Hamsten M, von Feilitzen K, Forsberg M, Persson L, Johansson F, Zwahlen M, von Heijne G, Nielsen J and Ponten F (2015) Proteomics. Tissue-based map of the human proteome. *Science (New York, NY)* **347**:1260419.

Unger BL, Faris AN, Ganesan S, Comstock AT, Hershenson MB and Sajjan US (2012) Rhinovirus attenuates non-typeable Hemophilus influenzae-stimulated IL-8 responses via TLR2-dependent degradation of IRAK-1. *PLoS Pathogens* **8**:1002969.

Vachier I, Vignola AM, Chiappara G, Bruno A, Meziane H, Godard P, Bousquet J and Chanez P (2004) Inflammatory features of nasal mucosa in smokers with and without COPD. *Thorax* **59**:303-307.

Val S, Kwon HJ, Rose MC and Preciado D (2015) Middle ear response of muc5ac and muc5b mucins to non-typeable *Haemophilus influenzae*. *JAMA Otolaryngology–Head & Neck Surgery* **141**:997-1005.

van der Linden L, Bruning AH, Thomas XV, Minnaar RP, Rebers SP, Schinkel J, de Jong MD, Pajkrt D and Wolthers KC (2016) A molecular epidemiological perspective of rhinovirus types circulating in Amsterdam from 2007 to 2012. *Clinical Microbiology and Infection* **22**:1002 e1009-1002 e1014.

van Schilfgaarde M, Eijk P, Regelink A, van Ulsen P, Everts V, Dankert J and van Alphen L (1999) *Haemophilus influenzae* localized in epithelial cell layers is shielded from antibiotics and antibody-mediated bactericidal activity. *Microbial Pathogenesis* **26**:249-262.

Vanhaesebroeck B, Guillermet-Guibert J, Graupera M and Bilanges B (2010) The emerging mechanisms of isoform-specific PI3K signalling. *Nature Reviews Molecular Cell Biology* **11**:329-341.

Vareille M, Kieninger E, Edwards MR and Regamey N (2011) The airway epithelium: soldier in the fight against respiratory viruses. *Clinical Microbiology Reviews* **24**:210-229.

Verra F, Escudier E, Lebargy F, Bernaudin JF, De Cremoux H and Bignon J (1995) Ciliary abnormalities in bronchial epithelium of smokers, ex-smokers, and nonsmokers. *American Journal of Respiratory and Critical Care Medicine* **151**:630-634.

Vestbo J, Hurd SS, Agusti AG, Jones PW, Vogelmeier C, Anzueto A, Barnes PJ, Fabbri LM, Martinez FJ, Nishimura M, Stockley RA, Sin DD and Rodriguez-Roisin R (2013) Global strategy for the diagnosis, management, and prevention of chronic obstructive pulmonary disease GOLD executive summary. *American Journal of Respiratory and Critical Care Medicine* **187**:347-365.

Vieira Braga FA, Kar G, Berg M, Carpaij OA, Polanski K, Simon LM, Brouwer S, Gomes T, Hesse L, Jiang J, Fasouli ES, Efremova M, Vento-Tormo R, Talavera-

López C, Jonker MR, Affleck K, Palit S, Strzelecka PM, Firth HV, Mahbubani KT, Cvejic A, Meyer KB, Saeb-Parsy K, Luinge M, Brandsma C-A, Timens W, Angelidis I, Strunz M, Koppelman GH, van Oosterhout AJ, Schiller HB, Theis FJ, van den Berge M, Nawijn MC and Teichmann SA (2019) A cellular census of human lungs identifies novel cell states in health and in asthma. *Nature Medicine* **25**:1153-1163.

Vlahos R and Bozinovski S (2014) Recent advances in pre-clinical mouse models of COPD. *Clinical Science* **126**:253-265.

Vogel AR, Szelestey BR, Raffel FK, Sharpe SW, Gearinger RL, Justice SS and Mason KM (2012) SapF-mediated heme-iron utilization enhances persistence and coordinates biofilm architecture of *Haemophilus influenzae*. *Frontiers in Cellular and Infection Microbiology* **2**:42.

Wack A, Terczynska-Dyla E and Hartmann R (2015) Guarding the frontiers: the biology of type III interferons. *Nature Immunology* **16**:802-809.

Wang JH, Kwon HJ and Jang YJ (2009) Rhinovirus enhances various bacterial adhesions to nasal epithelial cells simultaneously. *Laryngoscope* **119**:1406-1411.

Wang W, Dou S, Dong W, Xie M, Cui L, Zheng C and Xiao W (2018a) Impact of COPD on prognosis of lung cancer: from a perspective on disease heterogeneity. *International Journal of Chronic Obstructive Pulmonary Disease* **13**:3767-3776.

Wang Y, Xu J, Meng Y, Adcock IM and Yao X (2018b) Role of inflammatory cells in airway remodeling in COPD. *International Journal of Chronic Obstructive Pulmonary Disease* **13**:3341-3348.

Wark PA, Grissell T, Davies B, See H and Gibson PG (2009) Diversity in the bronchial epithelial cell response to infection with different rhinovirus strains. *Respirology* **14**:180-186.

Whitsett JA (2018) Airway epithelial differentiation and mucociliary clearance. *Annals of the American Thoracic Society* **15**:S143-S148.

Wilkinson TMA, Aris E, Bourne S, Clarke SC, Peeters M, Pascal TG, Schoonbroodt S, Tuck AC, Kim V, Ostridge K, Staples KJ, Williams N, Williams A, Wootton S and Devaster JM (2017) A prospective, observational cohort study of the seasonal dynamics of airway pathogens in the aetiology of exacerbations in COPD. *Thorax* **72**:919-927.

Wilkinson TMA, Hurst JR, Perera WR, Wilks M, Donaldson GC and Wedzicha JA (2006) Effect of interactions between lower airway bacterial and rhinoviral infection in exacerbations of COPD. *Chest* **129**:317-324.

Xu X, Steere RR, Fedorchuk CA, Pang J, Lee J-Y, Lim JH, Xu H, Pan ZK, Maggirwar SB and Li J-D (2011) Activation of epidermal growth factor receptor is required for NTHi-induced NF-κB-dependent inflammation. *PloS One* **6**:e28216.

Yaghi A, Zaman A, Cox G and Dolovich MB (2012) Ciliary beating is depressed in nasal cilia from chronic obstructive pulmonary disease subjects. *Respiratory Medicine* **106**:1139-1147.

Yamaguchi S, Nambu A, Numata T, Yoshizaki T, Narushima S, Shimura E, Hiraishi Y, Arae K, Morita H, Matsumoto K, Hisatome I, Sudo K and Nakae S (2018) The roles of IL-17C in T cell-dependent and -independent inflammatory diseases. *Scientific Reports* **8**:15750.

Yi G, Liang M, Li M, Fang X, Liu J, Lai Y, Chen J, Yao W, Feng X, Hu, Lin C, Zhou X and Liu Z (2018) A large lung gene expression study identifying IL1B as a novel player in airway inflammation in COPD airway epithelial cells. *Inflammation Research* **67**:539-551.

Zhang X, Sebastiani P, Liu G, Schembri F, Zhang X, Dumas YM, Langer EM, Alekseyev Y, O'Connor GT, Brooks DR, Lenburg ME and Spira A (2010) Similarities and differences between smoking-related gene expression in nasal and bronchial epithelium. *Physiological Genomics* **41**:1-8.

Zhou H, Wang X, Brighton L, Hazucha M, Jaspers I and Carson JL (2009) Increased nasal epithelial ciliary beat frequency associated with lifestyle tobacco smoke exposure. *Inhalation Toxicology* **21**:875-881.

Zhu J, Message SD, Mallia P, Kebadze T, Contoli M, Ward CK, Barnathan ES, Mascelli MA, Kon OM, Papi A, Stanciu LA, Edwards MR, Jeffery PK and Johnston SL (2019) Bronchial mucosal IFN-alpha/beta and pattern recognition receptor expression in patients with experimental rhinovirus-induced asthma exacerbations. *The Journal of Allergy and Clinical Immunology* **143**:114-125 e114.

Ziegler M and Niere M (2004) NAD+ surfaces again. *Biochemical Journal* **382**:e5-6.

Zuo WL, Yang J, Gomi K, Chao I, Crystal RG and Shaykhiev R (2017) EGF-amphiregulin interplay in airway stem/progenitor cells links the pathogenesis of smoking-induced lesions in the human airway epithelium. *Stem Cells* **35**:824-837.